DOWNWASTING AND SUPRAGLACIAL LAKE EVOLUTION ON THE DEBRIS-COVERED NGOZUMPA GLACIER, KHUMBU HIMAL, NEPAL

Kathryn Ann Hands

A Thesis Submitted for the Degree of PhD
at the
University of St Andrews

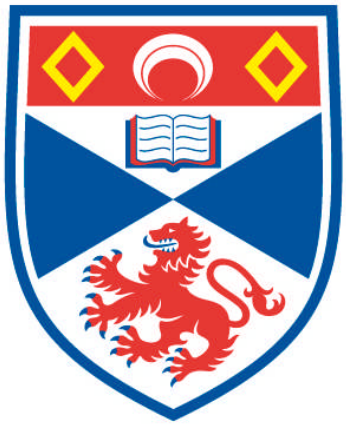

2004

Downwasting and Supraglacial Lake Evolution on the Debris-Covered Ngozumpa Glacier, Khumbu Himal, Nepal

A thesis presented by

Kathryn Ann Hands

to the University of St Andrews
in application for the degree of
Doctor of Philosophy

January 2004

Declarations

I, Kathryn Ann Hands, hereby certify that this thesis, which is approximately 60,000 words in length, has been written by me, that it is the record of work carried out by me and that it has not been submitted in any previous application for a higher degree.

Date 25/5/04 *Signature of candidate*

I was admitted as a research student in January 2000, and as a candidate for the degree of Doctor of Philosophy in the January 2000; the higher study for which this is a record was carried out between September 1999 and December 2003.

Date 25/5/04 *Signature of candidate*

I hereby certify that the candidate has fulfilled the conditions of the Resolution and Regulations appropriate for the degree of Doctor of Philosophy in the University of St Andrews and that the candidate is qualified to submit this thesis in application for that degree.

Date 25/05/04 *Signature of supervisor*

In submitting this thesis to the University of St Andrews I understand that I am giving permission for it to be made available for use in accordance with the regulations of the University Library for the time being in force, subject to any copyright vested in the work not being affected thereby. I also understand that the title and abstract will be published, and that a copy of the work may be made and supplied to any bona fide library or research worker.

Date 25/5/04 *Signature of candidate*

Acknowledgements

Firstly I would like to thank my supervisor Doug Benn for all his support and guidance over the years, and for his invaluable help during the October-November 1999 and October-November 2001 field seasons. If it were not for him, I would have opted for an English degree and missed out on a lot of wonderful opportunities.

The research was funded jointly by the University of St Andrews, the Department of Geography and Geosciences and the Cobb Scholarship Trust. Financial assistance for the three field seasons in Nepal was generously provided by the Carnegie Trust for the Universities of Scotland, the Russell Trust, the Bill Bishop Trust and my parents.

I am very grateful to Lindsey Nicholson and Seonaid Wiseman for their assistance and all the laughter, both in the field and the office. Dr Charles Warren, Andrew Wakefield, Stephen Varga, Tim Harrison and Sue Fielding kindly provided assistance in the field. Thanks must also go to our porters/field assistants Gyenbadur and Loxuman in October 2000, Mr and Mrs Sharma of the Gokyo Resort Lodge and the owner of the lodge at Thagnak. Permission to work in Nepal was given by R. Aryal, B. Rana and others at the Department of Hydrology and Meteorology.

Additional thanks must go to Dr Jack Jarvis for his help with equipment and data analysis, to John Reynolds and Sean Richardson at Reynolds Geosciences for providing SPOT images of the Ngozumpa Glacier and to Dr Nick Spedding for some useful notes and chats.

Finally, I would like to thank Peter, my mum and dad, Jack, Paul and Clare for their love, encouragement and support.

Abstract

In recent decades, the downwasting of several debris-covered glaciers in the Himalaya has led to the formation of large and potentially hazardous moraine-dammed lakes. The frequency of Glacial Lake Outburst Flood (GLOF) events in the Himalaya has steadily increased since the 1970s and as global temperatures continue to rise this trend is set to continue in the future.

Downwasting of the debris-covered Ngozumpa Glacier in the Khumbu Himal, Nepal, has resulted in the abandonment of the lateral and terminal moraine crests, leaving them standing several tens of metres above the glacier surface. The moraines have exerted a control on the drainage of meltwater from the glacier surface and have encouraged ponding of meltwater on the glacier surface. The present study examines the evolution of perched supraglacial ponds on the Ngozumpa Glacier and assesses how the growth of these ponds affects the rate of downwasting of the glacier surface. The expansion rates of perched ponds can be rapid, up to 21,609 $m^2 a^{-1}$, but the growth of these ponds tends to be terminated when contact is made with the englacial drainage network. The thesis documents for the first time a complete cycle of perched supraglacial pond growth and drainage and also provides direct evidence for internal ablation during pond drainage, a process that has only been inferred in previous research.

The western lateral moraine has dammed back drainage from the western tributary valleys, resulting in the formation of laterally-dammed lakes. The research presented here examines the processes and rates of paraglacial reworking of the Ngozumpa moraines in order to assess the stability and longevity of the moraine dam.

Approximately 1 km from the Ngozumpa terminus a large Spillway Lake has formed. Meltwater from upglacier is channelled into the lake and exits the glacier surface through an over-spill channel cut down through the western lateral moraine. The level of the Spillway Lake is thereby controlled by the height of the

spillway channel through the western lateral moraine. The rate of expansion of the Spillway Lake is lower than that of the perched ponds upglacier, but as the Spillway Lake continues to enlarge and surface downwasting of the glacier surface proceeds, the lake could enter a period of rapid and unstable growth. By analogy with other glaciers in the Khumbu Himal, it is possible that a large and potentially hazardous lake will form on the Ngozumpa within the next two decades.

Table of Contents

List of Figures

Chapter 4: Perched Supraglacial Pond Evolution

Chapter 5: Evolution of the Spillway Lake Basin

Chapter 6: Paraglacial Reworking on the Ngozumpa Moraines

List of Tables

Chapter 1

Introduction and Aims

1.1. Introduction and Rationale

The downwasting of debris-covered glaciers has long been associated with the formation of large and potentially hazardous lakes in high mountain regions. In recent decades there has been an increasing awareness of the problem of Glacial Lake Outburst Floods (GLOFs) and many potentially hazardous lakes have been identified. However, it is likely that if the current warming trend continues, many more glaciers may develop potentially hazardous lakes in the future. There is therefore a need to examine the early stages of lake development in order to provide early identification of the associated hazards. Research into the development of potentially hazardous lakes has already been carried out (Yamada & Sharma, 1993; Watanabe et al., 1994; 1995; Chikita et al., 1997; 1998; 1999; 2000a; 2000b; 2001; Sakai, 1998; 2000a; 2000b; 2001; Yamada et al., 1998; Ageta et al., 2000; Benn et al, 2000; 2001). However, many questions still remain unanswered. These include: ascertaining the processes of pond expansion; determining the rates of melting and calving around pond margins; and establishing the processes and rates of paraglacial reworking of moraine dams.

Thick accumulations of debris covering the surface of a glacier retard ablation of the underlying ice and alter the sensitivity of the glacier to climate change. Debris-covered Himalayan glaciers extend to lower altitudes than neighbouring clean-ice glaciers and, during periods of negative mass balance, debris-covered termini have a tendency to stagnate and become de-coupled from the active ice upglacier. This

allows the development of extensive and persistent glacier karst features and englacial drainage networks.

Deposition of debris around the margins of debris-covered Himalayan glaciers also results in the formation of large lateral and terminal moraines that can form continuous ramparts around a glacier from the headwalls down to and around the glacier terminus. As downwasting proceeds, these moraines can eventually be left standing tens of metres above the glacier surface. The formation of this type of moraine affects the drainage of meltwater from the glacier surface and encourages ponding of meltwater. Moraines can also impede the drainage from tributary valleys and can result in the formation of laterally-dammed lakes.

Melting of debris-covered glaciers tends to be focussed where ice is exposed at the glacier surface, such as around crevasses and areas of subsidence on the glacier surface and by slumping of debris from ice-cored debris mounds. The highest rates of ablation occur by melting and calving of exposed ice faces around the margins of supraglacial pond basins. As downwasting proceeds and overall glacier surface slope decreases, the number and size of supraglacial ponds on a debris-covered glacier tends to increase. The ponds are usually perched above the base level for englacial drainage and the impermeable glacier ice holds the pond water in place. Once formed, perched supraglacial pond basins can undergo rapid enlargement, particularly if water levels in the pond are high enough to initiate calving retreat at exposed ice faces around the pond margins. The growth of perched ponds is held in check by connection with established englacial conduit networks below the water level, which allows partial or complete drainage of pond basins.

In certain circumstances, the rapid supraglacial pond growth on debris-covered Himalayan glaciers is not constrained by periodic drainage events. Unrestricted pond growth can result in the development of very large lakes dammed by dead ice or moraine at the termini of debris-covered glaciers. These large unstable lakes have the potential to rapidly flood out downstream and can cause human casualties and

severely damage infrastructure. In the Nepal Himalaya, glacier lake outbursts floods or GLOFs are occurring with an increasing frequency, and if the current warming trend continues it is likely that many more debris-covered glaciers in the region will develop large potentially hazardous lakes at their termini (Shrestha et al., 1999; Nakawo et al., 1999; Benn et al., 2001). To date, the major trekking areas have not been overly affected by GLOFs but if global warming continues and glacier downwasting rates increase, more glaciers could be seen to be developing these large and potentially hazardous lakes. A report from the UN Environment Programme (UNEP) in 2002 listed 44 lakes in Nepal and Bhutan as being potentially hazardous (Pearce, 2002). This is a conservative estimate, however, and there may be many more lakes in a similar state that have not yet been recognised. At present, it is estimated that over a ten year period three GLOF events will occur in the Himalaya. By 2010 it is reckoned that there will be a GLOF once every year (Pearce, 2002). It is therefore necessary to identify the processes that cause supraglacial pond growth on debris-covered glaciers so that a better understanding is reached of how the development of large potentially dangerous lakes occurs.

1.2. Thesis Aims

The aim of this research is to understand and quantify the role of supraglacial ponds in the downwasting of debris-covered valley glaciers in the Khumbu Himal with particular reference to evolving Glacier Lake Outburst Flood (GLOF) hazards. The research was carried out on the debris-covered Ngozumpa Glacier in the Khumbu Himal, Nepal (Figure 1.1). The Ngozumpa is a 25 km long debris-covered valley glacier and is the longest glacier in Nepal. The Ngozumpa is also believed to have the highest concentration of supraglacial ponds of any glacier in the Khumbu region and is thought to be a candidate for the development of a large and potentially hazardous moraine-dammed lake (Benn et al., 2001). The moraines surrounding the Ngozumpa stand between 20 and 120 m above the glacier surface and have restricted the drainage of meltwater from the glacier to two over-spill channels in the moraine near the glacier terminus. The western lateral moraine has also dammed drainage from five tributary valleys, causing the formation of five laterally-dammed

lakes (Figure 1.1). Most of the meltwater leaving the surface of the Ngozumpa is channelled into the large Spillway Lake before exiting through the over-spill channel cut down through the western lateral moraine. The Spillway Lake is believed to be a possible nucleus for the growth of a large and potentially hazardous lake on the Ngozumpa Glacier.

The main aims of the research at the Ngozumpa are to:

- Determine the processes that govern perched supraglacial pond growth and drainage;
- Evaluate the rate of melting and calving around perched supraglacial pond basins;
- Examine the rates and mechanisms of basin enlargement at the Spillway Lake;
- Assess the potential for the development of a large and potentially hazardous lake at the terminus of the Ngozumpa Glacier;
- Ascertain the processes and rates of paraglacial reworking on the Ngozumpa moraines;
- Estimate the longevity of the western lateral moraine with reference to possible flood events from the laterally-dammed lakes in the western tributary valleys.

The research was carried between October 1999 and October 2001 and builds upon previous investigations of supraglacial lake evolution on the Ngozumpa Glacier by Benn et al., (2000; 2001) and Wiseman (2004) between October 1998 and October 1999. This has allowed the examination of the processes that affect supraglacial pond basin development on the Ngozumpa over four years.

1.3. Thesis Structure

The structure of the thesis has been designed to build up a model of supraglacial pond development on the Ngozumpa Glacier. Chapter 2 reviews the literature pertaining to the downwasting of debris-covered glacier surfaces, the backwasting of exposed ice faces, the development of glacier- and moraine-dammed lakes and the

associated problem of GLOF, and the paraglacial reworking of moraines. Chapter 3 provides a detailed description of the study area and outlines the methods used to achieve the aims of the research. Chapter 4 examines the processes and rates of pond growth and drainage at three case study basins on the Ngozumpa and provides a model for perched supraglacial pond development on the Ngozumpa. Chapter 5 investigates the mechanisms and rates of growth at the Spillway Lake basin and describes the function of the lake in relation to drainage of meltwater from the glacier surface. Chapter 6 looks at processes of paraglacial reworking and determines the average rate of retreat on the inner lateral moraines of the Ngozumpa. It also estimates the longevity of the western lateral moraine in order to assess the possibility of flooding from the moraine-dammed lakes in the western tributary valleys. Chapter 7 discusses the major findings of the research at the Ngozumpa and synthesises the results of the various investigations to provide a comprehensive overview of the mechanisms and rates of development of supraglacial ponds on debris-covered Himalayan glaciers. It also examines the possibility of the development of a large and potentially hazardous moraine-dammed lake on the Ngozumpa Glacier. The chapter goes on to describe the role of the Ngozumpa moraines and summarises the processes and rates of paraglacial reworking. Suggestions are then made as to how rapid growth of the Spillway Lake could be mitigated in order to protect lives and infrastructure of people living along the floodplain of the Dudh Kosi. Finally, proposals with regards to the direction of future research are made in order to help answer any questions raised by this research.

Chapter 1 Figures

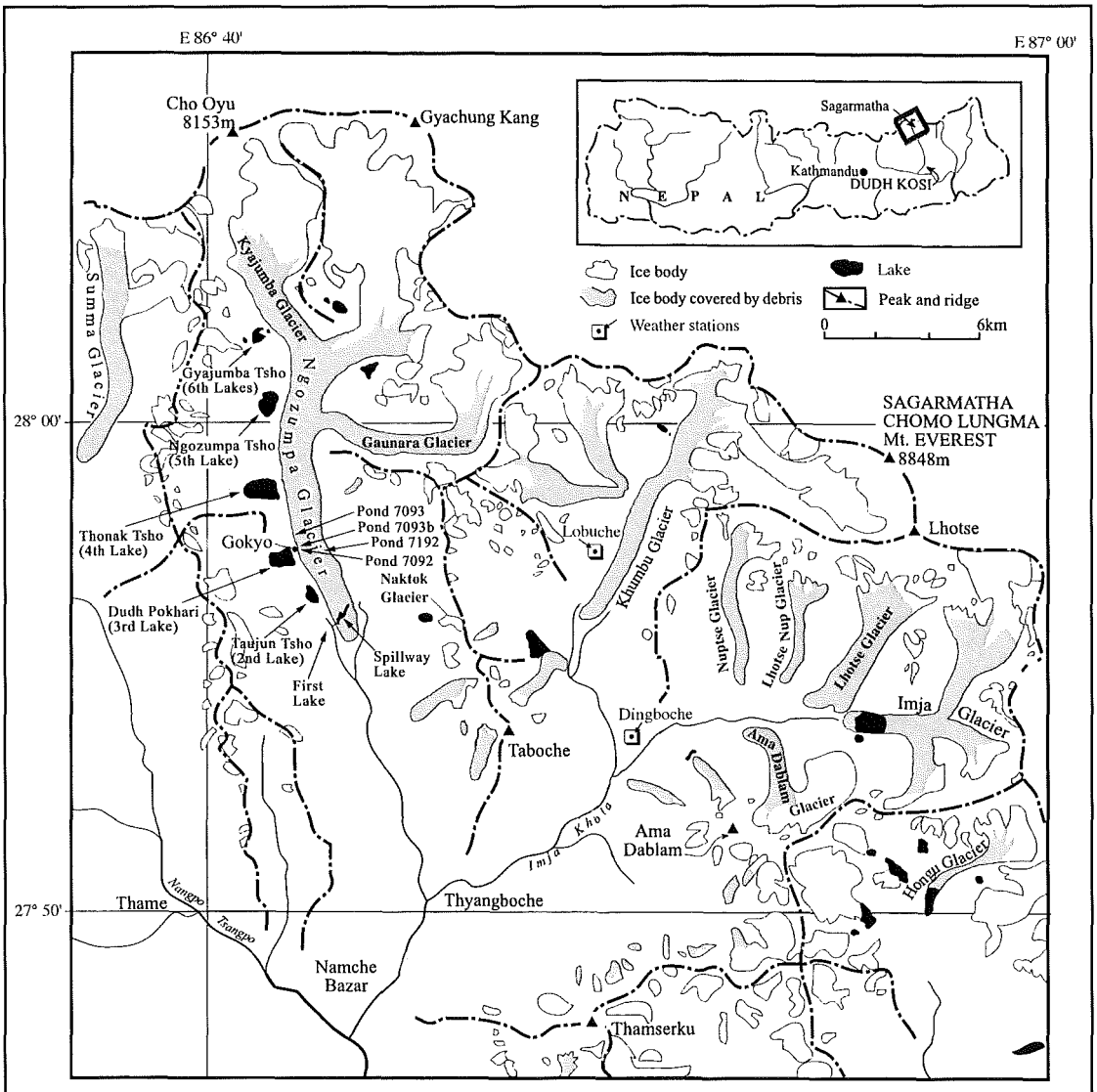

Figure 1.1. Location map showing the glaciers of the Khumbu Himal and the study sites on the Ngozumpa Glacier. Adapted from Higuchi et al. (1980).

Chapter 2

Downwasting of Debris-Covered Glaciers

2.1. Introduction

This chapter sets out the background of the thesis by reviewing the available literature relevant to the research. Firstly, the chapter examines the ablation of debris-covered glaciers as compared with clean-ice glaciers, giving a detailed description of how a debris cover is formed and how it affects the ablation of a glacier surface. The chapter then looks at the development of an undulating surface topography and glacier karst on debris-covered glaciers during periods of negative mass balance and wastage. Following this, the literature pertaining to the development of supraglacial ponds will be discussed. Section 2.5 looks at the phenomenon of glacier lake outburst floods (GLOFs) from both ice-dammed and moraine-dammed lakes, before specifically focusing on GLOFs in the Himalaya. The final part of the chapter examines the paraglacial reworking of the moraines of downwasting debris-covered glaciers.

2.2. Glacier Ablation

Processes of ablation are those which cause a glacier to lose mass. Most glacier ablation takes place below the equilibrium line in the glacier ablation zone (Paterson, 1994). The main processes of ablation are melting followed by runoff, evaporation, sublimation, calving, and wind ablation (Paterson, 1994; Benn & Evans, 1998; Purdie & Fitzharris, 1999). Melting is the main process of ablation on many glaciers and will occur when air temperatures exceed 0°C during part of the year and the ice temperature is raised to the melting point (Benn & Evans, 1998). Melting, evaporation and sublimation of ice surfaces require a net input of radiation or thermal energy. The energy balance determines the amount of energy available for melting of a glacier surface. The four components of the energy balance are short-wave radiation, long-wave radiation, the sensible heat flux, and

the latent heat flux (Benn & Evans, 1998). Given no horizontal transfer of heat, the energy balance at any point on the surface at any instant can be written as follows (Paterson, 1994).

$$M + \Delta G = R + H - L_v E + L_f P^l$$

Where:

M is the energy (W m^{-2}) used to melt snow and ice (either positive or negative)

ΔG is the rate of gain of heat of a vertical column from the surface to the depth at which vertical heat transfer is negligible (W m^{-2})

R is the net radiation (W m^{-2})

H is the sensible heat flux (W m^{-2})

L_v is the specific latent heat of vaporisation (2.8 x 10^6 J kg^{-1})

E is the rate of evaporation from the surface (kg m^{-2} sec^{-1})

L_f is the specific latent heat of fusion of ice (3.34 x 10^5 J kg^{-1})

P^l is the precipitation rate of rain (kg m^{-2} sec^{-1})

The net radiation (R) is,

$$R = Q(1 - \alpha) + I_i - I_0$$

Where:

Q is the incoming solar radiation at the surface (W m^{-2})

α is the surface albedo (dimensionless ratio)

I_i is the incoming long-wave radiation at the surface (W m^{-2})

I_0 is the emission of long wave radiation (W m^{-2})

2.2.1. Short-Wave Radiation

The most important component of the energy balance during the daytime is solar radiation, often termed the net short-wave radiation flux (Paterson, 1994). The amount of short-wave radiation that can be used to melt a glacier surface depends on the amount of cloud cover, the albedo of the ice surface, ice surface slope

aspect and angle, and the azimuth of the sun (Benn & Evans, 1998). The albedo is the measure of the reflective properties of a surface. Bright surfaces, such as fresh snow, have high albedos and reflect short-wave radiation (Paterson, 1994); dark surfaces, such as dirty ice or debris, have low surface albedos and absorb short-wave radiation (see Table 2.1). Receipts of short-wave radiation on overcast, cloudy days are lower than on clear days due to reflection and diffusion of short-wave radiation by cloud surfaces.

Table 2.1. Characteristic Albedo Values for Different Surface Types of the Djankuat Glacier, Russia (from Bozhinsky et al., 1986) and the Khumbu Glacier, Nepal (from Takeuchi et al., 2000a).

Surface Type	Albedo	
	Djankuat	Khumbu
Clean Ice	0.34 - 0.42	0.44
Slightly Soiled Ice (area of debris is much less than that of ice)	0.26 - 0.33	
Moderately Soiled Ice (areas are comparable)	0.21 - 0.25	0.21
Soiled Ice (debris area predominates)	0.15 - 0.20	
Continuous Debris Cover	0.05 - 0.14	2.1

2.2.2. Longwave Radiation

Longwave radiation is emitted from the atmosphere and from surfaces that have been heated by incoming short-wave radiation (Benn & Evans, 1998). Longwave radiation receipts are highest during periods of high humidity and on cloudy, overcast days because clouds are very good radiators (Kayastha et al., 1999). Rock surfaces overlooking valley glaciers also radiate longwave and this can aid in the melting of glacier margins. This process is particularly important in high-sided valleys that have reduced receipts of short-wave radiation due to the obstruction of parts of the sky (Arnold et al., 1996; Kayastha et al, 1999).

2.2.3. Sensible Heat Flux

The sensible heat flux of a glacier is the transfer of thermal energy between the ice surface and the atmosphere. The heat transfer is at its most efficient when the air is warmer than the ice surface and there are strong winds, or a rough glacier surface, causing eddying and turbulence of the air above the glacier (Paterson,

1994). The sensible heat flux is most associated with local air circulation, such as the movement of valley or Föhn winds (Benn & Evans, 1998).

2.2.4. Latent Heat Flux

The latent heat flux is associated with phase changes between solids, liquids and gases. The processes of melting, evaporation and sublimation consume energy, whereas condensation, freezing and deposition release energy. Latent heat transfer is the main energy exchange involved in the formation of weathering crusts (Müller & Keeler, 1969). The refreezing of water droplets deep within a snow pack or just beneath the glacier surface causes a transfer of latent heat to the surrounding ice particles; this creates a more porous ice structure which is more readily melted in the future (Bennett & Glasser, 1996).

2.2.5. Effect of a Debris Cover on Glacier Mass Balance

Debris on a glacier surface can affect the ablation rate in two ways. Thin debris covers of less than 2 cm will tend to speed up melting of underlying ice surfaces because rock tends to have a lower albedo than glacier ice and will heat up more rapidly and radiate long-wave energy. Maximum ablation rates under a debris layer occur when the debris layer is between 0.5 and 1 cm thick (Østrem, 1959; Loomis, 1970; Nakawo, 1979; Bozhinsky et al., 1986; Mattson & Gardner, 1989). Layers of debris which exceed a critical thickness of between c. 1-3 cm will serve to insulate and reduce the ablation rate of the underlying ice surface (Østrem, 1959; Loomis, 1970; Nakawo, 1979; Nakawo & Young, 1981; 1982; Bozhinsky et al., 1986; Mattson & Gardner; Nakawo & Rana, 1999). The thicker the debris layer the greater the insulation of the underlying ice. Debris layers greater than 2-3 m will almost cease the ablation of the underlying ice (Østrem, 1959; Bozhinsky et al., 1986; Watanabe et al., 1986; Clark et al., 1994; Kirkbride, 1995).

A thick debris layer causes a delayed response to short-term air temperatures and radiative energy due to the lag in heat transfer through the debris. Heat stored within a debris layer can cause melting of the underlying ice at night after air temperatures at the surface have dropped below 0°C (Benn & Evans, 1998;

Takeuchi et al., 2000a). It is not certain how much nocturnal melting occurs under thick debris layers. It has been suggested that contrary to prolonging melt, sinking of cold air down through the porous debris layer at night will replace the heat stored within the debris layer and maintain the base of the layer at the minimum daily temperature (Clark et al., 1994). Negative sensible and latent heat transfers also cause reduced melting at the debris/ice interface (Takeuchi et al., 2000a). As well as debris thickness, several other variables affect the insulative qualities of a debris mantle, including particle size, packing density, porosity, rock type, surface albedo, slope angle and aspect, and topographic shading (Loomis, 1970; Nakawo & Young, 1981; 1982; Bozhinsky et al., 1986; Kayastha et al., 1999; Nakawo & Rana, 1999). The main components of the heat balance responsible for the melting of ice surfaces under a debris layer are solar radiation and the advective and conductive heat transfers (McSaveney, 1975; Inoue & Yoshida, 1980; Bozhinsky et al., 1986; Kirkbride & Warren, 1999; Takeuchi et al., 2000a). Purdie & Fitzharris (1999) found that for the Tasman Glacier, New Zealand, conduction of heat accounted for 99% of ice melt at the base of the debris layer; compared with 1% of melt attributed to advective heat transfers. Similar findings were recorded on the Tasman by Kirkbride (1989) and also by McSaveney (1975) at the Sherman Glacier, Alaska.

2.2.5.1. Ablation of Debris-covered Glaciers

On debris-mantled glaciers the debris cover can be very thick and almost continuous over the ablation zone. The debris-cover alters the ablation rate and mass balance of the glacier. Debris-covered glaciers can extend down to much lower altitudes than clean ice glaciers because of their protective debris-mantle (Aoki & Asahi, 1998; Shroder et al., 2000). On the debris-covered G2 Glacier, Nepal, Nakawo (1979) estimated that ablation rates under debris covers thicker than 8 cm were one-third the rate for bare ice surfaces. If the overall net balance of a debris-covered glacier is negative, then the terminus of the glacier can often become stagnant and decoupled from the active ice up-valley (Kodama and Mae, 1976; Fushimi, 1977; Nakawo, 1979; Fushimi et al., 1980) and will melt in situ by thinning downwards towards its bed (Kirkbride, 1993). Significant glacier ablation is restricted to areas of the glacier surface that have become exposed,

such as on ice faces too steep to support a debris cover, around the edges of supraglacial ponds, and in areas of conduit roof collapse. Exposed ice surfaces melt and retreat by backwasting and downwasting.

The average melt rate of exposed ice cliffs on the Lirung Glacier, in the eastern Nepal Himalaya, is between 10 and 30 times the average melt rate in the debris-covered area. This could account for between 20 and 69% of the total ablation in this area (Sakai et al., 1998; 2000; 2001; Nakawo & Rana, 1999). Melting of bare ice on the Tasman Glacier accounts for 80% of the total ice loss (Purdie & Fitzharris, 1999). Melt rates of bare ice faces on the Tasman Glacier, New Zealand, average around 96 mm day^{-1} as compared to 6.7 mm day^{-1} under the debris layer (Purdie & Fitzharris, 1999). Kirkbride (1989) ascertained that backwasting rates of these bare ice faces in the debris-covered area were c. 20 m a^{-1}. Exposed conduit walls undergo similarly rapid backwasting retreats. Krüger (1994) found that medium sized conduits exposed at the surface of Myrdalsjökll, Iceland, increased in size by over 2 m $month^{-1}$ in the ablation season.

2.3. Debris Mantle Formation and Reworking

Varying thicknesses of different rock types mantle the surfaces of debris-covered glaciers over much of their lengths. Melting in the ablation zone is largely restricted to areas where the debris-cover is broken and ice is exposed at the glacier surface. The supraglacial debris cover is formed and developed by a number of processes.

2.3.1. Avalanching

Many glaciers in the Himalaya are nourished by avalanching in the upper catchments and are termed either *Turkestan-type glaciers* after Kalesnik (1937) or *Firnskessel glaciers* after Adolf Schlagintweit in 1856 (Kick, 1962; Glazyrin, 1975; Inoue, 1977; Benn & Lehmkuhl, 2000; Shroder et al., 2000). Avalanching in mountainous areas is strongly influenced by climate, vegetation and topography. Optimum slope angles for avalanche activity are between 25-50°, and especially on those slopes with angles between 35-45° (Luckman, 1977; Wenshou; 1992). Slopes steeper than the optimum angle are often unable to

accumulate the necessary volume of snow for avalanching to occur and failures will tend to occur as a series of small sloughs. However, it is possible for smaller failures on the upper slopes from gullies, ledges and cornices to trigger larger avalanching on the lower slopes (Luckman, 1977). Avalanching in the Himalaya can occur throughout the year above the snowline but the type of avalanche activity may be influenced by the season. In the pre-monsoon and post-monsoon thaw periods, larger avalanche events involving the whole depth of the snow pack are likely to occur (Zimmermann et al., 1986; Wenshou; 1992). As avalanches travel down slope they scour and pluck at the rock walls and entrain any loose weathered rocks from the slopes and gullies. The avalanched snow and rock is thereby transferred to the glacier surface (Shroder et al., 2000) and can remain at elevations lower than ordinary snow cover due to the thickness and density of the avalanche cones (Luckman, 1977).

2.3.2. Transport of Debris to the Glacier Surface

Snow and ice avalanching on the glacier headwalls brings down large quantities of shattered rock debris, which is then incorporated within the snow pack forming stratified planes of debris within the ice (englacial debris bands). The englacial debris bands are rotated as they are transported downglacier and then exposed by ablation below the equilibrium line to form part of the supraglacial debris mantle (Souchez; 1971; Small, 1983; Gomez & Small, 1985; Ensminger et al., 2001). Alongside debris from frost shattering, rockfall, rock avalanching and slope processes active on the steep valley walls, debris can also be delivered to the glacier surface from the lateral moraines (Nakawo, 1979; Small, 1983; Nakawo et al., 1986; Vere & Benn, 1989; Whalley et al., 1996; Owen, 1991; Owen et al., 1998; Jansson et al., 2000). Debris delivered to the ablation zone is transported either supraglacially or, if it falls down into a crevasse or shaft in the ice, incorporated into the englacial system and brought to the surface in debris bands downglacier (Small et al., 1979; Anderson, 2000). Supraglacial moraines formed in this way have been termed ablation-dominant (AD) moraines (Eyles & Rogerson, 1978; Gomez and Small, 1985; Vere & Benn, 1989).

On many debris-mantled glaciers in the Himalaya, the debris cover is almost continuous from the base of avalanche cones in the upper catchments down to the glacier terminus. The debris mantle is often only broken in places where lakes have formed, ice faces have been exposed, or cracks have opened on the glacier surface. The existence of such a continuous debris cover suggests that the equilibrium lines for these types of glacier may lie at around the same altitude as the avalanche cones in their upper catchments.

Medial moraines can also form on the surface of debris-mantled glaciers below the junction of two glaciers, providing a further source of supraglacial debris. Moraines of this type have been labelled *ice-stream interactive (ISI) moraines* (Eyles & Rogerson, 1978; Gomez and Small, 1985; Bozhinsky et al., 1986; Vere & Benn, 1989). Debris entrained in medial moraines is often derived from supraglacial lateral moraines and rockfall material weathered out of the slopes above the junction between the glaciers (Small & Clark, 1974; Kirkbride & Warren, 1999). If a glacier convergence occurs above the firn line, then the material will become incorporated into the glacier body and will then melt out downglacier in the ablation zone (Small & Clark, 1974). Material produced by glacier convergence below the firn line is predominantly carried supraglacially, although material may still be entrained into the englacial debris system via crevasse and meltwater structures. Once at the surface, the moraine may spread out creating a continuous debris cover (Small & Clark, 1974; Small et al., 1979; Kirkbride & Warren, 1999).

Englacial debris can be exposed at the glacier surface in a number of ways: by the melt-out of debris from debris bands both sub-aerially and sub-aqueously; by falling from debris bands exposed in ice cliffs; and by the exposure of debris on conduit floors by the collapse of conduit roofs. Debris can also be distributed throughout the body of the glacier by supraglacial and englacial fluvial processes (Knighton, 1973; Shaw & Archer, 1979; Watson, 1980; Wright, 1980; Kirkbride, 1995). Supraglacial stream action can redistribute debris across the surface and can deliver surface debris to englacial positions via moulins and crevasses. Furthermore, due to the high levels of energy involved in the drainage of

supraglacial ponds, substantial amounts of debris can be transferred from supraglacial to englacial positions. Englacial debris can similarly be brought to the glacier surface via discharge from conduits into supraglacial lakes. There is evidence from Gígjökull and Kvíárjökull in Iceland and from the Tasman and Mueller glaciers, New Zealand, that material from the bed of a glacier can be transferred up into the englacial meltwater system via conduits (Näslund & Hassinen, 1996; Kirkbride & Spedding, 1996; Spedding, 2000). Spedding (2000) explained the upward movement of water through the glacier by invoking an overdeepening in which rising water pressure forces the meltwater up into higher channels. Once in the englacial transport system debris can be deposited as channel fill structures, which can then melt out onto the glacier surface.

In addition to these debris sources, debris can be thrust upwards along englacial shear zones to the glacier surface from subglacial positions (Clayton, 1964; Boulton, 1967; Glazyrin, 1975; Gomez & Small, 1985; Bozhinsky et al., 1986; Kirkbride, 1995; Krüger & Aber, 1999; Ensminger et al., 2001). However, given the lack of data available for glacier bed conditions in the Himalaya, it is not known whether this process is important in Himalayan glaciers. Kodama and Mae (1967) and Fushimi (1977) suggested that a shear zone existed on the debris-mantled Khumbu Glacier 3 km from the glacier terminus whilst the tongue itself remained stagnant with ice flow vectors directed either upglacier or irregularly. In later studies, Nakawo et al. (1986) and Watanabe et al. (1986) suggested a migration of the Khumbu Glacier shear zone to around 6 km upglacier from the terminus. Benn and Owen (2002) described shear planes at the margin of the Batal Glacier in the Indian Himalaya. Low ice flow velocities promote glacier thinning and thickening of debris layers (Lundstrom et al., 1993; Nakawo et al., 1999). Richardson & Reynolds (2000a) describe the stagnation of the Tsho Rolpa and Thulagi Glacier termini, giving further evidence of low flow velocities and stagnation of debris-covered glaciers in Nepal. From research undertaken on the debris-mantled Tasman Glacier, New Zealand (Kirkbride, 1995) and on the Klutlan Glacier, Canada (Watson, 1980; Wright, 1980) it is apparent that the area of debris-mantled ice is inversely related to ice velocity. The development of various thermokarst features such as sinkholes, englacial

meltwater tunnels and small supraglacial ponds are testament to the fact that ice velocities have slowed to the point where conduits and voids within the ice are able to remain open for long periods of time.

2.3.3. Reworking of the Debris Mantle

The surface debris mantle on debris-covered glaciers thickens up from the base as englacial debris is melted out. Debris mantles are not of a uniform thickness and are constantly reworked and spread out across the glacier surface by a variety of slope, fluvial, and thermokarst processes (Vere & Benn, 1989; Kirkbride & Warren, 1999). Topographic relief on Himalayan Glaciers is commonly up to c. 50 m, largely due to varying thicknesses of debris on the surface. The presence of ogives in the body of a glacier downstream from an icefall may also exert an influence on the topography of the glacier, as has occurred on the Khumbu glacier downstream of the Khumbu icefall (Fushimi et al., 1980) and at several glaciers in the Arolla Region of Switzerland (Small & Clark, 1974; Small et al., 1979). On the Klutlan Glacier, Canada, some of the original glacier forms and patterns have persisted after over 200 m of downwasting (Watson, 1980; Wright, 1980).

At the point of emergence, deposits of debris on a glacier surface will insulate the underlying ice forming mounds and increasing the topographic relief. The debris mounds grow in size and height until the mound slopes become too steep to retain their debris cover (Loomis, 1970; Drewry, 1972; Small & Clark, 1974). Slumping and other mass movement processes will thereby remove material from the top of the debris mound and ablation will increase where the ice core is exposed (Clayton, 1964; Watson, 1980; Wright, 1980; Drewry, 1972; Small & Clark, 1974; Kirkbride, 1993).

More generally, topographic highs are found where there are very thick accumulations of debris on the glacier surface. This is due to the retardation of ablation under thick debris layers (Østrem, 1959; Loomis, 1970; Souchez, 1971; Drewry, 1972; Nakawo, 1979; Watson, 1980; Wright, 1980; Nakawo & Young, 1981, 1982; Small, 1983; Watanabe et al., 1986). The topographic high points

are usually in the form of large conical mounds and ridges, although there are also some plateaux formed from former lake beds. Conversely, the topographic lows are areas where sediment accumulations are initially less thick and therefore undergo proportionally more melting than the surrounding high areas. Fluvial incision by supraglacial streams and processes of supraglacial pond development (see Section 2.4) further accelerates melting in the low areas of the glacier surface (Healy, 1975; Watson, 1980; Watanabe et al., 1986). Over time the redistribution of debris by slope and fluvial processes across the glacier surface will bring about the process of topographic reversal; whereby topographic highs become lows and vice-versa (Clayton, 1964; Boulton, 1967; Drewry, 1972; Watson, 1980; Wright, 1980; Small, 1983). Far from being a solitary event, topographic reversals can occur many times during the downwasting of debris-covered glaciers (Watson, 1980). The process of topographic reversal causes the lateral transfer of debris across the glacier surface (Kirkbride & Warren, 1999) and brings about a fairly uniform average downwasting rate (Watson, 1980; Nakawo et al., 1999).

During periods of negative mass balance, debris thicknesses increase and downwasting rates decrease in a downglacier direction causing a reduction of the glacier gradient (Kirkbride & Warren, 1999; Reynolds, 2000). As a consequence the surface topographic relief also decreases progressively downglacier (Loomis, 1970; Small et al., 1979; Nakawo, 1979; Kirkbride & Warren, 1999). Loomis (1970) described the increase and subsequent decrease of topographic relief downglacier on the Kaskawulsh Glacier, Yukon, as "waxing and waning" of the moraines driven by the thickness of the moraine cover. A similar waxing and waning moraine pattern was reported as occurring on the Tsidjiore Nouve Glacier, Bas Glacier d'Arolla and Haut Glacier d'Arolla, Switzerland by Small et al. (1979).

2.4. Supraglacial Pond Development

The stagnation of a debris-covered glacier and the development of a complex hummocky topography provide perfect conditions for ponding of glacial meltwater and precipitation. The ponding of water is often encouraged by the

existence of lateral-terminal moraines that impede the drainage of meltwater from the glacier. Water can be stored in englacial conduits and voids, in subglacial cavities, and in hollows on the glacier surface. Small isolated ponds begin to appear once the overall surface slope of a glacier decreases to between 6 and 10°; larger discrete ponds occur where the surface slope is between 2 and 6 ° (Reynolds, 2000). Once the slope of the glacier surface reaches a critical threshold, precipitation and snow and ice melt will begin to pond in glacier surface hollows. The small supraglacial ponds that form have distinct characteristics in terms of their water inputs/outputs, basin size/shape, calving rates, sediment concentrations, temperature profiles, and current circulation. These characteristics determine the way in which ponds will develop and enlarge.

2.4.1. Energy Balance of Supraglacial Ponds

The study of supraglacial ponds is important to the understanding of ablation rates on debris-covered, downwasting glaciers. On the debris-mantled Lirung Glacier, in the Langtang Valley of the Nepal Himalaya, Sakai et al. (2000a) found that supraglacial ponds had average net energy receipts of 170 W m^{-2} during the summer monsoon season. This is around 7 times higher than the average for the whole debris-covered area. It was estimated that around half of this heat energy is lost by outflow of water through englacial conduits. The warmed pond water causes increased melting of the ice faces surrounding a pond and internal melt as it drains out, enlarging the conduits and facilitating the collapse of conduit roofs (Sakai et al., 2000a; Reynolds, 2000). These processes in turn expose new areas of ice cliffs and further increase the ablation of the glacier (Kirkbride, 1993; Sakai et al., 2000a).

Sakai et al (2000a) used a full energy balance approach to describe the heat balance of supraglacial lakes on the Lirung Glacier (see also Figure 2.1). They gave the heat balance of a supraglacial pond as:

$$dS/dt = Q + I - D - M_d - M_i$$

Where:

S	is the heat storage of the pond
t	is time
Q	is the net input at the water surface
I	is the heat advection from meltwater inflow
D	is the heat loss by water outflow
M_d	is the latent heat for ice melt under the debris layer
M_i	is the latent heat for ice melt of exposed ice cliffs below the water surface

Figure 2.1. Heat Balance at a Supraglacial Pond

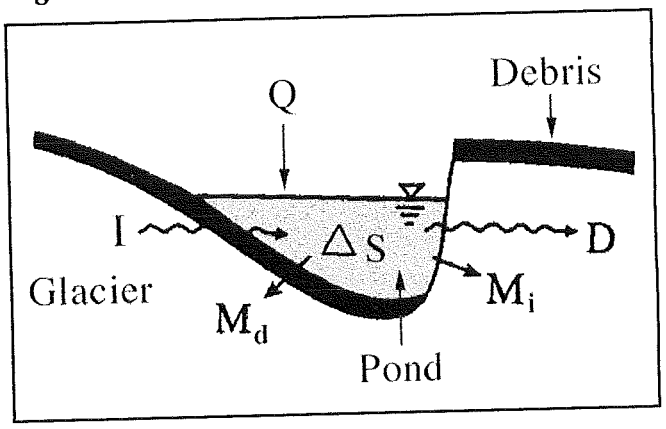

(from Sakai et al., 2000, p.122)

Heat input at the pond surface (Q) was calculated from meteorological measurements and expressed as:

$$Q = SR(net) + LR + H + E + P + F$$

Where:

SR(net)	is the net shortwave radiation
LR	is the longwave radiation
H	is the sensible heat flux
E	is the latent heat flux
P	is the heat flux with rainfall (av. 1.6 W m^{-2}, considered negligible)
F	is the heat flux from the edge of the ice cliff (< 3.5 x 10^{-4} W m^2, also considered negligible)

Errors in the measurement of the energy from shortwave radiation, longwave radiation and the sensible and latent fluxes are ±3.5 W m^{-2}, ±23 W m^{-2}, ±6.7 W m^{-2} and ±5.1 W m^{-2}, respectively. This gives a total error of ±40 W m^{-2} (23.5%) for the incoming energy to a pond surface.

Heat for ice melt (M_d and M_i) were given as:

$$M_d = k(T/\Delta z)(A_d/A)$$

Where:

T is the temperature difference between water and the ice melting point

A_d is the debris-covered area at the bottom of the pond (assumed to be equal to the pond surface area, A)

Δz is the debris thickness at the bottom of the pond, assumed to be the same as the thickness observed at the edge of the ice cliff.

K is the average heat transfer coefficient for the fully turbulent flow of a fluid over a flat plate (Eckert & Drake, 1959; Weeks & Cambell, 1973) adapted for fresh water.

Heat discharged from a pond (D) is the residual of the model after all the other terms are accounted for and is attributed to water discharge from a pond (q_0):

$$q_0 = D/c_w\rho_w T_s$$

The findings of the research carried out by Sakai et al. (2000a) on the Lirung Glacier and by Inoue and Yoshida (1980) on the Khumbu Glacier show that supraglacial ponds play a large role in determining the ablation rate of debris-covered glaciers. The research also suggests that internal melt by thermal enlargement of englacial conduits caused by the flow of relatively warm pond water is an important process of ice loss on debris-covered glaciers. However, the energy balance approach used in calculating the energy absorbed at a pond surface is limited by uncertainties in the input terms, many of which are subject to error. Sakai's model depends on the assumption that all the energy balance

terms are correct and assumes that the residual energy, over half the energy absorbed at the pond surface, is discharged from a pond by outflow of pond water. However, this assumption is unfair because no evidence of permanent outflows from supraglacial ponds on the Lirung Glacier is provided. Furthermore, Sakai et al. (2000a) only looked at rates of ice melt and did not take into account the role played by ice face calving around the edges of supraglacial ponds.

2.4.2. Water Inputs and Outputs

The main water inputs to supraglacial ponds are from precipitation and from melting snow and ice in the ablation zone of the glacier. The volume of water entering a pond will largely be determined by annual variations in precipitation, meltwater production and evaporation (Benn et al., 2001). In the Himalaya, water inputs are highest during the summer monsoon. Meltwater can enter a pond directly from the surrounding ice faces, from surface meltwater streams, from melting icebergs that have calved into the pond, and via englacial conduits. Over the winter months many supraglacial ponds freeze over and the englacial conduit systems of a glacier can shut down. Ice loss is largely by sublimation and ponds therefore receive little water input from melting ice and snow.

Water can exit a supraglacial pond via subaqueous englacial conduits or surface streams. Evaporation is also an important process of water loss from supraglacial ponds. The importance of these processes to basin expansion and melt rates depends on whether a pond is connected to the drainage system of the glacier. 'Closed' or 'perched' basins will not lose water via meltwater streams or conduits unless the basin expands and taps into the englacial conduit system below the water level of the pond (Benn et al., 2000; 2001) (See Section 2.4.4).

2.4.3. Basin Expansion

It has already been described how the melt rate of exposed ice faces is more rapid than for debris-covered ice surfaces (Section 2.2.2) and how the heat absorbed by supraglacial ponds further contributes to ice melt rates around the pond margins (Section 2.4.1). However, expansion of a supraglacial pond is not

dependent solely on ice melt rates around the pond margins. The basin expansion rate, and therefore the contribution to the glacier ablation rate, will also depend upon the size and depth of the pond; the percentage of exposed ice around the pond margin; the temperature and sediment concentration of the pond water; the amount of melting at the floor of the basin; and the calving rate of the ice faces surrounding the pond (Chikita et al., 1997; 1998; 1999; Benn et al., 2000; 2001).

2.4.3.1. Water Temperature

Supraglacial ponds have low surface albedos (<0.05) and consequently efficiently absorb solar radiation at their surfaces (Chikita et al., 1998; 1999; Benn et al., 2001). Temperatures of around 5°C can be experienced at the water surface of ponds during the daytime (Chikita et al., 1997; 1998; 1999). The warm surface water of a pond causes thermal erosion of exposed ice faces at the water-line, which results in the development of a notch. Thermo-erosional notches at the Austerdalsisen Glacier, Norway, undercut parts of the ice cliff by several metres and can extended over a metre vertically above the water-line (Theakstone, 1989). At the Maud Glacier, New Zealand, the roof of the thermo-erosional notch would collapse once the notch depth had reached between 3-4 m (Kirkbride & Warren, 1997). Notch-controlled calving will be examined in section 2.4.3.4.

During the summer, the temperature of a pond will decrease with depth. High surface water temperatures can cause thermo-erosional notching at the water level and induce water-line calving events. Cold water in contact with the ice margin or entering the lake as meltwater will be forced downwards and outwards, away from the ice face (Chikita et al., 1997; 1998; 1999). The circulation of this cold water during the daytime will undoubtedly slow the melt rate towards the bottom of the ice margin resulting in a tapering of the ice face at the base. The melt out of large calved ice bergs can reduce the temperature of a pond temporarily and this can slow the rate of thermo-erosional notching and water-line calving (Benn et al., 2001). The heat produced by debris falling into a pond is considered to have a negligible effect on pond temperature (Sakai et al., 2000a).

In the winter, the formation of a cover of ice on a pond alters the thermodynamics of a pond. The ice cover increases the albedo of the pond surface, reducing the amount of shortwave radiation available for heating the pond surface. The ice cover also reduces the amount of mixing and turbulence in the pond because it inhibits wind-induced currents. An ice cover also reduces the loss of longwave radiation from the pond, and this brings about a change in the thermal structure of the pond: producing warmer temperatures at the base of the pond than at the surface. In this way, subaqueous melting around the pond margins and at the pond floor can continue throughout the year.

Biological heating by mats of algae can substantially contribute to local water temperatures (Reynolds, 2000). Temperatures of between 5 and 8.5°C have been recorded within algae mats at the Thulagi Glacier Lake, Nepal (Reynolds, 2000).

2.4.3.2. Sediment Concentration

Suspended sediment concentrations affect the water density, temperature distributions and amount of stratification within supraglacial ponds (Chikita et al., 1997; 1998; 1999; Warren & Kirkbride, 1998). Water in ponds connected to the englacial drainage system is usually grey in colour due to mixing of suspended sediment particles by water inflow. Perched ponds are often stagnant and unmixed, except where disturbed by wind or debris falls, producing a grey-green water colour (Hochstein et al., 1995). Low transparency of pond water and high turbidity causes solar radiation to be absorbed mainly at the water surface (Chikita et al., 1997). The density of pond water at depth is largely driven by the suspended sediment concentration rather than by the water temperature (Warren & Kirkbride, 1998). Density-driven underflows laden with sediment travel along the floor of the lake away from the ice margins. The sediment-laden underflows could decrease melting at the pond floor by depositing further layers of sediment onto the pond floor and by decreasing the temperature gradient between the bottom water and the underlying ice (Chikita et al., 1999).

2.4.3.3. Currents

Wind-driven currents can bring about the advective diffusion of heat within the upper water column of a supraglacial pond (Chikita et al., 1999). In larger ponds and lakes, diurnal valley winds can transport the heated water surface layers towards ice face margins increasing the amount of melting and thermo-erosional notching (Chikita et al., 1999; Benn et al., 2000). Counter currents set up by the cooling of water at the ice margin will be transported away from the ice margin, reducing melt rates of ice at depth and along the floor of the basin. This cold water will eventually upwell downlake from the ice margin (Chikita et al., 1999).

2.4.3.4. Calving

Calving of ice blocks from steepened ice margins can result in rapid basin expansion and ice loss at supraglacial pond margins (Benn et al., 2000; 2001; Reynolds, 2000). Four types of calving typically occur around the edges of small supraglacial ponds: (1) full-height slab calving; (2) thermo-erosional notch-controlled calving; (3) spalling of thin flakes of ice from the middle of the subaerial ice face; and (4) subaqueous calving (Kirkbride & Warren, 1997; Benn et al., 2000; 2001). The calving process is not fully understood and research has been concentrated on calving rates and processes at glacier and ice sheet termini. Very little research has been published concerning the mechanisms of calving from ice faces bordering small supraglacial ponds on debris-covered glaciers.

Full-Height Slab Calving

Large pillars, slabs or flakes of ice have a tendency to calve along structural weaknesses present within and immediately behind the ice face (Powell, 1983; Theakstone, 1989; Warren et al., 1995, 1995b; Kirkbride & Warren, 1997; Benn et al., 2000; 2001). Cracks can propagate along old crevasse traces, englacial channels, foliation planes, debris bands and voids; the cracks are often, but not always, aligned parallel to the ice face (Theakstone, 1989; Kirkbride & Warren, 1997; Benn et al 2000; 2001). Once opened, bending stresses will help to further extend the crack down through the ice (Warren, 1992), debris and meltwater entering the crack may also help to develop it further (Van der Veen, 1998; Hanson & Hooke, 2000). Tensile stresses across failure planes increase with ice

flake/block height, as does the amount of oversteepening which occurs (Warren, 1992; Warren et al., 1995b). Benn et al. (2001) suggested that calving will occur where the ice faces around a supraglacial pond exceed 15 m in height. Eventually the resulting flake or pillar of ice becomes unstable and rapid failure at the base causes the detached ice block to calve into the pond (Warren, 1992).

Notch-Controlled Calving

Exposed ice at the water level will also be subject to the process of thermo-erosional notching and notch-controlled calving. Relatively warm surface water in supraglacial ponds causes the thermal erosion of exposed ice faces at the water-line, resulting in the formation of a thermo-erosional notch. As a thermo-erosional notch is deepened, stress-release fractures propagate behind the overhanging section of ice down to the water-line and eventually the roof of the notch calves into the pond. Steep ice faces undercut by thermo-erosional notches retreat at rates of between 3 and 5 times greater than more gently sloping debris-covered pond margins (Kirkbride, 1993). Notch-controlled calving events are more frequent than full slab calving events but they produce much smaller icebergs (Kirkbride & Warren, 1997).

Subaqueous Calving

Together with basin enlargement due to the retreat of surrounding ice faces, a pond basin may increase in size through melting taking place at the bottom of the water column. Melting of the pond floor is the most common process of achieving this, but under certain circumstances subaqueous buoyancy-driven calving can also occur.

Thermo-erosional notching, decreasing rates of subaqueous melting with depth, and calving of blocks above the water-line, may bring about the development of a tapering ice slope below the water level (Warren et al., 1995; Kirkbride & Warren, 1997; Warren & Kirkbride, 1998; Benn & Evans, 1998). This tapering ice slope is often termed an 'ice foot' or 'proglacial ramp' in proglacial lake and marine settings. These 'ramps' may be covered over by debris falling from the top of the ice face as it retreats. The development of subaqueous ramps can result

in buoyancy-driven subaqueous calving events. Calving of large blocks upward through the water column occurs where structural weaknesses, such as old crevasse traces or debris bands, exist within a protruding 'ice ramp' at the floor of the pond (Warren, 1992; Hanson & Hooke, 2000). Density differences between ice and water exert an upward buoyant force on the ice foot causing blocks of ice to break away and float up to the surface (Warren et al., 1995b; Kirkbride & Warren, 1997; Benn & Evans, 1998; Hanson & Hooke, 2000), often several metres away from the subaerial ice face.

Cycle of Calving

Kirkbride and Warren (1997) suggested that for the grounded ice margin of the Maud Glacier, New Zealand, there are four 'sequential stages of calving'. The first stage is the small-scale calving of thermo-erosional notch roofs. In the second stage the overhang is accentuated by the calving of thin ice flakes from the main ice face which promotes propagation of crevasses. In stage three, the crevasse propagation and bending stresses will bring about a full-slab calving event. Finally it is possible that a subaqueous calving event from the projecting 'ice ramp' will occur, although this happens far less frequently than the other three forms of calving events. If this hypothesis is correct then the calving rate in supraglacial ponds is driven by the rate of melting at the water-line (Kirkbride & Warren, 1997; Warren & Kirkbride, 1998). However, at the Ngozumpa Glacier Benn et al. (2001) found that some calving processes in supraglacial ponds occurred independently of the rate of water-line melting. Instead they argued that the rate of calving is mainly determined by ice face height and the location and spacing of suitably orientated weaknesses with exposed ice faces around a pond basin.

The calving of ice blocks into a supraglacial pond induces further increases in lake water volume as the calved icebergs melt in the relatively warm pond water. If the water level is deep enough, the icebergs produced by glacier calving will drift away from the ice face toward the ice margins (Warren & Kirkbride, 1998; Benn et al., 2000; 2001). If water levels are shallow then the iceberg can become grounded near to the ice face and will melt out in situ (Warren & Kirkbride,

1998). Melt out of icebergs will increase the water volume and depth of supraglacial ponds, further exacerbating the melt and calving rates of the exposed ice margins (Benn et al., 2000, 2001).

2.4.4. Pond Drainage

The drainage of ponds from basins connected to supraglacial or englacial drainage pathways has already been mentioned in Section 2.4.2, above. 'Perched' ponds will drain if they expand and tap into the englacial drainage system of the glacier below the water level (Benn et al., 2000; 2001). Once initiated, the drainage of a supraglacial pond can be very rapid and accelerates over time as the draining pond water enlarges the conduit walls by thermal erosion (Sakai et al., 2000a). If the conduit is tapped near or at the basin floor then the entire lake can drain out leaving an empty basin containing only a few isolated, shallow ponds (Benn et al., 2000; 2001). Drained 'perched' basins can be re-flooded, initiating further cycles of growth and drainage until the pond level coincides with the base level for englacial drainage. After the pond is connected at the base level, it will no longer undergo cycles of rapid drainage and will continue to expand and amalgamate with surrounding supraglacial ponds (Benn et al., 2001).

2.4.5. Pond Amalgamation

Glaciers with surface slopes of less than 2° promote the coalescence of supraglacial lakes (Reynolds, 2000). Lakes that are hydraulically connected at the base level for englacial drainage will expand freely until their basins amalgamate. The coalescence of supraglacial lakes and processes of basin expansion outlined above can eventually result in the formation of very large lakes at the termini of debris-covered glaciers, retained by moraine or ice dams (Kirkbride, 1993; Hochstein et al., 1995; Reynolds, 2000; Benn et al., 2000; 2001). If the lake deepens and extends down to the glacier bed, then a rapid calving retreat of the glacier will ensue (Kirkbride, 1993; Hochstein et al., 1995; Kirkbride & Warren, 1999).

2.5. Glacial Lake Outburst Floods

Costa and Schuster (1988) outlined nine types of ice-dammed lake: supraglacial lakes, marginal ponded lakes, converging ice stream ponded lakes, tributary stream-valley ponded lakes, tributary glacier-valley ponded lakes, interglacially ponded lakes, lakes dammed by a tributary glacier, proglacial ice-dammed lakes, and miscellaneous lakes (e.g. ice-dammed lakes above a volcano and large englacial or subglacial water bodies) (Figure 2.2). There are also two types of moraine-dammed lakes, supraglacial moraine-dammed lakes and pro-glacial moraine-dammed lakes (Figure 2.2).

Glacial lake outburst floods (GLOFs) are a direct result of the build up of large volumes of lake water behind moraine and ice dams. Due to the temporary and unstable nature of these natural ice and moraine dams, the lakes that form behind them have the potential to drain catastrophically causing large torrents of water downstream. The floodwater carries massive quantities of debris, and can travel many kilometres downstream at great speed and over several hours. The 1994 outburst from the Lugge Tsho, northern Bhutan caused river levels 200 km from the flood source to rise by about 2 m (Richardson & Reynolds, 2000b). Lake drainage can take place over a few days or can take only a few hours. The destructive force of these torrents has been well documented and several glacial lake outburst floods have resulted in widespread damage to housing, farmland and infrastructure; and they have caused the deaths of many humans and animals. Moreover, there are indications that GLOFs have become more frequent in the last few decades due to increased rates of glacier recession, which have been brought about by the amelioration of global climate (Lliboutry et al., 1977a; Yafeng & Jinwen, 1990; Clague & Evans, 2000; Reynolds, 1999; Richardson & Reynolds, 2000a; 2000b; Pearce, 2002). It is important therefore that the threat of GLOF be recognised and that those hazardous glacier lakes that have the potential to burst out are identified. The investigation of the processes by which large and potentially dangerous moraine- and ice-dammed lakes form, and accurate forecasting of lake growth rates are therefore required in order that predictive, and preferably preventative, measures can be implemented to protect people and infrastructure situated directly in the flood paths.

Outburst floods from glaciers have been reported from many locations world-wide. Much of the literature available has concentrated on floods which have occurred in Iceland, Canada, the North American Rockies, Alaska, the Nepalese, Chinese and Bhutanese Himalayas, Peru, India, Pakistan, Khazakhstan, the European Alps, Norway, Greenland, Russia and the Andes (Lliboutry, 1971; Eisbacher & Clague, 1984; Clague 1987; Costa & Schuster, 1988; Clague & Evans, 1992; 1994; Benn & Evans, 1998; Yamada, 1998; Richardson & Reynolds, 2000a; 2000b; Pearce, 2002).

2.5.1. Types of Glacial Lake Outburst Floods

Moraine and ice dammed lakes may form in subglacial, supraglacial and lateral/marginal positions. The type and impact of an outburst flood depends upon a number of factors: (1) the nature and integrity of the dam; (2) the structure and height of the dam; (3) the existence of weaknesses within the dam material; (4) the volume and temperature of water contained within a dammed lake; (5) the failure mechanism; (6) the position of the glacier(s) relative to the lake; (7) the type and gradient of the ice margin; (8) glacier mass balance; (9) the topography of the surrounding area; and (10) the volume of water discharged during a single outburst event. In some cases, moraine and ice dams may regain their integrity during or after an outburst flood event and the lake basin may refill, or in the case of complete drainage, another lake may form in its place (Clague, 1987). This can result in multiple outburst floods from the same source over the period of deglaciation in an area. Over time outburst floods originating from a single source tend to become less severe, especially in the case of moraine-dammed lakes where the volume of the stored lake water is determined by the height of the breach.

2.5.1.1. Terminology

The terminology used in the literature concerning glacier outburst floods is slightly confusing. Terms such as "*glacial lake outburst flood*" *(GLOF)*, "*jökulhlaup*" from the Icelandic meaning "glacier burst", "*débâcle*" from the French, and "*alluvióne*" in South America, have all been used to denote outbursts of floodwater from glaciers (Lliboutry, 1971; Eisbacher & Clague, 1984; Benn &

Evans, 1998). It is therefore important that a definition of the term GLOF be made in order that distinctions can be made between different types of glacier floods. For the purposes of this thesis the term GLOF will be used to refer solely to outburst floods from subaerial lakes which are controlled by glacier or moraine topography. This definition is important as it allows a separation to be made between the terms GLOF and jökulhlaup: lakes that burst out from subglacial positions.

2.5.2. Subaerial Lakes and GLOFs

The growth of large supraglacial lakes at the termini of many debris-covered glaciers has been reported from several locations around the world since the 1950s. In many cases the lakes are dammed by metastable lateral and terminal moraines, by dead ice melting at the glacier termini, or by a combination of the two. There has also been a similar increase in the growth and number of outbursts from subaerial lakes dammed by glacier ice and moraines which block off drainage from major and tributary valleys and other ice marginal areas.

Subaerial lakes can be identified both on the ground and in aerial and satellite photography. Potentially hazardous subaerial lakes are therefore much more easily recognised than subglacial lakes and their growth rates can be carefully studied and monitored. Furthermore, the processes by which ice and moraine dams fail can be observed and researched far more readily than outbursts from subglacial lakes. GLOFs also tend to be highly seasonal. In the European Alps around 95% of ice-dam failures occur during the ablation season, between June and September (Tufnell, 1984 in Costa & Schuster, 1988). Moraine-dammed lakes in Peru have a tendency to fail during the rainy season between October and April (Lliboutry et al., 1977a). In the Himalaya, 79% of outburst floods from moraine-dammed lakes occur in the period of maximum ablation during the Asian Monsoon season; between July and August (Yongjian & Jingshi, 1992; Xu & Feng, 1994). Outburst floods from glacier-dammed lakes in the Himalaya mainly occur between the end of August and the end of September when the storage capacity of lakes are at their maximum (Yongjian & Jingshi, 1992; Xu & Feng, 1994). Many floods are triggered in the evening or late at night (Xu &

Feng, 1994). The existence of these seasonal trends suggests that the occurrence of GLOFs can be correlated with increased volumes of meltwater and precipitation.

Given the relative ease of access for study and monitoring, mitigation and prevention of GLOFs from potentially dangerous subaerial lakes can be achieved far more readily than for subglacial lakes. Some of the techniques used in the draining of subaerial lakes and the implementation of warning systems in valleys threatened by dangerous subaerial lakes will be outlined in Section 2.5.4 of this literature review chapter.

2.5.2.1. Moraine-Dammed Supraglacial and Proglacial Lakes

The retreat of glaciers world-wide since the late neoglacial or "Little Ice Age" (Grove, 1988) has sometimes resulted in the build up of subaerial lakes behind steep-sided moraines. Moraine dams can be composed of a single moraine ridge or a series of ridges built up by several glacier advances and can range from a few tens of metres to over 100 m in height (Clague & Evans, 1994). Supraglacial and proglacial moraine-dammed lakes, although they occur less frequently than ice-dammed lakes (Clague, 1987), are arguably the most unstable due to the inherent instability of the moraine dams. It is this type of lake that is likely to form on the Ngozumpa Glacier (See Chapters 5 and 7). The instability and structure of moraine dams, together with the processes active on moraine slopes, will be examined more thoroughly in Section 2.6 of this chapter and in Chapter 6.

The trigger mechanisms for outbursts from supraglacial moraine-dammed lakes are numerous and the floodwaters resulting from these types of outbursts are heavily sediment-laden, which increases the amount of damage that can be inflicted downstream to settlements and infrastructure. Failure of a moraine dam most often results from overtopping and consequent notching of the moraine dam (Lliboutry et al., 1977a; Costa & Schuster, 1988; Clague & Evans, 1994, 2000; Hanisch et al., 1998; Richardson & Reynolds, 2000a; 2000b). Overtopping of moraine dams mainly occurs when large waves, termed *seiche* waves, are

propagated through a lake as a result of ice avalanching, large calving events, rock falls, debris slides or similar events into the up-glacier end of the lake. The waves are propagated through the lake at depth, and are typically over 10 m in height (Costa & Schuster, 1988). At the far end of the lake, seiche waves can overtop and exploit any weaknesses in the moraine dam, creating an outflow channel. Once a breach in the dam has been initiated, water will be rapidly evacuated from the lake. The initial breach will be excavated by mechanical erosion caused by the high discharge of out-flowing lake water until a peak flood discharge is attained. As an outflow channel through the moraine dam is continually incised by floodwater, the drainage of a moraine-dammed lake can continue until the lake has completely drained out. A moraine-dammed lake will normally develop and fail only once (Clague, 1987). In a few cases, however, a section of bedrock beneath the moraine is reached or the outlet channel becomes armoured by the development of a bouldery lag and the flooding will cease (Clague & Evans, 1992; 1994). In the case of these self-arresting moraine-dam failures the threat of multiple outburst floods from the same glacier should be recognised.

The low strength of moraine dams allows rapid drainage of a subaerial lake once an initial breach has been made and therefore peak flood discharges are likely to be higher for moraine dammed lakes than ice-dammed lakes (Costa & Schuster, 1988). Moraine dams are also susceptible to greater rates of failure than ice dams due to active paraglacial reworking of the moraine slopes, melting ice cores, earthquake activity, and high pore water concentrations in the moraine material. High pore water pressures within a moraine dam can also induce piping or seepage of water through the dam structure that will inevitably lead to the future failure and collapse of the moraine (Hanisch et al., 1998). Other triggers for outburst floods from moraine-dammed lakes include: the build up of pressure exerted by lake water on a moraine dam following an advance of the glacier tongue into the lake; heavy rainstorm events; rapid drainage of a glacial lake upglacier; or the generation of excessive meltwater during rapid glacier retreat (Costa & Schuster, 1988; Clague & Evans, 1994; 2000).

The longevity of moraine-dams is difficult to predict and some dams may remain in place for centuries after deposition. The presence of ice cores within moraine dams can add further complications to the prediction of failure rates. The melt-out of buried ice cores can destabilise a moraine dam, causing subsidence and lowering of the moraine and initiating slope failures (Richardson & Reynolds, 2000a; 2000b). Structures within the ice cores can also compromise the moraine stability by providing conduits that allow lake water to seep deep into the dam (Richardson & Reynolds, 2000a). The moraine dam at an un-named composite glacier flowing westward from the Nevado Hualcán, Peru, was lowering at a rate of c. 11 cm per month between 1985 and 1988 due to the melt-out of buried ice cores (Richardson & Reynolds, 2000a). The lowering of a moraine dam by melt-out of ice cores lowers the lake freeboard and leaves it more vulnerable to overtopping (Richardson & Reynolds, 2000a). Ice cores can melt out on decadal and centennial timescales depending on local climatic conditions (Costa & Schuster, 1988; Clague & Evans, 1994). However, if global temperatures continue to rise, this is likely to facilitate melting in the near future.

Local rates of paraglacial reworking and the occurrence of earthquakes also affect the longevity of moraine dams. As a general rule low, wide moraine dams are far more stable than high narrow moraine dams over-looked by steep rock slopes (Clague & Evans, 1994, 2000; Richardson & Reynolds, 2000b). Moraine dams that are composed of coarse blocky material can retain stability for longer periods irrespective of their morphology (Clague & Evans, 2000).

2.5.2.2. Moraine-Dammed Lakes in Marginal Subaerial Positions

Glacier ice and moraines also have the potential to block off drainage from nearby valleys, dry valleys and tributary valleys. This has happened in the Ngozumpa Valley and will be examined more closely in Chapter 6. The outburst mechanisms for moraine-dammed lateral lakes are the same as those described above for moraine-dammed supraglacial lakes (see section 2.5.2.1): overtopping and notching of the moraine dam, failure of the dam material, melt-out of buried ice cores, and piping or seepage of water through the dam. Marginal lakes dammed by lateral moraines also have the potential to burst out onto the surface

of a glacier if the altitude of the lake is higher than that of the glacier surface. Floodwater released by an outburst from a large marginal lake onto a glacier surface could conceivably cause further destabilisation of supraglacial lakes at or near to the glacier terminus and cause a secondary GLOF to occur of much greater magnitude.

2.5.3. Glacial Lake Outburst Floods in the Nepal Himalaya

Large supraglacial lakes have been forming on debris-covered Himalayan glaciers with surface gradients of $<2^{\circ}$ since the late 1950s (Reynolds, 2000). Table 2.2 (See page 44) gives details of some of the documented GLOFs that have occurred in the eastern Himalaya. The total number of glacial lake outburst floods that have occurred in the Nepal Himalaya is not known due to the inaccessibility of many of the mountainous regions. The GLOFs that are most widely known, and therefore the most intensively studied, are those that have occurred in populated areas and which therefore have had large impacts on the people living directly in the flood paths. Alongside the problems relating to the loss of life and the destruction of property and infrastructure, the threat of GLOFs also causes problems for water resource planners in the Himalaya. For instance, the development of hydro-electric power stations in Nepal could generate much needed revenue, but the threat of GLOFs pose many logistical and financial problems for any prospective developers of these water resources. The same is true for potential irrigation and industrial projects developed on Himalayan rivers.

The largest concentration of known outbursts from moraine-dammed lakes in the Himalaya has occurred in the area around Mt Everest (Yongjian & Jingshi, 1992), although many other areas are also affected. In early 2002, the UN Environment Programme named 44 lakes that are considered to be potentially dangerous throughout Nepal and Bhutan. This is a conservative estimate and there could be many more dangerous lakes that have not been identified. Among those lakes identified as dangerous in Nepal are the Tsho Rolpa at the terminus of the Trakarding Glacier in the Rolwaling Valley, the Imja Lake in the Imja Valley, and the Thulagi Glacier Lake in the Manaslu Himal. Zimmermann et al.

(1986) and Yamada & Sharma (1993) also predict future outburst floods in the Lobuche Khola Valley, the Gokyo Valley, the Hinku Valley, and the Hunku Valley. At present a glacial lake outburst flood in the Himalaya is expected to occur once every three years (Yamada & Sharma, 1993), by the year 2010 there is expected to be one GLOF every year (Reynolds, in Pearce, 2002). It is interesting to note that although the number of GLOFs occurring every year has been steadily increasing in the Nepal Himalaya, only the Tsho Rolpa Lake in the Rolwaling Valley, in the eastern Nepal Himalaya is presently undergoing a drainage programme.

2.5.4. Controlled Drainage of Potentially Hazardous Lakes

The draining of potentially hazardous subaerial lakes is an expensive business and the correct drainage procedures must be considered carefully for each specific site. As a first step a hazard impact assessment is required to determine the likelihood of failure from any ice- or moraine-dammed lake. Once the seriousness of the GLOF threat has been established a number of methods may be employed to mitigate the flood hazard. These include:

- Implementing early warning systems along valleys threatened by GLOF
- Pumping or siphoning of water from the lake
- Trenching across the surface of the dam
- Excavation of existing spillways
- Tunnelling through rock, moraine or ice
- The stabilisation of outlet streams through moraine-dams with paved revetments
- Increasing the lake freeboard of moraine-dammed lakes by building low earthen dams
- Construction of protective retention basins in valleys with low gradients to contain floodwater and sediment

(Lliboutry et al., 1977; Eisbacher, 1982; Eisbacher & Clague, 1984; Costa & Schuster, 1988; Clague & Evans, 1994; Richardson & Reynolds, 2000b).

The most effective way of dealing with the problem of GLOFs is to recognise the

potential threat before a large and unstable lake has fully developed. Early remediation, such as the excavation of spillway channels, is cheaper and more effective than siphoning of lake water and other engineering solutions, which if not executed with great care can trigger outburst floods.

2.6. Paraglacial Processes Initiated by Downwasting of the Glacier Surface

The study of moraines in the Himalaya is important to improving our understanding of rates and processes of paraglacial reworking. However, for several Himalayan glaciers, the rate of paraglacial reworking of the lateral and terminal moraines has further reaching consequences due to the threat of Glacial Lake Outburst Flood (GLOF). Progressive thinning of moraine dams by paraglacial reworking reduces the dam integrity and increases the likelihood of failure and the occurrence of a GLOF event. This applies to both supraglacial and lateral moraine-dammed lakes. Knowledge of the integrity of a moraine dam surrounding a potentially dangerous lake is fundamental to our understanding of why moraine dams fail and also the rate at which a dam will become destabilised.

2.6.1. Paraglacial Reworking of Moraines

Slope erosion and fluvial reworking of sediments are greatly increased during periods of glacier recession due to the abundance of loose morainic material and meltwater. Because of the glacial influence on these processes, they are defined as being *paraglacial*, a term first introduced by Ryder (1971) to describe the aggradation of alluvial fans in British Columbia. Church & Ryder (1972) later defined the term as "non-glacial processes that are directly conditioned by glaciation". The definition was extended to encompass a *paraglacial period*, which describes the time-scale over which paraglacial processes take place. The rates of paraglacial reworking of sediments and the length of the paraglacial period are dependent on a number of factors including: the basin shape and size, regional climate, catchment hydrology, availability of glacial deposits, rate of glacial recession, the presence of ice cores within the sediment accumulations, moraine slope aspect, vegetation succession rates, and tectonic activity (Johnson,

1971, 1984; Church & Ryder, 1972; Lliboutry et al., 1977a; Lewkowicz, 1987; Mattson & Gardner, 1991; Yamada & Sharma, 1993; Blair, 1994; Ballantyne, 1995; Ballantyne & Benn, 1996). In the Himalaya, the rates of paraglacial sediment reworking are high due to large glacier catchments with long steep slopes, large amounts of poorly consolidated moraine sediments, large volumes of meltwater from both glacier and snow melt, a monsoon climate, limited vegetation above 4,000 m, and ongoing tectonic uplift (Owen et al., 1998; Owen & Sharma, 1998). Although the rates of paraglacial reworking for the Himalaya are high, moraine deposits can still remain for millennia after deglaciation in suitable locations. Owen and Sharma (1998) suggested that the paraglacial period for the Garhwal Himalaya, in northern India, is around 100,000 years because of the lack of surviving moraines from before this period. It is conceivable that the paraglacial period in the Khumbu Himal could be similar, or perhaps greater than, the Garhwal Himal because of the well-developed u-shaped valley systems in the eastern Himalaya, which are more conducive to the preservation of glacial evidence over longer time periods (Owen et al., 1998). The oldest moraines that have been dated in the Khumbu at present are around 35 k a (Finkel et al., 2003).

2.6.2. Moraine Deposition at Downwasting Debris-Covered Glaciers

Debris-mantled glaciers are often flanked by extensive lateral and terminal moraines, the crests of which stand several tens of metres above the glacier surface along much of their length. These lateral and terminal moraines are complex in form and provide evidence for several episodes of moraine aggradation. The present day moraines of the debris-covered Khumbu and Lhotse Nup Glaciers, in the eastern Nepal Himalaya, were most probably built up periodically during the Chhukung Stage (either a Late Glacial or Holocene advance) and the Late Holocene (Little Ice Age) glacial stages (Richards et al., 2000).

The moraines of debris-covered glaciers in the Khumbu Himal are often of the Ghulkin type (Owen and Derbyshire, 1989; Owen, 1991; 1994), formed when rock debris from the glacier surface and from englacial debris bands sloughed off

the ice margins forming an extensive apron of lateral and terminal moraines (Small, 1983). The delivery of debris to the moraines is augmented by the ice velocity patterns in the terminus region of a glacier due to the tendency of valley glaciers to distribute debris towards the ice margins (Kirkbride, 1995).

Due to the nature of the depositional processes the moraines are composed of loose unconsolidated materials ranging from very fine silts and sands to large boulders over 4 m in length. In addition, large blocks of ice may be deposited during the moraine building periods and become buried by subsequent debris deposition. Snow layers too can be buried in the moraines; cementing material around them and creating the conditions for slopes with higher angles of repose (Johnson, 1971; 1984). The lateral moraines slope away from the glacier towards the valley walls forming "ablation valleys" or lateral morainic troughs at their foot (Owen & Derbyshire, 1989; Hewitt, 1989; 1993; Benn et al., 2003).

As debris-covered Himalayan glaciers begin to recede, meltwater exits the glacier surfaces over the lateral and terminal moraines and mobilises the loose, readily entrainable outer moraine material resulting in alluvial fan formation, debris flow and other sliding failures. As glacier downwasting continues and the glacier surfaces are lowered below the level of their moraines, the supply of meltwater to the outer moraine often becomes restricted to one or more spillway channels cut down through the lateral or terminal moraines near to the terminus of the glacier (Figure 2.3). At present, most outer moraine slopes of debris-mantled glaciers in the Himalaya are well vegetated and generally stable, although relict slope failure scars, terracing and fan features provide abundant evidence that these slopes were once highly active.

2.6.3. Paraglacial Reworking of Inner Moraine Slopes

Ice-distal slopes of moraines tend to adopt stable slope gradients during deposition. In contrast, ice-proximal moraine slopes are often over-steepened upon ice withdrawal and undergo rapid reworking. These ice-proximal slopes are long, steep and unvegetated as a result of the continued lowering of the glacier surface, and hence the base level of the slope toes. Slope instability is influenced

by slope gradient and length, the character of the material and slope foot conditions, and can be triggered by climatic and tectonic events. Many slope processes are active on the inner moraine slopes including sliding, rock fall, debris flow, gullying, debris avalanche, and wind erosion. As a result of these processes the inner moraine slopes are undergoing rapid parallel and vertical retreat.

2.6.3.1. Glacier Downwasting and Moraine Instability

Downwasting of the glacier surface encourages instability of the lateral moraines by steepening and undercutting the ice-proximal slopes (Johnson, 1984; Hochstein et al., 1995; Owen & Sharma, 1998; Kirkbride & Warren, 1999; Reynolds & Richardson, 2000). Work on the debris-mantled Tasman Glacier, New Zealand, by Blair (1994) established that dry moraine walls become unstable when the vertical relief between the glacier surface and the moraine crest exceeded 129 m ±10 m. The critical height decreases during periods of rain and snowmelt due to increases in pore water pressures within the moraine sediments. The removal of support at the base of the moraine slope causes debris avalanching and sliding failure of large blocks along shear zones within the moraine (Johnson, 1984; Cooke & Doornkamp, 1990; Richardson & Reynolds, 2000b). The fallen blocks can often modify the moraine in such a way as to produce several crests and the appearance of having being formed by several glaciations. Similar moraine structures were described by Johnson (1971) on the Donjek Glacier in Canada, and by Blair (1994) and Kirkbride & Warren (1999) on the Tasman Glacier, New Zealand.

2.6.3.2. Debris Flows

Small debris flows and mud flows are a common occurrence on inner moraine slopes. Ballantyne and Benn (1996) stated that debris flow is the main process responsible for hillslope reworking of glacial drift deposits in Fåbergstølsdalen, Norway. Mud and debris flow activity is increased during and after periods of heavy rainfall or snow melt. The presence of melt or rain water creates a rise in pore-water pressures in the drift slopes and gullies, lowering the strength of the slope material and causing flow-type failures to occur (Theakstone, 1982;

Johnson, 1984; Van Steijn et al., 1988; Cooke & Doornkamp, 1990; Blair, 1994; Owen, 1991; Mattson & Gardner, 1991; Owen & Sharma, 1998; Palacios et al., 1999). In the Himalaya, the sustained and intense rains during the monsoon season cause a rise in pore water pressures in the moraine sediments and initiate debris and mud flows on the inner moraine slopes (Owen & Sharma, 1998). Previous studies of hillslope debris flows suggest that debris flow initiation favours slopes with gradients greater than 28-30° (Innes, 1983; Ballantyne & Benn, 1996; Palacios et al., 1999). Debris and mud flow in gullies scours and removes any loose debris which has settled against the gully floor and walls, redistributing it over the lower slopes and producing gentler drift slopes below (Statham, 1976; Ballantyne & Benn, 1996; Van Steijn et al., 1988).

2.6.3.3. Ice Cores

During periods of negative mass balance on debris-covered glaciers, ice at the glacier margins can become covered by thick debris and incorporated within terminal moraines forming an ice core (Richardson & Reynolds, 2000b). Debris flow, mud flow, rotational sliding and other forms of mass movement on moraine slopes can also be initiated by the melt-out of buried ice cores (Johnson, 1971, 1984; Whalley, 1973; Mattson & Gardner, 1991; Ballantyne & Benn, 1996; Richardson & Reynolds, 2000a). Degradation landforms such as kettle holes are also formed by the melt-out of buried ice cores (Richardson & Reynolds, 2000a). Ice cores present within the moraines can act as a failure plane over which rapid sliding failures can occur. At the Boundary Glacier, Canada, during the summers of 1984 and 1985, 83% of all the sliding failures over ice cores which occurred were triggered after periods of heavy rainfall (Mattson & Gardner, 1991). This can be explained in two ways: firstly, the saturation of the overlying sediments can add to the mass of overburden material and on a slope this will increase the shear stress; and secondly, the presence of water at the ice core/moraine interface can reduce the shear resistance (Mattson & Gardner, 1991). The presence of ice cores is often marked by the appearance of tension cracks parallel to the moraine (Johnson, 1984). Once exposed at the surface a melting ice core will cause the direct input of water to the moraine slope increasing the adjacent pore water pressures and facilitating mudflow failure of the surrounding moraine sediments

(Johnson, 1971, 1984). Failure of slopes around an ice core may uncover further cores within a slope setting up a positive feedback cycle (Mattson & Gardner, 1991). Johnson (1984) reported that the melt-out of ice cores within the moraines of the Donjek Glacier, Yukon Territory, Canada, caused erosion rates of up to 1.5 m per week during the summer months. An ice-cored kame terrace in Adams Inlet, Alaska was measured as having a surface lowering rate of c. 0.25 m a^{-1} and backwasting rates between 1966 and 1983 were calculated to be 4.3 m a^{-1} (McKenzie & Goodwin, 1987). Melt-out above ice cores at the Thso Rolpa moraine dam, Nepal, caused maximum lowering rates of 22.3 m yr^{-1}, which was considerably higher than the average moraine lowering rate of 1.05 m yr^{-1} (Richardson & Reynolds, 2000a).

In addition to exposure by low magnitude slope failure events, ice cores can also be uncovered by the debuttressing of moraine slopes during a rapid calving retreat (Kirkbride & Warren, 1999), during large glacier flood events (Johnson & Power, 1985), and during earthquake activity. The stability of moraine slopes underlain by ice cores will only be achieved after the melt-out of all the cores present within those slopes.

2.6.3.4. Buried Snow Layers

The presence of buried snow layers within a moraine was reported to have a similar effect as buried ice cores on the Jampa Glacier, Mexico (Palacios et al., 1999). Snow layers within a moraine can be formed when slope failure overrides a layer of fallen snow and buries it at a depth where the snow layer is insulated and becomes dense and frozen in place. Frozen layers of snow within a moraine can form an impermeable layer, causing the saturation of overlying sediments during rain fall and snowmelt events. The saturated layer can then fail over the snow shear plane as a mud/debris flow or slump.

2.6.3.5. Gullying

Gullying causes the parallel retreat of the moraine edge. The threshold for the initiation of gullying on a slope is calculated to be between 30 and 35° (Ballantyne & Benn, 1996). Once formed, a gully becomes self-perpetuating,

channelling snowmelt and rainfall, which cause further excavation of the rill. Extensive gullying of lateral moraines may also result from the melting out of buried ice cores (Mattson & Gardner, 1991; Ballantyne & Benn, 1996).

2.6.3.6. Toppling Failure

The toppling of large boulders from the crests of the moraines is another process of moraine edge retreat. Rocks and boulders embedded within the moraine have also been observed to fall out of the moraine matrix that supports them. The toppling and falling of boulders from the moraine may trigger further rockfall events and slope failures, such as debris avalanching, on the lower moraine slopes (Blair, 1994). After periods of wet weather or snow melt, shrinkage of the fine supporting matrix during drying can also cause large blocks to fall out of the moraine (Blair, 1994).

2.6.3.7. Seismic Activity

Tectonic disturbances can trigger landsliding, debris flow and other mass movements in moraine deposits (Johnson, 1984; Hanisch et al., 1998) and can also expose ice cores buried within the moraine, leading to increased erosion rates subsequent to an earthquake event. During an earthquake at the Safuna Glacier, Peru, Lliboutry et al. (1977a) measured a lowering of the moraine crests by c. 1 m. The unpredictable nature of earthquake activity can cause rapid and unexpected failure of moraines damming large supraglacial lakes.

2.6.3.8. Vegetation

The presence of vegetation on a moraine slope has a stabilising effect because it increases the shear strength of the slope (Coppin & Richards, 1990). The plant roots bind together and strengthen the topsoil, whilst shoots and leaves protect the surface from rainsplash and aeolian erosion, which in turn helps to prevent rill erosion and gullying. A good vegetation cover will also act as an insulator protecting any buried snow layers or ice cores within the moraine (McKenzie & Goodwin, 1987). However, vegetation colonisation rates on Himalaya moraines and glacier forelands are low because of the extreme climate, the effects of altitude and the high rates of paraglacial slope reworking (Sharma, 1990). The

establishment of vegetation on bare moraine slopes or slopes that have been stripped of their vegetation cover can therefore take a long period of time.

2.7. Concluding Remarks

This chapter has discussed the literature on the downwasting of debris-covered glaciers: the effect of debris cover on rates of glacier ablation, the development of supraglacial ponds, the associated problems of glacier lake outburst floods, and the paraglacial reworking of moraines. The remainder of the thesis aims to build upon this current knowledge and will examine these processes in detail in relation to the downwasting of the debris-covered Ngozumpa Glacier in the Khumbu Himal, Nepal. The thesis focuses on the processes and rates of supraglacial pond evolution on the Ngozumpa Glacier and examines the mechanisms and probability of the formation of a large and potentially hazardous moraine-dammed lake at the glacier terminus. The thesis also investigates the mechanisms and rates of paraglacial reworking of the Ngozumpa moraines and evaluates the possibility of glacier lake outburst floods from the moraine-dammed lakes in the tributary valleys to the west of the glacier.

Table 2.2. Historical outburst floods in the Eastern Himalaya

Year	Lake Name and Location	Flood Volume/ Discharge	Cause of Failure	Damage Caused
450 yrs ago	Machhapuchare Lake (Seti Kola basin, Annapurna Region)	Lake area was approximately 10 km^2.	Ice-cored moraine dam collapse	Covered Pokhara in 50-60 m of debris
Aug 1935	Taraco Glacier Lake (Sun Kosi basin)		Ice-cored moraine dam collapse following seepage	Damage to fields, trails etc. Several livestock killed.
Sep 1964	Gelhaipco Lake (Arun basin)	23 million m^3 of water drained out of the lake	Glacier sliding into the lake caused moraine dam collapse	Damage to the highway and 12 trucks.
1964	Zhangzangbo Lake (Sun Kosi basin)	Water level in the river rose 8 m	Moraine collapse due to seepage	No real damage
1964	Longda Lake (Trisuli basin)	No data available		
1968	Ayaco Lake (Arun basin)			Roads and bridges etc. damaged
1969	Ayaco Lake (Arun basin)			Roads and bridges etc. damaged
1970	Ayaco Lake (Arun basin)			Roads and bridges etc. damaged
Sep 1977	Nare Lake, Nare Drangka Glacier on the southern slope of Ama Dablam (Dudh Kosi basin)	Lake volume was estimated to be around 500,000 m^3. The flood was recorded at Rabuwa Bazaar, 90 km downstream from the origin where discharges were 800 m^3/s. The peak discharge 8.6 km from the source was c. 1900 m^3/s, the total amount of water was about 5 million m^3. The flood lasted for 6 hours.	Collapse of a series of ice-cored moraine dams.	The ensuing flood triggered many landslides along the Dudh Kosi. Houses and a mini-hydro plant were destroyed. Two to three people were killed. All bridges were destroyed over a distance of 35 km downstream from the source.
1980	Phucan Lake (Arun basin)	River water levels rose 20 m.		Damage to forest, river bed etc.
July 1981	Zhangzangbo Glacier (Sun Kosi basin)	19 million m^3 of water drained out of the lake. The initial discharge was c. 16,000 m^3/s. This had slowed to 2400 m^3/s 50 km from the breach.	Piping of water through the dam followed by a moraine breach caused by a calving event	Destroyed the Arniko Highway, the friendship bridge, Sun Kosi hydro-power station, farm land etc.
Aug 1982	Jinco Lake (Arun basin)		Collapse of moraine dam due to glacier sliding into the lake.	1600 livestock killed, roads and bridges and 187,000 m^3 farmland damaged, and the houses of 8 villages washed away.
Aug 1985	Dig Tsho, Langmoche Glacier (Langmoche Khola, Bhote Kosi and Dudh Kosi)	In 5 hours approx. 5 million m^3 of water and 8.8 x 10^5 m^3 of moraine material was discharged through the breach. The peak discharge reached was 2350 m^3/s 7.1 km from lake. Average velocity in the reach 27 km from the source was 1375 m^3/s and the flood travelled a total distance of around 90 km. 3 million m^3 of sediment were eroded and deposited along the flood route. Flood duration was between 6-8 hours.	Ice avalanche (1-2 x 10^5 m^3) caused 4-6 m high wave to propagate, breaching the moraine dam.	Destroyed nearly completed Namche HEP station, 30 houses, 14 bridges, 3 humans and several livestock killed. Farm land and trails washed away, banks undercut, slope failure and destruction of forest. Around 3,000,000 m^3 of sediment was eroded and deposited in the valley downstream.
July 1991	Chubung Lake, Ripimo Shar Glacier (Tama Kosi basin)	Run out exceeded 10 km.	Moraine dam breached following an ice avalanche into the lake.	Destroyed houses, farm land, 3 flour mills and a bridge in the villages of Na and Beding. Several livestock and one person killed.
Oct 1994	Lugge Tsho, northern Bhutan	Floodwave reached a height of 2 m over 200 km from the source.	Failure of ice-cored moraine dam.	21-27 people killed at village of Punakha.
May 1995	Unknown source in the Kali Gandaki basin			

References: Zimmermann et al. (1986), Yamada and Sharma (1993), Xu & Feng (1994), Yamada (1998), Reynolds (1999, 2000), Pearce (1999;2002), Ageta et al. (2000), Richardson & Reynolds (2000b), Cenderelli & Wohl (2001).

Chapter 2 Figures

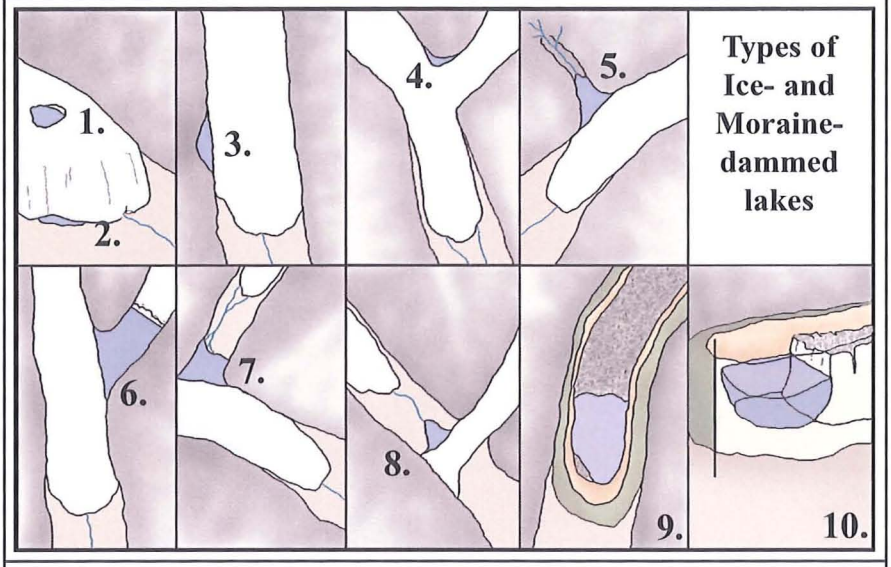

Figure 2.2. Types of ice- and moraine-dammed lake.

1. Supraglacial lake
2. Proglacial ice-dammed lake
3. Marginal ice-dammed lake
4. Converging ice stream dammed lake
5. Tributary stream-valley dammed lake
6. Interglacially ice-dammed lake
7. Tributary glacier-valley dammed lake
8. Lake dammed by a tributary glacier
9. Moraine-dammed supraglacial lake
10. Moraine-dammed proglacial lake

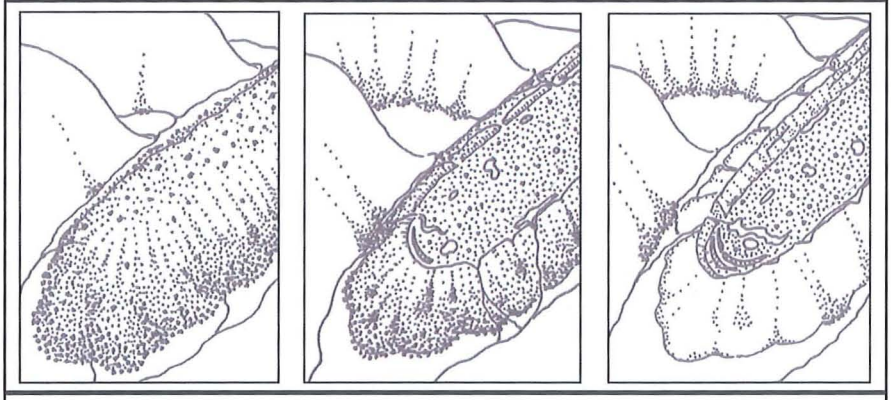

Figure 2.3. Formation of Ghulkin-type moraines

Chapter 3

Introduction to the Study Area and Methods

3.1. Introduction

This chapter introduces the study area on the Ngozumpa Glacier and describes the methods used. The chapter begins with an overview of glaciation in the Khumbu Region. This is followed by a description of the methods used in the research at the Ngozumpa Glacier. The chapter will then go on to describe the location and supraglacial environment of the Ngozumpa Glacier and examine the evolution of the glacier surface since the formation and abandonment of its Holocene lateral-terminal moraines.

3.2. Introduction to the Study Area

The Khumbu Himal in eastern Nepal is a high mountain region containing three of the world's highest peaks, Mount Everest (8848 m), Lhotse (8501 m) and Cho Oyu (8153 m). The Khumbu region forms the uppermost part of the watershed of the Dudh Kosi. The area is heavily glacierised and contains various types of glaciers, including small clean-ice valley and cirque glaciers, large debris-covered valley glaciers, reconstituted glaciers, hanging glaciers, niche glaciers, ice aprons and rock glaciers (Figures 3.1 and 3.2). Of the 664 glaciers listed in the glacier inventory of the Khumbu Himal region (Higuchi et al., 1978), only 47 are debris-covered (Fushimi et al., 1980). However, debris-covered glaciers occupy approximately 80% of the total glacierised area (Nakawo & Rana, 1999; Sakai et al., 2000b). The glaciers in the Khumbu Himal are predominantly fed by snow and ice avalanching from the steep valley headwalls (Figure 3.3) and most of the annual accumulation takes place during the summer monsoon (Ageta & Higuchi, 1984; Kayastha et al., 1999).

3.2.1. Geology

Since the collision of India and Asia c. 50 Ma, convergence of the plates has caused horizontal shortening, crustal thickening and regional metamorphism in the Himalaya and beneath southern Tibet (Searle et al., 2003). The High Himalayan slab is bounded by two major shear zones dipping north: the South Tibetan Detachment along the top and the Main Central Thrust along the base (Searle 1999a; Searle et al., 2003). These shear zones were simultaneously active around 22 – 16 Ma and are possibly still active today (Searle, 2003). The South Tibetan Detachment bounds the northern part of the High Himalayan wedge and consists of two major normal faults, the upper Qomolangma detachment and the lower Lhotse detachment. The Qomomlangma detachment separates sedimentary rocks above from greenschist-facies carbonates and shales below. The lower Lhotse detachment lies between Everest series greenschists on top and lower high-grade sillimanite-cordierite gneisses containing over 50% leucogranite sills and sheets. The leucogranites occur as 1 – 1500 m thick layer-parallel sills (which in the Everest region lie above the Greater Himalayan sequence below the South Tibetan detachment low-angle normal fault), or less frequently as cross-cutting dykes that intrude into the sillimanite grade gneisses (Searle, 1999b; Searle et al., 2003). The emplacement of the leucogranites occurred sometime during the Oligocene – early Miocene. They were formed by passive magmitic intrusion along fractures parallel to the country rocks and were later exhumed by uplift along the Khumbu Thrust, normal faulting along the top of the Lhotse Detachment slab coupled with thrusting along the Main Central Thrust, and by erosion (Searle, 1999a; 1999b).

The surface debris on the glaciers in the Khumbu mainly composed of two types of rock: weakly metamorphosed sedimentary rocks (Tibetan Formation) and granitic rocks (Himalayan Gneisses) (Zimmermann et al; 1986; Searle & Treloar, 1993; Sharma, 1990). The metamorphic rocks are a type of schistose material composed of black schist, hornfels and marble-like limestone, whilst the granitic rocks are typically granites (leucogranites with tourmaline, muscovite, biotite and garnet; adamellites with occasional sillimanite, andalusite and cordierite; migmatites; mica

schists containing garnets and tourmalines; and quartzites). There are also gneisses with pegmatites (Fushimi et al., 1980; Vuichard, 1984; Zimmermann et al; 1986; Sharma, 1990; Nakawo et al., 1999; Searle, 1999b; Searle et al., 2003).

3.2.2. Climate

The Khumbu Himal experiences four marked seasons. The spring, pre-monsoon period occurs between March and June and is typified by warm dry weather. The summer monsoon period between mid-June and mid-September brings heavy rain to the region, which falls as snow in the upper catchments above 5,500 m (Haffner, 1979; Zimmermann et al., 1986). Approximately 70-85% of the total annual precipitation occurs during the summer monsoon (Yamada, 1998; Ageta et al., 1980; Zimmermann et al., 1986; Cenderelli & Wohl, 2001). The post-monsoon season, between mid-September and the beginning of November is cooler and dry, although heavy snowfall events can occur. The winter season, between November and February, is cold with some heavy snowfalls that can occasionally last for 2-3 weeks (Brower, 1983; Zimmermann et al., 1986).

3.2.3. Glaciation of the Khumbu Himal

The number and age of glacial stages in the Khumbu Himal, and indeed across the Himalaya, are still incompletely known (Iwata, 1976, 1984; Benedict, 1976; Fushimi, 1977, 1978; Müller, 1980; Williams, 1983; Röthlisberger & Geyh, 1986; Hanisch et al., 1998; Owen et al., 1998; Richards et al., 2000). Optically stimulated luminescence dating in the Khumbu and Imja valleys (between 8 and 15 km east of the Ngozumpa Valley) have provided evidence of three stages of glacial advance (Richards et al., 2000). The earliest advance dated is the Periche Stage of c. 18-25 ka, which correlates with the last Glacial Maximum of the Laurentide and Eurasian Ice Sheets (Iwata, 1976; Fushimi, 1977; Richards et al., 2000). Equilibrium line altitudes during the Periche Stage were estimated at c. 200-300 m lower than present day altitudes (Richards et al., 2000). The second glacial advance stage, which culminated c. 10 ka, corresponds to either a Late Glacial or Holocene advance that Richards et al. (2000) termed the Chhukung stage. A smaller Late Holocene

advance, which pre-dates the Little Ice Age, was dated at c. 1-2 ka and is backed up by radiocarbon dates carried out by Müller (1980), Benedict (1976) and Fushimi (1978). Research conducted by Mayewski & Jeschke (1979) and Mayewski et al. (1980) showed that the glacial regime in the Himalaya has been dominantly one of retreat since AD 1850, with some glaciers experiencing minor re-advances or stand-stills during the periods AD 1870 to 1910 and 1920 to 1940. The advances and stand-stills appear to correlate with a strengthening of the monsoon between 1880 and 1920 (Mayewski et al., 1980).

3.2.4. Large and Potentially Hazardous Lake Formation

In recent decades, downwasting of many debris-covered glaciers in the Khumbu Himal, and other areas of the Himalaya, has resulted in the formation of numerous small and isolated supraglacial ponds. Given the right conditions, large and potentially unstable lakes can form at the termini of debris-covered glaciers, dammed by dead ice or lateral-terminal moraines. The transition from small isolated ponds into large moraine- or ice-dammed lakes can take place within two to three decades (Ageta et al., 2000; Benn et al., 2003). The formation of large moraine- and ice-dammed lakes has already occurred on many of the smaller debris-covered valley glaciers in the Khumbu Himal, and several GLOFs from these glaciers have been documented. Within the next two decades it is likely that many of the larger debris-covered valley glaciers will also develop large moraine- or ice-dammed lakes at their termini. However, not all large supraglacial lakes have the potential to flood out catastrophically. Indeed, many ice-dammed lakes in the Khumbu Himal appear to be relatively stable because thermal downcutting of over-spill channels allow drainage to occur slowly and safely. One such lake is the moraine- and ice-dammed Imja Tsho at the terminus of the Imja Glacier (Figure 3.4).

3.2.4.1. Moraine-Dammed Lakes and Ice Margin Classification

Moraine-dammed lakes are the most unstable type of glacial lake in the Khumbu Himal (See Chapter 2, Section 2.5.1). Moraine material is unconsolidated and subject to paraglacial reworking and retreat (see Chapter 6). Over time, progressive

thinning of a moraine dam increases the probability of failure and the possibility of a GLOF occurring. Failure of moraine dams can also be triggered by external factors such as tectonic activity or unusual weather events. The formation of large supraglacial moraine-dammed lakes on debris-covered glaciers is dependent upon the type of glacier margin.

Coupled Ice Margins

At coupled ice margins, where sediment is efficiently transported away from a glacier into the proglacial environment by powerful outwash streams, moraine development is limited (Benn et al., 2003). Where terminal moraines do form at a coupled ice margin, migratory meltwater streams at the glacier terminus rapidly destroy them (Benn et al., 2003). Drainage of meltwater from glaciers with coupled ice margins is unimpeded by moraines and very efficient, and thereby does not permit the development of moraine-dammed lakes. In the Khumbu Himal a typical example of a coupled ice margin is the Lhotse Glacier (Figure 3.5).

Decoupled Ice Margins

At debris-covered glaciers where the outwash discharge is insufficient to transfer sediment away from the glacier margin, repeated superposition of moraines results in the formation of large lateral-terminal moraines (Benn et al., 2003). This type of margin is said to be decoupled (Benn et al., 2003). During periods of negative mass balance, debris-covered glaciers with decoupled ice margins have a propensity to develop moraine-dammed lakes at their termini due to inefficient drainage of meltwater from the glacier surface. In the Khumbu Himal there are many debris-covered glaciers with decoupled ice margins that have developed, or have the potential to develop, large unstable moraine-dammed lakes at their termini (Figure 3.5). These include the Trakarding Glacier in the Rolwaling Valley, the Lhotse Nup Glacier in the Imja Valley, the Khumbu Glacier in the Khumbu Valley and the Ngozumpa Glacier in the Ngozumpa Valley. The Ngozumpa Glacier is therefore an ideal site to study the evolution of supraglacial ponds and the development of large and unstable moraine-dammed lakes.

3.3. Methods

The purpose of the research at the Ngozumpa was to quantify the rates of supraglacial pond growth and examine how different types of pond margin affect basin development. In addition, the processes and rates of paraglacial reworking were investigated to assess the stability of the Ngozumpa moraines. Moraine stability is important at the Ngozumpa Glacier because it is on the threshold of developing a large unstable moraine-dammed lake at its terminus. Furthermore, the western lateral moraine has dammed drainage from the western tributary valleys, resulting in the formation of five laterally-dammed lakes (see Figure 3.6), the largest of which have the potential to flood out following paraglacial retreat of the moraine.

The research at the Ngozumpa Glacier was conducted at selected case study sites on the glacier surface and its moraines between September 1999 and November 2001. The sites were carefully selected after observation of processes of pond evolution and paraglacial reworking of moraine slopes over much of the glacier ablation area. The research on the evolution of two perched pond basins and the growth of the Spillway Lake basin is a continuation of a previous study carried out by Benn et al. (2000; 2001) and Wiseman (2004) between October 1998 and October 1999. This has allowed monitoring of the processes and rates of pond development on the Ngozumpa over four years. It should be noted, however, that the author was present during the September – November 1999 field season and most of the photographic evidence presented in this thesis document the author's own observations of the period. Further information on pond development at the case study basins between October 2001 and October 2002, was kindly provided by Lindsey Nicholson who is currently working on the effect of debris on glacier ablation on the Ngozumpa and other glaciers.

3.3.1. Mapping Techniques

Mapping of the glacier surface and the moraines was carried out using stereoscopic pairs of 1:35,000 aerial photographs of the glacier surface in December 1984 (Swissair Photo & Surveys Ltd., photograph nos. 77, 98, 123 & 146). Further

mapping used a panchromatic SPOT image of the Ngozumpa Glacier (scene 227/294), taken on the 6th October 2000. The photographs and satellite image were used to map the following features on the glacier surface and the Ngozumpa moraines:

- The extent of the debris cover on the Ngozumpa.
- The morphology of the inner and outer lateral and terminal moraine slopes.
- Topographic features on the glacier surface.
- The distribution of ponds on the Ngozumpa Glacier surface and the terminus of the Gaunara Glacier.
- The Spillway Lake basin and the over-spill channel through the western lateral moraine.
- Supraglacial streams on the Ngozumpa surface and the terminus of the Gaunara Glacier.

3.3.2. Surveys

Surveys of perched pond basins, the Spillway Lake basin and the moraines of the Ngozumpa Glacier were carried out between October 1999 and October 2001 using a Leica TR1000 theodolite and Dior 3002S distomat. The accuracy of the measurements, to the nearest minute of arc, correspond to a percentage error of 0.001% or a horizontal accuracy of <0.03 m over the areas surveyed. The surveys were conducted from the western lateral moraine and the glacier surface using triangulation from measured baselines and also single survey stations using a reflector.

3.3.2.1. Triangulation from Measured Baselines

In order to conduct this type of survey, two survey points were established and the distance between the points was measured using a reflector and distomat (labelled X in Figure 3.7). A series of numbered survey points were then established on a rough sketch of the feature to be mapped. These points were then surveyed from both of the survey stations. In order to do this, the theodolite was zeroed on a known point,

such as a mountain peak, which enabled the angles between the peak and the selected survey points and survey stations to be determined as follows (Figure 3.7):

$a = a1 - a2$
$b = (360 - b1) + b2$

Having established angles a and b, angle c can also be determined. From this, the distances A and B were then calculated using the sine rule:

$X/\sin c = A/\sin a = B/\sin b$

Once all of the angles and lengths of the triangle had been calculated, trigonometry was employed to calculate the x and y co-ordinates of the survey point relative to Survey Station 1 (Figure 3.7):

$x = (\cos a)B$
$y = (\sin a)B$

After all of the points in a survey were converted into the x and y co-ordinate system, they were plotted as a graph using the program CA Cricket Graph III and converted into map form using Adobe Illustrator 6.0. and Adobe Photoshop 5.5.

By using the azimuth of the point to calculate the angle d, the height (Z) of any given survey point relative to the survey station could also be obtained as follows (Figure 3.7):

$Z = (\tan d)B$

3.3.2.2. Single Station Surveys

Single Station surveying is a much faster way of mapping a feature and does not require the use of a sketch showing the position of the points to be surveyed. Two

types of single station surveys were employed: reflector surveys and reflectorless surveys.

Reflector Surveys

The reflector surveys were conducted using a theodolite, distomat and reflector. The theodolite was zeroed to a known point, in the same way as the triangulation surveys. The survey points were then determined by placing a reflector at various points around the feature to be mapped. At each survey point the angle, azimuth and distance between the point and the survey station were measured. These measurements were then used to calculate the x and y co-ordinates of the points as follows (Figures 3.8 and 3.9):

$A = (\cos d) D$

$x = (\cos a) A$

$y = (\sin a) A$

Following the conversion of the measured points into x and y co-ordinates, mapping was carried out in the same way as outlined in Section 3.3.2.1 above. The height (Z) of a measured point relative to the survey station was calculated as follows (Figure 3.8):

$Z = (\sin d) D$

Reflectorless Surveys

Reflectorless surveys were the quickest method of mapping the perimeters of ponds. First of all, a series of points around a pond perimeter were measured using the reflector survey method described above in order to ascertain the height (Z) of a pond relative to the survey station. This was followed by measuring the azimuths and angles (relative to the zero point of the theodolite) of various points around a pond perimeter. Given that a pond surface is a horizontal plane, the distance A was

calculated for each reflectorless point using the value of Z determined for the reflector points (Figure 3.10).

$A = Z/\tan d$

The x and y co-ordinates of the points could then be calculated in the same way as for the reflector surveys (also see Figure 3.9).

3.3.3. Temperature and Bathymetry Measurements

Where pond surfaces were unfrozen, measurement of pond temperature and bathymetry were made from a small boat. Where a thick layer of ice covered a pond surface, holes were cut in the ice in order to carry out the measurements. Pond bathymetry measurements were made using a plumb line graduated at 1m intervals. Pond temperature was measured at 1m intervals using a thermistor attached to a graduated 30 m cable.

3.3.4. Moraine Retreat Rates

The rate of moraine edge retreat between October 1999 and October 2001 was calculated by annual measurement of the distance between the moraine edge and ten marked boulders using a tape measure. Repeated surveys of landslipped blocks were carried out using triangulation from measured baselines and single station reflector surveys. A reflector survey was also used to produce a transect of the moraine. Slope profiles on the moraine were measured using an Abney level, Suunto compass and tape measure.

3.4. The Supraglacial Environment of the Ngozumpa Glacier

Observations made between September 1999 and November 2001 have provided an understanding of the supraglacial environment at the Ngozumpa glacier and provide a context for the detailed case studies. The following section describes the

supraglacial environment of the glacier and examines the evolution of the glacier surface between 1984 and 2000.

The Ngozumpa Glacier is a debris-covered valley glacier in the upper Dudh Kosi catchment of the Khumbu Himal region, Nepal (Figure 3.6). The Ngozumpa is the longest glacier in Nepal and extends approximately 25 km southwards from the headwalls of Cho Oyu (8153 m) and Gyachung Kang (7992 m). The tributary Kyajumba Glacier enters the main Ngozumpa Glacier stream from the northwest at around 5000 m. A second tributary, the Gaunara Glacier, once entered the main ice stream from the east, around 8 km upglacier from the terminus, but is no longer dynamically connected to the Ngozumpa Glacier (Figure 3.11).

A layer of debris, of varying thickness, mantles the surface of the Ngozumpa Glacier. The debris cover is almost continuous and extends from the base of the avalanche cones and snowfields in the headwalls down to the glacier terminus (Figure 3.12). Several small clean ice streams, supplied by material from the snowfields at the base of Gyachung Kang (7992 m) and Cho Oyu (8153 m), break up the debris cover in the upper reaches of the glacier and taper out c. 5km from the glacier headwalls (Figure 3.13). The extent and continuity of the debris cover suggest that the equilibrium line for the Ngozumpa Glacier lies at around 5300 m, the same altitude as the avalanche cones in the upper catchments. The presence of a thick debris layer has inhibited the melting of the Ngozumpa surface, allowing the glacier to extend down to 4700 m, a much lower altitude than the smaller clean ice glaciers present in the region that terminate above c. 5500 m.

The debris cover in the glacier ablation area is only broken in places where supraglacial ponds have formed, ice faces have been exposed, or cracks have opened up on the glacier surface (Figure 3.12).

3.4.1. Description of the Ngozumpa Moraines

The Ngozumpa Glacier is encompassed by large multi-crested Ghulkin-type moraines (see Chapter 2, section 2.6.2). The moraines extend from the headwalls of the glacier down to and around the glacier terminus. Due to downwasting of the glacier surface, the moraine crests have been abandoned and, at present, they stand between c. 20 m and 120 m above the glacier surface. The exact timing of moraine formation and abandonment at the Ngozumpa is not known. However, by analogy with other glaciers in the Khumbu region (Iwata, 1976, 1984; Benedict, 1976; Fushimi, 1977, 1978; Müller, 1980; Röthlisbeger & Geyh, 1986; Williams, 1983; Aoki & Asahi, 1998; Owen et al., 1998; Richards et al., 2000), it is probable that deposition began during the Chhukung Stage (c. 10 ka). The innermost moraine units were probably abandoned at the onset of glacier thinning following the Little Ice Age maximum.

The outer moraine slopes are well vegetated and are reasonably stable at present, although the morphology of these slopes suggested that in the past they were highly unstable and underwent considerable paraglacial and fluvial reworking. The stabilisation and vegetation of the outer moraine slopes is likely to have occurred only after the abandonment of the moraine crests. The inner moraine slopes around the glacier terminus have a thin vegetation cover and are moderately stable, although there is localised evidence of recent slope failures. From a distance of around 1 km from the terminus the inner moraine slopes are steep and unvegetated and are undergoing rapid retreat by paraglacial reworking. Slope instability of the inner moraines is perpetuated by the continuous downwasting of the glacier surface. The slopes generally take the form of a free face and talus slope, although the general slope profile is frequently modified by the landslipping of detached blocks of moraine.

The western lateral moraine at the Ngozumpa dams back drainage from a series of tributary valleys causing the formation of five lateral moraine-dammed lakes (Figures 3.6 and 3.14). The size and volume of the lakes relate to the characteristics

of the basins in which they are situated: with the larger, glacierised basins favouring the development of larger lakes. The laterally-dammed Gyajumba Tsho lake that formed in the northern-most of the western tributary valleys drained out through the moraine onto the glacier surface sometime during 1998 (Wiseman, 2004), leaving behind a series of smaller ponds, colloquially referred to as the 'Sixth Lakes' (Figures 3.6 and 3.15).

3.4.2. Formation of the Debris Mantle

The main source of moraine material on the glacier surface is debris brought down by snow and ice avalanching from the steep slopes of Cho Oyu (8153 m) and Gyachung Kang (7922 m) (Figure 3.6). Other sources of debris include frost shattering and rock fall from steep rock slopes that overlook the glacier surface, and also debris from paraglacial reworking of the inner moraine slopes. Debris from avalanching and frost shattering on the headwalls is incorporated into the glacier as avalanched snow is turned into firn and eventually into glacier ice, thus forming stratified bands of debris within the ice. Most of the debris is passively transported in supraglacial and englacial pathways with some active transport of material by meltwater processes. Debris can also be transferred from supraglacial to englacial transport by falling into crevasses or moulins and through fluvial reworking of the debris layer. Crevasse-fills can form discordant debris bands within the ice. As the glacier flows down-valley, the bands of debris are rotated and are eventually melted out in the glacier ablation zone by downwasting of the glacier surface. As downwasting proceeds the debris mantle is thickened up from the base. The greatest debris thicknesses are found towards the glacier terminus as a result of cumulative melt-out of debris from the ice (see Chapter 6, section 6.3.1).

3.4.3. Glacier Surface Evolution

By insulating the glacier ice from solar radiation and other energy sources, the debris cover has influenced the morphology and development of topography on the Ngozumpa surface. Varying thicknesses of surface debris have resulted in uneven downwasting of the glacier surface, bringing about a hummocky relief across the

entire debris-covered area (Figure 3.16). Large ice-cored debris mounds and ridges, of up to c. 50 m in height, are separated by topographic lows and supraglacial ponds. The surface debris layer is very dynamic and is constantly reworked by downwasting, backwasting and slope processes.

Once ice-cored debris mounds and ridges reach a critical height and steepness, slope processes rework the protective debris cover down-slope exposing clean ice surfaces (see Chapter 2, section 2.3.3). Direct ablation of these exposed ice faces causes rapid backwasting and disintegration of the ice-core within the debris-mound or ridge. Over long periods of time, the glacier surface will undergo several grand topographic reversals whereby large ice-cored hummocks gradually become topographic low points and topographic low areas develop into ice-cored debris mounds as the glacier downwastes towards the bed (see Chapter 2, Section 2.3.3).

The rate of ablation of the glacier surface is increased in areas where ice is exposed and where small supraglacial ponds have formed on the glacier surface. Where the debris cover is broken, meltwater is produced and often collects to form small ponds in the surface topographic hollows. Once formed, small supraglacial ponds expand rapidly and contribute substantially to the downwasting of the glacier surface (see Chapter 4). As glacier downwasting proceeds, the overall surface gradient lowering and backwasting of ice faces increases the number of lakes present on the surface of the Ngozumpa, encouraging faster downwasting rates in a positive feedback cycle (see Chapter 6, section 6.3.1).

Wiseman (2004) investigated the present surface gradients of the Ngozumpa and found that between the altitudes of 4680 m and 5040 m (from the glacier terminus to the point where the Kyajumba Glacier feeds into the main glacier) the average surface gradient was 2.04°. The glacier surface gradient on the Kyajumba Glacier between 5000 m and 5160 m was 2.37°, and on the main Ngozumpa stream between 5000 m and 5160 m it was 3.01°.

3.4.4. Meltwater Drainage

The presence of the lateral-terminal moraine, the crests of which now stand several tens of metres above the glacier surface, influences the drainage of meltwater from the Ngozumpa Glacier and has encouraged ponding on the glacier surface (see section 3.4.5). Drainage of meltwater from the glacier surface has been mainly restricted to an over-spill channel cut down through the western lateral moraine c. 1 km from the glacier terminus (see Chapters 5 and 6). A second smaller spillway channels meltwater off the glacier surface through the southeastern terminal moraine. Meltwater draining from the Ngozumpa Glacier feeds directly into the Dudh Kosi River and southwards into the Arun Kosi River.

Most of the meltwater on the Ngozumpa glacier is transported englacially and is channelled into the large Spillway Lake basin and out through the over-spill channel in the western lateral moraine (Figure 3.14). The height of the over-spill channel therefore exerts a control on the drainage of meltwater from the glacier and marks the base-level for englacial drainage. At present, this over-spill channel is relatively stable and is armoured by large boulders. There is little evidence of rapid down-cutting of the channel.

The englacial conduit network of the Ngozumpa Glacier is thought to be extensive and there is abundant evidence for shallow englacial drainage. Backwasting of ice faces frequently exposes englacial conduits at the glacier surface (Figure 3.17). These conduits have often developed along planes of structural weakness within the ice, such as debris bands and crevasse traces. Meltwater exploits these planes of weakness in the ice and enlarges them by thermal erosion. Eventually, englacial conduits are formed and continue to enlarge by thermal and mechanical erosion, caused by the passage of relatively warm meltwater. It is believed that larger conduits may persist throughout the year because the rate of creep closure of englacial conduits and karst features near the glacier surface is very low. Many of the englacial conduits that were observed during the field seasons were dry and not channelling meltwater. This suggests that some conduits are seasonal, only operating

when meltwater inputs are at their highest level during the summer monsoon period. Englacial conduits can provide inputs of meltwater into perched supraglacial pond basins and can also cause partial or complete drainage of pond water (Figure 3.18) (see Chapter 4, Section 4.4).

Surface meltwater streams, although not uncommon on the Ngozumpa, exist only over short distances and surface water is usually channelled into the englacial conduit network via moulins or sinkholes at the glacier surface. The largest known supraglacial meltwater stream flows onto the Ngozumpa surface down the eastern lateral moraine from the terminus of the Gaunara Glacier. The meltwater stream cascades down the moraine onto the surface of the Ngozumpa and into a large moulin surrounded by many ice faces (Figure 3.19). After it enters the englacial drainage network it is unclear where the meltwater is channelled but it is almost certain to flow downglacier into the Spillway Lake and out through the spillway channel in the western lateral moraine. Evidence for surface flow along the eastern lateral moraine may be related to the existence of the Gaunara meltwater stream. At times of particularly high flow, or at the beginning of the meltwater season when the englacial drainage system is not fully developed, meltwater from the Gaunara could be channelled along the inner eastern moraine/glacier margin. The glacier surface along the eastern moraine margin shows evidence of elongated ponds, some of which have drained out, and small surface streams that follow the base of the moraines. Much of this surface meltwater apparently enters the eastern end of the Spillway Lake.

3.4.5. Ponding of Meltwater on the Glacier Surface

Small supraglacial ponds are present on the Ngozumpa surface up to an altitude of c. 5120 m. Ponding on the Ngozumpa has been encouraged by the negative mass balance of the glacier, the low surface gradient, the low ice velocities in the ablation zone, the development of an undulating glacier surface topography and the inhibition

of drainage from the glacier surface by the formation of the extensive Ghulkin-type moraines.

Supraglacial ponds are formed where ice faces are exposed by sliding and slumping of debris from the steepening slopes of ice-cored debris mounds (Figure 3.20). The impermeable nature of the underlying glacier ice allows the meltwater generated from the rapid backwasting of exposed ice faces to collect and pool in the topographic hollows at the base of the ice faces. Unless the exposed ice becomes covered over again, by debris sliding and slumping from above, the ice face will gradually steepen up over time. As the ice face steepens, debris will begin to slide away from the edges and the top of the face, lengthening and enlarging the exposure. This will lead to an increase in meltwater production and an enlargement and deepening of the pond. The mechanisms and rates of growth of perched supraglacial ponds are examined in detail in Chapter 4.

Perched pond basins on the surface of the Ngozumpa contribute substantially to the downwasting rate of the glacier surface. Downwasting of the glacier surface produces lower surface slope gradients and causes an increase in the number of perched supraglacial ponds present on the glacier surface. Higher incidences of supraglacial ponds result in a greater rate of surface downwasting, thereby further reducing the glacier surface slope gradient and allowing the inception of still higher numbers of ponds in a positive feedback cycle.

3.4.6. Pond Drainage

Perched supraglacial ponds on the Ngozumpa Glacier are ephemeral features. This is evidenced by the presence of large empty basins and raised deltas on the surface of the Ngozumpa Glacier (Figure 3.21). Comparison of the glacier surface using satellite imagery, aerial photographs and old picture postcard photographs provides further evidence of the appearance and disappearance of perched ponds over time. There is also evidence that several of the larger pond basins have undergone cycles

of drainage and re-flooding. Pond drainage on the Ngozumpa was found to occur all over the ablation zone from the glacier terminus up to, and possibly beyond, the confluence of the Ngozumpa with the Kyajumba Glacier.

Pond drainage predominantly occurs when backwasting of an exposed ice face, or melting of the pond floor, causes a connection to be made with an englacial conduit below the water-line. This results in the complete or partial drainage of the pond water from a basin. In this way connection with the extensive englacial network provides a check on rapid pond basin enlargement.

In some cases the drainage of a pond can be interrupted. On the 3rd of October 2001 a large pond on the eastern side of the glacier (Pond 7192) was discovered to be draining out through a large key-hole shaped conduit in the southern pond ice margin (Figure 3.22). The ice faces around the pond margin had a series of 13 consecutive thermo-erosional notches carved into them, each marking a progressive lowering of the pond level (Figure 3.23). Similar stepped pond level lowering was displayed in drapes of mud in areas immediately adjacent to the draining pond and also along the eastern lateral moraine, providing evidence that the pond had been considerably larger in area and volume before drainage began (Figure 3.23). The spacing between each of the thermo-erosional notches, after the initial two, was fairly uniform and it was therefore postulated that each notch represented a diurnal pond level. Larger gaps between the 1st, 2nd and 3rd notches provided evidence of initial rapid drainage followed by a much slower drainage over the following days. The large overhang formed by the series of thermo-erosional notches destabilised the western ice face causing two full-height calving events to occur (Figures 3.24 and 3.25). The older of the two failures occurred at the around the same time as the formation of the 2nd thermo-erosional notch and it is believed that icebergs from this calving event caused a blockage to occur in the conduit draining the pond. The choking of the conduit with floating ice debris consequently lowered the rate of pond drainage. Floating icebergs (~ 10^0 – 10^1 m^3 in volume) produced by a more recent calving event from the western ice face, were being rotated anti-clockwise

and carried into the conduit by a slow current set up in the pond, showing that some drainage was still occurring at the site (Figure 3.25). Several larger icebergs (up to ~ 10^2 m^3 in volume) remained grounded and melted out *in situ* in the relatively shallow pond.

Pond 7192 was revisited on the 19th of October 2001. Over the intervening 16 days, 50 cm of pond surface lowering had occurred. The appearance of two new thermo-erosional notches suggested that this lowering had happened in two stages: a 20 cm lowering followed by a further 30 cm. Part of the conduit roof that overhung the large thermo-erosional notch had calved into the pond, most probably due to the propagation of a stress-release fracture (Figure 3.26). Several icebergs remained grounded in front of the conduit entrance. The initial decrease in the rate of drainage of Pond 7192 was undoubtedly caused by blockage of the conduit by floating icebergs. However, this decrease in drainage rate is likely to have been augmented by a drop in pond temperatures caused by the *in situ* melting of grounded icebergs in the pond, nocturnal freezing of the pond surface, and the gradual shutting down of the englacial conduit network brought about by the onset of winter. Lindsey Nicholson visited the site again in October 2002 and reported that no further drainage of the pond was discernible. It can therefore be deduced that the production of icebergs by large calving failures during the drainage of perched supraglacial ponds can hinder or even stop the drainage of perched supraglacial ponds. The type of drainage witnessed at Pond 7192 is not considered to be atypical of perched supraglacial ponds on the Ngozumpa Glacier because sudden drainage of ponds can often trigger calving failure along structural weaknesses and above thermo-erosional notches at exposed ice faces around the pond margins.

3.4.7. Temporary Storage

Meltwater from draining pond basins is channelled downglacier and eventually enters the Spillway Lake basin before draining off the glacier surface through the over-spill channel in the western lateral moraine. However, many perched supraglacial ponds on the Ngozumpa receive inputs of water from englacial conduits

exposed in ice faces around the upglacier perimeter of the basin. It is therefore suggested that meltwater can be transferred between several pond basins before finally reaching the Spillway Lake and leaving the glacier surface. This process has been termed temporary storage.

3.5. Perched Supraglacial Pond Development Between 1984-2000

Figure 3.27 shows the change in the number of supraglacial ponds present on the glacier surface in 1984 and 2000. The 1984 map was drawn from aerial photographs of the lower Ngozumpa and the 2000 map from a SPOT image taken in October 2000. The overall shape and length of the glacier has remained unchanged since 1984 demonstrating the effective insulative properties of the continuous debris cover and the low ice flow velocities.

The most striking change that has occurred between 1984 and 2000 is the number of perched supraglacial lakes and exposed ice faces present on the Ngozumpa surface. The number of ponds present on the glacier surface increased from c. 48 in 1984 to c. 145 in 2000. These figures are a minimum estimate because many of the smallest ponds present on the glacier surface would not have been visible on the aerial photographs and satellite images, the total number of ponds therefore could potentially be much higher. The area that has experienced the most supraglacial lake development since 1984 is the section of glacier that lies between the Guanara Glacier (c. 8 km from the terminus) and the Dudh Pokhari (c. 3 km from the terminus) (Figures 3.6 and 3.27). In 1984, this area contained many topographic high points. Since 1984, the surface debris on the slopes of these large ice-cored debris mounds and ridges have evidently undergone much reworking by sliding and slumping as downwasting of the glacier surface occurred, causing new ice faces to become exposed and an overall lowering of the glacier surface gradient. The exposure of ice faces in this area has led to the inception of supraglacial ponding followed by extensive and rapid pond enlargement processes (see Chapter 4). The area of individual supraglacial ponds has not changed greatly between 1984 and 2000: this is due to complete or partial drainage of ponds that come in contact with

englacial conduits below the water-line (see Chapter 4). As supraglacial ponds expand, the likelihood of coming into contact with the englacial drainage network is increased. The extent of glacier karst and the englacial conduit network thereby exert a control over the maximum surface area attained by the perched supraglacial ponds. The only exception to this is at the glacier terminus where the Spillway Lake has formed.

3.6. Development of the Spillway Lake Basin Between 1984-2000

The development of the Spillway Lake has not followed the same patterns of development as the other supraglacial ponds on the Ngozumpa. This is due to the fact that the Spillway Lake is not perched but is continually supplied by meltwater from upglacier that subsequently drains out through an over-spill channel cut down through the western lateral moraine (see Chapter 5). The level of the Spillway Lake is regulated by the height of the over-spill channel and effectively controls the drainage of meltwater from upglacier. The rate of growth of the Spillway Lake has been extremely rapid. In 1984 the Spillway Lake did not exist in its present form (Figure 3.27). Surface drainage of meltwater from the glacier surface was via two supraglacial streams that exited the moraines through channels in both the western and eastern terminal moraine. By October 1998 a large lake had formed, extending almost the entire width of the glacier, and had captured almost all of the meltwater drainage from upglacier, directing it out through the over-spill channel in the western lateral moraine (Figure 3.27). The eastern moraine over-spill channel is still in existence to date but surface drainage via this channel has evidently been reduced since 1984. The rapid appearance and growth of the Spillway Lake is a major concern as it is a perfect candidate for development into a large and potentially hazardous moraine-dammed lake. A GLOF from a large lake on the Ngozumpa would feed directly into the Dudh Kosi River and could potentially endanger the lives of hundreds of residents and visitors to the Sagarmatha National Park downstream from the village of Jorsale, some 16 km from the glacier terminus. The growth of the Spillway basin will be examined in greater detail in Chapter 5.

Chapter 3 Figures

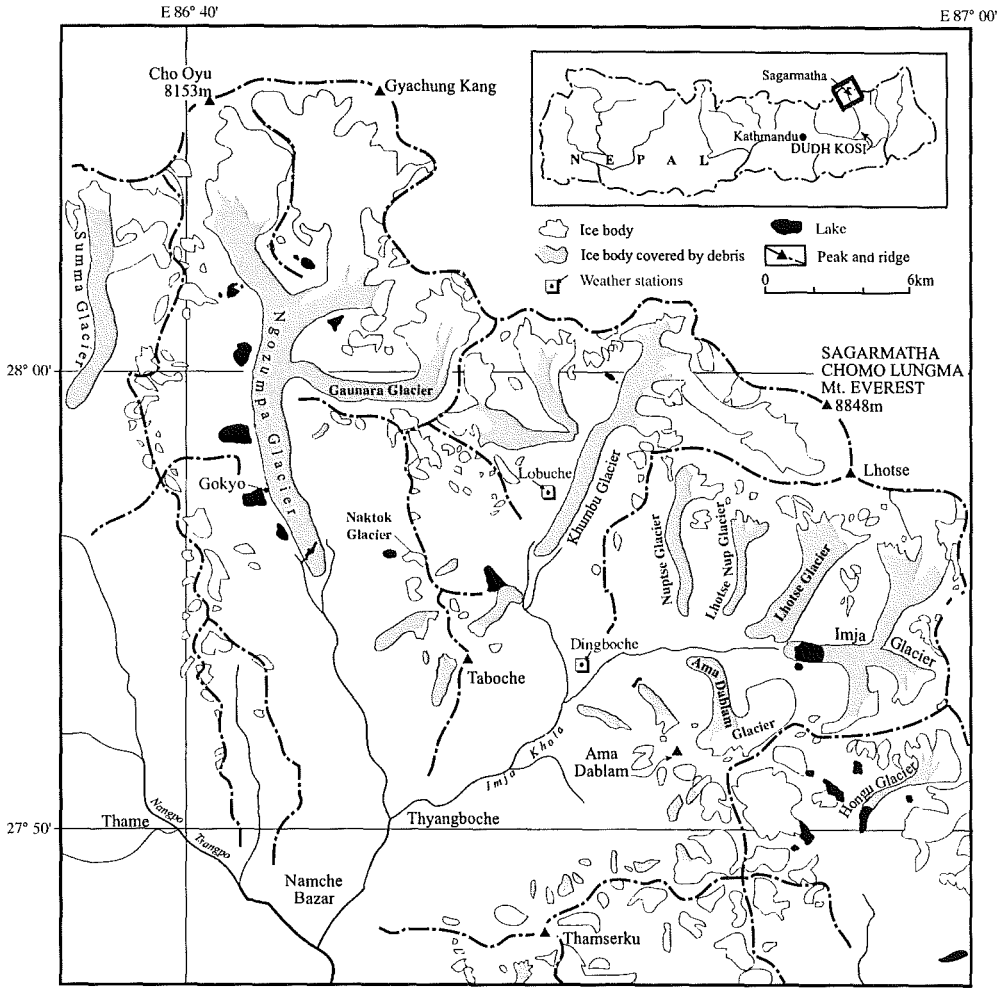

Figure 3.1. Map showing the glaciers of the Khumbu Region. Adapted from Higuchi et al. (1980).

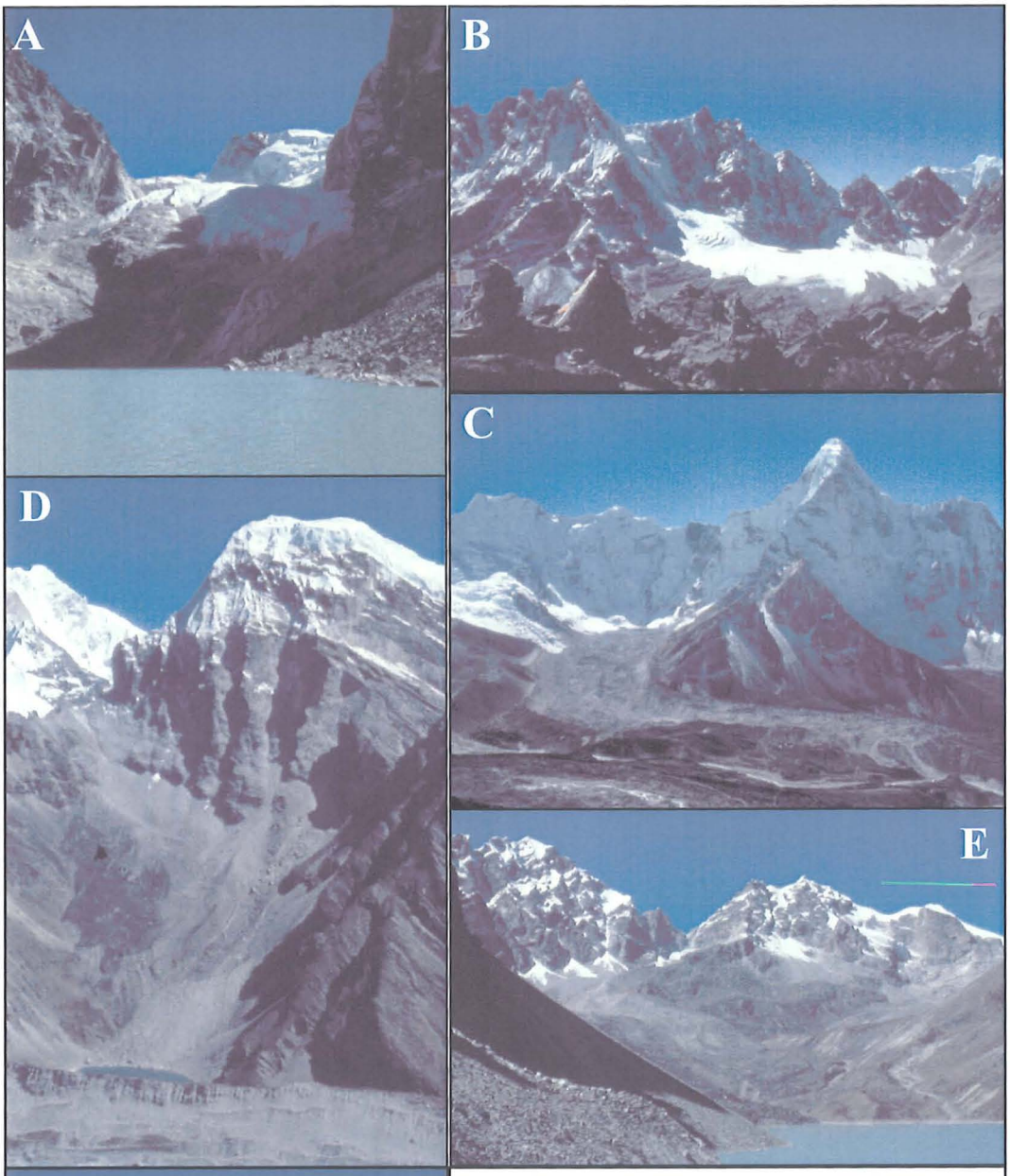

Figure 3.2. Different types of glaciers in the Khumbu Himal.

A. The clean-ice Naktok Glacier, Naktok Valley.
B. An un-named clean ice glacier, Ngozumpa Valley.
C. The debris-covered Ama Dablam Glacier, Imja Valley.
D. A small rock glacier, Ngozumpa Valley.
E. Three rock glaciers near Thonak Tsho, Ngozumpa Valley.
F. A hanging glacier, Naktok Valley.

Figure 3.3. Avalanche debris is the main source of moraine material on the Ngozumpa Glacier.

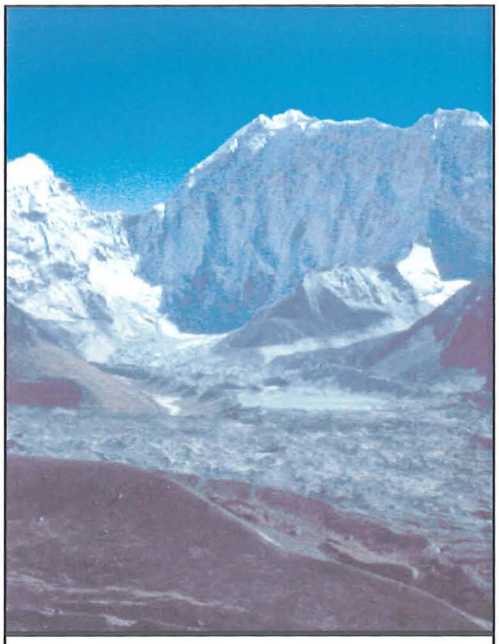

Figure 3.4. The moraine- and ice-dammed Imja Tsho on the Imja Glacier. At present the lake is relatively stable and draining out slowly and safely.

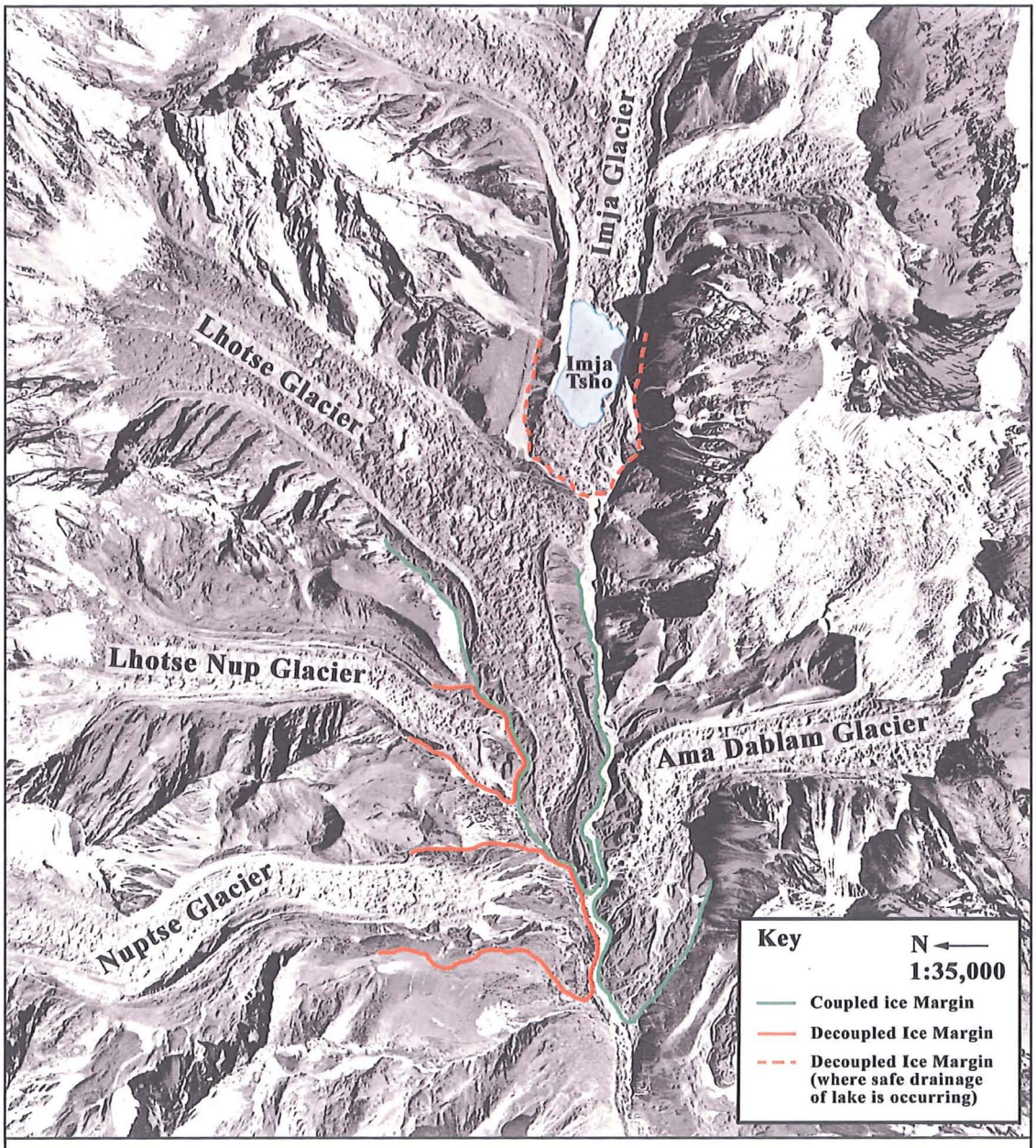

Figure 3.5. Aerial photograph of the Imja Valley, Khumbu Himal, showing coupled and decoupled ice margins. (Photograph copyright of the University of new Hampshire).

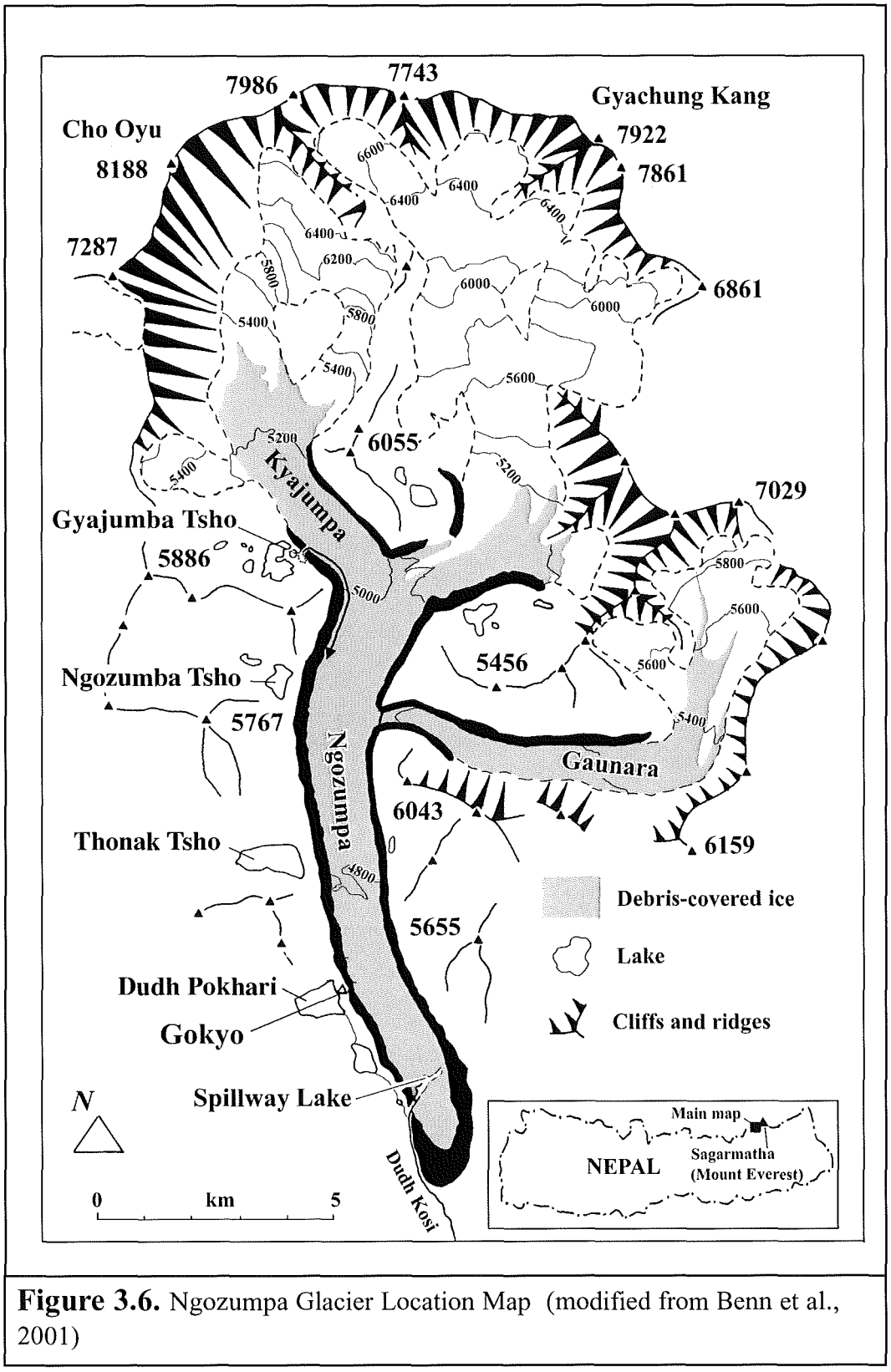

Figure 3.6. Ngozumpa Glacier Location Map (modified from Benn et al., 2001)

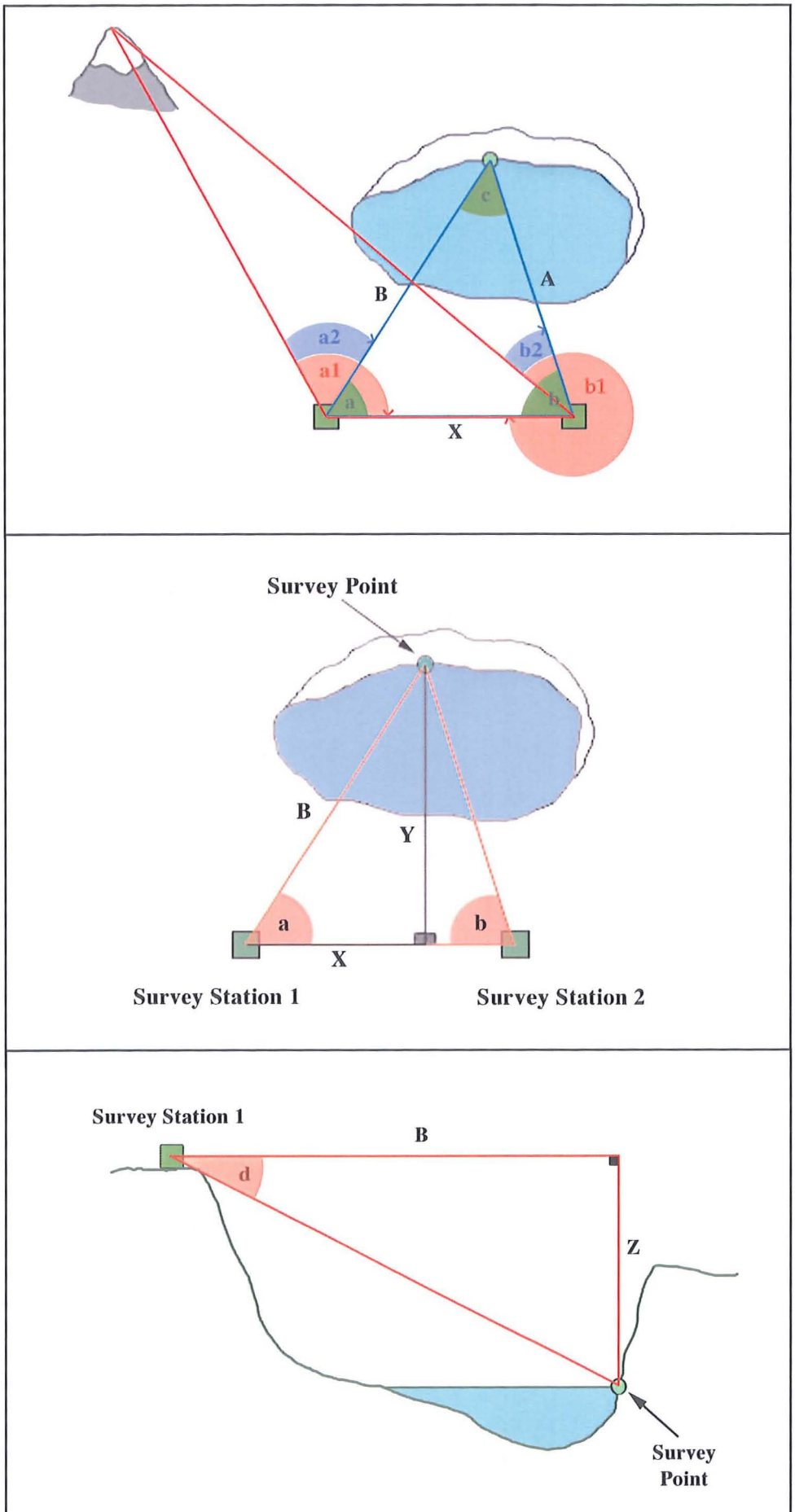

Figure 3.7. Method of surveying using triangulation from a measured baseline

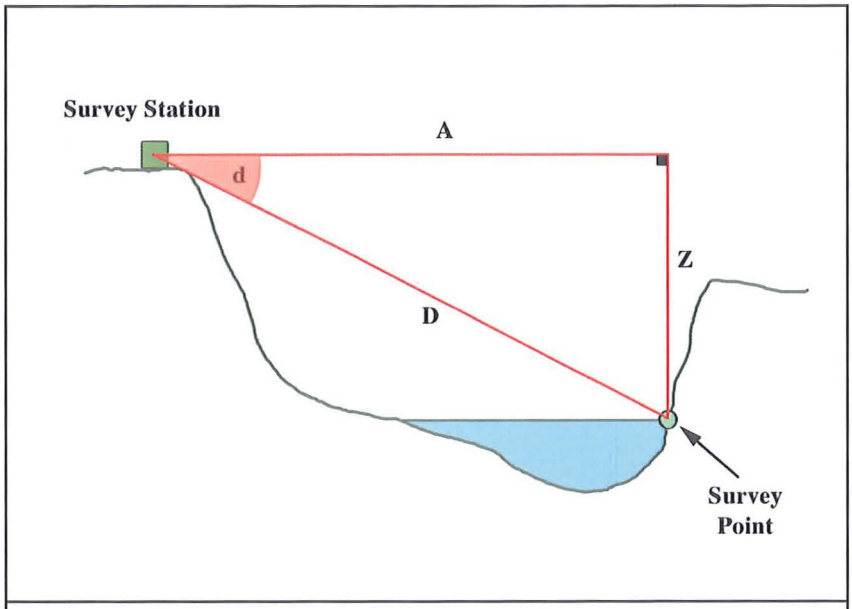

Figure 3.8. Single Station Reflector Survey. Calculation of distance A.

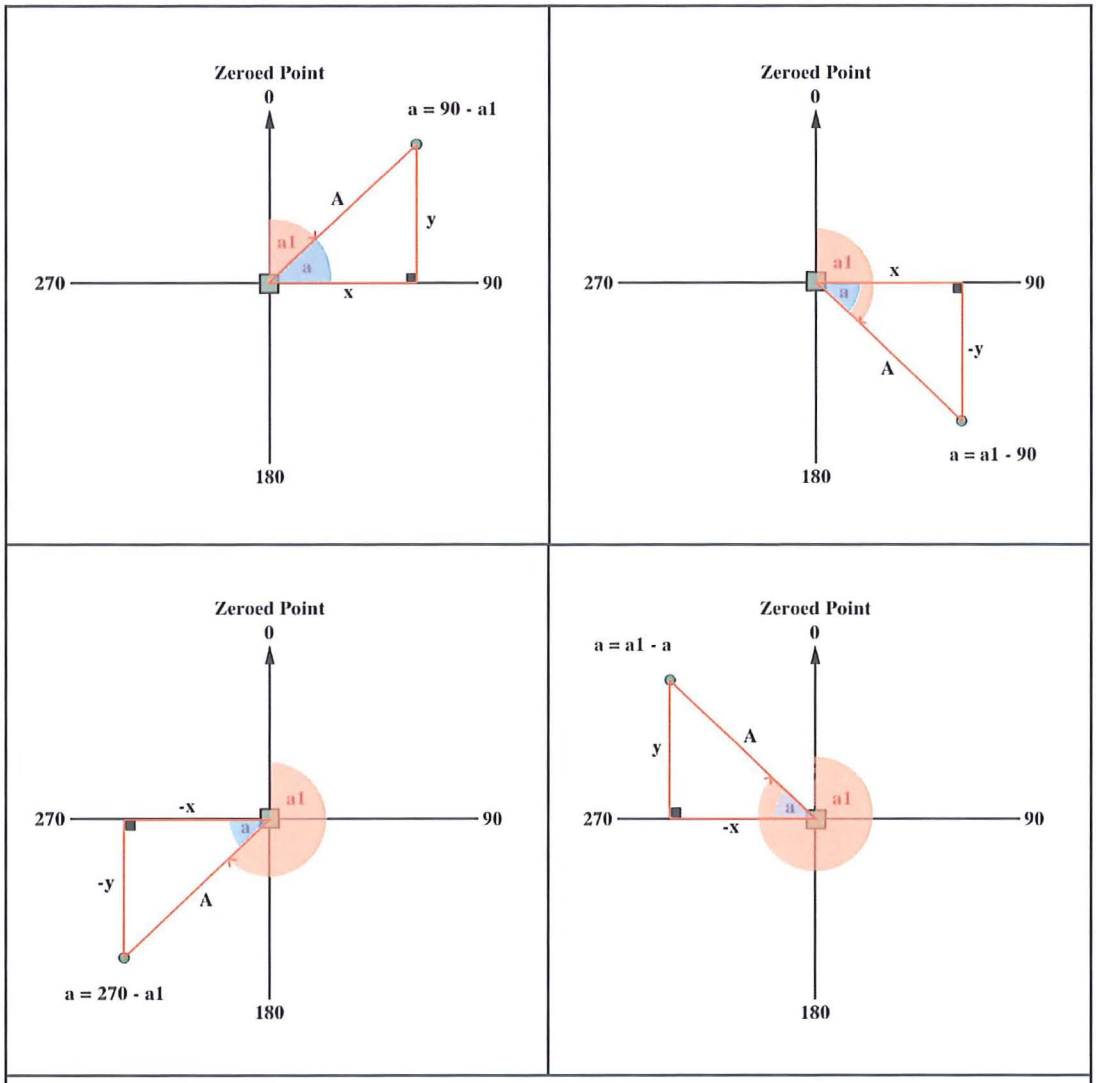

Figure 3.9. Single Station Reflector Survey. Calculation of angle a.

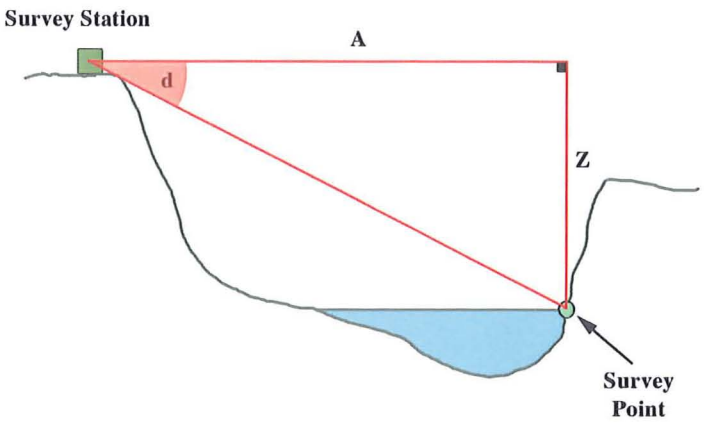

Figure 3.10. Reflectorless surveys.Calculation of A.

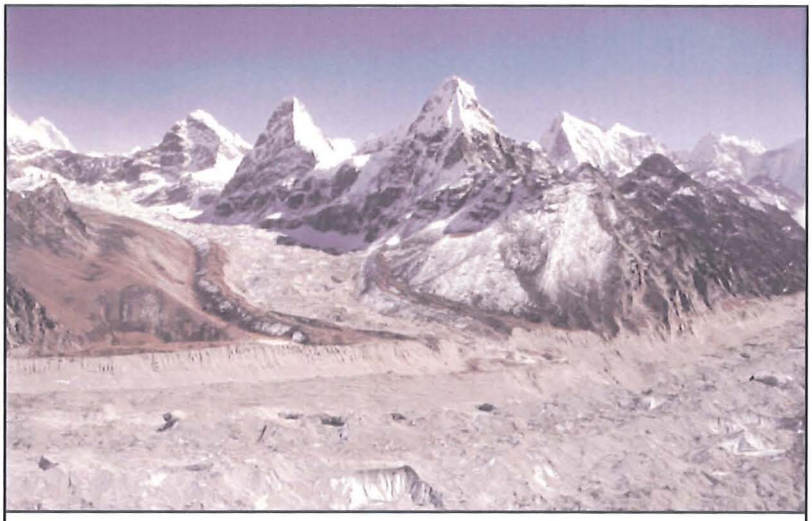

Figure 3.11. Ice no longer flows into the Ngozumpa Glacier from the once tributary Gaunara Glacier.

Figure 3.12. The debris mantle covering the surface of the Ngozumpa. The mantle is only broken where supraglacial ponds have formed, ice faces have become exposed, or cracks have opened up on the glacier surface.

Figure 3.13. A clean ice stream containing little englacial debris supplied with material from the snowfields at the base of Gyachung Kang (7992m).

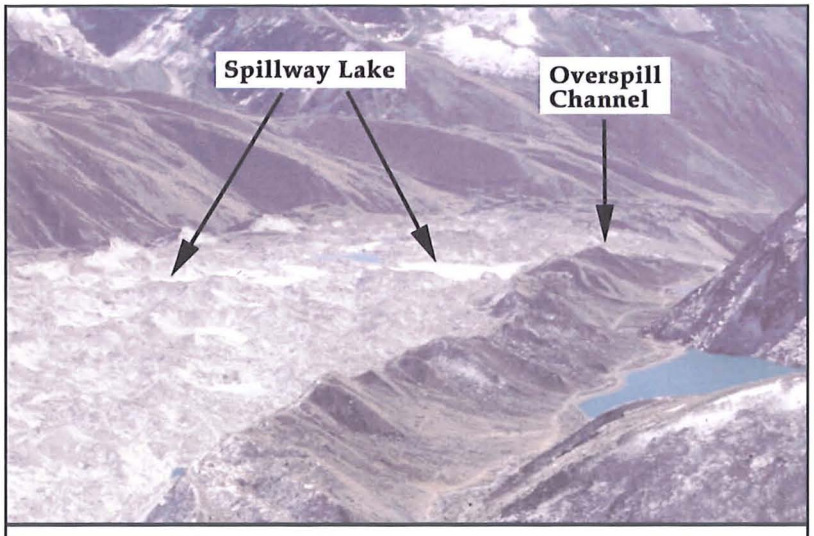

Figure 3.14. Most of the meltwater from the Ngozumpa enters the Spillway Lake near the glacier terminus and drains out through the western lateral moraine. The moraine has dammed drainage from the western tributary valleys.

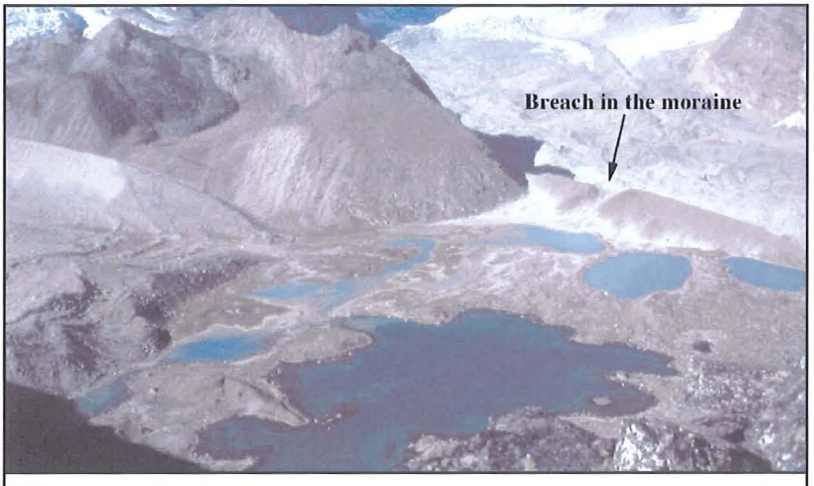

Figure 3.15. The Sixth Lakes left behind when the Gyajumba Tsho flooded out onto the Ngozumpa surface.

Figure 3.16. Hummocky surface topography on the Ngozumpa caused by differential downwasting of the glacier surface.

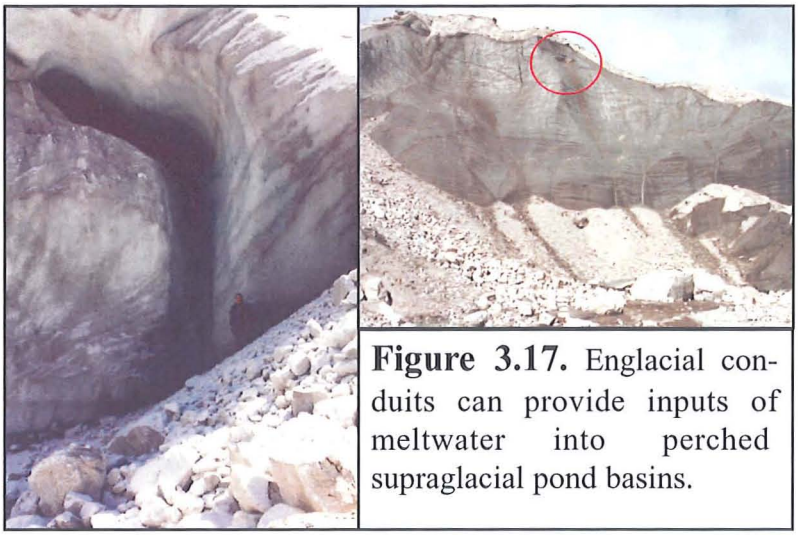

Figure 3.17. Englacial conduits can provide inputs of meltwater into perched supraglacial pond basins.

Figure 3.18. Exposed englacial conduit responsible for the drainage of a perched supraglacial pond.

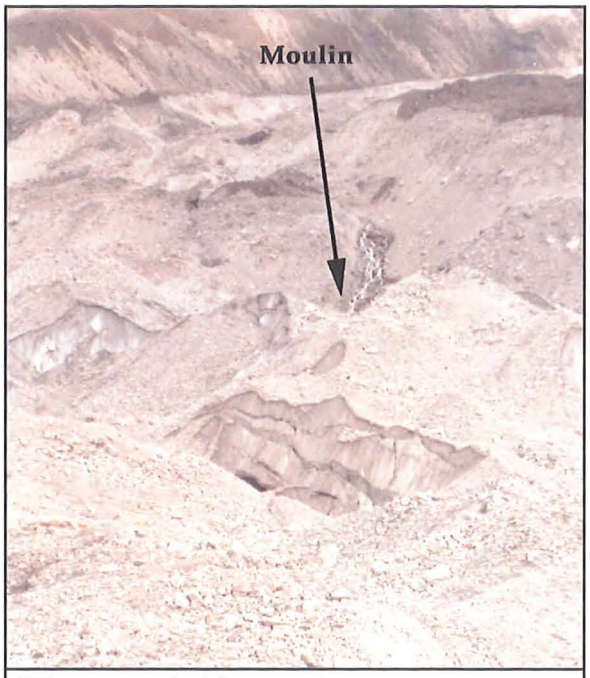

Figure 3.19. Meltwater from the Gaunara Glacier flows onto the surface of the Ngozumpa and into a large moulin surrounded by exposed ice faces.

Figure 3.20.

Slumping and sliding of debris can cover exposed ice faces with a layer of insulative debris.

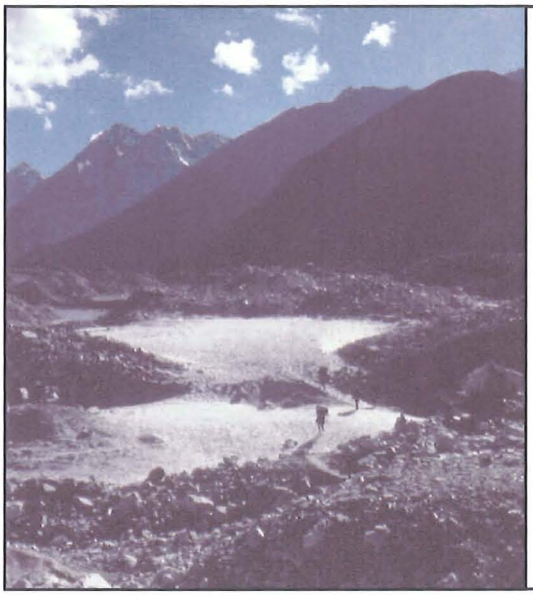

Figure 3.21.

Raised deltas on the glacier surface provide evidence for pond drainage.

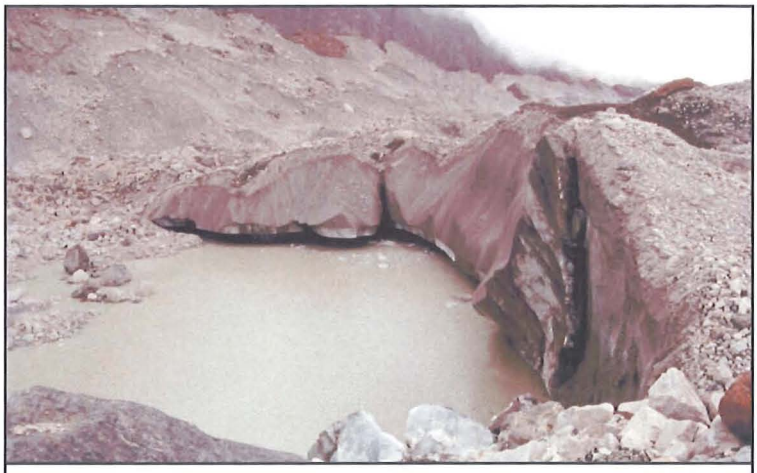

Figure 3.22. Drainage of Pond 7192 through an englacial conduit in the southern ice margin.

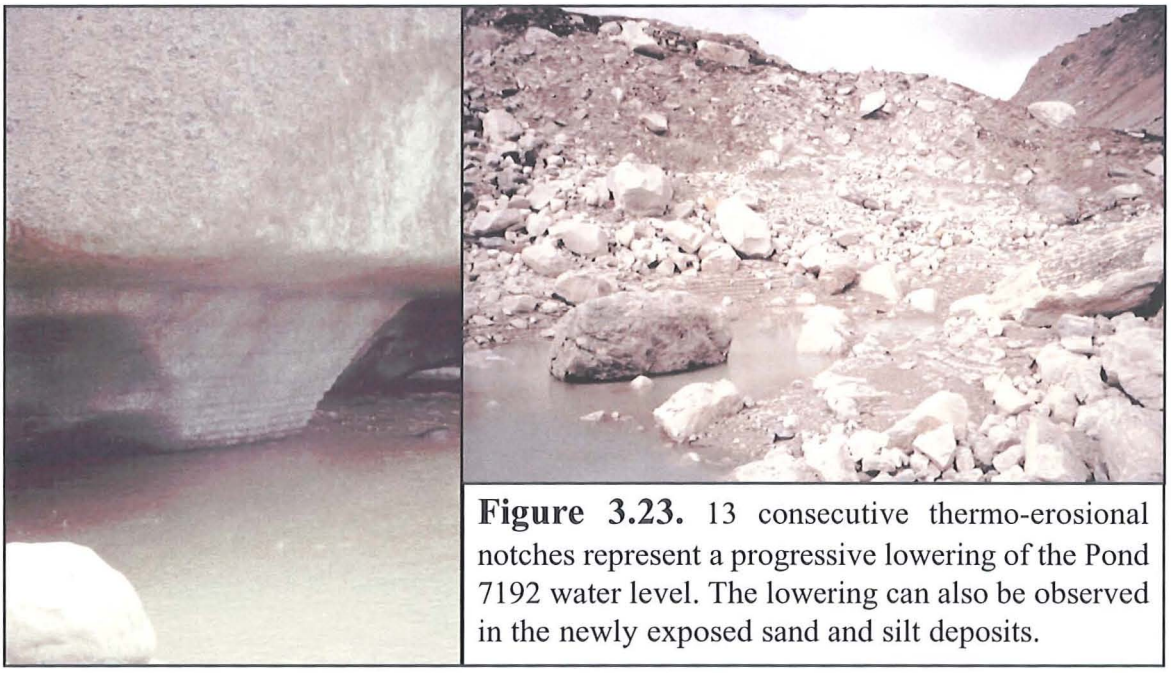

Figure 3.23. 13 consecutive thermo-erosional notches represent a progressive lowering of the Pond 7192 water level. The lowering can also be observed in the newly exposed sand and silt deposits.

Figure 3.24. Grounded icebergs produced by the second calving failure event since drainage of Pond 7192 began.

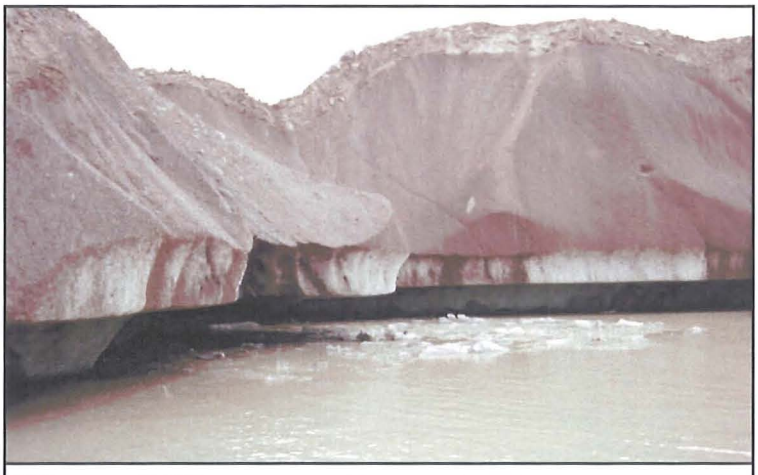

Figure 3.25. Icebergs floating into the conduit indicated that the drainage of Pond 7192 was still ongoing.

Figure 3.26. Pond 7192. Collapse of part of the conduit entrance caused by propagation of a stress-release fracture in the ice above the large thermo-erosional notch.

Figure 3.27. Surface Morphology and Pond Location in 1984 and 2000. Drawn from the 1984 1:35,000 aerial photograph No. 123 (Figure 3.28) and a panchromatic SPOT image (scene 227/294) taken on 6th October 2000 (Figue 3.29).

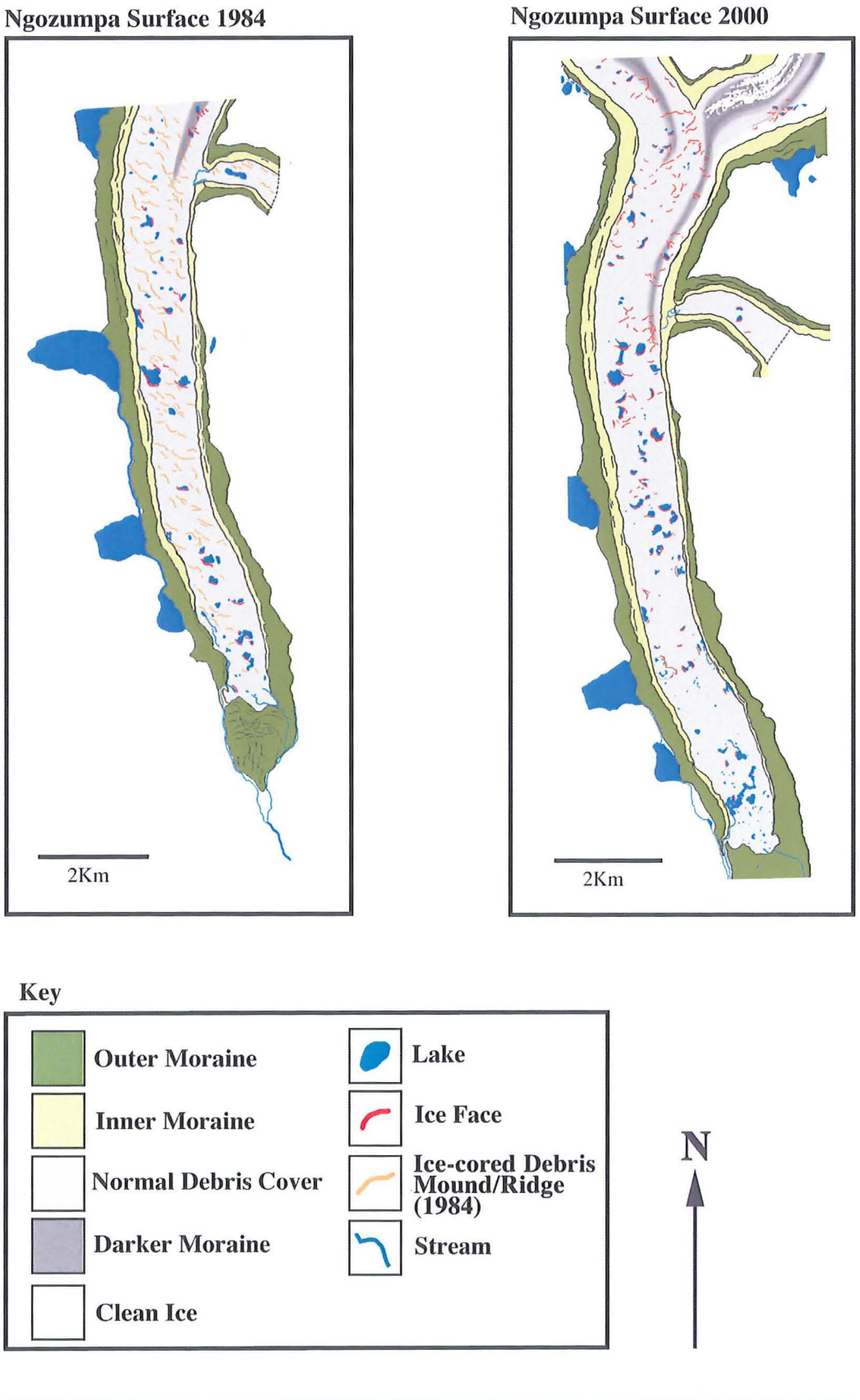

Figure 3.28. Aerial photograph of the Ngozumpa Glacier No. 123 (1984). Scale 1:35,000.

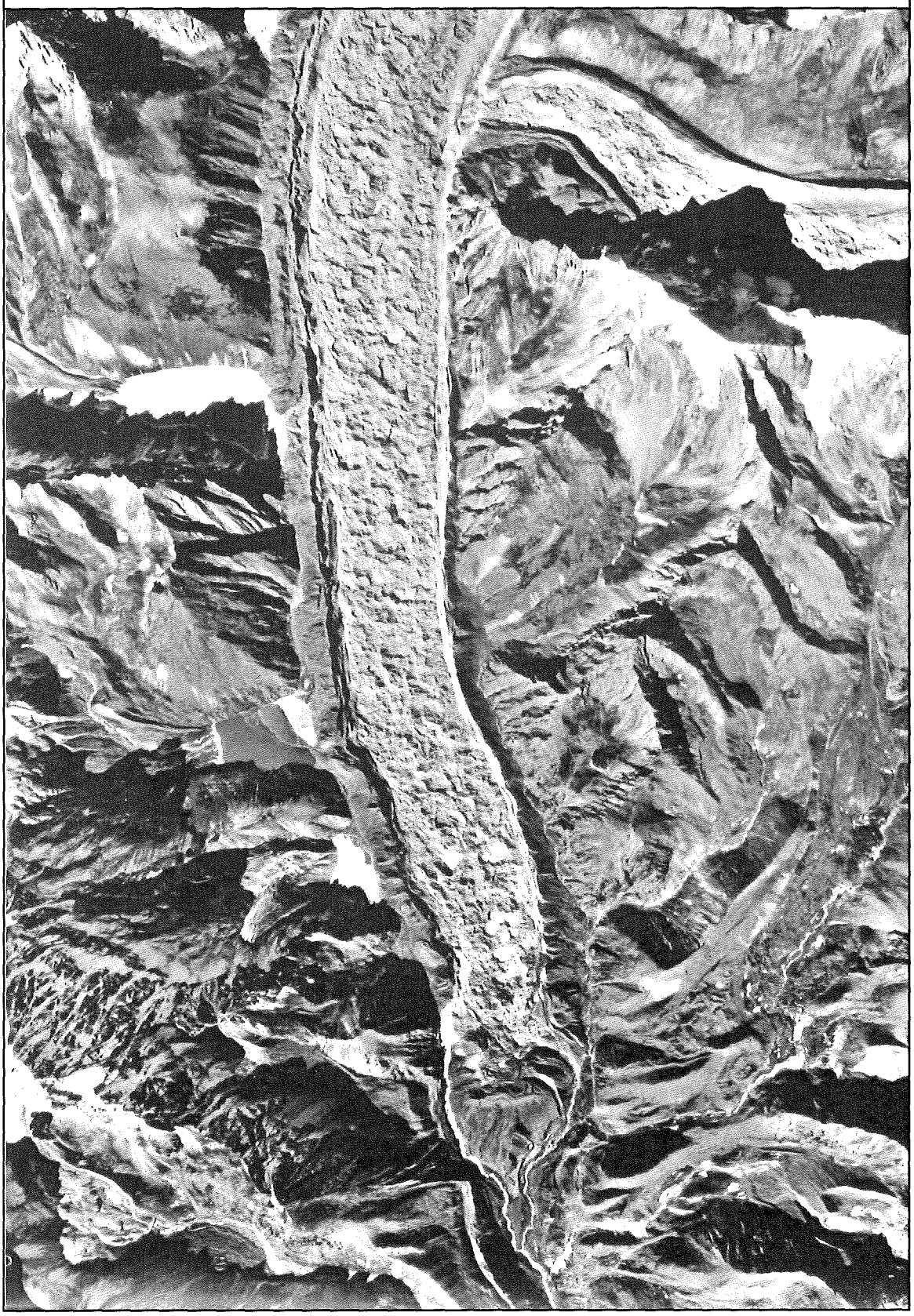

Figure 3.29. Panchromatic SPOT image of the Ngozumpa Glacier (scene 227/294) taken on 6th October 2000.

Chapter 4

Perched Supraglacial Pond Evolution

4.1. Introduction

To develop a quantitative understanding of the processes and rates of perched supraglacial pond development, detailed case studies were conducted at three basins on the surface of the Ngozumpa Glacier between September 2000 and November 2001 (Figure 4.1). The main aims of the case studies were:

- To determine mean rates and mechanisms of ice face retreat
- To establish the controls on calving at exposed lake-contact ice margins
- To monitor lake level changes within the basins
- And to examine the role of debris cover within and around the pond basins

The three ponds selected for this study were considered typical of perched supraglacial ponds on the Ngozumpa Glacier. Two of the case studies (Ponds 7092 and 7093) follow and build upon previous research undertaken between 1998 and 1999 (Benn et al., 2000; 2001; Wiseman, 2004). Taken together, the case studies and the earlier work allow the development of these perched supraglacial ponds to be followed over a four-year period, between October 1998 and October 2001.

4.2. Case Study 1: Pond 7093b

Pond 7093b is a small supraglacial pond located around 4.2km upglacier from the terminus of the Ngozumpa (Figures 4.1, 4.2, 4.3 and 4.4). The pond is situated close to but not in contact with the western lateral moraine and is surrounded by exposed ice and debris-covered ice perimeters. Two surveys of the pond were conducted; the first was carried out on the 11th October 2000 and then repeated on 7th October 2001.

4.2.1. October 1999 - October 2000

Although the first survey of the site was not conducted until October 2000 (Figure 4.2), photographic evidence proves the existence of Pond 7093b during the post-monsoon season of 1999 (Figure 4.5). The pond was much smaller than in October 2000 and appeared to have formed as the result of the exposure and subsequent melting of an ice face on an ice-cored debris mound. As melting and backwasting of the ice face proceeded, the meltwater produced collected in the small topographic hollow at the base of the ice face to form a shallow perched supraglacial pond. In 1999, the ice perimeter stretched along the southern, eastern and western margins of the pond. The northern margin was a debris-covered ice perimeter.

Pond 7093b was visited again during September-October 2000 (Figure 4.2). Since the previous post-monsoon season there had been a substantial change in the size of the pond basin, the depth of the pond and the extent of the ice perimeter. The pond had increased in surface area and was measured to be c. 2395 m^2. The ice margin had extended further around the eastern and western margins of the pond. The length of the exposed ice perimeter was 145.7 m. No ice had been exposed at the northern pond margin due to the low surface relief around the northern pond perimeter. A second smaller pond (Pond 7093c) had appeared 15 m south of Pond 7093b. Pond 7093c had an area of around 67 m^2 and was situated c. 8 m above the water level of Pond 7093b (Figure 4.6). An exposed ice perimeter surrounded the southern, western and eastern margins of Pond 7093c.

4.2.1.1. Exposure of Clean Ice Faces

Between October 1999 and October 2000, the length of the ice perimeter around Pond 7093b increased. Several different processes brought about the increase in the amount of exposed ice surrounding the pond. Melting and backwasting of the exposed ice faces around the pond margins, and calving along the water-line, caused the enlargement of the pond basin around the southern, eastern and western margins, increasing the length of the exposed ice perimeter. Furthermore, slumping and

sliding of debris at the edges of the steepening ice faces had converted more of the debris-covered ice margin into exposed ice margin.

4.2.1.2. Calving

Melting at the water-line had caused a thermo-erosional notch to develop along the whole length of the ice margin. When Pond 7093b was first revisited in October 2000, there were several floating and grounded icebergs in the pond from a recent water-line calving event caused by the collapse of a thermo-erosional notch roof at the southern ice margin, recorded by a fresh failure scar (Figure 4.6). At the eastern perimeter there was evidence of an older water-line calving event that had taken place along a fracture above the thermo-erosional notch (Figure 4.6). The crack had propagated further to the south of the failure scar and caused a third water-line calving failure to occur between the 26th and the 30th October (Figure 4.7).

A large crack had also opened up along the southern ice margin 9 m above the fresh failure scar, and parallel to the water-line (Figure 4.8). This crack is interpreted as a stress-release fracture that developed in response to the removal of support at the base of the ice face by the enlargement of the thermo-erosional notch and the previous calving event (Figure 4.6 and 4.9). Between the 26th-30th October a large flake calving event occurred along the fracture, removing a large volume of ice from the southern ice margin of the pond. The failure scar was approximately 53 m long, 9 m high and along most of the scar length extended the full depth of the thermo-erosional notch at the water-line (Figure 4.7).

The only other visible structural weakness was a diagonal crack in the southern face of the Pond 7093c (the small pond to the south of Pond 7093b) (Figure 4.7). A string of boulders embedded along the crack suggested that it had formed along a debris band within the ice that may represent a former crevasse. No calving events were witnessed at Pond 7093c during the field season in 2000 although a thermo-erosional notch had formed around the ice perimeter.

4.2.1.3. Creation of a Spit

The southeast margin of Pond 7093b, although an ice margin at the water-line, had a considerable debris cover over the top part of the face and had a much lower surface angle than the surrounding ice perimeter (Figure, 4.7). This led to a higher rate of debris deposition in the southeast corner of the Pond 7093b basin, compared with the rest of the basin. As the ice faces around the basin backwasted over time, the higher rate of debris deposition at the southeast pond margin gradually brought about the formation of a spit of ice-cored debris that extended into the pond at point S (Figures 4.2 and 4.10). In this way, variations in the debris cover and topography around the basin impose similar variations on the newly created glacier surface below retreating ice faces.

4.2.2. October 2000 - October 2001

Pond 7093b was re-surveyed on the 7th October 2001. The southern ice margin had retreated except where a large debris fan had formed covering the ice face at point A (Figures 4.3, 4.4 and 4.11). The retreat of the southern ice face had increased the length of the exposed ice perimeter to 157.5 m. The average retreat rate at the southern pond margin was calculated to be 11.9 m a^{-1} (Table 4.1, p118). The western pond margin had not retreated between October 2000 and 2001 and the eastern-most part of the ice face had advanced towards the pond due to burial of the exposed ice margin by debris. In contrast, the southeast pond margin had lost its protective covering of debris. Despite the increased length of the exposed ice perimeter and the retreat of the southern pond margin, the surface area of Pond 7093b decreased. The water stored in the basin had become divided into three separate ponds: one large pond in the centre measuring c. 1620 m^2, and two small ponds to the east and west measuring 71.5 m^2 and 87.5 m^2 respectively, giving a total area of 1779 m^2 (compared with 2395 m^2 in October 2000). This decrease in surface area can largely be accounted for by a measured 2.1 m drop in the pond water level. This is also evident when the level of the pond relative to a large white boulder situated on the north western shore of the pond, is compared between 2000 and 2001 (Figures 4.7 and 4.11). The decrease in depth was also responsible for the break up of the main

pond into three separate ponds. The most probable explanation for the decreased pond depth is the evaporation of water from the pond as there was no evidence of pond drainage through englacial or sublacustrine conduits.

Pond 7093c had drained when the site was revisited in October 2001. The exposed ice face at the southern end of the drained basin had retreated in the intervening year and the ice face at the eastern end of the basin had become connected to the southern ice margin of Pond 7093b (Figures 4.3 and 4.11). It is suspected that the drainage of Pond 7093c took place in two stages. Partial drainage of Pond 7093c into Pond 7093b could have occurred as the southern ice face of Pond 7093b retreated. The drainage of Pond 7093c into Pond 7093b could explain the formation of the large talus cone down the southern ice margin of Pond 7093b (Figure 4.11). Further drainage of Pond 7093c would have occurred when the backwasting southern ice margin connected with an englacial conduit below the water-line (Figure 4.12). The conduit exploited a debris band running diagonally across the ice face: most probably a lateral extension of the debris band observed in the southern face in October 2000 (Figure 4.7). It is not known where water entering the conduit resurfaces. It is possible, however, that water entering the conduit is channelled into the neighbouring Pond 7092 through an englacial meltwater stream that enters the latter 107.5 m south and 55.8 m east of the hole that drained Pond 7093c. However, it is also feasible that the conduit channels meltwater into the Spillway Lake or any of the small supraglacial ponds in between.

4.2.2.1. Calving

Only two calving events were observed to have occurred during October-November 2001. A large flake calving event occurred on the 7th October at the southern ice margin of Pond 7093b (Figure 4.13). The failure scar extended around 65 m in length and was 11.7 m high at the highest point. The most probable explanation for the failure was the development of a stress-release fracture in the ice above a thermo-erosional notch. A second stress-release fracture in the southern ice margin extended west along the ice margin above the failure scar and parallel to the

underlying thermo-erosional notch. A small water-line calving event occurred along this fracture sometime before the 19th October (Figure 4.14).

4.2.3. October 2001-October 2002

Photographs of Pond 7093b taken by Lindsey Nicholson in October 2002 show that the exposed ice margins around the pond had retreated further (Figure 4.15). The pond depth had increased sufficiently to submerge the eastern spit that had been created as a result of deposition of debris from the retreating ice margins. However, in the centre of the southern exposed ice margin progradation of the large talus cone, that had formed at the base of the ice face between October 2000 and October 2001, was forming a new spit perpendicular to the direction of ice face retreat. The ice faces to the south of Pond 7093b, that had once surrounded Pond 7093c in October 2000, had become covered over with debris once more.

4.2.4. Summary

Pond 7093b formed sometime prior to October 1999, after sliding and slumping from an ice-cored debris mound exposed an ice face. As melting and backwasting of the ice face proceeded, meltwater and precipitation collected in the small topographic hollow below the exposed ice face. Between October 1999 and October 2000, the pond basin expanded rapidly by a combination of backwasting and calving retreat at the exposed ice perimeters surrounding the pond. As the area of the pond increased, the length of the exposed ice perimeter around the pond was also increased. This led to higher rates of basin expansion in a positive feedback cycle. Slumping and sliding of debris at the edges of the steepening exposed ice margins also brought about increases in the length of the ice perimeter. The northern debris-covered ice margin was the only margin that did not experience a rapid retreat. This was mainly due to the low surface relief at the northern margin. The southern exposed ice margin of Pond 7093b continued to retreat between October 2000 and October 2001 at a rate of 11.9 m a^{-1}. In contrast, the surface area and depth of the pond in the basin had decreased. This was due to evaporation of pond water from the basin and the progradation of debris cones at the western exposed ice margin. By

October 2002, the pond depth had increased once more and the exposed ice margins around the pond had experienced further retreat.

As the exposed ice margin in the southwest corner of Pond 7093 retreated, high inputs of debris sliding from the face created a spit of debris that extended into the pond from the northern margin perpendicular to the direction of ice face retreat. The spit was submerged as the depth of the pond increased between October 2001 and 2002. However, a new spit began to form in October 2001 due to the progradation of a talus cone at the centre of the southern ice margin. As the ice face retreated between October 2001 and 2002, the continued high rate of debris delivery developed the talus cone into a spit of debris extending perpendicular to the direction of retreat.

Calving around the Pond 7093b basin was predominantly controlled by thermo-erosional notching at the water-line. Enlargement of the thermo-erosional notch tended to cause stress-release fractures to propagate sub-parallel to the water-line causing failure of the notch roof and small-scale flake calving events directly above the notch. The mean ice face retreat of 11.9 m a^{-1} probably represents annual waterline melt followed by collapse of the overlying ice.

A smaller perched pond appeared to the north of Pond 7093b (Pond 7093c) between October 1999 and October 2000. The pond subsequently drained between October 2000 and 2001, most probably during the summer monsoon when retreat rates at the exposed ice margins were higher. Complete drainage of Pond 7093c occurred when ice face retreat connected the pond with an englacial conduit in the southern ice margin below the water level. In this way, the extensive englacial conduit network at the Ngozumpa Glacier plays an important role in limiting the life-spans of perched supraglacial ponds.

4.3. Case Study 2: Pond 7093

Pond 7093 is situated 350 m north of Pond 7093b (Figure 4.1). The first survey of Pond 7093 was carried out in October 1998 and repeated in November 1999 (Benn et al., 2000; 2001; Wiseman, 2004). However, the photographs presented here of the Pond 7092 basin in October 1999 were taken by the author and record personal observations of the site. For the present study two new surveys were conducted. The first of the new surveys was made on the 11th October 2000 and then repeated a year later on the 7th October 2001 (Figures 4.16, 4.17, 4.18, 4.19 and 4.20). These data provide the opportunity to examine the development of the Pond 7093 basin over four field seasons.

4.3.1. Previous Work: October 1998 - October 1999

In October 1998, Pond 7093 was c. 170 m long and occupied an area of 3870 m^2 (Figures 4.16 and 4.21). Two types of margin surrounded the pond in 1998: the southern, eastern and northern pond perimeters were debris-covered ice margins, whereas the western pond margin was delimited by the western lateral moraine. A large west-facing ice face, 106 m long and between 30 and 70 m in height, was exposed about 100 m east of the pond perimeter. Several smaller ice faces were also becoming exposed in an area of hummocky surface relief near to the southeast pond margin where there was a high level of slumping activity. The presence of fine sand and silts between the eastern pond perimeter and the large ice face indicated that the pond had previously occupied a much larger area of the basin. Around 150 m northeast of Pond 7093 there was a large circular depression in the glacier surface. The slopes surrounding this depression lay at an angle of around 45° and were predominantly debris-covered, although punctuated by small exposures of ice.

By the pre-monsoon season in 1999, the water level had increased by 2 m and the pond area had increased. The increased water level brought the pond perimeter into contact with the small ice faces to the southeast creating an exposed ice margin. The large ice face to the east had not changed position. The pond level rose by a further 7 m over the summer monsoon season. By October 1999, the pond had increased in

length to 250 m and occupied an area of c. 13,550 m^2 (Figures 4.17, 4.22 and 4.23). The expansion of the pond area was largely due to flooding of the relatively low-lying ground to the north. However, where the small ice-contact margin had developed prior to the monsoon season, backwasting of the exposed faces and calving retreat at the southeast pond margin had caused an enlargement of the pond basin towards the southeast. The exposed ice pond margin had increased in length and extended along 120 m (20%) of the pond perimeter with heights of between 10 and 27 m above the level of the pond. The retreat rate at the exposed ice perimeter of the pond between 1998 and 1999 was 51.6 m a^{-1}. This is much higher than the retreat rate experienced at the large ice face to the east, which was measured to be 15 m a^{-1} for the October 1998-1999 period.

4.3.1.1. Calving Retreat

The high retreat rate experienced at the southeast pond margin can be explained by rapid calving retreat during the summer monsoon season. Several calving events were witnessed at the exposed ice margin of Pond 7093 between October and November 1999 (Figures 4.24). Calving around Pond 7093 was predominantly controlled by the rate of thermo-erosional notching of the ice face at the water-line and small-scale flaking and spalling of ice from the face (Figures 4.25). However, there were several larger full-height slab calving events that involved large blocks or pillars of ice that gradually became detached from the main face before toppling into the pond. These large blocks of ice form where planes of weakness within the ice intersect. Prior to calving, a detached block becomes increasingly separated from the main ice face above the water-line as old planes of weakness are reactivated. Eventually the block of ice topples into the pond in a single event leaving a deep failure scar that extends back further than the depth of thermo-erosional notch at the water-line, indicating that these events are not controlled by the rate of water-line notching. Figure 4.25 shows the separation of a large ice block from the eastern face of Pond 7093 in November 1999. A fan of debris extended into the pond from behind the block and was formed as debris fell from the top of the ice face into the widening gap. To the right of the block a recent failure surface from a notch-

controlled calving event can be seen. The icebergs present in the pond are the result of a previous full-height slab calving event that occurred at the southeast pond margin.

A fourth type of calving event, subaqueous calving, was also observed at Pond 7093 during October 1999. The event was heralded only by a rushing noise immediately followed by the appearance of a large dark-coloured block of ice approximately 10 m out from the ice cliff at the southeast pond margin. Subaqueous calving does not occur frequently at the Ngozumpa and this was the only such event observed in a supraglacial pond on the glacier over the study period. The lack of subaqueous calving at the Ngozumpa is probably due to the large thicknesses of debris, which mantle the glacier surface. The weight of the debris covering the floor of a perched supraglacial pond offsets the buoyancy forces that drive subaqueous calving, resulting in a much lower subaqueous calving rate than in a pond with little or no debris cover at the pond floor. Given the infrequent occurrence of subaqueous calving events, this type of calving is considered to play only a minor role in the enlargement of supraglacial perched ponds on the Ngozumpa (Benn et al., 2001).

4.3.1.2. Development of a Moulin

In October 1999, the large depression to the north of Pond 7093 had developed into a large active moulin 130 m by 65 m wide and 80 m deep. Slumping and sliding of the surface debris had exposed large ice faces around the inner slopes of the depression (Figure 4.22). The inner east-facing wall of the depression was c. 35 m lower than the surrounding inner slopes. Meltwater and debris from the exposed ice faces were funnelled down to the base of the depression and could be seen and heard entering the moulin. It is believed that this moulin connected with an englacial conduit that channelled meltwater beneath Pond 7093 towards the glacier terminus, although it is not known exactly where the englacial meltwater entering the moulin re-emerged.

4.3.2. October 1999 - October 2000

Between October 1999 and October 2000 the water level in the pond had risen by 1 m but the pond area had decreased to 11260 m^2 (Figures 4.18, 4.20, 4.26 and 4.27). The decrease in pond area was due to the progradation of talus fans in the southeast corner of the pond. The exposed faces around the southeast corner (Face E, Figure 4.18) had retreated and were no longer in contact with the pond perimeter. The height of the ice face ranged from between 9 m and 32 m and the face had increased in length to c. 130 m. The retreat rate for this face was calculated to be 17.9 m a^{-1} (Table 4.1, p118), and was mainly by melting. It is therefore probable that during the course of the year the deposition of debris from the top of the ice face and the progradation of talus cones into the pond protected the base of the exposed ice faces at the southeast pond margin and inhibited calving at the face. As backwasting continued, the ice face became further removed from the pond perimeter decreasing the retreat rate of the ice face.

The exposed ice face to the east of Pond 7093 had also continued to retreat (Face C, Figure 4.18). Slumping and sliding of debris from the top of the face had partially covered the northern end of the face and had brought about a reduction in the face length by c. 35 m to 71.26 m. Ice face heights ranged between 6.6 m and 25.6 m. The annual retreat rate at the face was calculated to be 24.5 m a^{-1} (Table 4.1, p118), 9.5 m a^{-1} higher than the previous year. This gave an average retreat rate for the ice face of 19.7 m a^{-1} over the two-year period.

There was no change in the western pond perimeter, indicating the relative short-term stability of moraine margins when compared with debris-covered and exposed ice margins.

4.3.2.1. Disappearance of the Moulin

The moulin to the north of Pond 7093 was no longer active in October 2000 (Figure 4.27). The exposed ice faces surrounding the moulin no longer formed a funnel shaped depression as melting and backwasting had removed the lower ice faces to

the west (Face A, Figure 4.18). The eastern wall of the moulin had developed into a slightly curved ice face measuring 130 m wide and between 13 m and 25 m high. The annual retreat rate of the ice faces at Face A was c. 7.85 m a^{-1} (Table 4.1, p118). A connecting southwest facing ice face (Face B, Figure 4.18) had become exposed at the southern end of the main face, making the total length of the exposure c. 177 m. Face B had a higher annual retreat rate of 11.7 m a^{-1} (Table 4.1, p118). Several large debris fans had built up by sliding and slumping of debris down the central part of the ice face and had completely covered over the area where the entrance to the moulin had been situated in October 1999 (Figure 4.27). The deposition of debris down face A could partly explain the lower retreat rates experienced at the face between October 1999 and 2000. The appearance and disappearance of this moulin over two years illustrates the highly mutable nature of the englacial drainage network at the Ngozumpa Glacier.

4.3.3. October 2000 - October 2001

The water level in pond 7093 had dropped by 1.5 m by October 2001 and the pond area had decreased by 30 m^2 to 11230 m^2 (Figures 4.19, 4.20 and 4.28). This decrease in area was largely attributed to the continued progradation of talus fans at the southeast perimeter of the pond, although evaporation of water from the pond may also have been a contributing factor. The western perimeter of the pond bordered by the relatively stable lateral moraine had changed very little between October 2000 and October 2001. On the eastern perimeter, however, around 482 m^2 of the debris-covered ice margin had been removed and replaced by pond water and a small ice face had opened up 5.5 m east of the new embayment (Face F, Figure 4.19). It is feasible that the ice face developed as an ice contact margin that became distanced from the pond perimeter by subsequent slumping and sliding of debris down the face combined with a drop in the pond water level. The retreat rate of the pond margin at Face F was approximately 0.9 m a^{-1} and this low rate could be explained by distancing of the ice face by progradation of talus fans soon after the ice contact margin was formed.

The large ice face near to the southeast margin had continued to retreat (Face E, Figure 4.19). Slumping and sliding of debris from the debris-covered surfaces above had divided the ice face into two separate faces (Figure 4.29). The southern-most face was situated at a distance of 48 m from the pond perimeter and was 71.6 m wide and between 4.8 m and 30.6 m in height. The annual retreat rate was calculated to be c. 21 m a^{-1} between October 2000 and 2001 (Table 4.1, p118). The smaller face was located 38 m from the pond perimeter and measured 32.3 m wide and 4.8-10.3 m high. The annual retreat rate between October 2000 and 2001 was calculated to be 17.3 m a^{-1} (Table 4.1, p118).

The large ice face to the east had also continued to retreat and was now positioned around 115 m from the eastern perimeter of the pond (Face C, Figure 4.19). The length of the face had been reduced to 57.5 m. The height of the ice face was around 11.5 m. The annual retreat rate of the face between October 2000 and 2001 was 13.6 m a^{-1} (Table 4.1, p118).

4.3.3.1. The Ice face Surrounding the Old Moulin

The moulin was still inactive in October 2001 and the ice face that had once formed the walls of the funnel-shaped depression above the active moulin in 1999 had continued to backwaste and retreat at a rate of 17.4 m a^{-1} (Figures 4.19 and 4.29). This rate was much higher than for the period between October 1999 and 2000. The length of the face had been reduced by c. 33 m to 143.7 m due to the slumping of debris from the top of the ice face and the build up of talus cones that had covered over the southern end of the face. The height of the ice face ranged between c. 10 and 18 m.

4.3.4. October 2001 - October 2002

Lindsey Nicholson photographed pond 7093 once more in October 2002 (Figures 4.30, 4.31 and 4.32). The water level appeared to have dropped between October 2001 and 2002, and there had been further progradation of the talus cones at the southeast pond perimeter. Along the eastern pond perimeter several patches of dark

sands and silts indicated the drop in water level. A small exposure of ice had appeared near the northeast pond margin, possibly as a result of slope movement caused by the drop in the pond water level.

The ice faces to the southeast of Pond 7093 had become almost entirely covered over by debris, with only a few limited exposures of ice remaining. The large face 115 m east of the pond perimeter had also disappeared. Sustained progradation of debris cones had reduced the area of exposed ice around the old moulin to the north of Pond 7093, although backwasting of the exposed ice had continued. The most significant change to the basin occurred at the base of the large ice-cored debris-mound between the site of the old moulin and the northern perimeter of Pond 7093. The 'growth' of the debris mound, relative to the downwasting glacier surface, had brought about an increase in the slope angles of the mound (see Chapter 2, Section 2.3.3). By October 2002, the increase in slope angles around the mound had destabilised the debris cover, causing slumping and sliding of debris to expose several ice faces around the base of the southern and western slopes of the debris mound (Figures 4.30 and 4.32). It is expected that melting and backwasting of these newly exposed faces will bring about a new phase of expansion in the Pond 7093 basin in the near future.

4.3.5. Summary

Pond 7093 experienced an increase in area of 7360 m^2 between October 1998 and 2001. The increase in pond area occurred between October 1998 and 1999 by backwasting and calving retreat at the exposed ice margins around the eastern and southeastern perimeters of the pond. Thermo-erosional notch-controlled calving, flake calving and several larger full-slab calving events characterised the calving retreat at the exposed ice pond margins. Although one sublacustrine calving event was witnessed in October 1999, this process is believed to be a rare occurrence in supraglacial ponds on glaciers with thick debris-mantles. This is due to the weight of the debris layer, which offsets the buoyancy forces that drive sublacustrine calving. After the initial expansion period between 1998 and 1999, the pond area began to

decrease as progradation of debris cones covered the exposed ice faces around the eastern and southeastern pond perimeters, distancing them from the pond and converting exposed ice margins into debris-covered ice margins. Debris-covered ice pond margins retreat at a much lower rate than exposed ice pond margins, reducing the rate of pond basin expansion and also decreasing the volume of meltwater entering the lake. Reduction of the length of exposed ice margin surrounding a pond perimeter reduces the rate of basin expansion. It can also lead to a decrease in pond water level and area if evaporation of pond water exceeds the volume of meltwater entering the pond. Between October 1999 and 2001, the progradation of talus-cones in the southeast corner of Pond 7093 not only distanced the ice faces from the pond perimeter, halting the rapid calving retreat and converting an exposed ice margin into a debris-covered ice margin, but also caused the area of the pond to decrease. The observations of debris reworking around the margins of Pond 7093 are important because they illustrate the role that the debris budget plays in pond basin evolution. Deposition of debris around pond margins can slow or halt the growth of a pond basin and exposure of ice by debris reworking can trigger backwasting and increase rates of basin growth.

4.4. Case Study 3: Pond 7092

Pond 7092 is located at the western glacier margin c. 213 m south of Pond 7093b (Figure 4.1). The first surveys of the pond basin were conducted in September 1998 and repeated in October 1999 (Benn et al., 2000; 2001; Wiseman 2004) (Figure 4.33). The photographic evidence presented in this thesis for Pond 7092 in October 1999 is taken from the author's own collection and record personal observations made at the site during this time. The surveys were repeated for this study on the 3rd October 2000 and on the 4th October 2001 (Figures 4.34, 4.35, 4.36 and 4.37).

4.4.1. Previous Work: September 1998 - May 1998

In September 1998, three ponds (labelled A-C) occupied a large basin, measuring approximately 300 m in length and 200 m in width (Figures 4.33 and 4.38). These ponds had a combined surface area of c. 17,890 m^2 and covered around 46% of the

basin floor (Wiseman, 2004). In the areas of the basin floor not occupied by pond water, deposits of laminated sands and silts provided evidence for a much deeper and more extensive pond in the past. The northern basin margin was a debris-covered ice margin, the eastern and southern margins were exposed ice margins punctuated by large talus cones, and the western margin was a relatively stable moraine margin. The bases of many of the exposed ice-cliffs were protected by prograding talus fans and therefore were not in contact with the pond water in the basin; however, there were limited sections of the face that did terminate in the shallow ponds. Wiseman (2004) also noted that the exposed ice faces in the south and east of the basin had extensive planes of weakness such as planes of old crevasse fill and open cracks.

By April 1999, although there had been little change in the basin size and shape, the water level in the basin was estimated to have increased by c. 2 m (Benn et al., 2001; Wiseman, 2004), causing the two small ponds in the south of the basin to amalgamate and increase in surface area. The rise in water level had submerged many of the protective talus cones around the bases of the exposed ice faces bringing these faces into direct contact with the pond water and initiating calving and spalling of ice from the eastern and southeastern ice faces.

4.4.2. October - November 1999

When the basin was visited in October 1999, a dramatic change had taken place. The water level in the basin had continued to rise over the summer monsoon period and was 8.8 m deeper than in October 1998 (Benn et al., 2001) (Figure 4.34, 4.39 and 4.40). The rise in water level had created a single pond 52,550 m^2 in area that occupied c. 87% of the total basin area (almost 3 times the area of the pond in September 1998) (Wiseman, 2004). Measurements of the basin bathymetry showed that the pond depth ranged between c. 3 m and 14 m. The deepest part of Pond 7092 was in the southwest part of the basin, in the area that had been occupied by the largest of the three small ponds in September 1998. The basin itself had also expanded in area and measured around 60,500 m^2. This basin expansion was due to

the retreat of the exposed ice margins in the eastern and southeastern parts of the basin where around 340,000 m^3 of ice and debris had been removed by calving of the exposed ice faces (Benn et al., 2001). The mean retreat around the eastern and southeastern margins was 31 m between September 1998 and October 1999 (Benn et al., 2001). The greatest retreat was experienced at the southeastern ice margin where the presence of a series of closely spaced longitudinal crevasses running parallel to the exposed face had enhanced the calving rate of the ice face. Along the northern pond margin slumping and sliding of debris had converted parts of the debris-covered ice margin into exposed ice margins. In contrast to the rapid retreat rate experienced in the eastern and southeastern margins, the western moraine margin and the debris-covered ice margin to the north of the basin had remained relatively unchanged.

4.4.2.1. Calving

Several calving processes were observed at Pond 7092 during September-October 1999. The most frequent type of calving at Pond 7092 was water-line calving controlled by the rate of thermo-erosional notching of exposed ice margins. The flooding of the basin during the summer monsoon had increased the water level in the basin above the height of the protective debris cones that had built up around the bases of the exposed ice faces. The loss of the protective debris cones increased the rate and degree of thermo-erosional notching along the water-line at the exposed ice margins and thereby enhanced the rate of water-line calving. At the lowest point of the eastern face the thermo-erosional notch depth was measured to be 3.8 m (Benn et al., 2001; Wiseman, 2004). This depth reflects the fact that there was no calving activity along this part of the face, allowing uninterrupted notch growth. The largest water-line calving event witnessed at Pond 7092 took place on the 25th October at the eastern exposed ice margin and removed a flake of ice 1 m high and 28 m long (Figure 4.41). Smaller water-line calving events were observed along the southern ice margin and in one area had resulted in the formation of an arcuate indentation just above the water-line (Figure 4.42). The formation of arch-shaped 'caverns' above the water-line is not unusual in supraglacial ponds on the Ngozumpa and is

thought to occur primarily by exploitation of pre-existing weaknesses in the ice above and behind a thermo-erosional notch. The arch shape can subsequently be enhanced by preferential spalling of ice from the apex of the arch roof, where tensile stresses in the ice are greater than at the margins (Wiseman, 2004).

Spalling of flakes of ice occurred above thermo-erosional notches, from the tops of the exposed ice faces and from the middle parts of the faces. The controlling factor for this type of calving appeared to be the intersection of pre-existing weaknesses within the ice, such as old crevasse traces, foliation planes and debris bands.

Several full-height slab calving events occurred at Pond 7092 during September-October 1999. The largest of these events occurred at the northeast exposed ice margin. At the beginning of October 1999, a well-developed fissure c. 40 m long was observed to extend diagonally down through the ice face isolating a pillar of ice measuring approximately 20 m high, 40 m across and 6 m wide (Figure 4.43). The crack behind the pillar was gradually widened and limited flaking and spalling of ice occurred in the immediate vicinity until the pillar toppled on the 12th October. A smaller flake, which measured approximately 15 m x 15 m x 2 m, fell from the same location on the 20th October. By the 28th October a second crack had begun to open up parallel to the old failure surface (Figure 4.44) and on the 30th October another ice pillar toppled about 10 m west of where the previous pillar had calved (Figure 4.45). The rate and type of calving that occurred in the northeast corner suggests that there were several parallel planes of weakness in the ice behind the northeastern pond margin. These planes of weakness are most likely to be old crevasse traces that are reactivated as they come into close proximity with the pond margin. Large pillars of ice form where two or more structural weaknesses intersect.

The calving rate along the exposed ice margins of Pond 7092 was greatest in the southeastern bay where structural weaknesses, in the form of a series of closely spaced longitudinal crevasses, promoted the occurrence of full-height slab calving events above a thermo-erosional notch (Figure 4.46). Wiseman (2004) suggesteds

that the calving mechanism at this face is the process of 'ice slumping' whereby large blocks of ice fail along structural weaknesses above thermo-erosional notches and fall directly downwards. The presence of the notch creates a torque within the ice above and the rotational force generated results in tensile stress at the top and behind the face, and compressional stress at the back of the notch (Wiseman, 2004). Fractures are propagated from the top of the face downwards and eventually the block fails. The process of 'ice slumping' differs from conventional slab calving where cracks are propagated down from the surface and gradually widen until toppling failure occurs.

4.4.2.2. Conduits

In early October 1999, an elongated englacial conduit channelled meltwater into the southeastern margin of Pond 7092 (Figure 4.47). The conduit shut down after the 19th-20th October 1999 when a metre of snow fell in the valley and many of the supraglacial ponds on the glacier froze over. The existence of a conduit in this part of the basin is most probably due to the high degree of structural weakness and amount of fracturing within the ice around the southeast pond margin. Several other conduits were observed in ice faces in the southern and southeastern part of the Pond 7092 basin but these did not appear to be active during the September-October 1999 field season (Figure 4.48). It is probable that these conduits were active during the summer monsoon period when the volume of meltwater present on and within the glacier is higher. Meltwater was also observed to emerge from under the debris cover on the northern shore of Pond 7092 and entered the pond at the water level.

Water entering the Pond 7092 basin via englacial conduits could have been partly responsible for the flooding of the basin during the summer monsoon. However, volumetric comparison of the increase in lake volume and the loss of ice volume from the surrounding pond margins showed that most of the water level rise in Pond 7092 was probably due to melting of calved icebergs (Benn et al., 2001).

4.4.3. October 1999 - October 2000

Sometime during July or August 2000 Pond 7092 was almost entirely drained leaving behind six very small and shallow ponds (A-D) in the lowest parts of the basin (Figures 4.35, 4.37 and 4.49). The position of these ponds mirrored the position of the shallow ponds present in the basin during September 1998. The basin had continued to expand by calving retreat and backwasting during the early summer monsoon months increasing the basin size to c. 82,023 m^2. In total, approximately 21,522 m^2 of ice and rock were removed from around the margins of the basin. The mean retreat rate for the eastern exposed ice margin (Face 1, Figure 4.35) was calculated to be c. 25.8 m a^{-1} (Table 4.1, p118). The largest annual retreat rate of 32.4 m a^{-1} was recorded in the southeast corner (Face 2-3, Figure 4.35 and Table 4.1, p118). The high rates of retreat at the northeastern and southeastern ice margins are attributed to the presence of structural weaknesses within the ice (Figures 4.50 and 4.51). In contrast, the northern and southern debris-covered ice margins had retreated very little and the position of the western moraine margin had remained unaltered. By October 2000, the northern pond margin had become almost entirely debris-covered. The southern exposed ice margin had been partially buried by two large talus fans formed by debris falling and sliding into the basin from the slopes above leaving three separate exposures of ice measuring 115.7 m, 21.6 m, and 22.8 m in length respectively.

4.4.3.1. Conduits

Three large holes were discovered in the southeastern exposed ice margin of the basin in October 2000 (labelled C1-C3 in Figure 4.35). The shape and structure of all three holes showed them to be englacial conduits. Meltwater was observed to be flowing inside conduit C2 and from conduit C3.

The entrance to C1 was a large arcuate recess at the base of the ice face around 25 m long, 3 m high and 4 m wide (Figures 4.52). The roof of the recess had been smoothed and scalloped by the passage of water. The floor was covered by drapes of fine silts and sands. To the northeast of the recess a large inverted T-shaped conduit

extended for about 10 m before ending abruptly (Figures 4.53 and 4.54). The shape of the conduit was consistent with simultaneous downcutting and widening of a pre-existing conduit at a time of high discharge. The size and shape of the lower part of conduit C1 suggested that the conduit experienced a rapid influx of water flowing at, or near, full-pipe flow. The upper part of the conduit coincided with a debris band within the ice.

At the northeastern-most end of the conduit, light was observed to enter from a small hole near the roof of the tunnel, indicating that the tunnel opened up onto the surface of the glacier. At the base of the hole a cone of debris had built up (Figure 4.54). At the western end of the arcuate recess the roof showed clear evidence of collapse, rapidly diminishing in height with distance from the conduit entrance.

A second conduit (C2) was exposed 54 m west of conduit C1 (Figure 4.35). The conduit was exposed at the floor of a hole in the base of the ice face (Figure 4.55). The roof of the hole had been smoothed and scalloped by water and looked distinctly like the roof of an thermo-erosional notch (Figure 4.56). Subsequent to the drainage of Pond 7092 the collapse of ice blocks in front of the hole enclosed the hollow forming an ice cave approximately 5 m wide and 2-3 m high (Figure 4.56). The entrance to the conduit at the back of the hole was approximately 65 cm high and 1 m long (Figure 4.57). Further investigation revealed that water was running in a northeast to southwest direction in the conduit (Figure 4.57). The size of the conduit was large compared with the size of the stream and a bank of debris had been built up on the southern side of the conduit, indicating that the water level had previously been much higher. It was concluded that conduit C2 was the downstream continuation of the conduit at C1.

The third conduit (C3) was exposed in the southeastern ice margin about 3 m above the floor of the basin (Figure 4.58). The conduit was in the shape of an inverted 'L' (c. 4 m wide x 6 m long) and appeared to have originally formed along a large band of debris in the ice before eroding downward through the ice. Meltwater was running

from the conduit into a small pool on the basin floor. Water flowed out of the pool in a small supraglacial stream for several metres before disappearing into the thick debris mantle covering the floor of the basin.

4.4.3.2. Drainage Mechanism

The location and form of englacial conduits C1 and C2 indicates that they were utilised and enlarged by floodwaters draining from Pond 7092. It is inferred that as calving and backwasting of the exposed ice faces proceeded in the southeast corner of the basin, a connection was made with an englacial conduit below the water-line. As a result of this connection, the pond water was drained from the basin. The field evidence suggests that drainage was triggered when a calving event in the southeast corner of the basin intersected the northeast-southwest orientated conduit at C1. As drainage of the pond proceeded, the conduit widened due to thermal erosion of the walls and the pond drained with increasing rapidity. Downcutting of the conduit floor, before and during the initial stages of pond drainage, elongated the shape of the conduit. This was followed by a period of rapid thermal erosion as the pond water drained out of the basin producing the inverted T-shape. The large size of the conduit suggested that the pond drained rapidly and continuously until the basin was emptied. The existence of a single deep thermo-erosional notch around the southeastern exposed ice face also suggests that the lake drained as a single rapid event rather than being a protracted drainage that occurred over a number of days (Figure 4.59). As the conduit widened during the drainage of the pond a second much smaller entrance to the conduit was opened up at C2. This must have happened at a late stage in the drainage of Pond 7092 because only a small amount of thermal erosion of the conduit entrance had taken place. After the pond had drained, the conduit entrance at C1 experienced collapse and subsidence at the southern end. The floodwater from Pond 7092 most probably entered the large Spillway Lake before finally exiting the glacier surface via the over-spill channel cut down through the western lateral moraine. Evidence for conduit enlargement and collapse further down glacier due to the drainage of Pond 7092 will be examined in Chapter 5, Section 5.5.

4.4.3.3. Temporary Storage

The Pond 7092 basin is a perfect example of the temporary storage of meltwater on debris-mantled glaciers. Although most of the flooding of Pond 7092 in 1999 was caused by the melt out of calved icebergs in the pond, part of the flooding may also have been caused by meltwater entering the basin via an englacial conduit in the northern section of the southeast ice margin. The meltwater entering the basin through this conduit could have derived from a number of sources up-glacier from Pond 7092 including meltwater from exposed ice faces, rainwater channelled into the englacial conduit system, and flood water from the drainage of another supraglacial pond or ponds. Flooding of the 7092 basin increased the rate of calving retreat at the exposed ice faces around the pond and caused rapid enlargement of the basin. Eventually a connection was made with a conduit below the water-line and the basin was emptied, releasing the pond water downglacier. It is inferred that the pond water from Pond 7092 was channelled directly into the Spillway Lake and out through the spillway in the western lateral moraine (See Chapter 5, Section 5.5). Following the drainage of the pond the conduits were shut down, melted out, or filled in by the progradation of debris cones and the expansion rate of the basin was decreased. This process effectively re-seals the basin in readiness for the next cycle of flooding and rapid expansion. Given the relative proximity of the basin to the Spillway Lake and its large size it is expected that the 7092 basin will undergo several such cycles as downwasting of the glacier surface proceeds.

4.4.3.4. Post Drainage Basin Development

Following the drainage of Pond 7092 the exposed ice faces around the basin margins continued to retreat but at a much slower rate. The decreased rate of backwasting brought about a relaxation in the slope angles of the exposed ice margins and allowed the progradation of talus fans at the base of these ice faces. As a result of these processes the basin experienced a reduction in the area of exposed ice around the margins. This in turn led to a further reduction in the rate of basin expansion in a positive feedback cycle.

4.4.4. October 2000 – October 2001

When Pond 7092 was visited in October 2001, the basin had increased in size to c. 98,559 m^2 (Figures 4.36, 4.37 and 4.60). Between October 2000 and October 2001 some 16,526 m^2 of debris and ice had been removed from around the margins of the basin. The amount of basin expansion experienced between October 2000 - 2001 was considerably lower than for the periods between October 1998 - 1999 and October 1999 - 2000. This is largely due to the cessation of calving following the drainage of the basin during the summer monsoon 2000, but also reflects the decreased length of the exposed ice perimeter around the basin during 2001 compared with previous years (Figure 4.36).

4.4.4.1. Ice Margin Retreat Rates

The highest retreat rates of between 36.1 m a^{-1} and 58.5 m a^{-1}, at the exposed ice perimeters were once again recorded in the southeast corner of the basin (Table 4.1, p118). These retreat rates were recorded for the northern- and eastern-most faces of the southeast corner of the basin (Face 2, Figure 4.36) and not in the vicinity of the conduit C1, as was expected. The annual retreat rate of 58.5 m a^{-1} recorded for the western-most section of Face 2 seems unusually high. It is likely that this rate does not reflect the retreat of the ice margin by backwasting and instead indicates a change in the position of the ice exposure. This was brought about as slumping and sliding of debris covered over the exposed ice face at the base of the slope and uncovered a fresh exposure of ice near the top of the slope.

The annual retreat rates of the southwest- and west-facing northeast ice margin (Face 1, Figure 4.36) were 20.9 m a^{-1} and 28 m a^{-1} respectively (Table 4.1, p118). The rate at the western most edge of Face 1 was around 5 m a^{-1} lower than in the previous year. The most likely explanation for this is that as the ice face retreated between October 2000 and 2001, the crevasse traces that had been reactivated by calving processes during 1999 had been removed. Following the removal of the structurally weak ice, backwasting continued but at a lower rate.

The lowest retreat rates of between 5.9 m a^{-1} and 9.2 m a^{-1} were recorded at the north-facing Faces 3 and 4 (Figure 4.36 and Table 4.1, p118). This was due to the progradation of talus cones that had almost completely covered the exposed ice margins where the faces at C1 and C2 had intersected with the englacial conduit that drained the pond during the 2000 summer monsoon (Figures 4.36 and 4.61). The continued progradation of talus cones had also reduced the length of the exposed ice margin. As backwasting at the southeast ice margin proceeded between October 2000 and 2001, the conduit at C3 melted out (Figure 4.62).

4.4.4.2. Ponding and Meltwater

Between October 2000 and October 2001, the four largest ponds (A-D) in the bottom of the Pond 7092 basin had changed in shape and size but not in position (Figure 4.36). Pond A had decreased in size from 3659 m^2 to 2691.3 m^2 as a result of net evaporation from the basin. Pond B had also decreased in size through evaporation from 583.6 m^2 to 173.7 m^2. In contrast, Pond C had increased in size from 2970.2 m^2 to 3112.6 m^2. The pond lay in the vicinity of a small stream that entered the basin from underneath the debris cover during October 1999; the increase in the pond size is therefore liable to reflect meltwater inputs from this source combined with rainwater inputs during the summer monsoon. Pond D had increased in size from 511.8 m^2 to 819.6 m^2 and was continually being supplied by meltwater exiting an englacial conduit at the water level (Figure 4.63). The other two ponds situated below the northeastern ice margin in October 2000 had been filled in by debris falling from the top of the ice face and a new pond had opened up in October 2001 at the southernmost end of this face.

In addition to the ponding of water, a small supraglacial stream was also present in the 7092 basin. The stream exited the pond situated below the southern end of the eastern ice perimeter (Face 1, Figure 4.36) and flowed southwards for several metres before disappearing beneath the debris cover. There was further evidence of supraglacial meltwater flow in the basin during 2001 in the form of holes in the debris cover (Figure 4.64). In total 16 holes were observed within the sand and silt

drapes covering the floor of the Pond 7092 basin during October 2001 (Figure 4.36). The holes were distributed in linear chains that did not follow the topography of the basin floor. It is believed that these holes were not created by collapse of an englacial conduit because the holes were very small and the subsidence of silts was very localised. Also no ice had become exposed by the formation of the holes. It is therefore suggested that the holes were created by meltwater and rainwater flowing along structural weaknesses in the ice at the ice-debris interface. The planes of weakness were exploited and gradually enlarged downwards by thermal erosion causing the overlying drapes of silt and sand to collapse, forming the holes. Crevasse-fill structures, observed in a crevasse at the top of Face 1, provided further evidence for this process (Figures 4.36 and 4.65). The laminated crevasse-fill was interpreted as evidence of a former perched pond basin situated at a higher altitude than the present day basin. Laminae in the crevasse-fill sag downwards, with decreasing deformation upsection, indicating syndepositional melt and downward enlargement of the crevasse. The formation of the crevasse-fill structure in Face 1 and the holes along the floor of the Pond 7092 basin provide convincing evidence of localised bottom melting along structural weaknesses in the ice at the floor of Pond 7092. It can thereby be concluded that localised bottom melting occurred along structural weaknesses at the floor of the Pond 7092 during the flooding of the basin and continued following the drainage of the pond water.

4.4.4.3. Calving and Thermo-Erosional Notching

Only two calving events occurred during the 2001 field season and both occurred on the 28th September. Some time during the night or in the early morning the ice above a thermo-erosional notch at the southernmost end of the eastern ice margin failed (Figure 4.66). At the same time another section of ice failed above an thermo-erosional notch on a large block of ice c. 38 m west of the main face (Figure 4.67). The block of ice was believed to be part of a debris-covered 'ice foot' that had become isolated from the main face as the ice cliff retreated. As the 'ice foot' melted out *in situ*, meltwater had ponded around the base causing the development of a deep thermo-erosional notch where ice had become exposed (Figure 4.68). A small

conduit was also observed in the eastern side of the block and was probably formed as supraglacial meltwater was channelled along the side of the exposed block during the summer monsoon period (Figure 4.69).

Following the calving event on the 2nd of October, the rate of thermo-erosional notching was measured over two days on a calved block grounded in the small pond at the southern most end of the eastern ice margin. Over the two-day period a notch 16.7 cm deep was melted into the block of ice. This rate of melt was 4 times faster than the melt rate experienced on the subaerial part of the iceberg face. The average temperature at the pond surface was measured to be 2.2°C with a range of 1.4°C - 3.1°C. After two days the iceberg was no longer grounded in the pond and the experiment was ceased.

In October 2001, the northeastern ice margin was no longer as crevassed and fractured as it had been in October 2000. This was not because the structural integrity of the ice behind the margin was better than in previous years. Indeed a large crevasse trace was visible just behind the exposed ice face (Figure 4.70). The cessation of rapid calving retreat and the consequent relaxation of the ice face angle are thought to provide a more reasonable explanation of why the face was not as broken up and fractured as had previously been observed.

4.4.5. October 2001 – October 2002

Photographs taken of the Pond 7092 basin in October 2002 by Lindsey Nicholson show the continued progradation of talus cones in the basin (Figure 4.71). The ice margins in the southeast and south parts of the basin had almost entirely been converted into debris-covered ice margins. The northeastern and eastern ice margins had also been affected by the progradation of debris cones and the area of ice exposed around these margins and length and height of the exposures had also been greatly decreased.

The floor of the basin appeared to have undergone a few small changes in terms of the position and size of the shallow supraglacial ponds. The water level in Pond A appeared to have fallen as a small island of debris had appeared in the centre of the pond. Pond B had disappeared completely. Pond C, in contrast, appeared to have increased in size again and had amalgamated with two very small ponds to the east. Pond D was no longer in contact with an exposed ice face and dark muddy patches around the margins indicated that it too had undergone a decrease in water level. The conduit that supplied pond D with meltwater from upglacier in October 2001 did not seem to be active. The small pond at the southernmost end of the eastern ice face was still present but was no longer in contact with the ice margin due to the deposition of debris cones at the base of the ice face. A new pond had been formed where the debris-covered 'ice foot' had melted out *in situ*.

4.4.6. Summary

Observations of Pond 7092 over the four year study period covered a complete cycle of basin flooding, expansion, and drainage, and allowed the sequence of events to be determined in detail. In October 1998 the Pond 7092 basin contained three small ponds covering around 46% of the basin floor. However, layers of silt and sand at the floor of the basin provided evidence for a much more extensive pond in the past. By April 1999, the water level in the basin had increased by c. 2 m. The increased water level caused the amalgamation of the two ponds in the southern half of the basin and submerged many of the protective debris cones that had formed at the base of the exposed ice margins, bringing the ice faces into direct contact with the pond water. During the summer monsoon the water level in the basin rose by a further 6.8 m creating a single pond the depth of which ranged between 3 m and 14 m. The water level rise was attributed to several different processes, including: meltwater inputs from backwasting and calving of the exposed ice margins; melting at the debris-covered ice margins; displacement of the water level by high inputs of debris from the basin margins; precipitation inputs during the monsoon; a small meltwater stream emerging from under the debris at the northern basin margin; and the in-flow of water from an englacial conduit exposed in the northern ice margin of the

southeast corner of the basin. The increased depth of the pond encouraged rapid calving retreat at the exposed ice margins, particularly at the eastern and southeastern margins. Calving and backwasting of the exposed ice margins between October 1998 and October 1999 removed some 340,000 m^3 of ice and debris from around the basin perimeter, increasing the size of the basin to c. 60,500 m^2. As calving and backwasting proceeded, the length of the exposed ice perimeter was increased. This in turn increased the rate of basin expansion in a positive feedback cycle. Sliding and slumping at the edges of the steepening ice perimeters had also caused the length of the exposed ice perimeter to increase.

Calving around the basin took the form of thermo-erosional notch controlled calving at the water-line, flaking and spalling of ice from the face, ice 'slumping', and full-height slab calving events. Rapid calving occurred where the height of the ice face above the level of the pond was greater than 15 m. The most rapid calving retreat in the Pond 7092 basin occurred at the northeast and southeast ice faces where parallel planes of structural weakness existed immediately behind the ice faces. Where two or more structural weaknesses intersected, large pillars of ice formed and later failed as full-height slab calving events.

During the summer monsoon in 2000, Pond 7092 drained out through conduit C1 in the southeastern exposed ice margin of the basin. The conduit was exposed below the water-line as the ice faces in the basin retreated by calving. As drainage proceeded conduit C1 was rapidly enlarged by thermal erosion. The large size of the conduit and the inverted 'T'-shaped profile, together with the existence of a single, well-defined thermo-erosional notch in the southeastern ice face, suggested that the pond drained in a single rapid event. As the conduit widened a second connection to the conduit was made at C2, although it is suspected that this occurred towards the end of the drainage of Pond 7092. Following the drainage of Pond 7092, the roof of conduit C1 began to collapse and subside at the southern end. In October 2000, there were six small shallow ponds on the floor of the basin, with the three largest of them occupying the same areas as in October 1998.

Between October 2000 and October 2001, the basin had continued to expand, but at a lower rate. The cessation of calving around the exposed ice margins brought about a relaxation of the ice face slope angles. The reduced slope angles allowed the progradation of talus cones down the exposed ice margins, reducing the area of exposed ice around the margins and converting parts of the exposed ice margin into debris-covered ice margin. The progradation of debris cones was especially noticeable in the southeast corner of the basin. At the floor of the basin there had been several changes in the size and distribution of the small ponds. Two of the ponds had disappeared completely due to in-filling by debris. Ponds A and B had decreased in size through evaporation. In contrast, Pond C had increased in size due to inputs of meltwater from a supraglacial stream running under the debris. Pond D had also increased in size due to inputs of meltwater from the adjacent ice face and an englacial conduit. Several holes that punctuated the silt and sand layers on the basin floor were interpreted as subsidence along supraglacial or shallow englacial meltwater channels that followed planes of structural weakness in the ice below the debris mantle. Sagging of debris layers within a crevasse-fill feature at the top of Face 1 also provided evidence for localised bottom melting along planes of weakness at the floor of a former basin.

Between October 2001 and October 2002, sliding and slumping of debris down the exposed ice faces and the progradation of debris cones had considerably decreased the length of the exposed ice perimeter. The exposed ice margin in the southeast corner of the lake (Face 3), where the connection with the englacial conduit had drained the pond in 2000, appeared to have been entirely converted into a debris-covered ice margin. Most of Face 4 had also been converted into debris-covered ice margin. Progradation of debris cones down Face 1 had considerably decreased the area of exposed ice in the northeast and eastern basin margins. Slumping of the debris cover at the southern margin appeared to be exposing a new ice face.

It seems likely that unless the Pond 7092 basin is flooded once more, the growth of the basin will proceed at a very slow rate. In the immediate future the exposed ice

faces along the northeast and eastern margins of the basin will continue to backwaste slowly, unless they too become converted into debris-covered ice margins by the progradation of talus cones. However, commercial posters and picture postcards of the Pond 7092 basin reveal that the basin experiences cycles of flooding and drainage. The basin appears to undergo periods of rapid enlargement followed by more quiescent periods when little retreat is experienced. Therefore, if the drainage from the Pond 7092 basin becomes blocked again in the future then the basin will refill and a new cycle of basin enlargement will begin.

4.5. Discussion

The three case studies have allowed a detailed examination of the mechanisms and rates of perched supraglacial pond evolution on the Ngozumpa. The following section synthesises the results of these case studies to provide an overview of the mechanisms of pond expansion and drainage.

4.5.1. Pond Expansion Mechanisms

Observation of Pond 7093b showed that ponding of meltwater in topographic hollows at the base of ice-cored debris mounds where ice has been exposed by sliding or slumping of the debris cover could cause the inception of a supraglacial pond. Following the initial formation of Pond 7093b, rapid backwasting and thermo-erosional notch-controlled calving around the exposed ice perimeter caused expansion of the basin in the direction of ice face retreat, and an increase in the length of the exposed ice margin. As backwasting and calving proceeded the exposed ice faces began to steepen, causing sliding of debris from the edges of the exposed ice faces, further increasing the length of the exposed ice margin. These processes of rapid basin enlargement were also occurring in the Pond 7092 and Pond 7093 basins between October 1998 and October 1999.

4.5.2. Retreat Rates

Rapid enlargement of the three pond basins between October 1998 and 2002 occurred around exposed ice margins. The average ice margin retreat rates around the three case study basins between October 1999 and October 2001 are presented in Table 4.1 (p118). The retreat rates were highest at southwest-, northwest- and west-facing ice faces respectively (Table 4.2, p118). North-facing ice margins experienced the lowest average retreat rates. In contrast, little retreat was recorded at debris-covered ice margins. Moraine margins were the most stable margin type. Over time, the reworking of the debris mantle around pond basins can initiate a shift in margin type from exposed ice margins to debris-covered ice margins and *vice versa.*

4.5.3. Calving

Retreat rates in the three basins were highest at ice faces undergoing calving retreat. Much of the calving in the three case study ponds was controlled by the rate of thermo-erosional notching of the exposed ice margins. This concurred with observations of other supraglacial ponds on the Ngozumpa. The most commonly observed types of calving in the case study ponds were the collapse of thermo-erosional notch roofs and flake calving above the water-line. Several larger full-height slab calving events were observed in Ponds 7093 and 7092. The full-height slab calving events tended to occur along planes of structural weakness that were reactivated as the ice margins retreated, and were not controlled by the rate of water-line melting. Re-activation of old crevasses around supraglacial ponds mainly occurred behind very steep ice faces over 15 m in height. This suggests that planes of weakness behind ice margins are re-activated after a certain critical ice face angle and height is exceeded. Most of the full-slab calving events observed involved pillars of ice that had formed where two or more planes of structural weakness intersected immediately behind an ice face. In October 1999, three consecutive ice pillar calving events occurred at the northeast exposed ice margin of Pond 7092 where there were extensive planes of weakness behind the ice margin. Planes of structural weakness were also responsible for the high retreat rates experienced at

the southeast exposed ice margin of Pond 7092 between October 1999 and October 2000. The observed calving events at this margin were 'ice slumping' events, however, given the height and angle of the face, it is possible that full-height slab calving events may also have occurred. During the three field seasons only one subaqueous calving event was witnessed and it is proposed that this is an infrequent process at the Ngozumpa Glacier. This is due to the thick debris mantles at the floor of supraglacial ponds that offset the buoyancy forces that drive subaqueous calving.

4.5.4. Controls on Pond Water Level

Increases in water levels in the three ponds were controlled by: inputs of meltwater from backwasting and calving ice margins; melting at debris-covered ice margins; precipitation; meltwater inputs from englacial conduits and supraglacial conduits emerging from under the debris; and displacement of the pond water by debris falling and sliding from the basin margins. Decreases in pond water levels were controlled by evaporation and drainage of pond water from the basin via englacial conduits.

4.5.5. Pond Drainage

Two pond drainage events occurred at the case study sites between October 1998 and October 2002. Both events were triggered when backwasting and calving around exposed ice margins caused a connection to be made with the englacial conduit system below the water level. Pond 7092 drained rapidly after backwasting and calving retreat at the southeast ice margin exposed an englacial conduit below the water level. Once the connection was made, rapid enlargement of the conduit walls by thermal erosion increased the rate of drainage in a positive feedback cycle until almost all of the pond water in the basin had drained out. It is suspected that the water from the Pond 7092 basin drained out into the Spillway Lake, causing extensive collapse of a conduit roof north of the Spillway Lake (See Chapter 5, Section 5.5).

Between October 2000 and 2001, a second smaller drainage event took place in Pond 7093c. Drainage of the pond was most probably triggered when ice face retreat at the southern exposed ice margin caused a connection with an englacial conduit below the water-line. It is possible that water draining out through this conduit was channelled into the Pond 7092 basin.

4.5.6. Temporary Storage

The drainage of perched pond basins via connections with the englacial conduit system implements a check on the positive feedback cycle of rapid basin expansion. The frequent exposure of englacial conduits within exposed ice faces indicates that the englacial conduit network is extensive and can exist at shallow depths within the glacier body. This is a reflection of the proliferation of glacial karst features within the stagnating glacier tongue.

The englacial conduit network not only provides a mechanism for the drainage of perched pond basins, but, as has been recorded above, can also provide them with inputs of meltwater. It is believed that inputs of meltwater from an englacial conduit exposed in Pond 7092 was partially responsible for the flooding of the basin between October 1998 and October 1999.

Given the extent of the englacial conduit network, it is inevitable that many englacial drainage connections will be made with the large number of perched supraglacial pond basins that exist on the Ngozumpa Glacier. This affirms the theory of temporary storage, whereby meltwater may be stored in several different supraglacial pond basins as it travels downglacier towards the Spillway Lake.

4.5.7. Progradation of Debris Cones

After a period of rapid expansion between October 1998 and October 1999, the Pond 7093 basin experienced a decrease in the rate of basin expansion between October 1999 and October 2000. This was due to the progradation of talus cones at the base of the ice faces. As the ice face retreated, high rates of debris delivery from the tops

of the exposed ice faces caused the build up of extensive debris cones at the base of the ice faces. These debris cones protected the ice face from thermo-erosional notching at the water-line, inhibiting calving and lowering the rate of ice face retreat. Between October 2000 and 2001, backwasting of the ice margins in the basin distanced them further from the pond perimeter. The cessation of calving gradually caused the ice face slope angles to decrease and further progradation of the talus cones brought about a decrease in the length of the exposed ice margin. By October 2002, most of the exposed ice margins had been converted into debris-covered ice margin.

Progradation of debris cones was also rapid in the Pond 7092 basin following the drainage of the pond during the 2000 summer monsoon. The cessation of rapid calving retreat and the consequent relaxation of the ice margin slope angles allowed extensive debris cones to build up around the backwasting ice margins. Between October 2000 and October 2002, the rate of basin expansion was progressively lowered as progradation of debris cones reduced the length and area of the exposed ice perimeter by converting exposed ice margins into debris-covered ice margins.

4.5.8. Cycles of Basin Expansion and Quiescence

Wiseman (2004) noted that in October 1998 there were patches of laminated sands and silts covering the floor of the Pond 7092 basin. These sediments were interpreted as evidence for more extensive ponding in the basin prior to October 1998. Commercial picture postcards of the glacier provide further evidence for higher water levels in the Pond 7092 basin prior to October 1998. Following the flooding of the Pond 7092 basin between April and October 1999, it was inferred that the basin experienced periods of flooding and rapid calving retreat followed by drainage and decreased rates of basin expansion (Wiseman, 2004). The rapid drainage of the Pond 7092 basin during the summer monsoon in 2000 and the decrease in basin expansion rate between October 2000 and October 2001 described in this study provides the first observational evidence of the cyclical nature of perched supraglacial pond basins. Furthermore, it is also provides the first evidence

for internal ablation and conduit enlargement by relatively warm floodwater, a process that was inferred by Sakai et al. (2000a). It is expected that if the drainage connections from the 7092 basin become blocked once more, the basin could undergo further cycles of rapid expansion, drainage, and quiescence in the future.

Table 4.1. Ice Face Retreat Rates (1999-2001)

Pond 7093b (2000-2001)					
	Main Face (N facing)				
Retreat Rate (m a^{-1})	11.91				
Pond 7093 (1999-2000)					
	Face 1 (NW facing)	**Face 2 (SW facing)**	**Face 3 (NW facing)**	**Face 4 (SW facing)**	**Moulin Face (W facing)**
Retreat Rate (m a^{-1})	17.85	7.25	24.54	11.7	7.85
Pond 7093 (2000-2001)					
	Face 1 (NW facing)	**Face 2 (W facing)**	**Face 3 (NW facing)**	**Moulin face (W facing)**	
Retreat Rate (m a^{-1})	20.96	17.27	13.64	17.36	
Pond 7092 (1999-2000)					
	Face 1 (W facing)	**Face 2 (W facing)**	**Face 3 (NW facing)**		
Retreat Rate (m a^{-1})	25.76	32.37	13.95		
Pond 7092 (2000-2001)					
	Face 1 (SW facing)	**Face 2 (W facing)**	**Face 3 (SW facing)**	**Face 4 (SW facing)**	**Face 5 (N facing)**	**Face 6 (N facing)**
Retreat Rate (m a^{-1})	20.92	28.03	58.51	36.1	5.86	9.17

Table 4.2. Ice Face Retreat Rates and Face Orientation

Face Orientation	**N Facing**	**SW Facing**	**W Facing**	**NW Facing**
Annual Retreat Rates in m a^{-1}	11.91 5.86 9.17	7.25 11.7 20.92 58.51 36.1	7.85 17.27 17.36 25.76 28.03	17.85 24.54 20.96 13.64 32.37 13.95
Average Annual Retreat Rates (m a^{-1})	**8.98**	**26.90**	**19.25**	**20.55**

Chapter 4 Figures

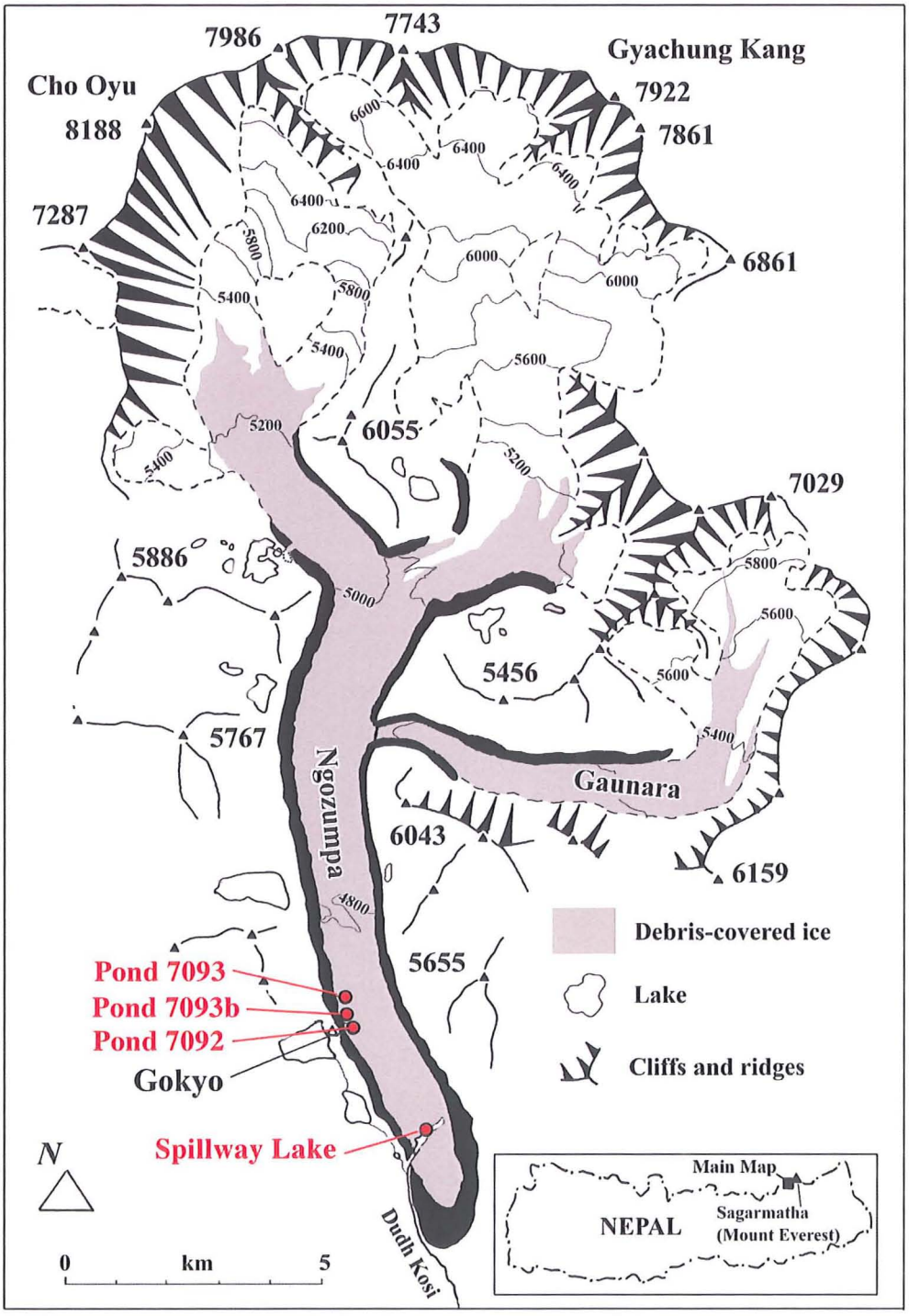

Figure 4.1. Pond Case Study Site Location Map. Modified from Benn et al. (2001).

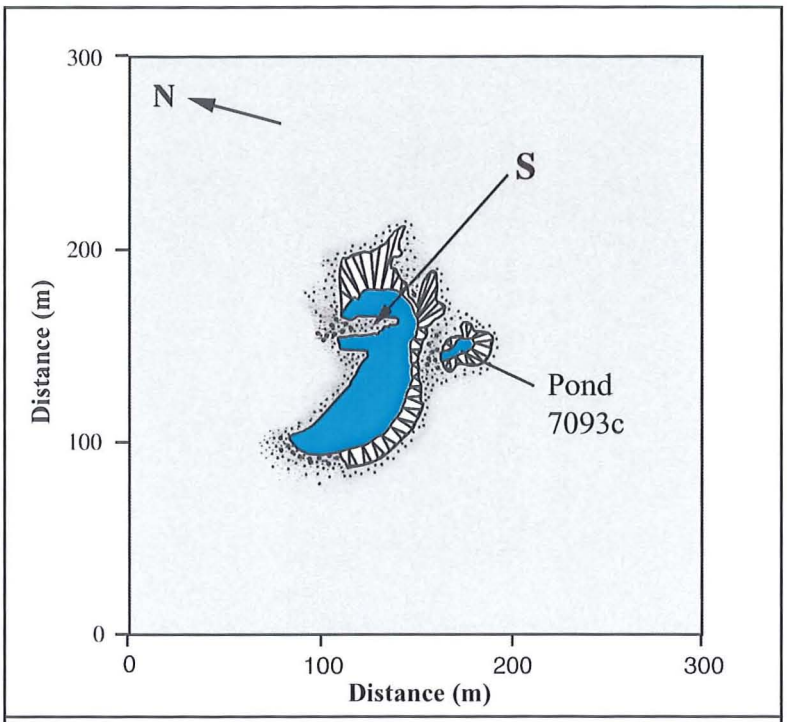

Figure 4.2. Pond 7093b Survey Map October 2000

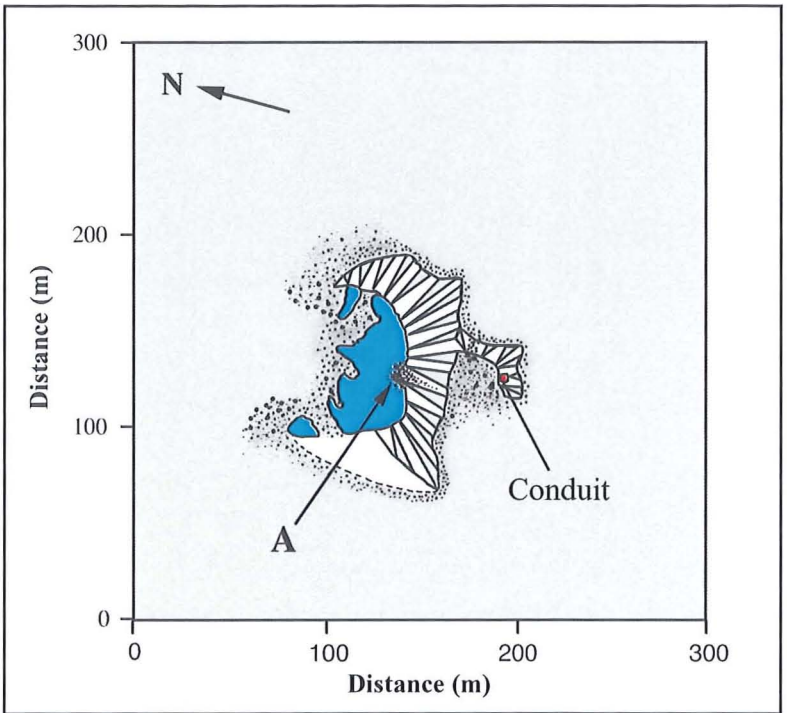

Figure 4.3. Pond 7093b Survey Map October 2001

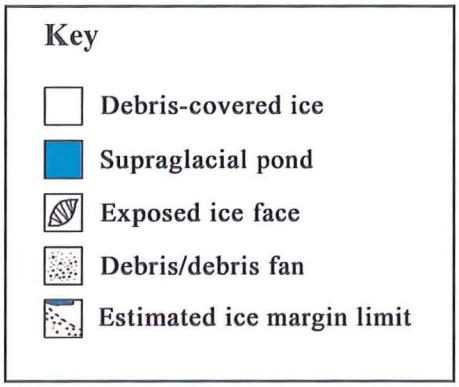

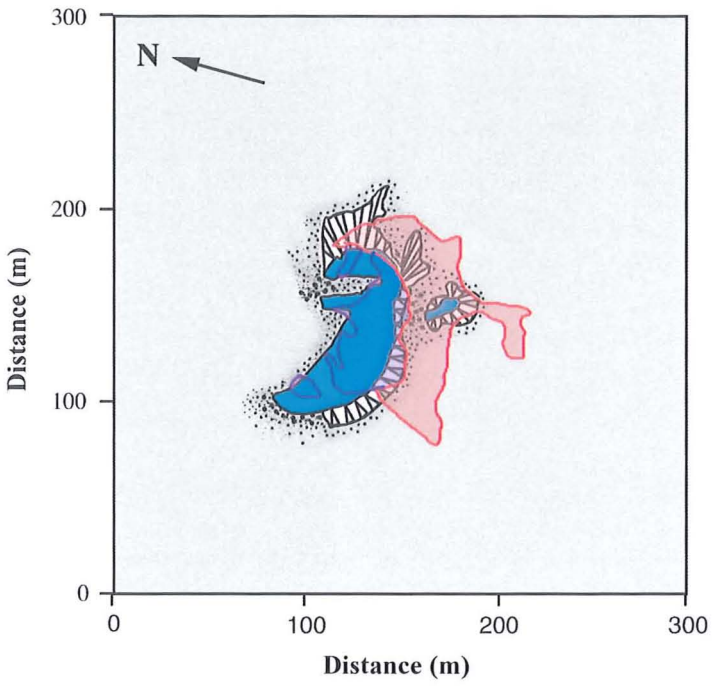

Figure 4.4. Pond 7093b Survey Comparison Map, October 2000 - October 2001

Key

- Debris-covered ice
- Position of pond in 2000
- Position of ice faces in 2000
- Debris/debris fan
- Position of ice faces in 2001
- Position of pond in 2001

Figure 4.5. Pond 7093b in October 1999. Viewed from the glacier looking west.

Figure 4.6. Pond 7093b 11th October 2000. The icebergs in the pond are from a waterline calving event at the southern ice margin. Note the previous failure scar and fracture on the eastern ice margin. Viewed from the western lateral moraine.

Figure 4.7. Pond 7093b 30th October 2000. A large flake calving event has occurred along a stress-release fracture above a thermo-erosional notch.

Figure 4.8. Pond 7093b in October 2000. Note the thermo-erosional notch around the pond perimeter and the stress-release fracture in the southern ice margin. Viewed from the north.

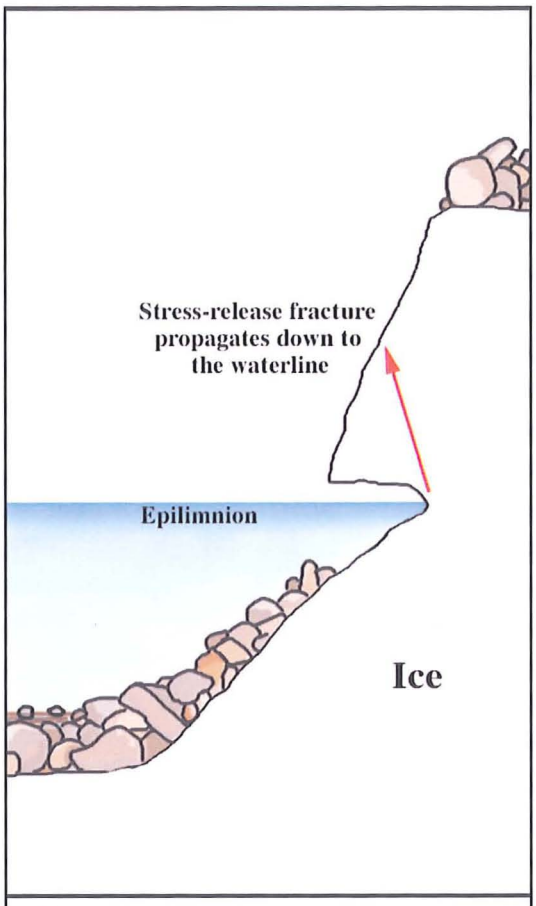

Figure 4.9. Diagram showing the propagation of a stress-release fracture above a thermo-erosional notch. This process causes flake calving events above the waterline.

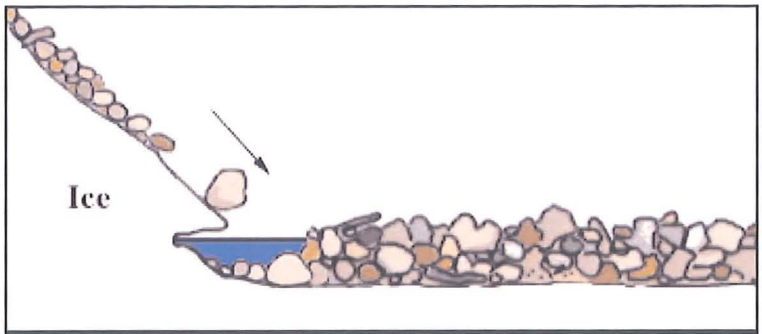

Figure 4.10. High rates of debris deposition at the base of an ice face can cause a spit to develop in a pond perpendicular to the direction of ice face retreat.

Figure 4.11. Pond 7093b on the 19th October 2001. Note the position of the white boulder indicating a decrease in the depth of the pond. Viewed from the north.

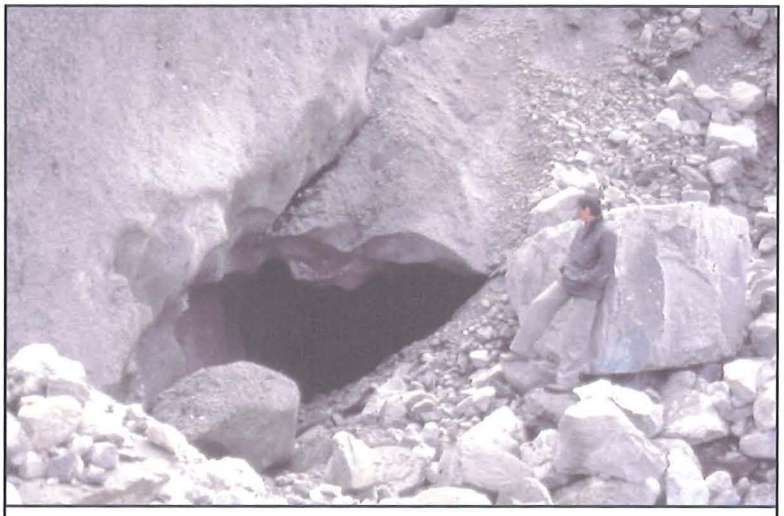

Figure 4.12. The englacial conduit that drained the small pond to the south of Pond 7093b. The conduit most probably formed along the existing debris band present within the ice. Person for scale.

Figure 4.13. Pond 7093b 7th October 2001 viewed from the north. Note the icebergs floating in the pond. These are a result of a large flake calving event at the southern ice margin.

Figure 4.14. Pond 7093b 19th October 2001 viewed from the north. A second waterline calving event has occurred below a stress-release fracture in the south-western ice margin.

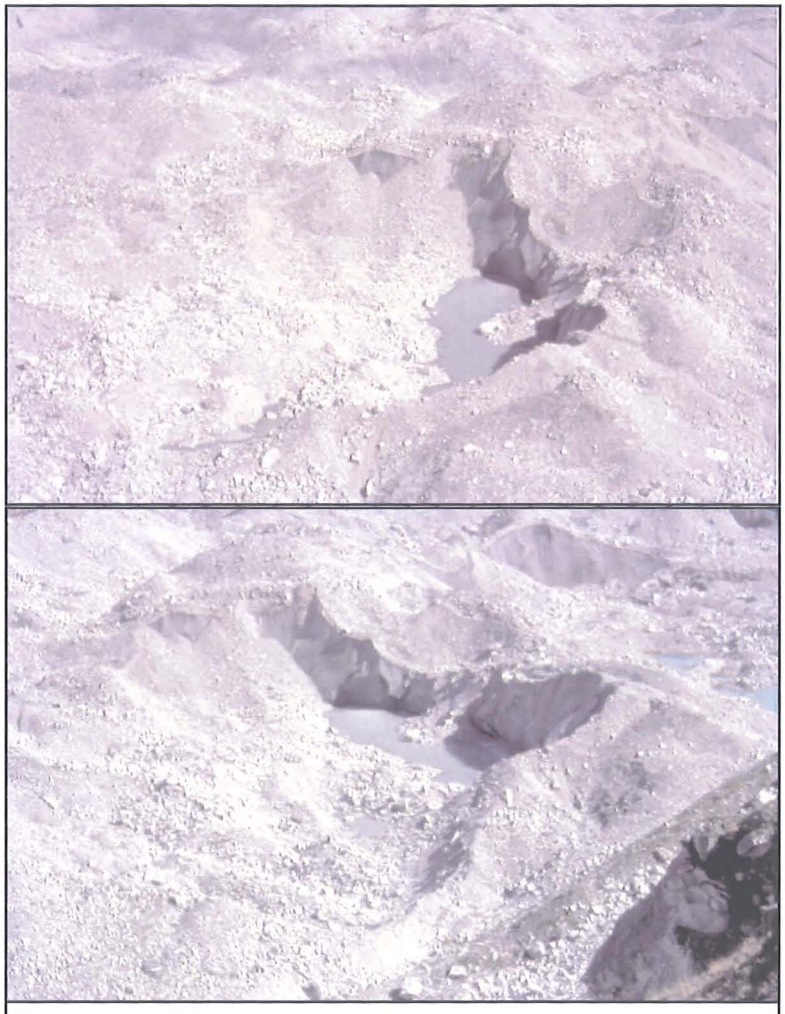

Figure 4.15. Two views of Pond 7093b during October 2002. Pictures taken by Lindsey Nicholson from the western lateral moraine.

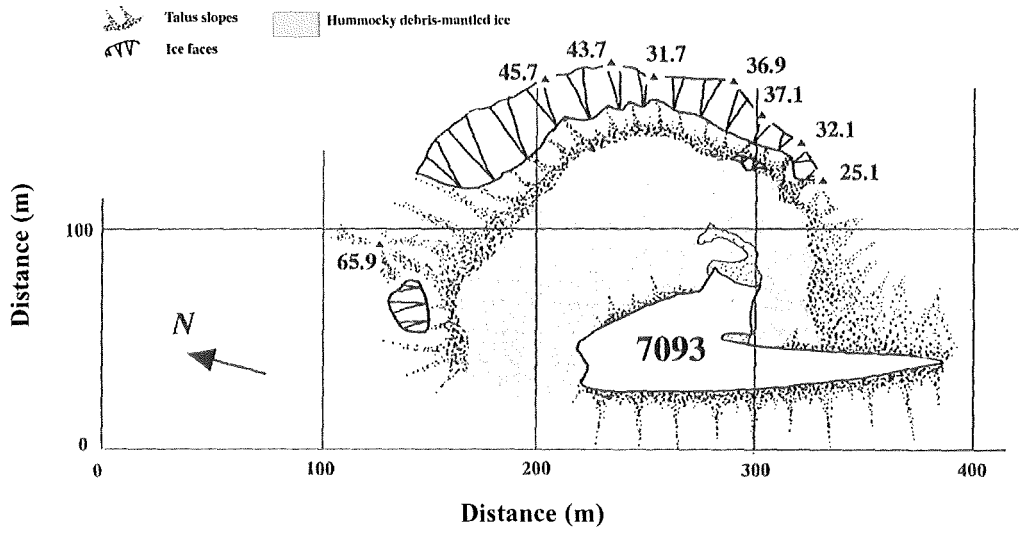

Figure 4.16. Pond 7093 Survey Map October 1998 (from Benn et al., 2001)

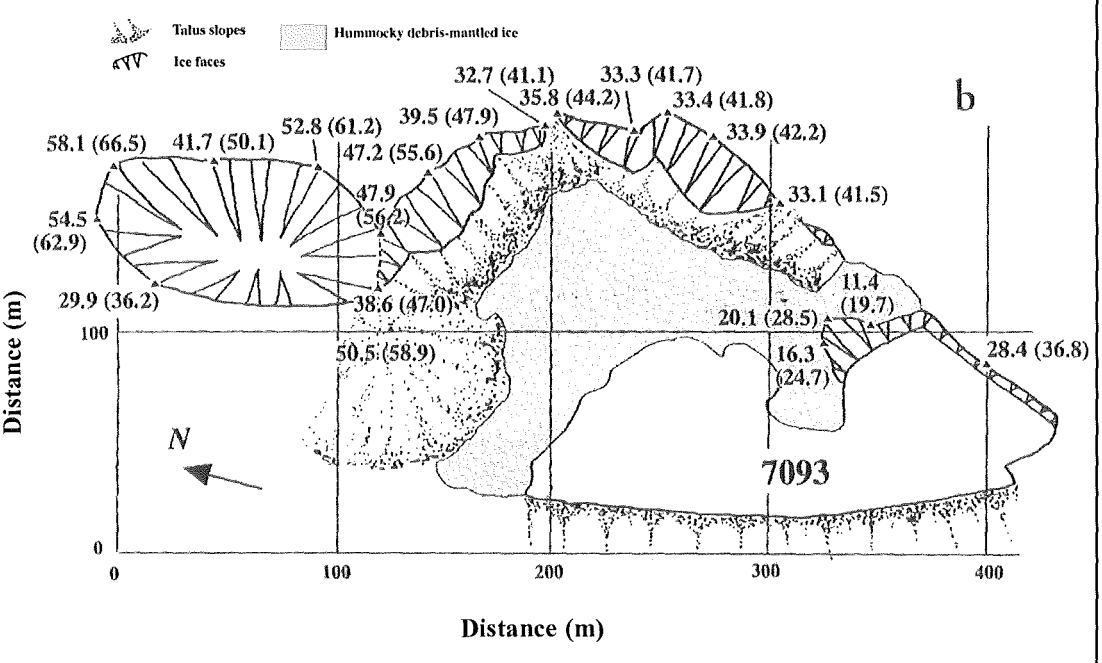

Figure 4.17. Pond 7093 Survey Map October 1999 (from Benn et al., 2001)

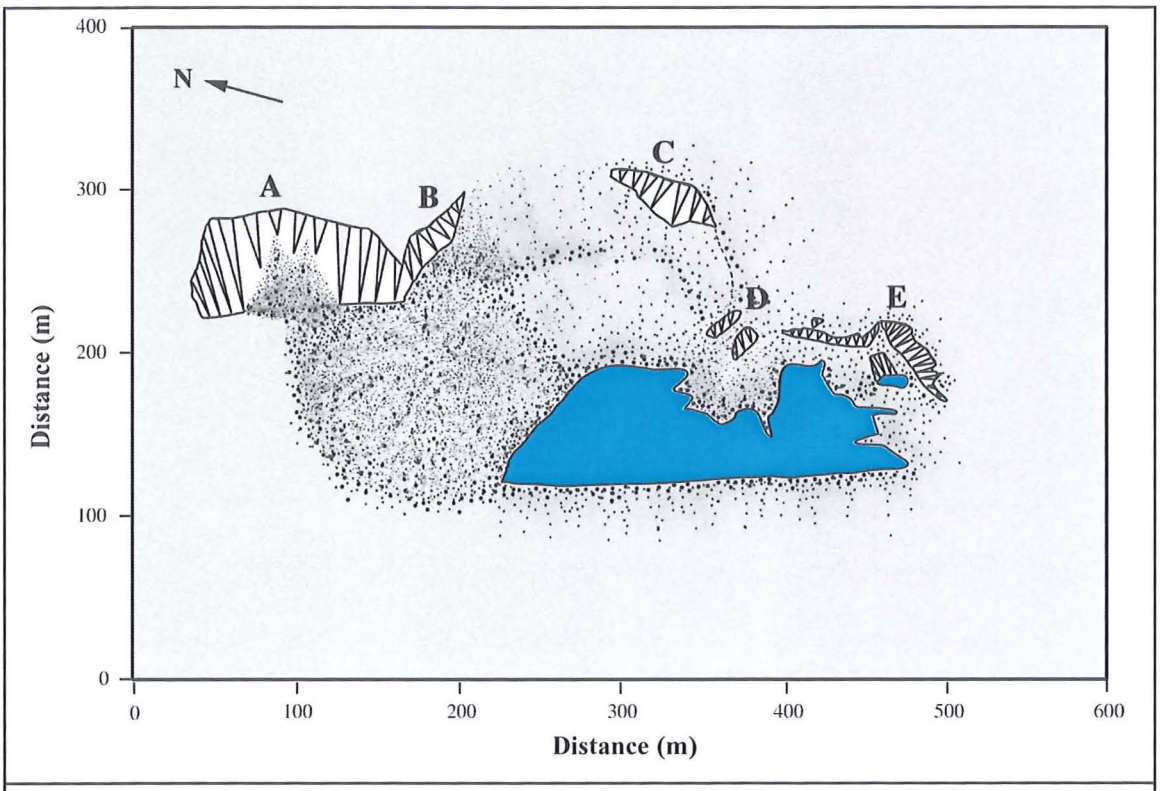

Figure 4.18. Pond 7093 Survey Map October 2000

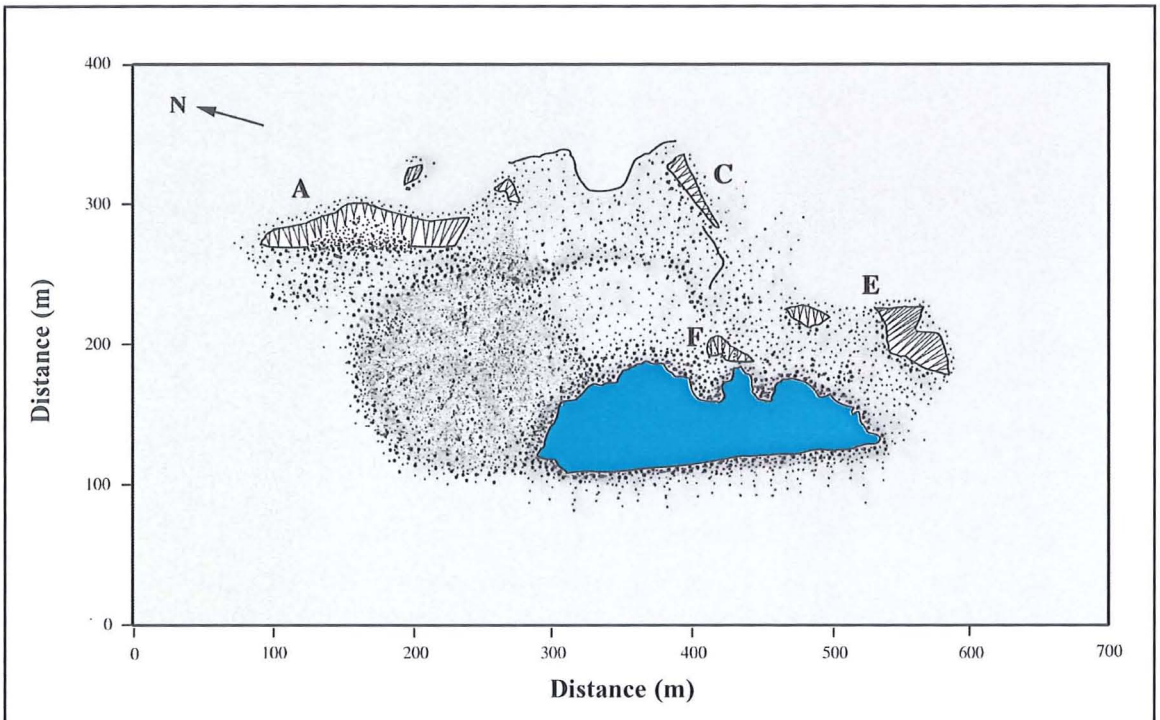

Figure 4.19. Pond 7093 Survey Map October 2001

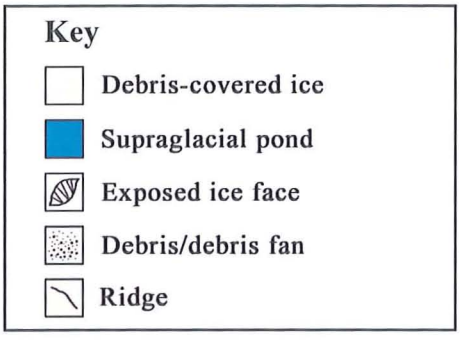

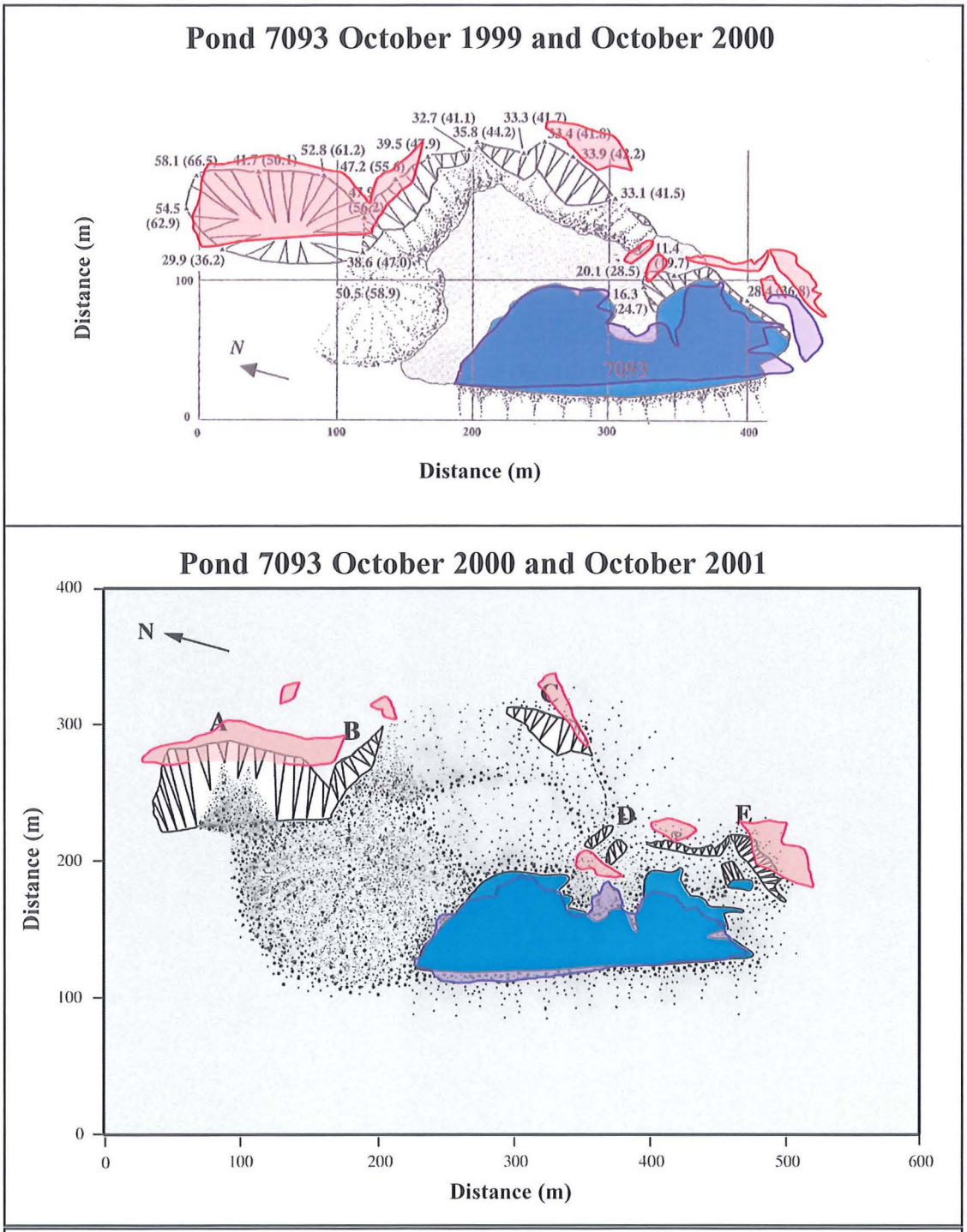

Figure 4.20. Pond 7093 Survey Map Comparison Map October 1999 - October 2001

Figure 4.21. Pond 7093 in September 1998 viewed from the western lateral moraine looking southeast. Photograph taken by Doug Benn.

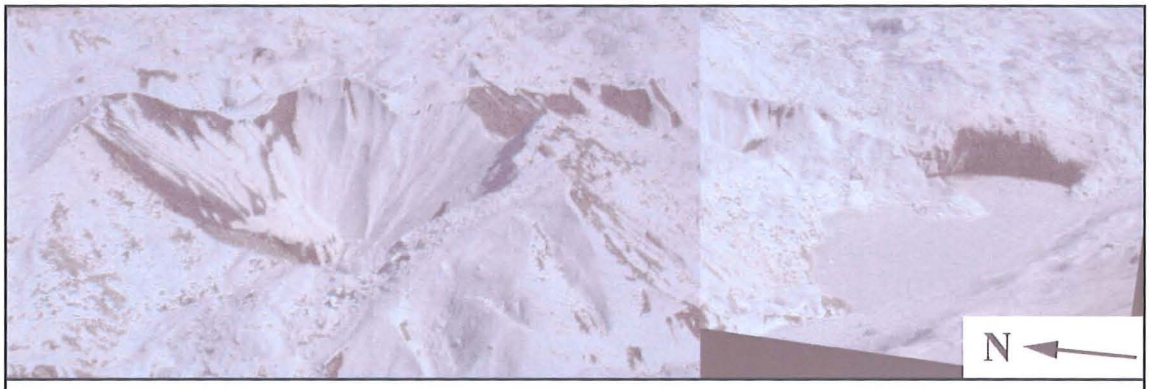

Figure 4.22. Pond 7093 in October 1999 viewed from the western lateral moraine looking southeast. The water level and the pond area had increased and the south-east pond margin had been converted into an exposed ice margin undergoing rapid calving retreat. Note the large active moulin to the north of the basin.

Figure 4.23. Pond 7093 in October 1999. Viewed from the western lateral moraine looking northeast.

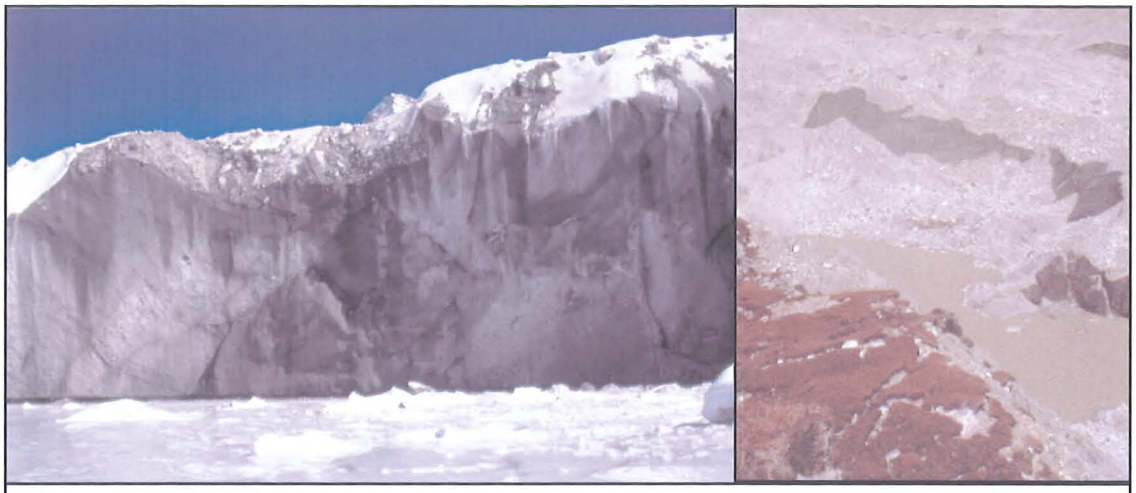

Figure 4.24. Pond 7093 in October 1999. Thermo-erosional notching and flake calving at the southeast exposed ice margin. Viewed from the pond surface looking east and from the western lateral moraine looking northeast respectively.

Figure 4.25. A block of ice is detached as intersecting planes of weakness are reactivated in Pond 7093 during October 1999 viewed from the pond surface looking east. Notice also the deep thermo-erosional notch to the right of the detached ice block.

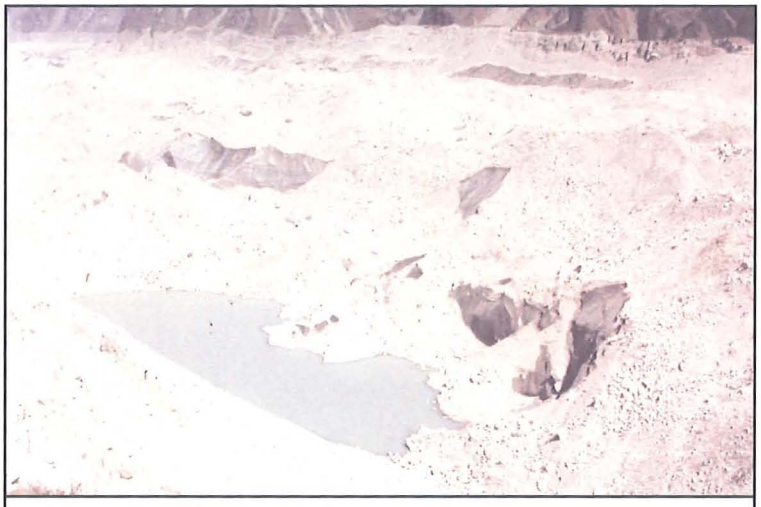

Figure 4.26. Pond 7093 in October 2000. Viewed from the western lateral moraine looking northeast.

Figure 4.27. Pond 7093 in October 2000 viewed from the western lateral moraine looking southeast. The water level had increased by 1m but the total pond area had decreased due to the progradation of debris cones around the pond margin. The large moulin feature to the north of the basin had become choked with debris and was no longer active.

Figure 4.28. Pond 7093 in October 2001 viewed from the western lateral moraine looking northeast. The pond area and water level had decreased. The progradation of talus cones and the continued backwasting of the ice faces had converted the southeastern exposed ice margin into a debris-covered ice margin.

Figure 4.29. Continued backwasting of the moulin feature to the north of Pond 7093. Viewed from the western lateral moraine looking northeast in October 2001.

Figure 4.30. Pond 7093 in October 2002 viewed from the western lateral moraine looking southeast. The water level of the pond appears to have decreased once more and the ice faces around the basin margin had become covered over by debris. A large section of ice had been exposed on the lower slopes of the large debris cone in the foreground due to slipping of debris on the steepening slope angles. Picture taken by Lindsey Nicholson.

Figure 4.31. Pond 7093 in October 2002 viewed from the western lateral moraine looking northeast. Picture taken by Lindsey Nicholson.

Figure 4.32. The ice faces around the moulin feature to the north had continued to backwaste and there had been further progradation of debris cones on the face. Viewed from the western lateral moraine looking northeast in October 2002. Picture taken by Lindsey Nicholson.

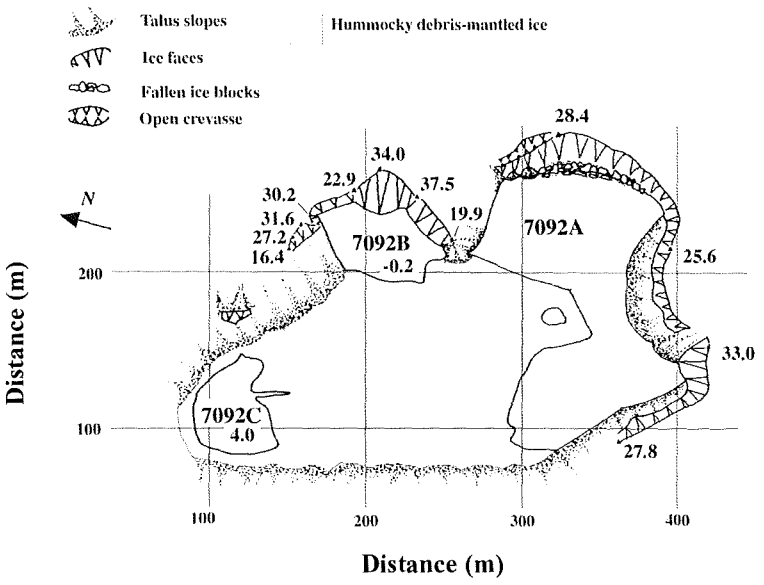

Figure 4.33. Pond 7092 Survey Map October 1998 (from Benn et al., 2001)

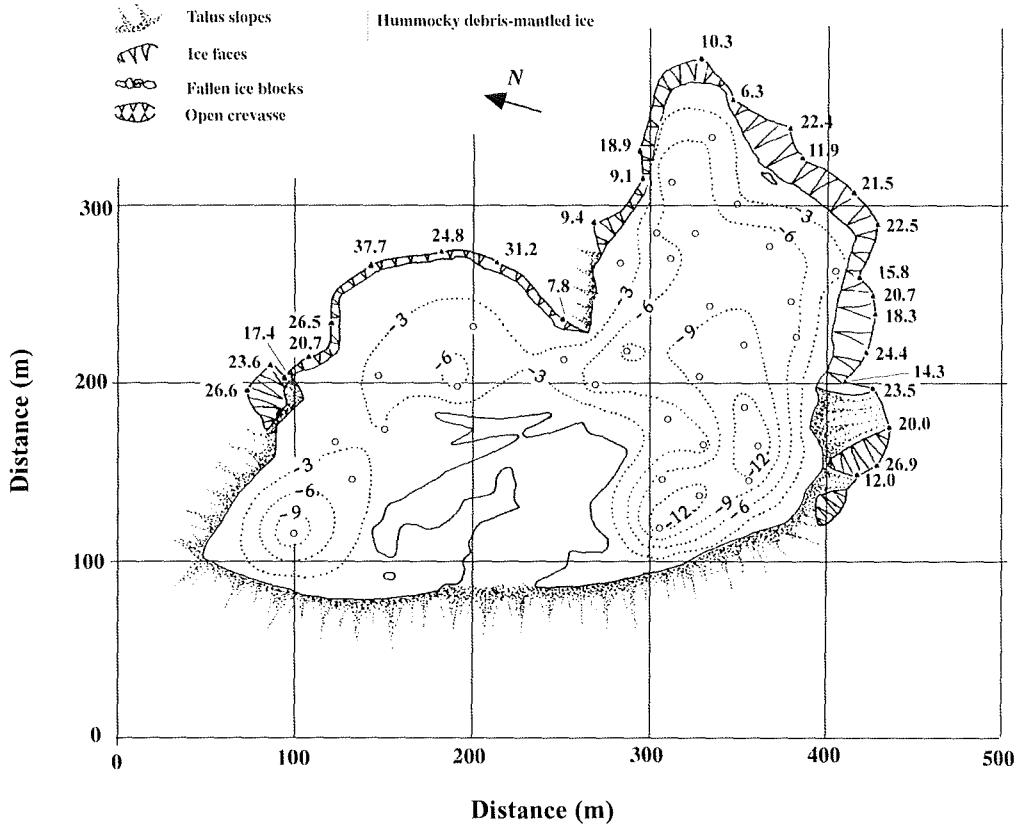

Figure 4.34. Pond 7092 Survey Map October 1999 (from Benn et al., 2001)

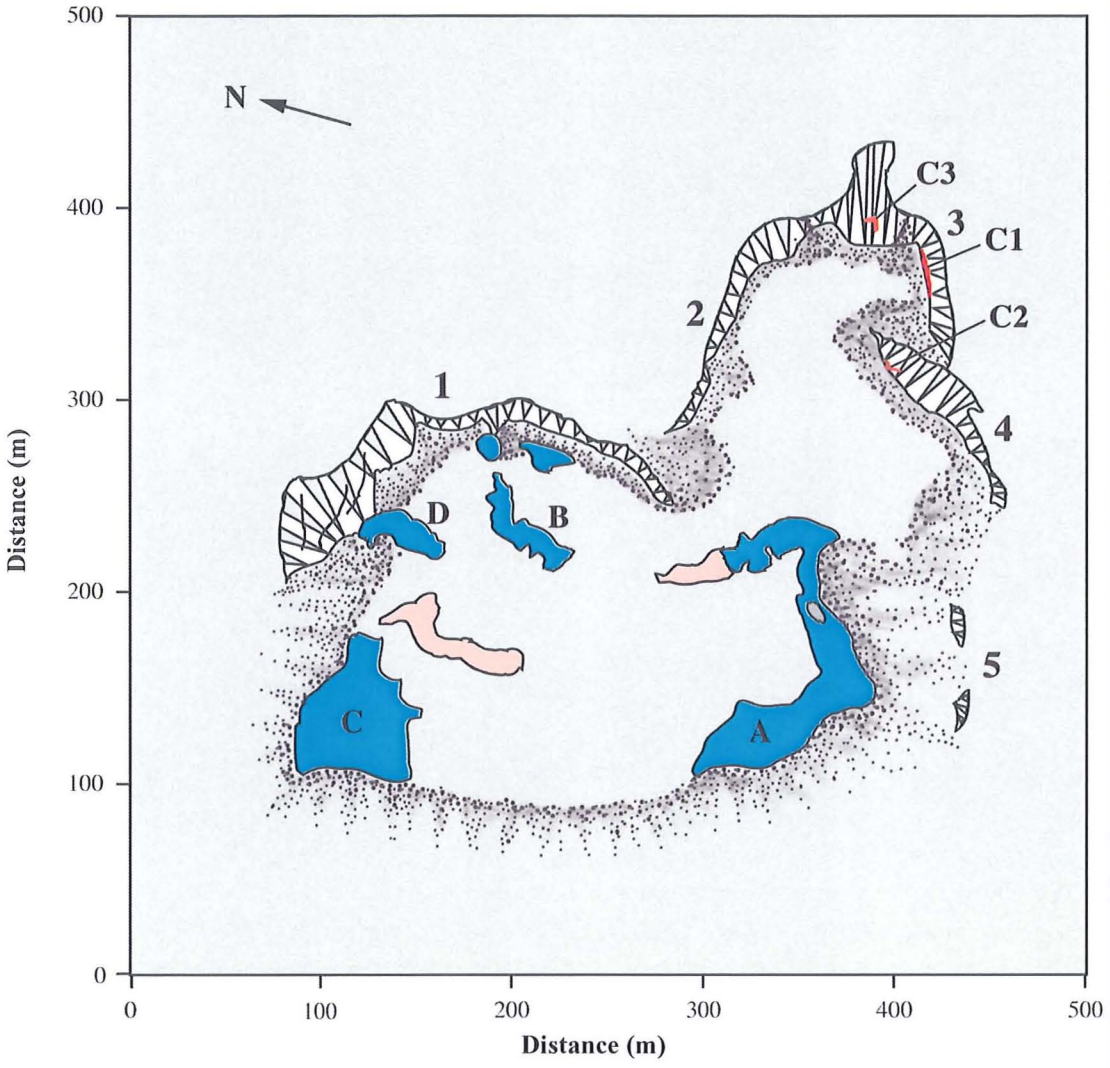

Figure 4.35. Pond 7092 Survey Map October 2000

Key

- Debris-covered ice
- Pond water
- Exposed ice face
- Silt/sand drapes
- Exposed conduit
- Crevasses
- Debris/debris fan

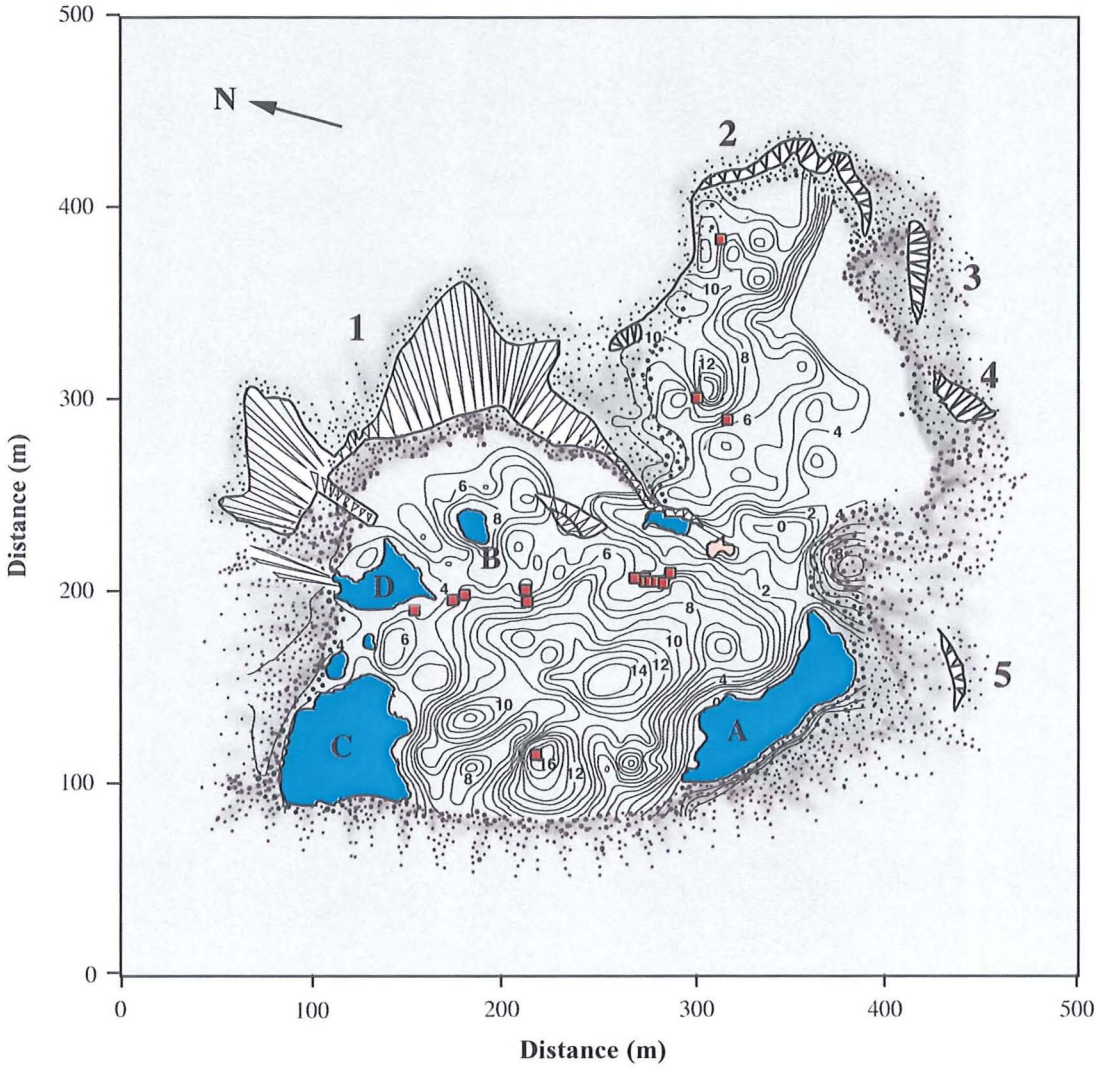

Figure 4.36. Pond 7092 Survey Map October 2001

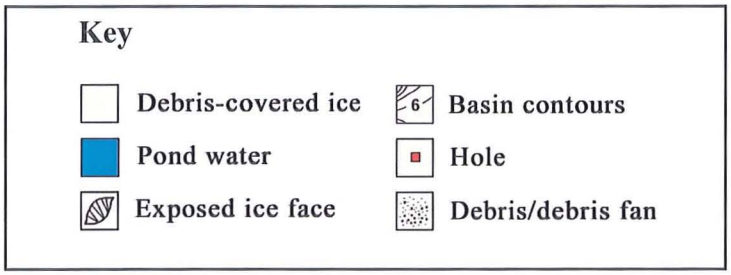

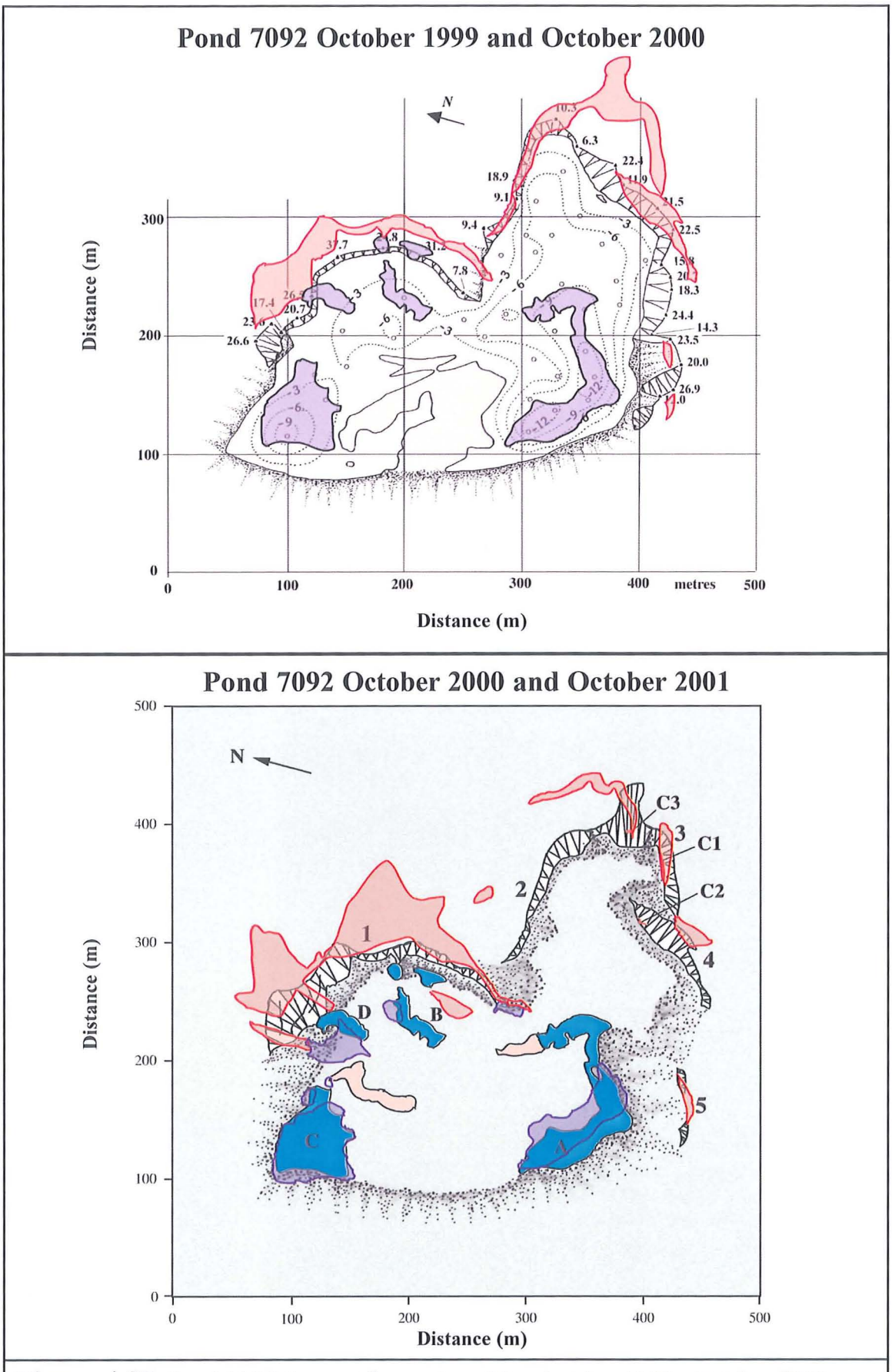

Figure 4.37. Pond 7092 Survey Comparison Map October 1999 - October 2001

Figure 4.38. Pond 7092 in September 1998 viewed from the western lateral moraine looking southeast. Photograph taken by Doug Benn.

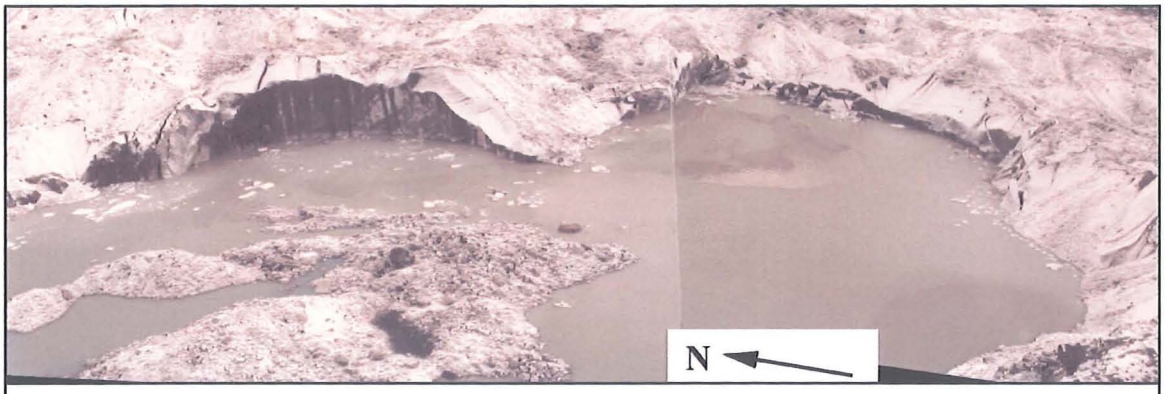

Figure 4.39. Pond 7092 in October 1999. Viewed from the western lateral moraine looking northeast. The basin flooded during the summer monsoon and rapid calving retreat was experienced at the northeastern and southeastern exposed ice perimeters. Note the full height calving failure scar on the left-hand ice face.

Figure 4.40. Pond 7092 in October 1999 viewed from the western lateral moraine looking southeast. Note the re-activated crevasse trace behind the ice face on the left.

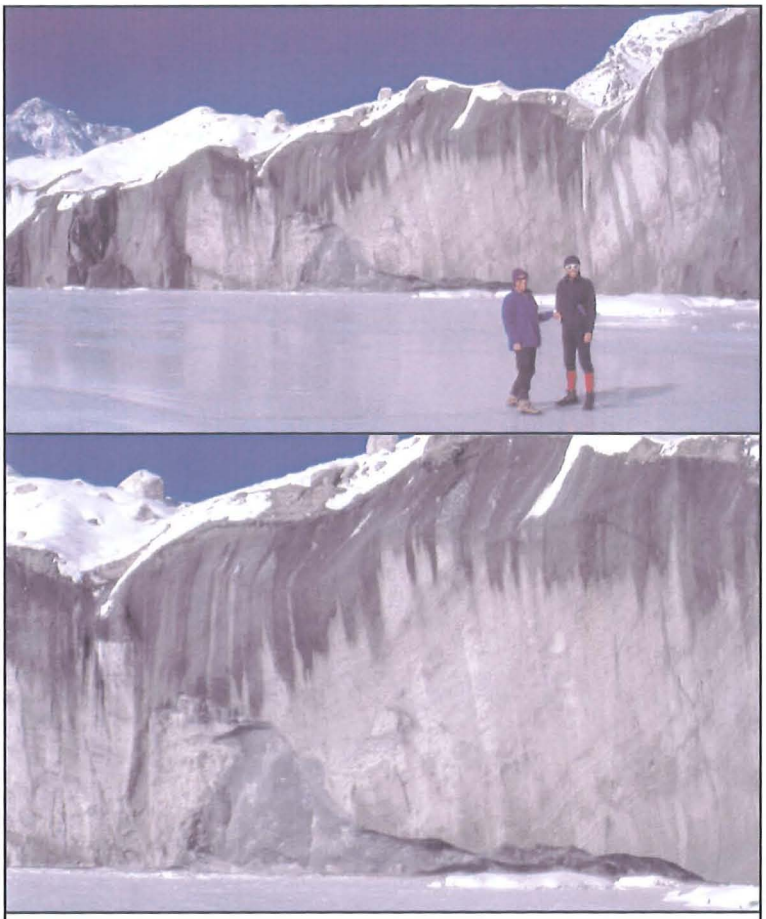

Figure 4.41. Pond 7092 in October 1999. Viewed from the pond surface looking east at the eastern exposed ice pond margin. A large flake calving event above a thermo-erosional notch removed a flake of ice 1m high and 28m long.

Figure 4.42. Pond 7092 in October 1999 viewed pond surface looking south. The failure of the roof of a thermo-erosional notch left a large arcuate recess in the base of the ice cliff. Person for scale.

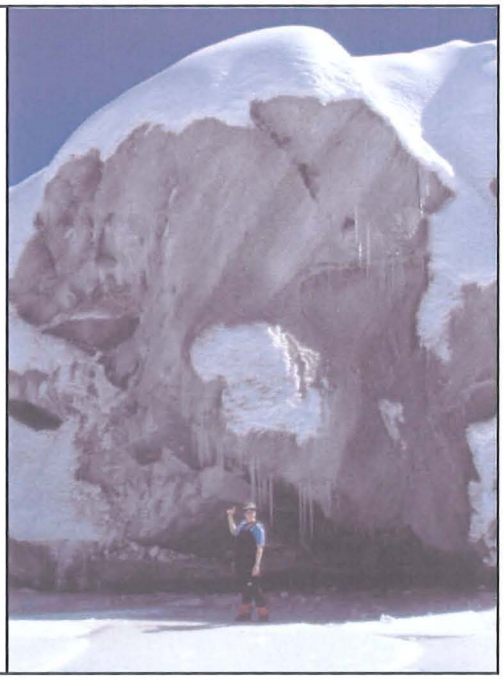

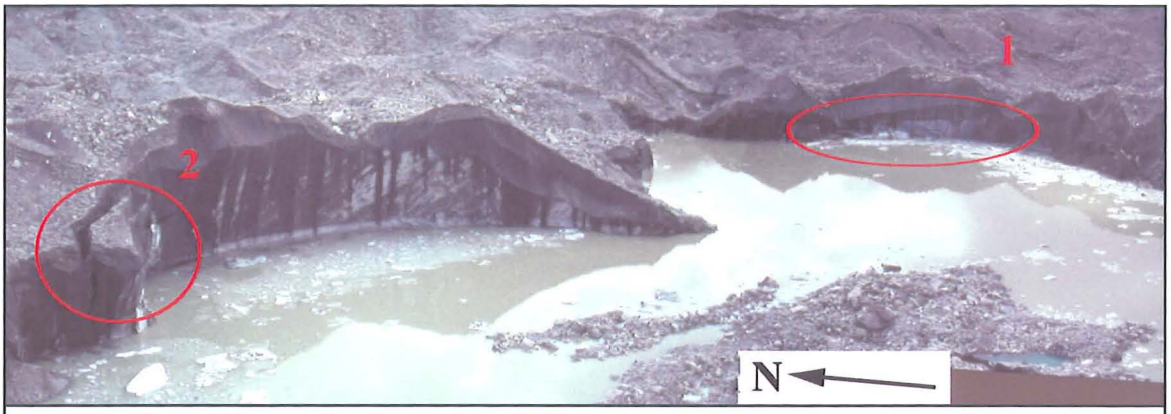

Figure 4.43. Pond 7092 in October 1999. Viewed from the western lateral moraine looking southeast. **1.** A large flake calving event above a thermo-erosional notch **2.** A pillar of ice is being separated from the main face due to the reactivation of an old crevasse. The icebergs in the water beneath the pillar are from a full-slab calving event that removed a section of ice from the front of the pillar.

Figure 4.44. The same ice face as above viewed from the pond surface looking north. A second pillar is forming in the same section of ice.

Figure 4.45. Pond 7092 in October 1999. Viewed from the western lateral moraine looking northeast. The second pillar of ice calved from the main 10m west of the previous calving events. Note that another large crevasse is being re-activated behind the ice face.

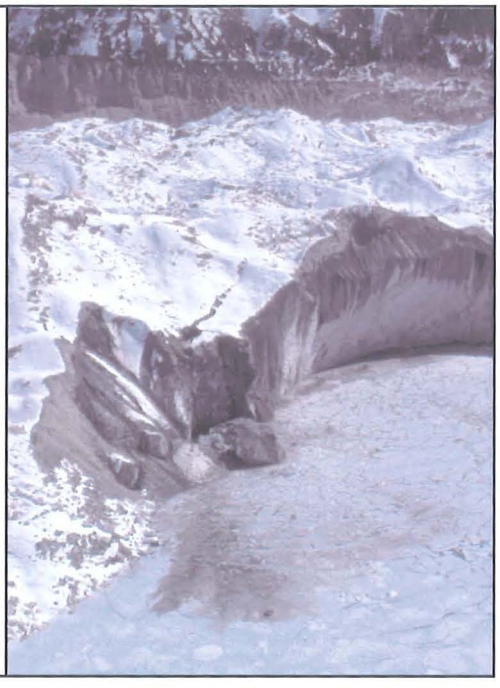

Figure 4.46. Stacked longitudinal crevasses behind the southeast ice margin and thermo-erosional notching at the waterline results in ice slumping . Viewed from the pond surface looking east.

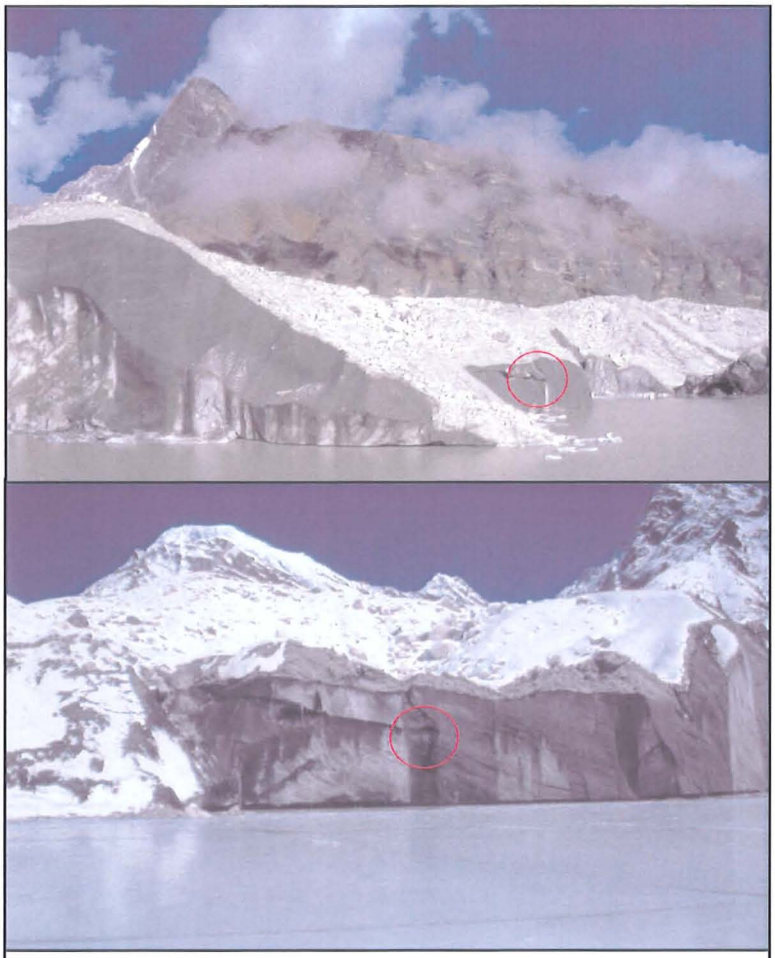

Figure 4.47. An englacial conduit in the southeast corner of the pond. A melt water stream entered the pond via this conduit in September 1999 but ceased to flow after a metre of snow fell on the valley during October. Viewed from the pond surface looking east.

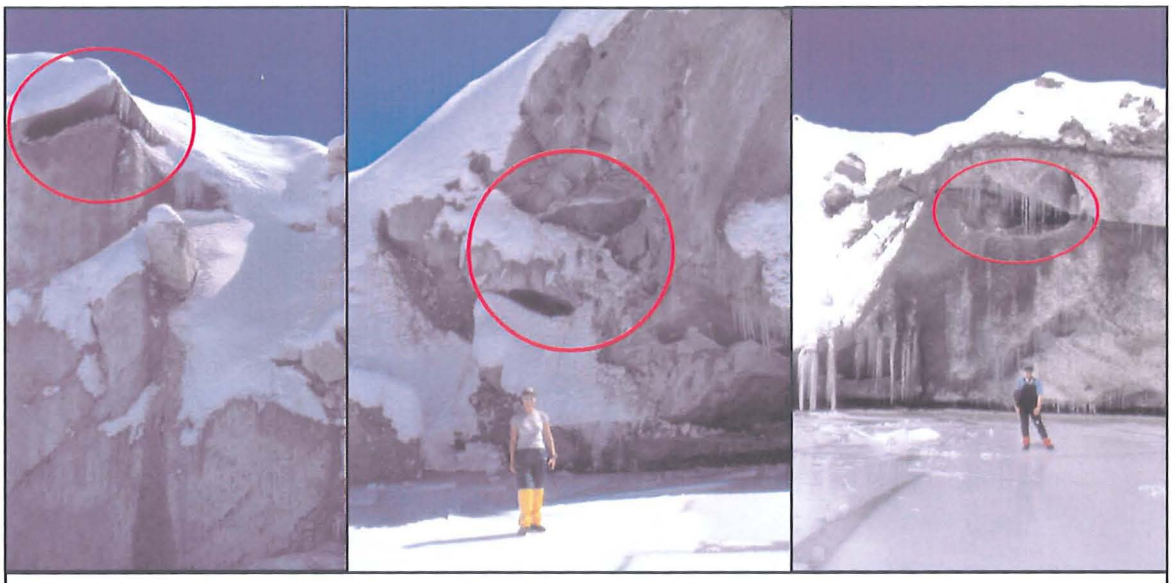

Figure 4.48. Several other dry conduits were observed in the ice faces around the southeastern corner of the pond. These conduits may have provided meltwater inputs into Pond 7092 during the summer monsoon.

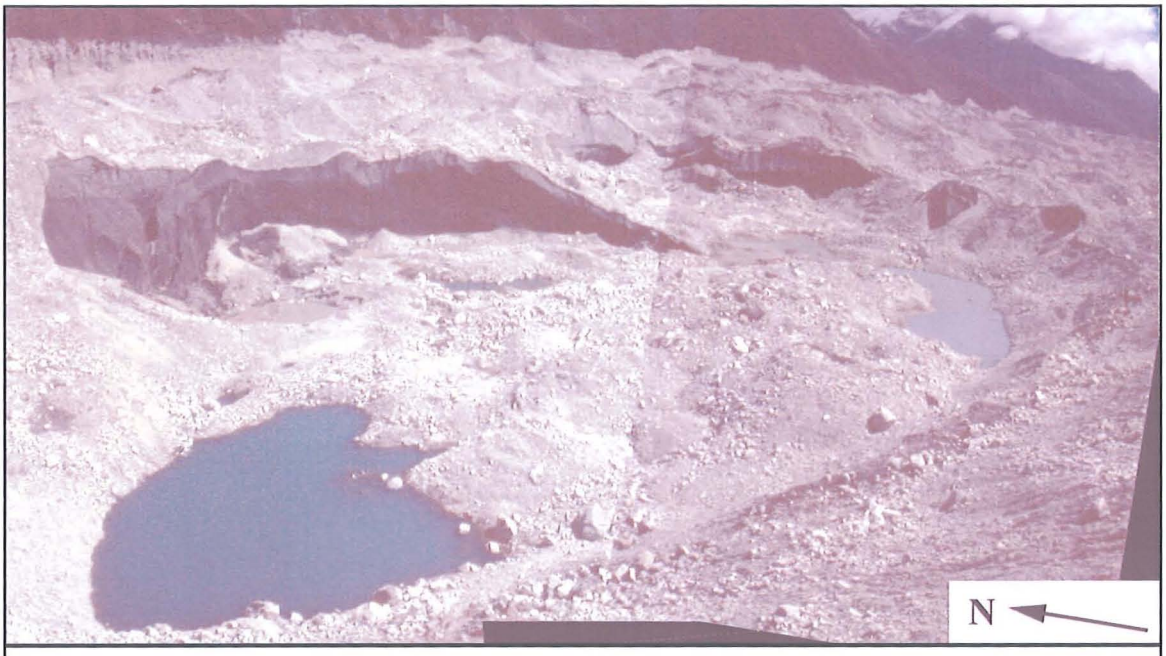

Figure 4.49. Pond 7092 in September 2000 viewed from the western lateral moraine looking southeast. The pond drained out through a conduit in the southeast margin.

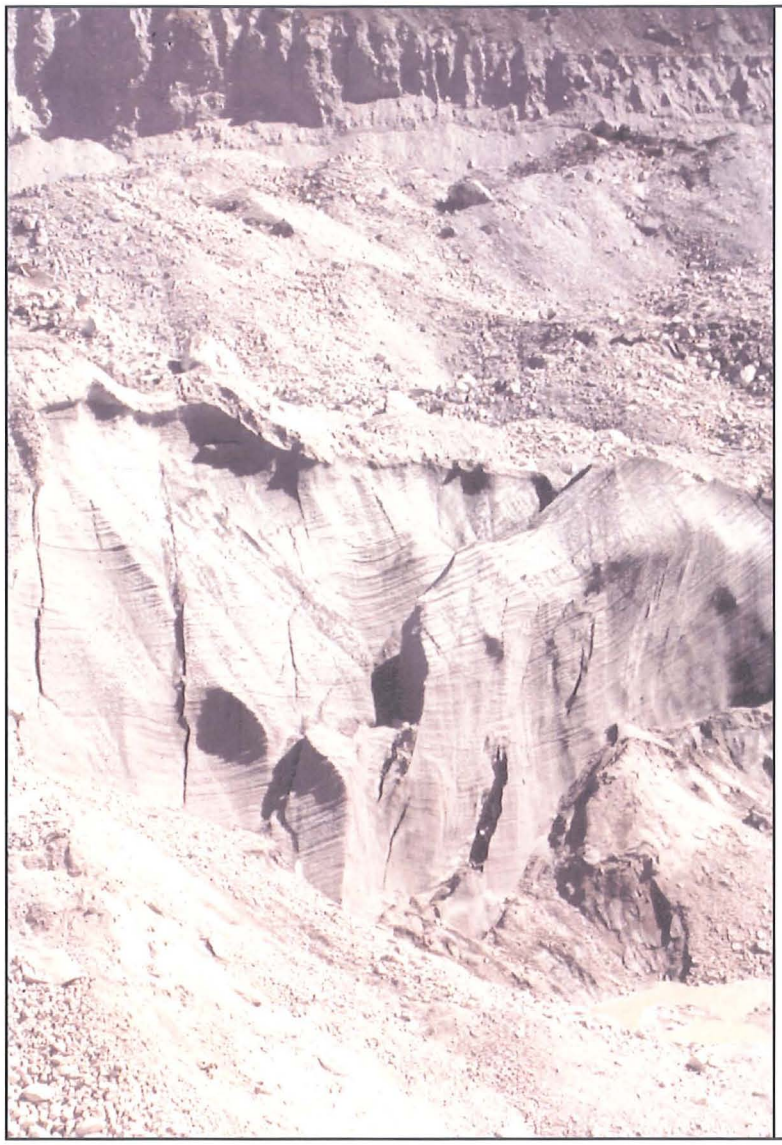

Figure 4.50. Stacked longitudinal crevasses becoming re-activated behind the northeastern exposed ice margin. Viewed from the glacier surface looking east.

Figure 4.51. The southeastern ice margin of the 7092 basin viewed from the basin floor looking southeast.

Figure 4.52. The entrance to conduit C1 where the pond water drained out of the basin. Note the water scoured roof and the drape of fine sediment on the floor. View looking south.

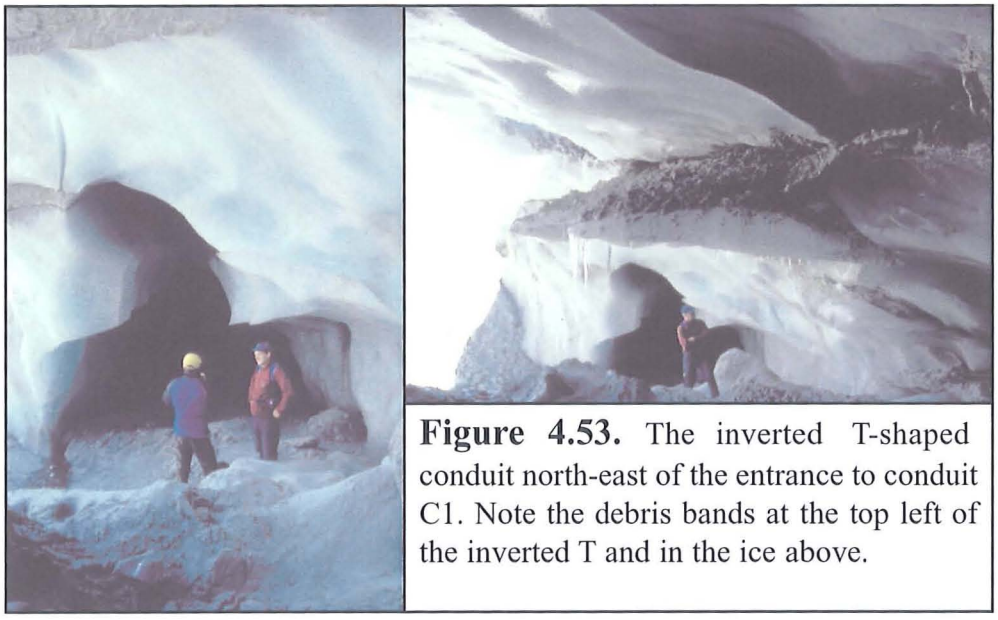

Figure 4.53. The inverted T-shaped conduit north-east of the entrance to conduit C1. Note the debris bands at the top left of the inverted T and in the ice above.

Figure 4.54. Two views inside the conduit at C1. The right-hand picture shows where the conduit ends. Person for scale.

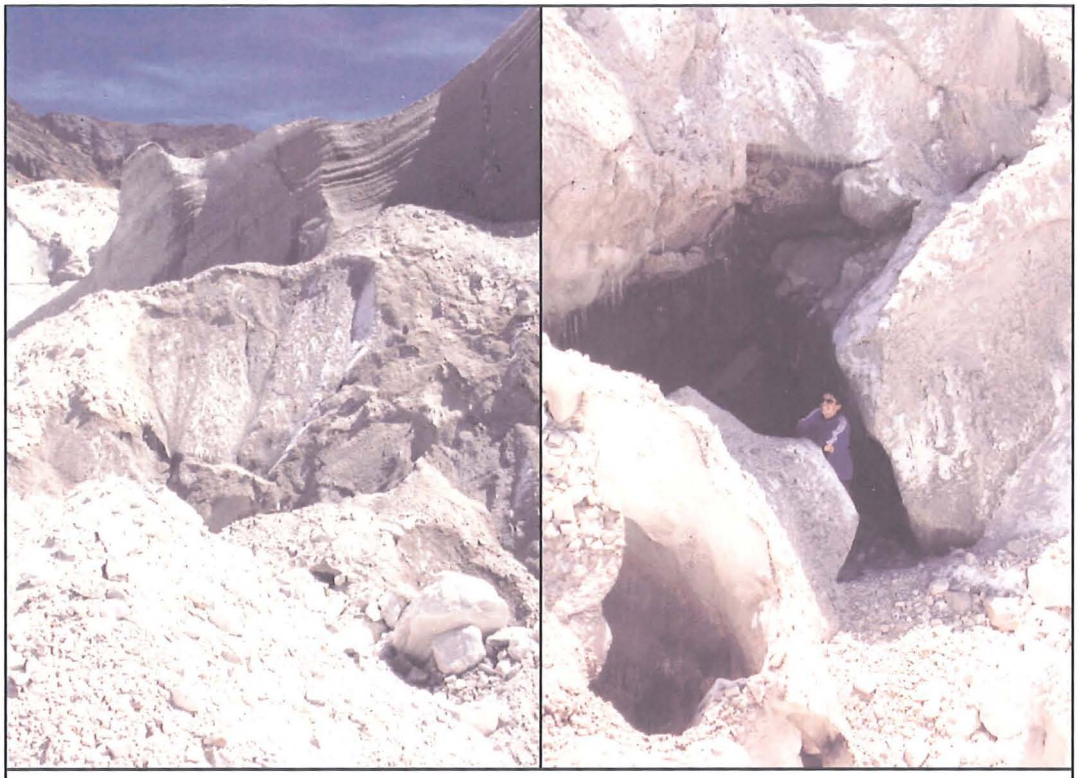

Figure 4.55. The entrance to the hole that links up to conduit C2 looking south-east. Person for scale.

Figure 4.56. Inside the hole that links up to conduit C2. Note the ripples in the ice at the floor of the hole in front of the conduit entrance (right of the person) and the water scalloped roof. Person for scale.

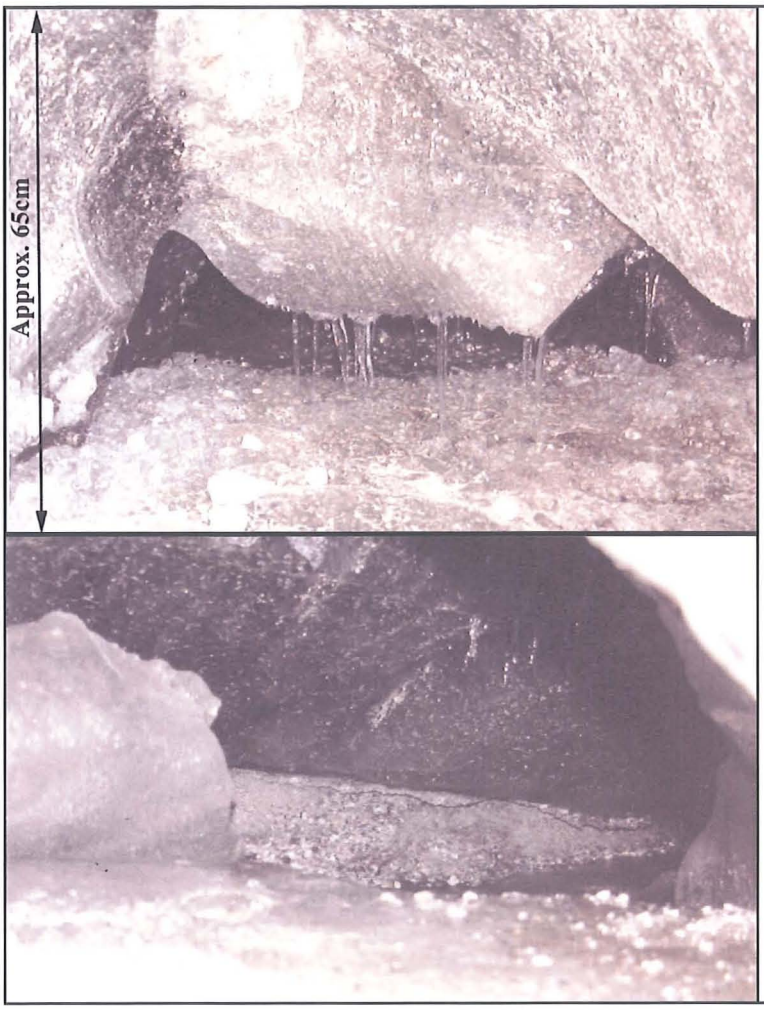

Figure 4.57. The top picture shows the entrance to conduit C2 at the back of the hole. The lower picture is a view inside the conduit showing an englacial stream flowing from left to right (northeast to southwest). The size of the conduit and the deposits of debris in the background are evidence that a much larger stream once occupied through the conduit.

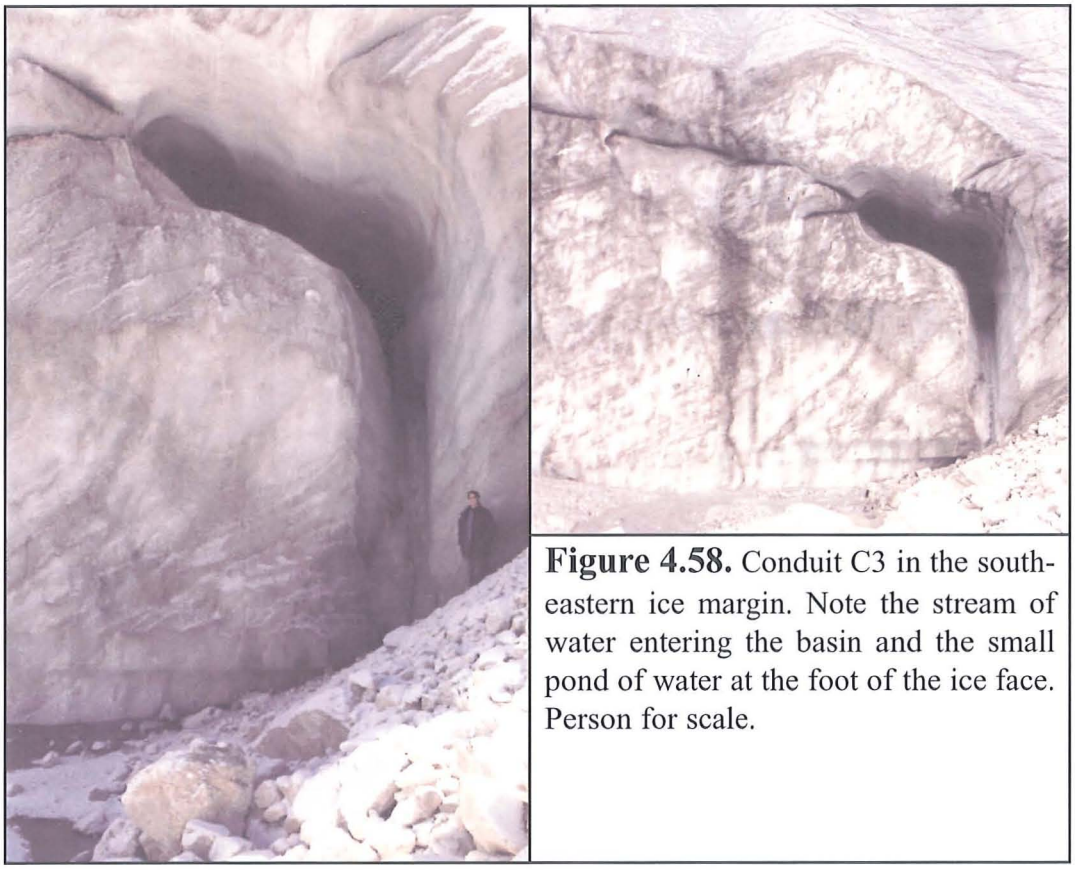

Figure 4.58. Conduit C3 in the south-eastern ice margin. Note the stream of water entering the basin and the small pond of water at the foot of the ice face. Person for scale.

Figure 4.59. A thermo-erosional notch in the southern ice margin.

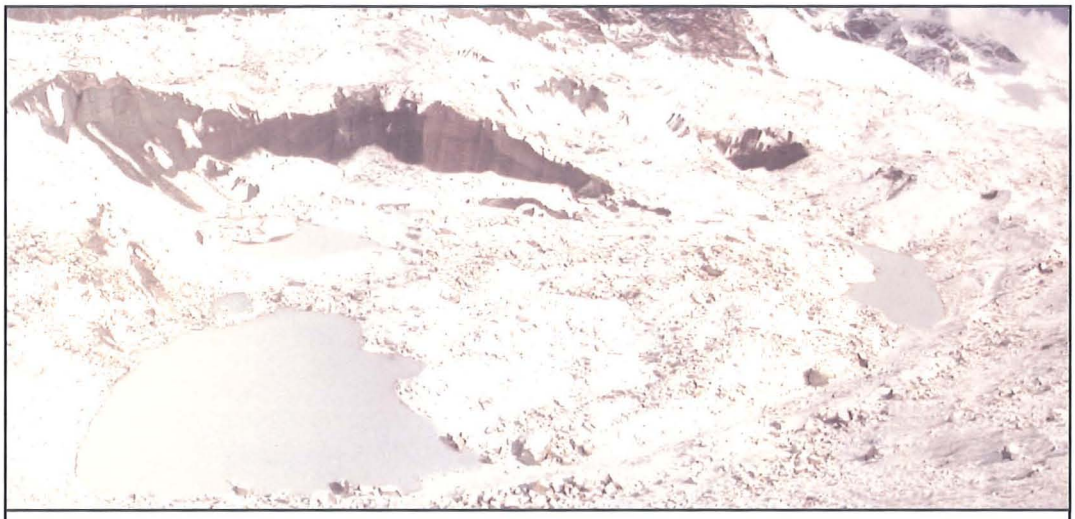

Figure 4.60. Pond 7092 in October 2001 viewed from the western lateral moraine looking southeast. Progradation of talus cones has converted some of the exposed ice margins into debris-covered ice margins. Note the exposed ice foot in front of the main ice face.

Figure 4.61. View looking southeast of the ice faces around the southeast margin. The progradation of talus cones had covered over the entrances to the englacial conduit at C1 and C2.

Figure 4.62. Ice face retreat around the southeast basin margin exposed the conduit at C3. Person for scale. View looking northeast.

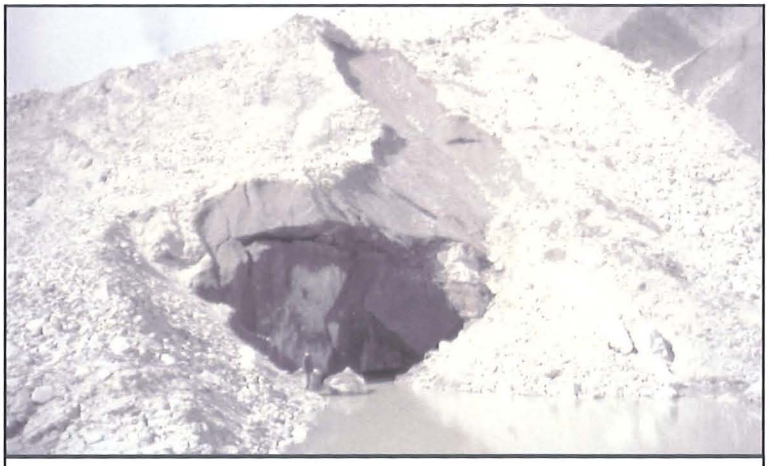

Figure 4.63. View looking north showing a meltwater stream entering Pond D at the water level via an englacial conduit. Person for scale.

Figure 4.64. A hole through the drape of laminated silts and sands on the floor of the Pond 7092 basin formed by subsidence above a supraglacial meltwater stream or shallow englacial conduit. Person for scale.

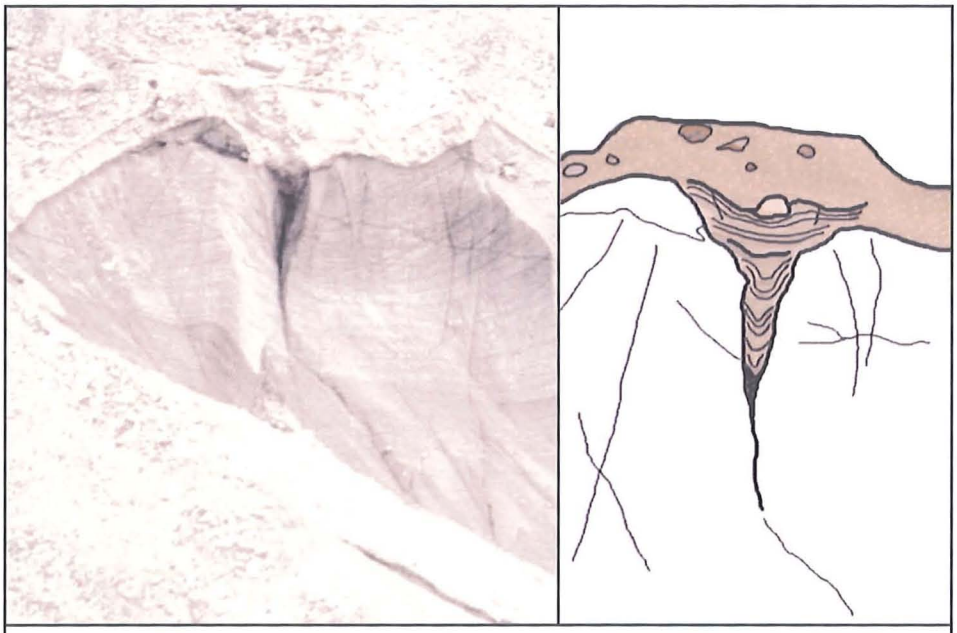

Figure 4.65. The photograph shows a crevasse in Face 1 filled with laminated silts and sands in October 2001. The diagram on the right was drawn from a field sketch of the crevasse-fill sediments. The upward decrease in the amount of sagging in the sediments suggests that the crevasse was melting downward. This feature provides evidence for localised bottom melting along structural weaknesses in supraglacial pond basins on the Ngozumpa.

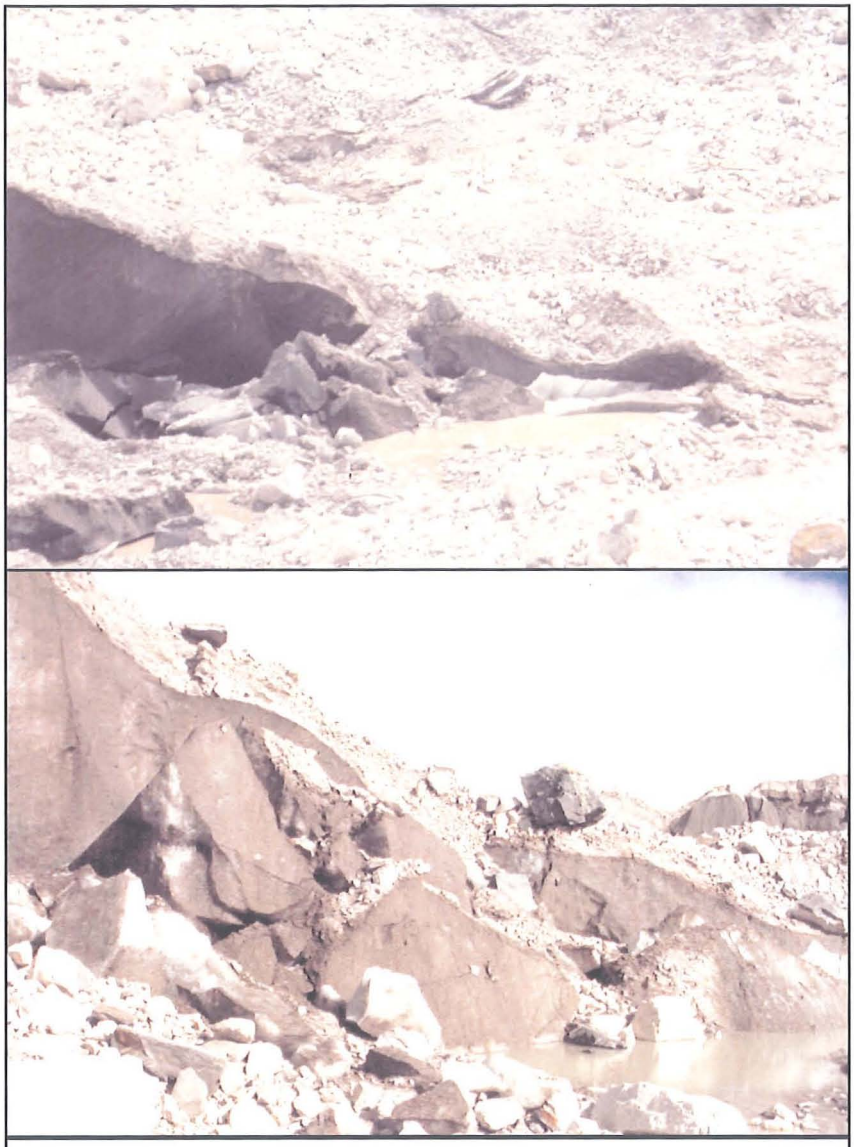

Figure 4.66. A thermo-erosional notch controlled calving event at the southern end of the eastern ice margin.

Figure 4.67. A second thermo-erosional notch controlled calving event occurred on the exposed ice foot in front of the eastern ice margin. View looking southeast from the western lateral moraine. Note also the crevasse in the ice face to the left of the picture and the exposure of another section of ice foot below the face.

Figure 4.68. An old ice foot detached from the main face as the ice margin retreated. Sliding of debris subsequently exposed the underlying ice. Note the deep thermo-erosional notch at the water level. Persons for scale. Photograph taken by Lindsey Nicholson.

Figure 4.69. The north and south end of a conduit in the eastern end of the old ice foot . The meltwater is flowing from north to south.

Figure 4.70. A crevasse immediately behind the northeastern ice margin. Viewed from the top of the ice face looking southwest.

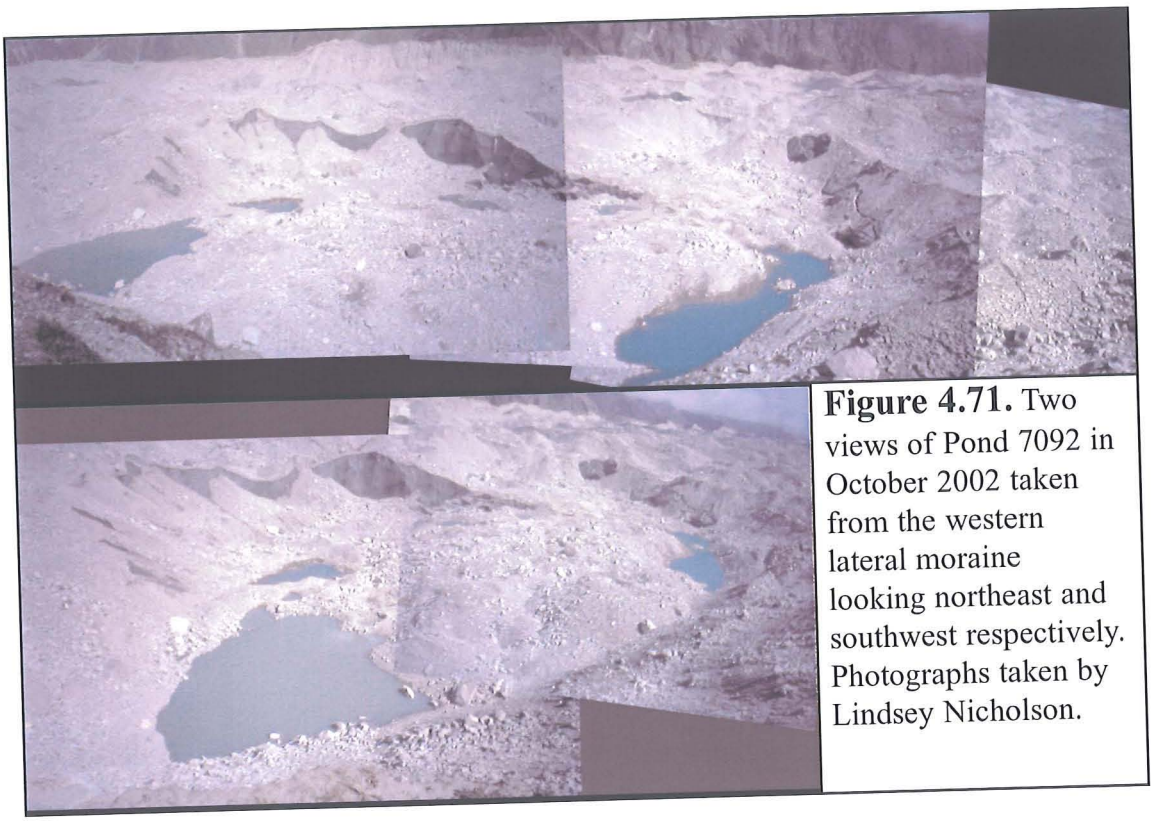

Figure 4.71. Two views of Pond 7092 in October 2002 taken from the western lateral moraine looking northeast and southwest respectively. Photographs taken by Lindsey Nicholson.

Chapter 5

Evolution of the Spillway Lake Basin

5.1. Introduction

The Spillway Lake is a long ribbon-shaped lake extending across almost the whole width of the Ngozumpa Glacier, about 1km up-glacier from the terminus (Figure 5.1). The Spillway Lake differs from the other supraglacial ponds present on the glacier surface in that it is not a closed or perched basin but has a continuous through-flow of that exits the glacier via a stream cut down through the western lateral moraine. The level of the spillway controls the drainage of meltwater from the glacier and determines the base level for drainage on and within the glacier. Due to the continuous input and drainage of lake water, the Spillway Lake does not undergo the cycles of rapid growth followed by complete or partial drainage experienced by the perched ponds up-glacier. The level of the over-spill channel and the rate of down-cutting through the moraine ultimately control the growth of the Spillway Lake. Provided that the spillway remains at the same elevation, the lake will continue to expand and deepen over time. For these reasons, the Spillway Lake is likely to be the nucleus for the formation of a potentially hazardous lake and requires careful monitoring.

The research carried out at the Spillway Lake was designed to examine the mechanisms and rates of basin enlargement at the Spillway Lake basin and follows on from previous research conducted at the site between October 1998 and October 1999 (Benn et al., 2000; 2001; Wiseman, 2004). Investigations were made into the rates of ice face retreat; the type of calving retreat experienced at exposed ice margins; the rate of melting at the basin floor; and the influence of meltwater flowing into the basin on the rate of basin enlargement. An evaluation of the glacier surface surrounding the lake was also made in order to identify the potential direction of future basin expansion.

5.2. Description of the Spillway Lake Basin

The Spillway Lake is approximately 700 m in length and has a maximum width of around 250 m at the western end (Figures 5.2 and 5.3). The lake consists of two distinct basins at the western and eastern extremities, linked together by a narrower channel containing several small embayments. The connecting channel has a very circuitous morphology and extends for around 375 m with an average width of about 50 m. The lake water flows as a stream through the thinnest section of the channel 220 m from the easternmost basin perimeter. The lake water from the eastern basin flows down through this narrow strait, which is approximately 10 m wide and relatively shallow, into the main channel.

Meltwater from up-glacier enters the Spillway Lake in two areas: (1) via a small subaerial stream which flows into the eastern end of the lake, and (2) through an englacial conduit which enters the northern shore of the lake at the water-line 150 m from the western lake margin. Several other conduits are present within the ice faces surrounding the Spillway Lake, but these were not observed to contribute significant discharges of water into the lake during the September-November field seasons. It is possible that these dry conduits channel into the Spillway during times of peak ablation and precipitation during the summer monsoon months. Other water inputs into the Spillway Lake include surface runoff under the debris, melting of the ice faces surrounding the lake, and direct precipitation.

Water exits the Spillway Lake via a river channel that has been cut down through the western lateral moraine. The river is about 8 m wide and has eroded a channel c. 36 m deep through the moraine and is the exit point for most of the meltwater leaving the glacier. The stream travels a distance of 395 m down the ice-distal front of the lateral moraine before joining a larger stream formed by drainage of the laterally dammed marginal lakes to the north. Large boulders in the moraine and on the glacier surface armour the channel and no changes to the channel depth or morphology were observed here between 1998 and 2001.

5.3. Growth of the Spillway Lake Between 1998-2001

Most of the Spillway Lake perimeter consists of debris-covered ice, and these margins experienced very little change over the period of observation. Basin enlargement was generally restricted to areas where ice faces were exposed. Between October 1998 and October 2001, ice faces were exposed in only three areas of the basin: (1) at the northeast margin of the western basin, (2) around a meltwater conduit which enters the north shore of the lake, and (3) around the eastern extremity of the lake (see Figures 5.2, 5.3 and 5.4). The growth of the Spillway Lake basin between 1998 and 2001 was mainly concentrated in these three areas.

5.3.1. The Western Basin (Area A, Figure 5.3)

Most of the perimeter of the western basin of the Spillway Lake is a debris-covered ice margin and consequently, little basin expansion was experienced around the southern, northern, and western lake shores. In the centre of the basin there are seven small debris-covered ice islands. Meltwater entering the western basin flows out through a channel in the southern shore and off the glacier surface via the spillway cut down through the western lateral moraine. Between October 1998 and 2001, the largest amount of basin expansion in the western basin took place at a west-facing ice face exposed in a large debris mound situated on the northeastern shore (Figure 5.5).

5.3.1.1. Previous Work: October 1998 – October 1999

In October 1998, the exposed ice margin on the northeast shore was 40 m long and c. 16 m high, and the southern end of the face tapered down into a debris-covered promontory (Wiseman, 2004) (Figure 5.5). The face was backwasting by a number of ablation processes including melting, thermo-erosional notching at the water-line, and the calving of undercut blocks. In April 1999, the ice face was not undergoing calving retreat and instead subaerial melting had become the dominant backwasting process, evidenced by several water-carved gullies in the face. Between October1998 and October1999, the ice face retreated at an average rate of 18.9 m a^{-1} and had increased in length to c. 80 m with a height range of between 5 and 20 m (Benn et al., 2001; Wiseman, 2004) (Figure 5.2).

5.3.1.2. October 1999 – October 2000

By October 2000, the ice face had retreated further and had become detached from the debris-covered promontory at the southern end (see Section 5.3.1.5 and Figure 5.2). The mean retreat rate of the exposed face was calculated to be 14.0 m a^{-1}. Backwasting processes and slumping of debris had caused further exposure of the ice face at the northern end. No calving events were witnessed at the ice face between October – November 2000, although the presence of a large thermo-erosional notch at the water level suggested that the face was susceptible to calving events.

5.3.1.3. October 2000 – October 2001

The annual retreat rate of the exposed ice face decreased to 7.5 m a^{-1} between October 2000 and October 2001 (Figures 5.3 and 5.4). The length of the exposure in October 2001 was 62.7 m and the height of the face above the lake water level ranged between 7 m and 14 m. Melting and thermo-erosional notching followed by small-scale calving failures continued to be the dominant ablation processes at the face. Several structural weaknesses were observed in the northern end of the ice face in 2001 (Figure 5.6). A large dry conduit filled with debris can be clearly identified in Figure 5.6. The photograph was taken in early November 2001 when the englacial conduit system was beginning to shut down and it is expected that this conduit would be active at times of peak melt at the Ngozumpa. Evidence for running water exiting the face was provided by the presence of icicles that extended from the conduit to the base of the ice face. The rate of thermo-erosional notching in the area directly below the conduit was also noticeably higher than for the rest of the ice face. This suggests that either the meltwater from the conduit was at a higher temperature than the lake water, or that there is a greater degree of mixing directly below the conduit due to turbulence caused by higher rates of debris delivery into the lake. The conduit and the planes of weakness surrounding it provided good conditions for calving retreat at the face and the greatest amount of retreat at the face between October 2000 and October 2001 had occurred in this area. It is expected that future retreat rates will be higher here than at the rest of the face until these weaknesses have been fully exploited.

Large-scale calving events were not observed at the exposed face between October 2000 and October 2001. This was apparently due to the absence of suitably orientated weaknesses within and immediately behind the ice face. The predominant backwasting processes between 2000 and 2001 were melting, spalling and flaking of ice from the face, and thermo-erosional notching at the water level; the same as in the previous year. The thermal erosion of notches at the water level during the monsoon and post-monsoon periods promoted instability and small-scale calving failures, such as flaking and spalling, near the base of the ice face.

5.3.1.4. Creation of Islands and Spits

The retreat of ice faces in the western basin has resulted in the formation of several small ice-cored islands. This process was observed directly between the field seasons in 1999 and 2000, when a new island was formed following backwasting of the large northeastern ice face (Figure 5.7). Retreat of the ice face caused a large debris-covered promontory to become separated from the lake perimeter, forming the island. As ice face retreat continued between October 2000 and October 2001, the island became further removed and isolated, and by October 2001, was positioned approximately 56 m from the shore. The height of the island visibly decreased between October 2000 and October 2001 due to continued wastage of the buried ice core (Figure 5.5). The other older islands present within the western Spillway basin showed little change in shape and size between 1999 and 2001, demonstrating that any ice cores present within these islands underwent limited ablation beneath a thick debris cover.

The position of islands and spits probably reflects variations in debris thicknesses. Where the debris cover at the top of the ice face is thick, progradation of debris cones at the base of an exposed ice face retard melting and create ice-cored debris mounds following the continued retreat of the face. As the ice face retreats, continued high rates of debris deposition could form a spit of debris extending from the base of the exposed face into the water, perpendicular to the direction of ice face retreat. If the supply of debris from the face were later to cease or be reduced, the deposited debris could eventually become isolated from the ice face producing an elongated ice-cored debris island. The formation

of debris spits in this manner was also observed at Pond 7093b (See Chapter 4, Section 4.2.2).

The processes described above were most likely responsible for the creation of all of the islands present within the western basin of the Spillway Lake. The same processes can also be evoked for the creation of other spits within the Spillway basin. The three parallel spits situated in the mid-basin (Figure 5.3, point G and Figure 5.8) may have been formed during the retreat of an ice face before the amalgamation of the western and mid Spillway basins. The general relief of the glacier surface around the spits is relatively low compared with the surrounding hummocky topography and could represent the position of former ice-cored talus cones left behind after the retreat of the ice face.

5.3.2. North Shore Meltwater Conduit (Area B, Figure 5.3)

The second area where significant expansion of the Spillway Lake has occurred is around a conduit where meltwater enters the lake on the northern shore 150 m east of the western-most lake perimeter (Figures 5.2, 5.3, 5.4 and 5.10).

5.3.2.1. Previous Work: October 1998 - October 1999

In October 1998 and October 1999, the only evidence to support the existence of a conduit was an upwelling point around 2 m from the northern lake shore. At the upwelling point, the flat lake surface was interrupted by a dome-shaped circle of upwelling water approximately 2 m in diameter (Figures 5.9 and 5.10). The water depth in the vicinity of the upwelling in 1999 was measured to be around 8.4 m. Two possible explanations for the upwelling phenomena exist. Firstly it could be the case that a vertical jet of water was forced upwards from a conduit that entered at the lake floor. Pressurised flow could force the jet of water through the lake water column, breaking the surface of the lake and forming the upwelling. The second, and more plausible, explanation is that a roughly horizontal conduit entered the lake below the water surface and buoyancy forces caused the water jet to rise through the water column to form the upwelling point (Figure 5.11). Water entering the Spillway via the englacial conduit was measured in 2001 to be around 0.2°C and contained very little suspended

sediment. The water in the Spillway Lake on the other hand has an average temperature of around 0.8°C and is a cloudy green colour, indicating a high concentration of suspended sediment. Since high suspended sediment concentrations increase the density of lake water, and the density maximum of pure water is at its most dense at 3.98°C, relatively cold, clear entering the Spillway Lake via a sub-lacustrine conduit will be driven upwards by buoyancy forces. Wiseman (2004) noted that there was no upwelling in this area during the pre-monsoon season in April 1999, which indicates that the upwelling is driven by seasonal meltwater influx into the Spillway Lake during the monsoon and post-monsoon seasons. The upwelling was still active in mid-November 1999 despite the formation of a 16 cm layer of ice on the surface of the lake suggesting that outflow from the conduit persists into the beginning of winter.

5.3.2.2. October 1999 – October 2000

In October 2000, the meltwater inflow point had migrated c. 26.5 m west of its position in 1999 (Figure 5.2) and entered the lake subaerially at the lake water level (Figure 5.10). A small ice face had been exposed around the outflow point, above the lake level. The average retreat of the ice face containing the conduit between 1999 and 2000 was 18.8 m a^{-1}. The processes most likely to be responsible for the rapid retreat of the ice surrounding the conduit are: high velocities of water flow in the conduit causing thermal and mechanical erosion of the inner conduit walls; conduit roof collapse; subaqueous melting of the conduit and surrounding ice by relatively warm lake water; and rapid influx of large volumes of water caused by the sudden drainage of large perched lakes up-glacier, including Lake 7092 (See Section 5.5).

5.3.2.3. October 2000 – October 2001

Between 2000 and 2001, the conduit and surrounding ice face continued to retreat, forming a narrow embayment through which meltwater continued to flow into the lake (Figures 5.3, 5.4 and 5.10). The annual retreat rate of the face between October 2000 and October 2001 was calculated to be 24.3 m a^{-1}. This rate was 5.5 m a^{-1} higher than for the period between October 1999 and October 2000 and probably reflects thermal erosion of the conduit walls and failure of the conduit roof.

5.3.3. Eastern Basin (Area E, Figure 5.3)

The third area in which significant lake growth has occurred is at the large north-facing ice face exposed in the eastern Spillway Lake basin. The eastern basin receives direct inputs of meltwater from up-glacier via a subaerial stream that enters the Spillway Lake (see Figures 5.3 and 5.12). The temperature of the in-flowing water was measured in October 2001 to be c. 2.2°C. Lake water is drained out of the eastern Spillway basin to the south through a narrow channel.

5.3.3.1. Previous Work: October 1998 – October 1999

The eastern Spillway Lake basin was not surveyed in 1999 but a photograph taken in 1998 by Wiseman (2004) shows that slumping of debris down a large debris mound situated on the southeastern perimeter of the basin was beginning to expose an ice core beneath the debris (Figure 5.13). No other exposures of ice along the debris-covered ice lake margins were observed.

5.3.3.2. October 1999 – October 2000

By October 2000, a large ice face had become exposed at the southeastern margin of the basin and a significant amount of retreat had occurred at this new exposed ice margin (Figure 5.13). No other changes in the shape of the basin or the type of margin surrounding the basin were detected from comparison with the photographs taken by Seonaid Wiseman in October 1999. Most of the basin perimeter was debris-covered ice margin, except for the exposure of the ice face in the southeast. The western margin was blanketed with a layer of white sands and silts. This is a delta graded to a former lake level 11.3 m above the present level of the Spillway Lake. It is possible that this was a perched pond visible on aerial photographs of the Ngozumpa Glacier taken in 1984 (Figure 5.12, see also Chapter 3, Figure 3.27).

5.3.3.3. October 2000 – October 2001

Between October 2000 and October 2001, the surface area of the water contained within the eastern Spillway Lake basin increased from 4098 m^2 to 6361 m^2 (Figures 5.3 and 5.4). The mean retreat rate of the exposed ice margin in the southeast was approximately 15.5 m a^{-1}. The main backwasting process operating

at this margin was subaerial melting of the exposed ice. There was a small amount of thermo-erosional notching of the ice face at the water level suggesting that notch-controlled flaking and spalling of ice from the face was also contributing to the rate of backwasting between 2000 and 2001. No calving events were witnessed at the ice face and this was probably due to a combination of shallow water depths in the lake, low water temperatures (Section 5.4) and the absence of structural weaknesses within or behind the ice face.

In 2001, several new ice faces had opened up on the northern shore of the eastern basin, following slumping and sliding of debris on the perimeter slopes (Figure 5.12). Backwasting of the exposed faces was predominantly by melting. The lower gradient slopes of the exposed ice margin had also undergone a small amount of gullying by meltwater running down the face. Thermo-erosional notching was limited at the eastern end of the ice face due to the build up of debris cones that protected the face at the water level. No calving, flaking or spalling events were witnessed at the ice face and there were no visible structural weaknesses within the ice. If debris slides and falls continue to expose ice in this area, the ice face is likely to enlarge further. However, the deposition of debris at and above the water level may inhibit thermo-erosional notching and decrease the retreat rate.

5.4. Bathymetry and Sublacustrine Processes

In order to evaluate the rate of enlargement of the Spillway Lake basin, it was necessary to examine the rates of melting at the bottom of the lake. To achieve this, depth measurements were made in the western Spillway Basin in the area in front of the exposed ice face at the northeast margin on the 8th and 10th of November 2001 (Area A, Figure 5.3 and Figure 5.14). Depths were also recorded in the eastern Spillway Lake basin and in the large perched lake south of the Spillway Lake on the 22nd October (Areas E and H, Figure 5.3 and Figure 5.15). The temperature of the water column was measured at 2 m intervals in the eastern basin and in the perched pond to the south of the Spillway Lake. Temperature measurements were also made at the bottom of the lake in the western basin.

5.4.1. West Basin Bathymetry

Lake depth and bottom temperatures were measured at twenty points within the western Spillway basin over two days on the 8th and 10th of November 2001 (Figures 5.14 and 5.16). A layer of ice several inches thick covered the lake at the time the measurements were taken. The depth of the lake at the measured points ranged from 1.4 to 6.4 m, giving an average depth of 4.4 m. Through comparison of the depth measurements in the western Spillway Lake with the position of the exposed ice face between October 1998 and October 2001 (Figure 5.14), it was possible to determine an average bottom melting rate of 2.4 m a^{-1} for the western basin, although this rate is spatially variable. Bottom melting rates at the Tsho Rolpa Lake on the Trakarding Glacier in the Nepal Himalaya were measured to be around 23.36 m a^{-1} (Chikita et al., 1997). This is around ten times the rate of melt calculated for the floor of the Spillway Lake basin.

5.4.2. East Basin Bathymetry

The depth and temperature of the Spillway Lake in the eastern basin was measured at 7 locations on the 22nd October 2001 (Figures 5.15 and 5.17). The depths recorded ranged from 4 m to 16.1 m with an average depth of 9.7 m. The depth of 4 m seems unusually low compared with the depth of the surrounding lake water and probably reflects submerged debris cones relating to thicker than average debris. Annual bottom melting rates could not be calculated directly from the former positions of exposed ice faces. However, examination of aerial photographs of the Ngozumpa Glacier constrains the formation of the Spillway Lake to between 1984 and 1992. This gives an estimated depth increase of 16 m in 10-18 years, or between 0.89-1.6 m a^{-1}. This should be considered as a minimum estimate of bottom melting rates because the glacier surface is likely to have lowered since 1984.

5.4.3. Bathymetry of the Perched Pond to the South

Bathymetry measurements were also made at eight points in the perched pond south of the Spillway Lake basin on the 24th October 2001 (Area H, Figure 5.3 and Figure 5.18). The depth of the lake ranged between 6.3 and 12.3 m with an average of 9.98 m. The pond perimeter was a continuous debris-covered ice

margin that did not undergo measurable retreat during the study period and so an accurate calculation of the rate of bottom melting was not possible. However, as with the eastern Spillway lake basin, the appearance of the pond can be constrained to between 1984 and 1992. This gives an estimated depth increase of 12 m in 18-10 years, or between 0.67-1.2 m a^{-1}. Again this is a minimum estimate of bottom melt rates in the pond due to downwasting of the glacier surface since 1984.

5.4.4. Lake Temperature

The lake temperatures at the bottom of the western Spillway Lake basin were measured at twenty points on the 8th and 10th November 2001 (Figure 5.14). The temperatures ranged from 0.6°C to 1.3°C. Figure 5.16 shows that the basal temperature of the lake increased slightly with depth. Proximity to the large ice face in the western bay appeared to have only a small influence on the temperature distribution at the lake bottom and most probably reflected the deepening of the lake towards the ice face. Furthermore, due to the cold weather conditions at the time of measurement, melting of the ice face in the western bay had almost ceased and therefore would not have played a large role in influencing the lake temperatures.

In the eastern Spillway Lake basin, temperature measurements were taken at 2 m intervals at 7 points on the 22nd October 2001 (Figure 5.15). Temperatures ranged from 0.4°C to 0.6°C at the surface and from 0.8°C to c.1°C at the lake bottom. The average lake temperature increased from 0.5°C at the surface to 0.8°C at 2 m depth before leveling out at 0.9°C below 4 m depth (Figure 5.17).

Water temperatures were also recorded in the perched lake south of the Spillway Lake basin on the 24th October 2001 (Figure 5.18). The surface water temperatures of the perched pond ranged between 8.1°C and 8.5°C, with an average of 8.3°C. Bottom temperatures ranged between 4°C and 7.9°C, with an average of 6.1°C. The average surface water temperature in the perched pond was 7.6°C warmer than in the Spillway Lake. The difference is attributed to cooling of the Spillway Lake by cold meltwater from conduits or subaerial

streams and exposed ice faces around the pond perimeter. The cooler water of the Spillway Lake results in earlier freezing of the lake surface. Freezing increases the albedo of the lake surface and enhances the cooling effect.

5.4.5. Inferred Lake Dynamics

The temperature profile of the eastern Spillway Lake basin resembled that of a dimictic lake in the winter phase (Smith & Ashley, 1985; Benn & Evans, 1998) (Figure 5.19). Although it was not possible to measure lake temperatures throughout the year, it is suggested that the Spillway Lake is dimictic and undergoes two overturning periods: one in late October and the other in April or May during the spring melt. During the summer, higher water temperatures at the lake surface induce thermo-erosional notching and notch-controlled calving retreat at exposed ice margins. As air temperatures are reduced during the autumn, the lake surface cools and develops an ice cover that inhibits thermo-erosional notching and calving retreat. The lake overturns near the end of the ablation season and enters the winter phase producing higher temperatures at the bottom of the water column than at the lake surface. This dimictic thermal regime would allow melting to occur at the bottom of the Spillway Lake throughout the year.

The decline of water temperature with depth in the perched pond (Area H, Figure 5.3 and Figure 5.18) produced a thermal profile that indicated that the pond was still in the summer phase (Figure 5.19). The summer phase of the perched pond in 2001 was more prolonged than inferred for the Spillway Lake, which had entered its winter phase in early November. This suggests that the Spillway Lake experiences lower average water temperatures than perched lakes with debris-covered margins on the Ngozumpa surface. Diurnal heating of the Spillway Lake water is considered to be lower than for perched ponds because of the continuous mixing with cold englacial meltwater entering the lake and drainage of lake water out through the Spillway overspill channel. The absence of surface ice at the other perched ponds in the vicinity of the Spillway Lake basin was taken as an indication that they too had not entered into the winter phase by early November 2001.

A thin layer of ice had formed on the Spillway Lake surface prior to the 21st October 2001. When the bathymetry and temperature measurements were made in the western basin, between the 8th and 10th November, this ice layer had thickened to approximately 15cm. The presence of a layer of ice during the winter phase influences the thermo-dynamics of a lake in several ways. The ice layer increases the albedo of the lake surface and thereby reduces the in-coming shortwave radiation. Furthermore, the cap of ice greatly reduces the amount of mixing and turbulence in the lake by inhibiting wind induced currents. However, the cold temperature of the ice layer also reduces the loss of longwave radiation from the lake surface allowing the water temperature at the lake floor to remain high enough to cause continued bottom melting, possibly throughout the winter period. In this way the dimictic nature of the Spillway Lake allows expansion and deepening of the lake basin to occur throughout the year. At the moraine-dammed Tsho Rolpa Lake on the Trakarding Glacier a similar dimictic lake regime appears to be in place (Chikita et al., 1997; Sakai et al., 2000; 2001). Average bottom temperatures in the Tsho Rolpa were recorded to be 2.7°C (Sakai et al., 2000b), 1.8°C higher than recorded in the Spillway Lake. Unfortunately, detailed comparisons of the thermal regimes of the Tsho Rolpa and the Spillway Lake are not possible at present due to the limited data available. However, as the Spillway Lake continues to grow, it is expected that the average lake temperatures will rise and that melting of the lake floor will play an increasingly important role in the expansion rate of the lake basin in the future.

5.5. Collapsed Surface Topography

Stagnation of the glacier tongue as it downwastes towards its bed is most evident near to the glacier terminus where ice flow velocities are low or approaching zero. Glacier karst features such as sink holes, ice caves and conduits become exposed at the glacier surface as the ice surface downwastes. Often the roofs of ice caves and conduits collapse as the glacier surface is lowered. If subsidence occurs at the foot of ice-cored debris mounds, sliding of debris into the hole can expose new ice faces. Furthermore, subsidence at the base of exposed ice faces can initiate further collapse as the above face undergoes fracturing or dry calving

above the hole. Once exposed at the surface, collapse features will melt out very rapidly due to direct ablation of ice faces, often facilitated by the presence of running or ponded meltwater. Consideration of collapsed surface topography in the environs of the Spillway Lake basin is important because it forms topographic low points that are potential sites of flooding following expansion of the Spillway Lake. Areas of collapse can also form nuclei for the development of perched supraglacial lakes that may become amalgamated with the Spillway Lake basin in the future.

An extensive area of collapse developed on the surface of the Ngozumpa to the north of the Spillway Lake between October 1999 and October 2001 (Figure 5.3, Area C). In 1999, several cracks and holes appeared in the glacier surface several metres north of the Spillway Lake. The collapse of a small ice face indicated that subsidence of the glacier surface was occurring above an englacial void or conduit (Figure 5.20). By October 2000, the ice face had greatly enlarged by backwasting, notch-controlled calving and presumably additional collapse events along fractures or weaknesses within the ice (Figure 5.21). Further subsidence had occurred to the north of this ice face (Figure 5.22), indicating that collapse of a conduit roof was responsible for the collapse features and topography in this area. To the north of the area of collapse a new perched supraglacial pond had also formed by October 2000, c. 283 m northeast of the conduit upwelling point in the Spillway Lake (Area D, Figure 5.3 and Figure 5.23).

The location of the area of collapse was directly up-glacier from the conduit in the north shore of the Spillway Lake (Figure 5.3, Area B) and it was considered likely that the collapse was occurring along the up-glacier continuation of this conduit. The rapid collapse of the conduit roof between October 1999 and October 2000 may have been initiated and exacerbated by the drainage of the perched Pond 7092 during the summer monsoon (Chapter 4, Section 4.4.3). It is hypothesised that the meltwater from the Pond 7092 basin drained out through the englacial conduit that up-welled into the Spillway Lake basin. As the rapid drainage of Pond 7092 proceeded, it caused enhanced thermal erosion of the walls along the length of the englacial conduit and brought about exposure of the conduit at the surface of the Spillway Lake at Area B (Figure 5.3). This caused

the cessation of meltwater upwelling into the Spillway Lake basin at this point and initiated the rapid retreat of the newly exposed ice margin on the north shore (Section 5.3.2). Immediately following the drainage of Pond 7092, the roof of the enlarged englacial conduit began to collapse c. 30 m north of the Spillway Lake, due to the proximity of the conduit to the surface of the glacier at this point.

By October 2001, a long u-shaped channel containing three small ponds had formed between the Pond D (Figures 3.5 and 3.23) and the Spillway Lake (Figure 5.24). Water could be heard running at depth, providing evidence that the line of collapse coincides with the drainage route. It is most likely that meltwater from the area of collapse enters the Spillway Lake via the conduit in the north shore, discussed in section 5.3.2 above. Continued backwasting of the conduit entering the Spillway Lake and the ice face surrounding the southernmost part of the collapsed zone will almost certainly cause coalescence and inundation of the collapsed conduit over the next few years. Further collapse along the length of the englacial part of the conduit would exacerbate this process.

5.6. Future Enlargement of the Spillway Basin

Expansion of the Spillway Lake basin is expected to continue where bare ice faces are exposed around the lake perimeter. The position and area of these ice faces frequently changes over time as slumping of debris exposes new areas of bare ice and causes older ice faces to become covered over and insulated once more. Little expansion of the basin is expected where the lake perimeter is composed of low-angled debris-covered slopes or large thicknesses of deltaic sediments. Enlargement of the Spillway Lake basin will also occur by amalgamation with surrounding supraglacial ponds and by flooding of areas of collapse in the immediate vicinity of the Spillway Lake. In 2001, four sites in the immediate vicinity of the Spillway Lake were identified as being areas of potential expansion within the next few years. These sites are: (1) the perched pond to the south of the Spillway Lake; (2) the area of collapse; (3) the two small lakes at the eastern end of Spillway Lake; and (4) continued melting of the lake floor (Figure 5.3).

5.6.1. Amalgamation with Smaller Supraglacial Lakes

It looks certain that the Spillway Lake will amalgamate with the perched pond situated 54 m to the south (Area H, Figure 5.3 and Figure 5.25). In October 2001, the water level in the perched pond was measured to be 1 m above the level of the Spillway Lake, although this level is liable to fluctuate slightly throughout the year. The intervening glacier surface is relatively low and in places is already studded with very small ponds in hollows. The topographic barrier between the two lakes varies in height, ranging between c. 1.2 m and 17.7 m. It is therefore, only a matter of time before this barrier downwastes far enough to allow the amalgamation of the perched pond and the Spillway basin.

5.6.2. Amalgamation with the Small Ponds to the East

The two small shallow ponds situated 41 m east of the Spillway Lake are also candidates for amalgamation with the Spillway Lake basin (Figures 5.3 and 5.26). In October 2001, a subaerial stream discharged meltwater from up-glacier into the westernmost of the two ponds and a second stream transported water from this pond into the eastern end of the Spillway Lake. The pond was expanding southwards due to backwasting of a small ice face, 38 m wide and 11 m high during the 2001 field season, and looked likely to join up with the neighbouring lake by 2002. A single water temperature measurement made in the pond during November 2001 was 1.6°C and a thin skin of ice had formed on the pond surface. The temperature of the subaerial stream that entered the pond was measured to be 1.4°C, suggesting that only a small amount of heating occurred while water was stored in the pond at this time. The ice face had been undercut by a deep thermo-erosional notch, indicating higher water temperatures and small-scale calving events may occur during the monsoon and early post-monsoon seasons. In the eastern perched pond, water temperature was much higher at 7.6°C and had no surface ice, demonstrating the cooling influence of meltwater from the ice face and the subaerial stream entering the neighbouring pond. It is expected that, in the near future, the ice face will continue to melt back by a combination of subaerial melting and notch-controlled calving processes that will enlarge the size of the pond causing the two ponds to coalesce first with each other and then with the Spillway Lake.

5.7. Discussion

The data presented above indicate that the Spillway Lake expands by melting around the lake perimeter and at the bottom of the lake. Basin expansion is greatest where ice faces have emerged from the debris-covered slopes around the edge of the lake. Where there were large thicknesses of surface debris or deltaic deposits little change in basin size or shape was observed between October1999 and November 2001. Melting at the Spillway Lake floor is likely to be a continuous process that occurs throughout the year.

The low temperature of the lake water lowers the rate of basin expansion compared with perched lakes on the glacier surface. The development of thermo-erosional notches at the water level is considerably slower than in other areas of the glacier and very few calving events were witnessed at the Spillway Lake basin between October 1999 and November 2001. This suggests that most ice face retreat around the Spillway Lake occurs by subaerial melting and small scale flaking and spalling of ice from exposed faces. In 2001, the Spillway Lake had frozen over by early November and appeared to have entered the winter stage of a dimictic thermal regime. In contrast, the perched pond to the north of the Spillway Lake had not frozen over in early November and displayed a summer-type thermal profile. The other perched ponds in the vicinity of the Spillway Lake basin had not frozen at the surface either and were therefore also assumed to still be in the summer stage. The early onset of lake overturning at the Spillway Lake basin is most likely to be the result of lower water temperatures caused by the continuous throughflow of relatively cold englacial meltwater. As a result, the ablation period is shorter and the basin expansion rate lower for the Spillway Lake than for the surrounding perched lakes.

Despite the lower expansion rate, the Spillway Lake basin will continue to develop and expand. Ice face melting, bottom melting, amalgamation with surrounding lakes, and flooding of areas of subsidence adjacent to the Spillway Lake basin will continue to increase the size and volume of the lake until the effect of cold englacial meltwater inputs becomes negligible. After this threshold is crossed diurnal heating of the water surface and mixing of warmer water to

depth will eventually cause the onset of more rapid melting and calving retreat. Evidence from the Imja Glacier and the Trakarding Glacier in Nepal (Watanabe et al., 1994; Chikita et al., 1997; 2000; Richardson & Reynolds, 2000) and from debris-covered glaciers in Bhutan (Ageta et al., 2000; Reynolds, 2000) indicates that once ponds develop near the terminus, presumably at the base level for englacial drainage, amalgamation and rapid growth ensue, encompassing all of the terminal zone on timescales of around 20 years. It is considered likely that the Spillway Lake will follow a similar pattern of evolution, and that a large and potentially hazardous lake will form within the next ~20 years, unless the level of the Spillway Lake is lowered by natural processes or human intervention.

Chapter 5 Figures

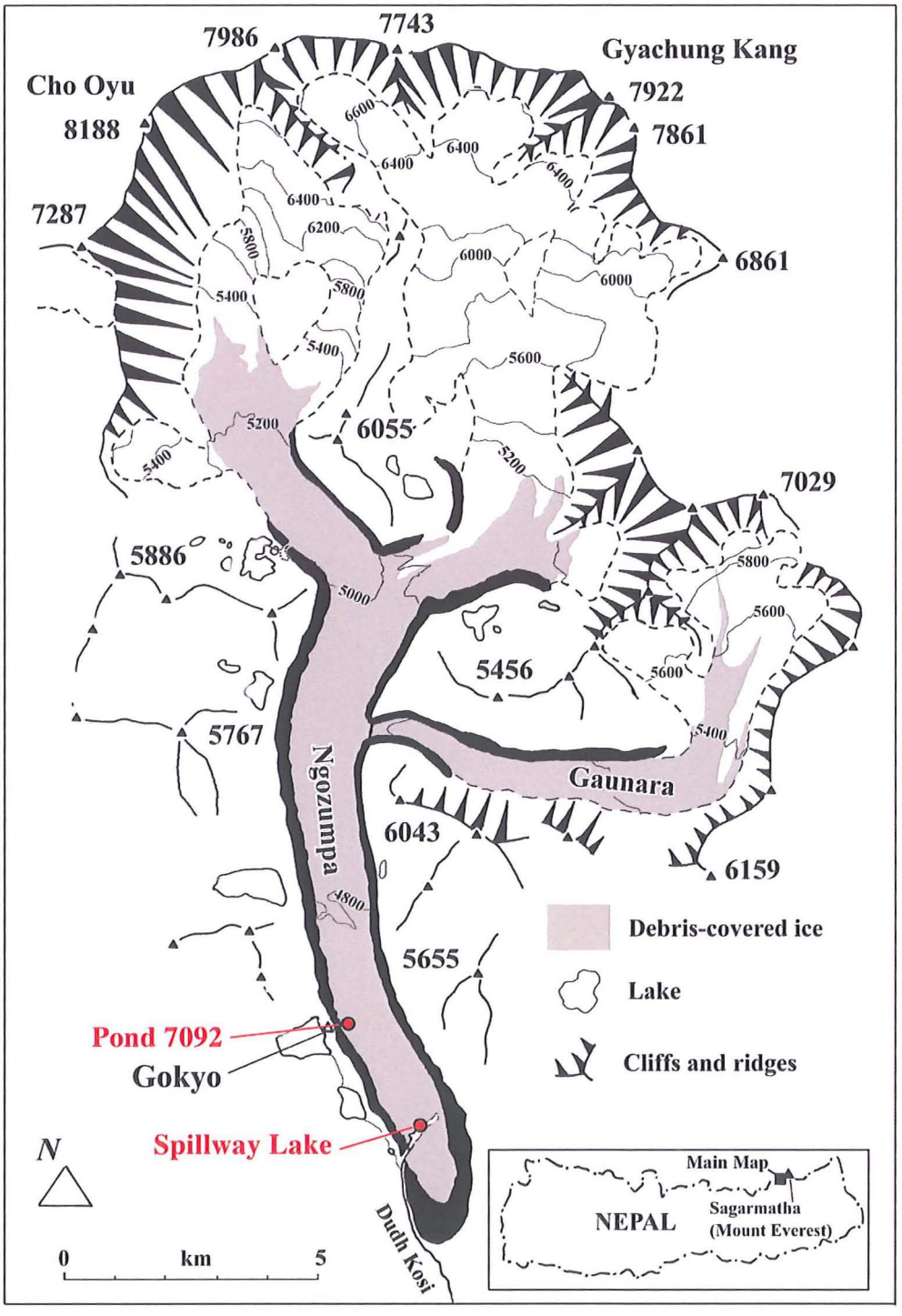

Figure 5.1. Location Map showing the Spillway Lake basin (modified from Benn et al., 2001)

Figure 5.2. Spillway Lake Survey Map showing the growth of the western Spillway basin between October 1998 and October 2000. From Benn et al (2001).

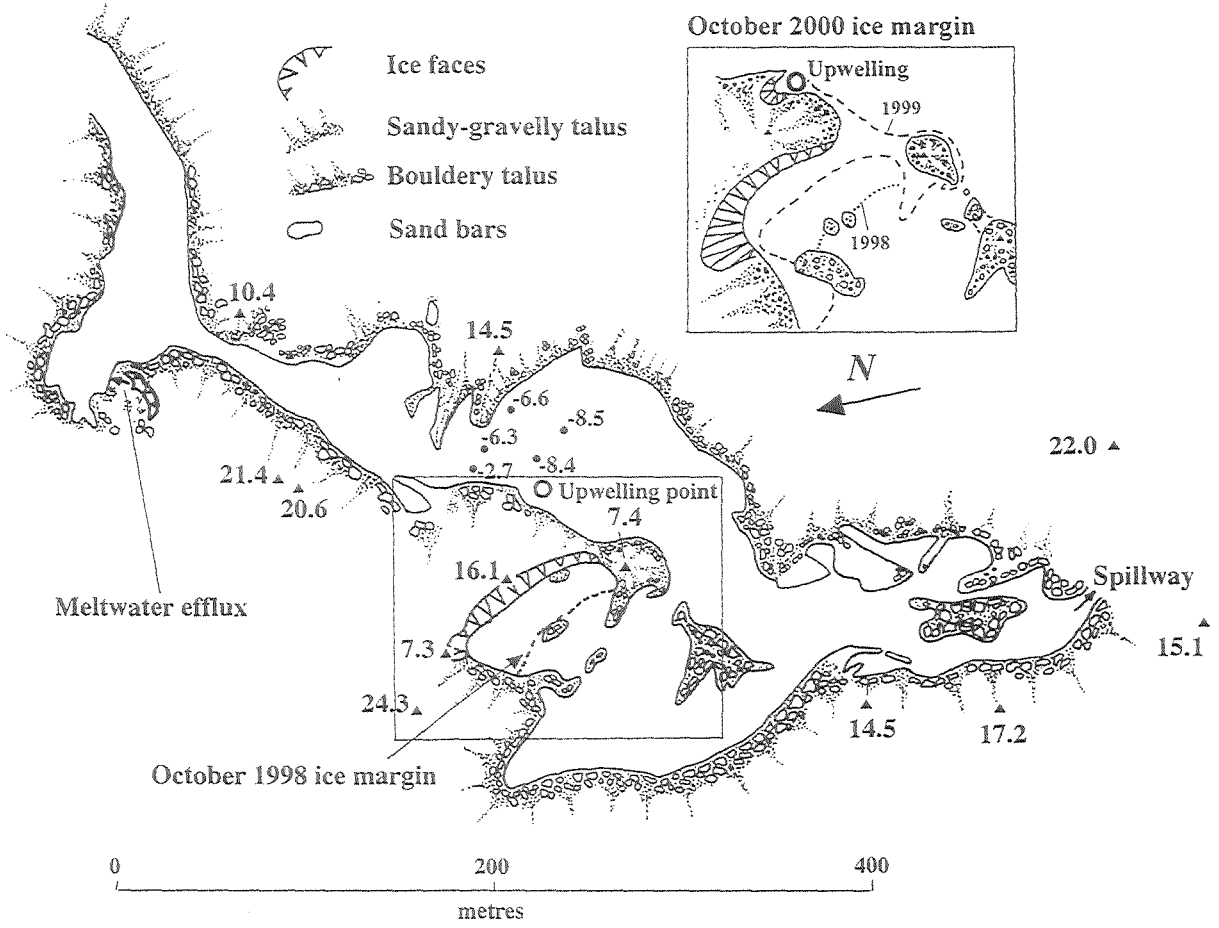

Figure 5.3. Spillway Lake Survey Map, October 2001

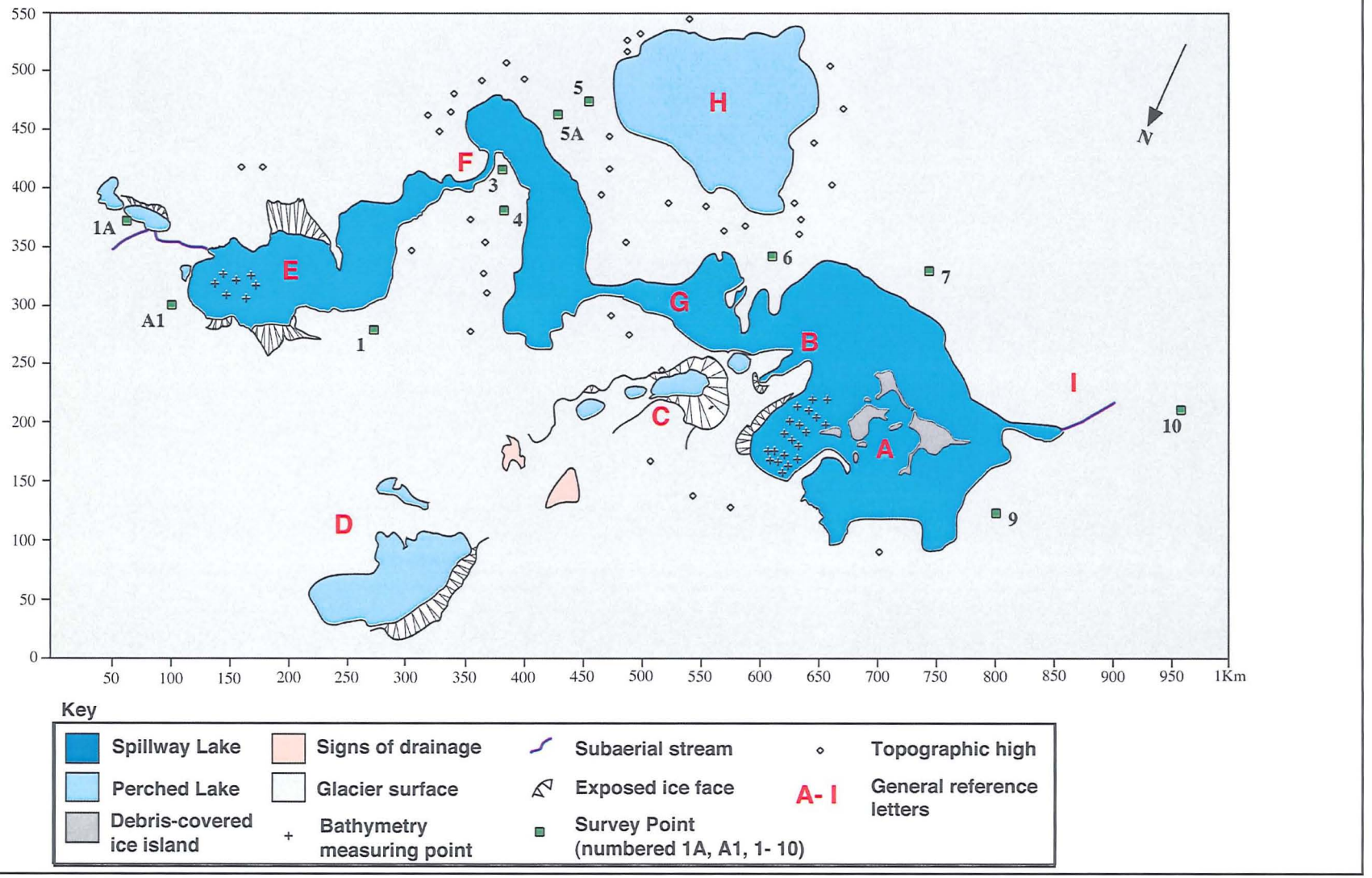

Figure 5.4. Ice face retreat in the western and eastern Spillway Lake basins between October 2000 and October 2001. For key see Figure 5.3.

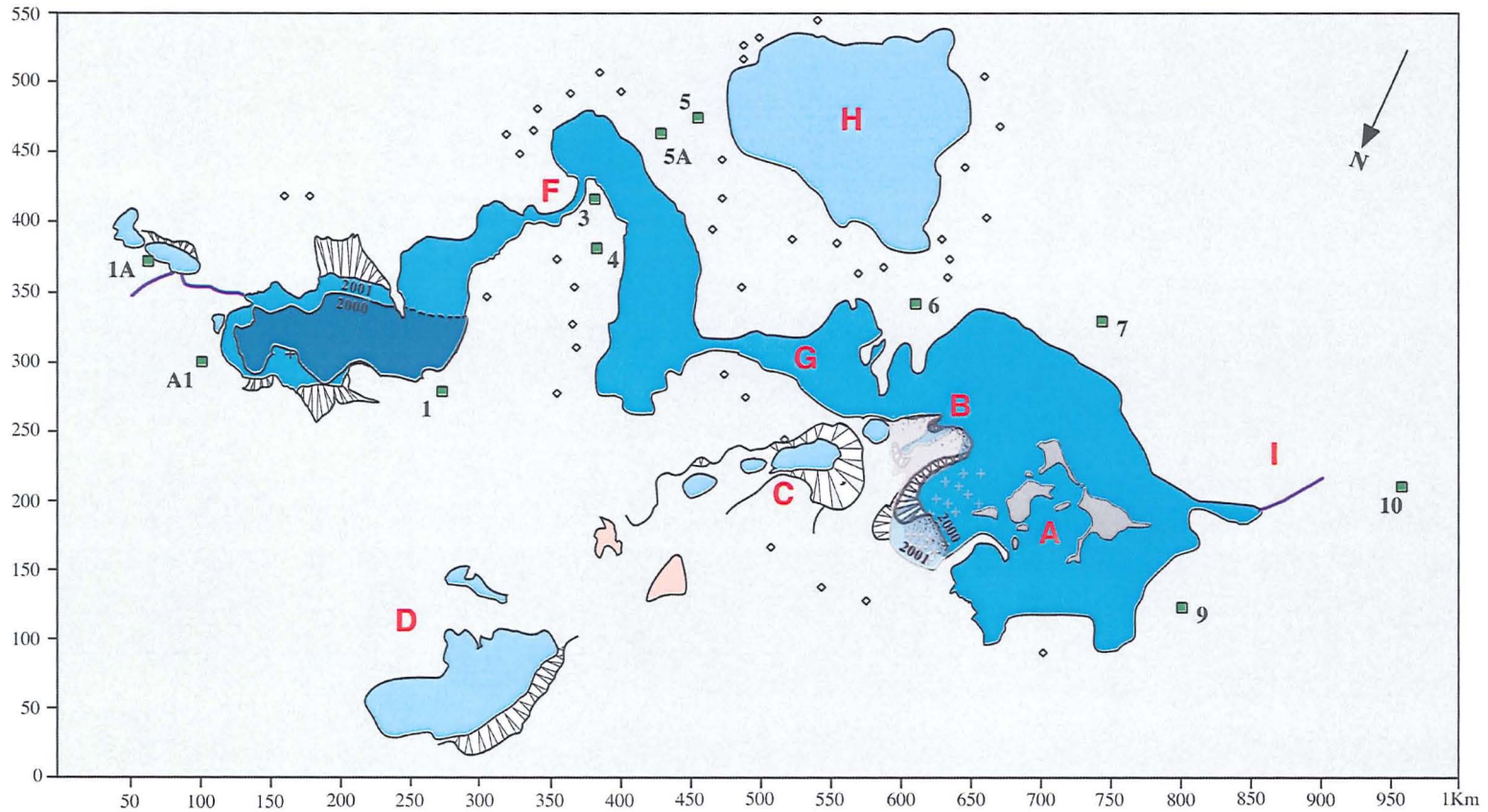

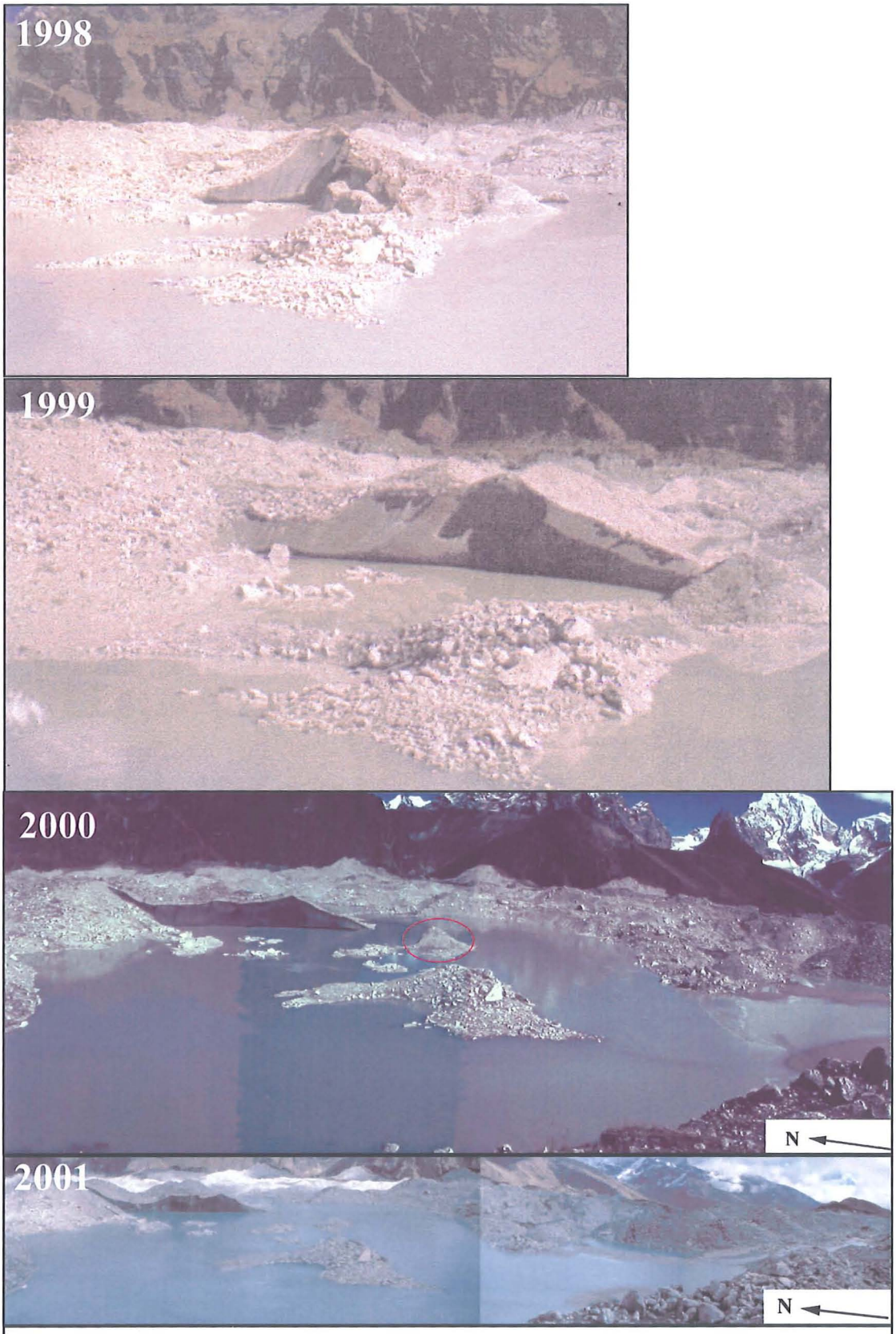

Figure 5.5. Retreat of the ice face in the western basin between October 1998 and October 2001. Retreat of the ice face between 1999-2000 caused the separation of a debris-covered promontory and the creation of an ice-cored debris island. The detached island promontory is lower in height in 2001 than in 2000. The first two pictures were taken by Doug Benn.

Figure 5.6. A conduit and planes of structural weakness in the exposed ice margin of western Spillway Lake basin. Person for Scale.

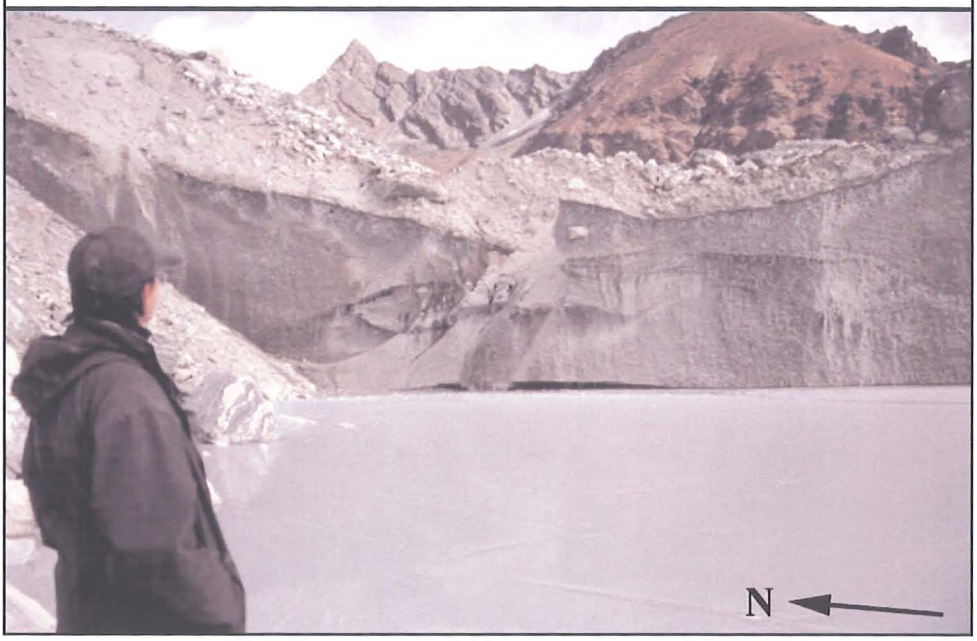

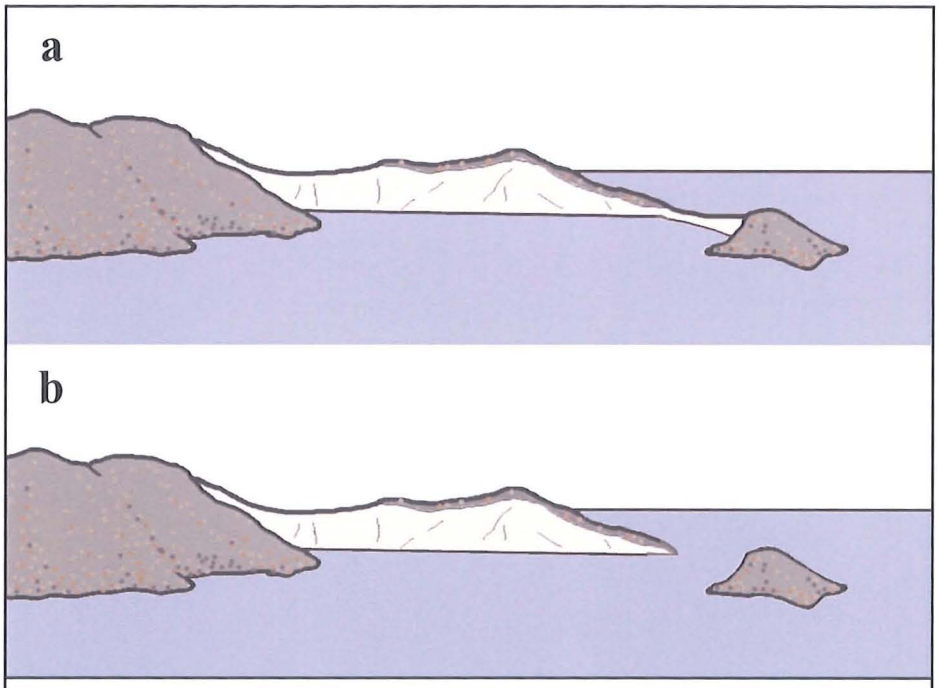

Figure 5.7. Formation of an ice-cored debris island through separation from a debris-covered promontory.

Figure 5.8. Mid Section of the Spillway Basin, October 2000. The spits may have formed where high levels of debris deposition occurred at a retreating ice margin.

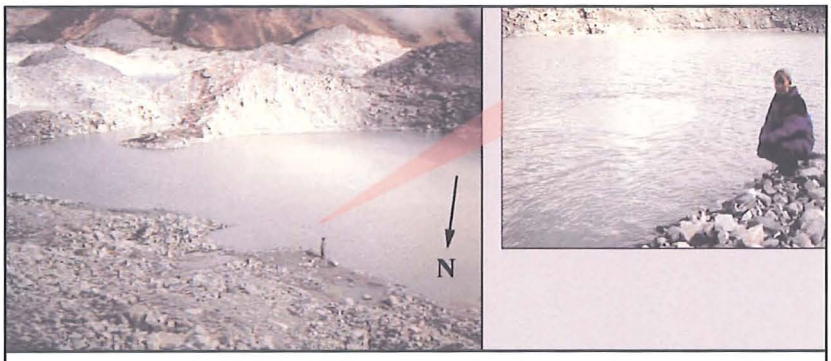

Figure 5.9. An upwelling point in the Spillway Lake photographed by Doug Benn in October 1998. Person for scale. View looking southeast.

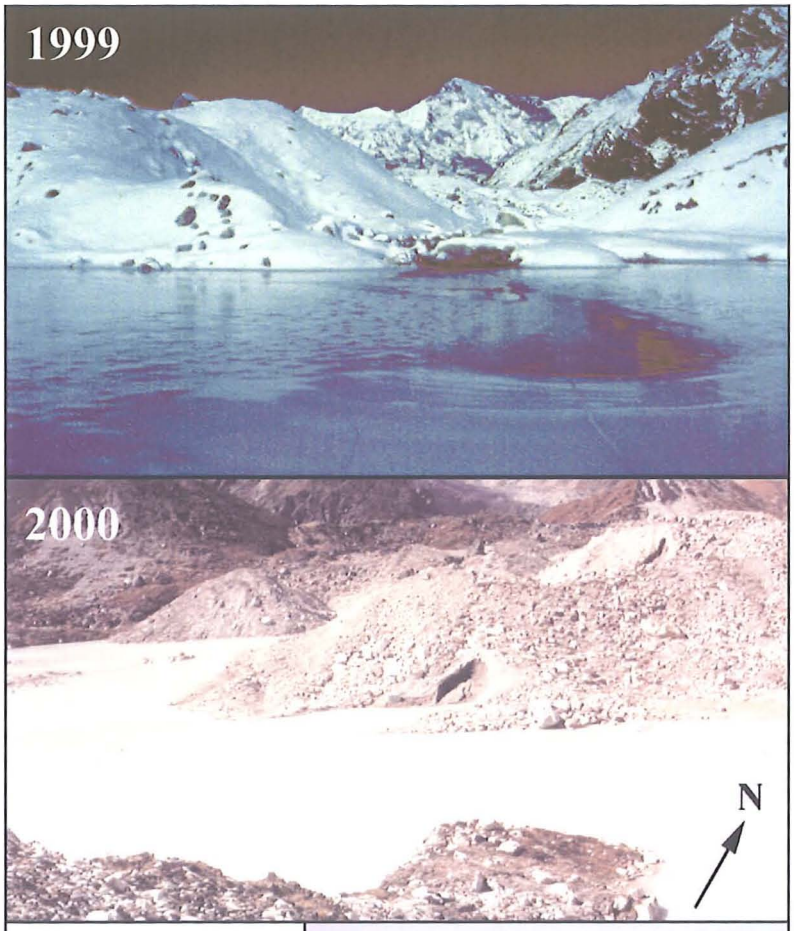

Figure 5.10.

Migration and exposure of an englacial conduit on the north shore of the Spillway Lake basin between 1999 and 2001. The top picture shows where water was upwelling in the lake. By 2000, thermal erosion of the conduit walls caused the conduit to become exposed at the level of the lake. Thermal erosion and melting of exposed ice caused rapid retreat around the conduit between 2000 and 2001.

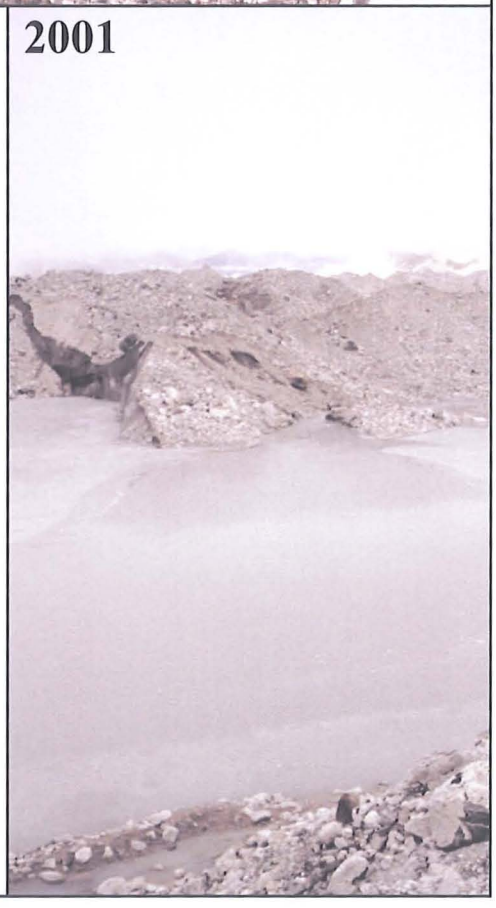

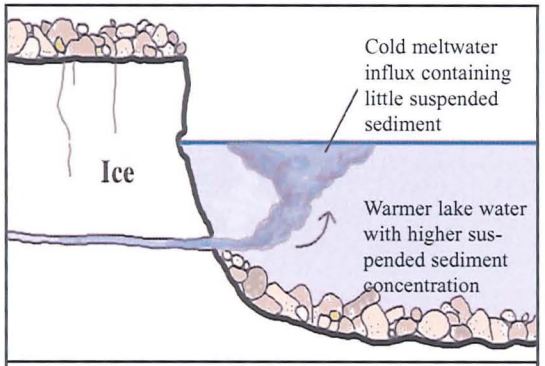

Figure 5.11. Temperature and density differences between in-flowing meltwater and lake water cause an upwelling to occur.

Figure 5.12. Slumping of debris from the perimeter slopes exposed new ice faces in the eastern basin between October 2000-2001.

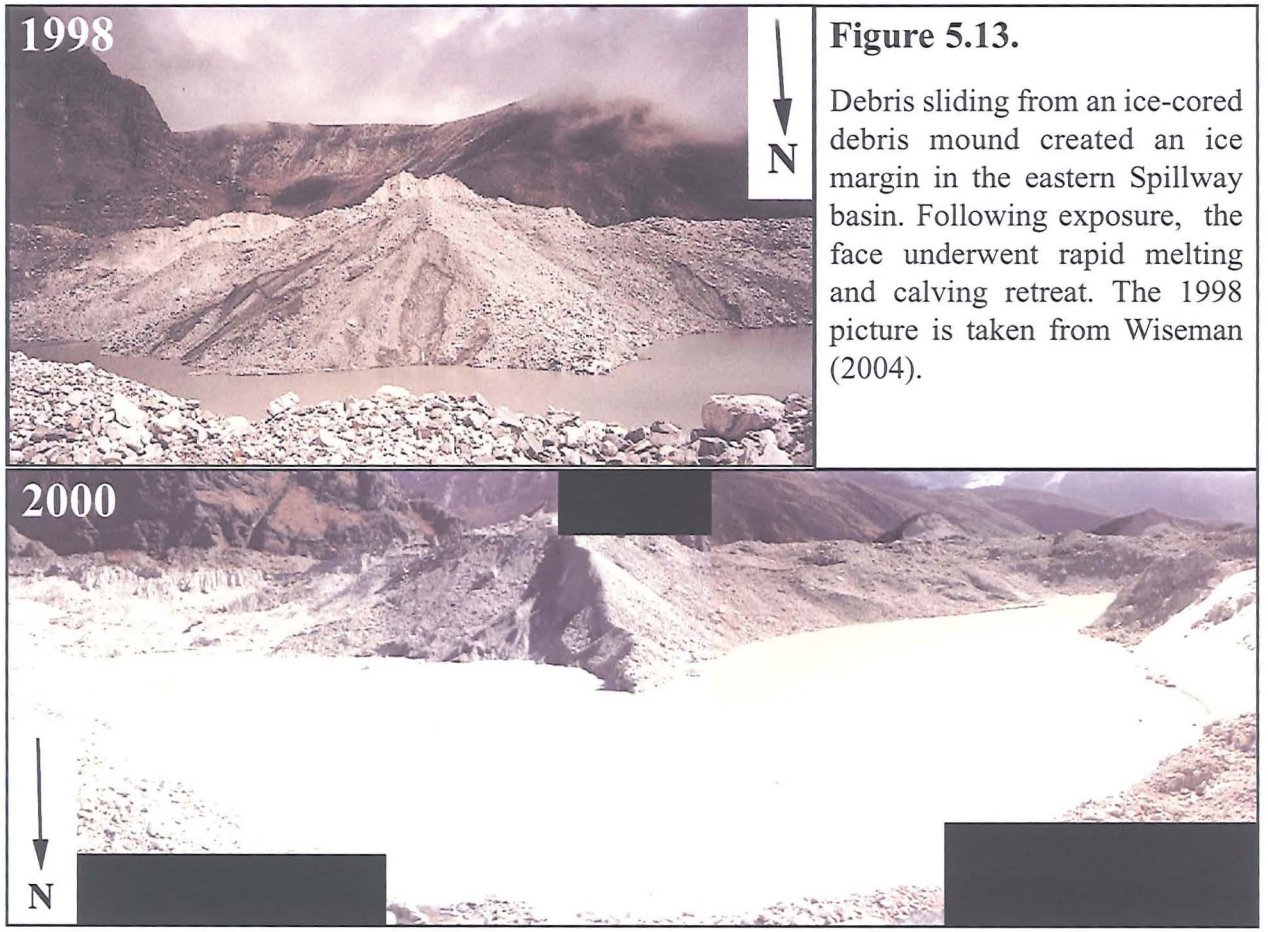

Figure 5.13.

Debris sliding from an ice-cored debris mound created an ice margin in the eastern Spillway basin. Following exposure, the face underwent rapid melting and calving retreat. The 1998 picture is taken from Wiseman (2004).

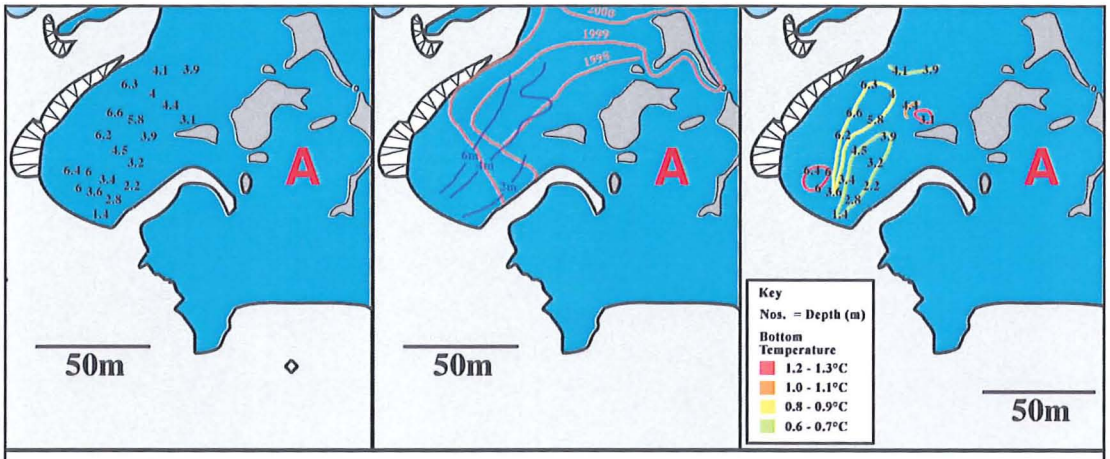

Figure 5.14. An excerpt from Figure 5.3. The left-hand map shows the depth measurements (m) taken in the western Spillway Lake basin in November 2001. The centre map shows the depth of the lake relative to the former positions of the lake margin between 1998 and 1999. The right-hand map shows the temperature distribuion (¡C) at the bottom of the lake in November 2001.

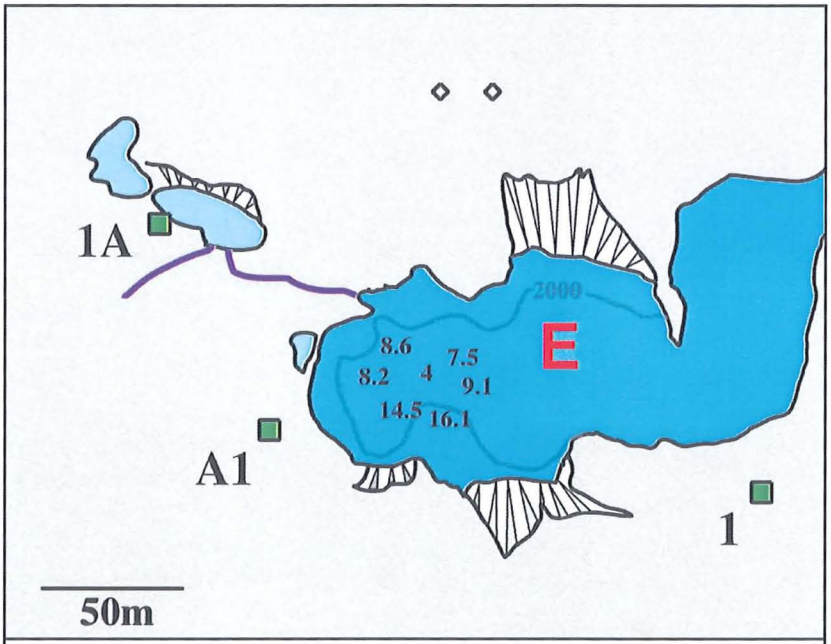

Figure 5.15. The map shows the depth measurements (m) taken in the eastern Spillway Lake basin in October 2001. The map is an excerpt from Figure 5.3.

Point	Depth	Bottom Temp
1	1.4	0.6
2	3.6	0.8
3	6	1.2
4	6	1.2
5	6.4	1.2
6	2.8	0.6
7	3.4	0.6
8	2.15	0.6
9	3.2	0.6
10	4.5	0.7
11	6.2	0.8
12	6.6	0.8
13	5.8	0.8
14	3.9	0.6
15	3.1	1.3
16	4.4	1
17	4	0.8
18	6.3	0.8
19	4.1	0.6
20	3.9	0.7
Av Depth	Av Temp	
4.3875	0.815	

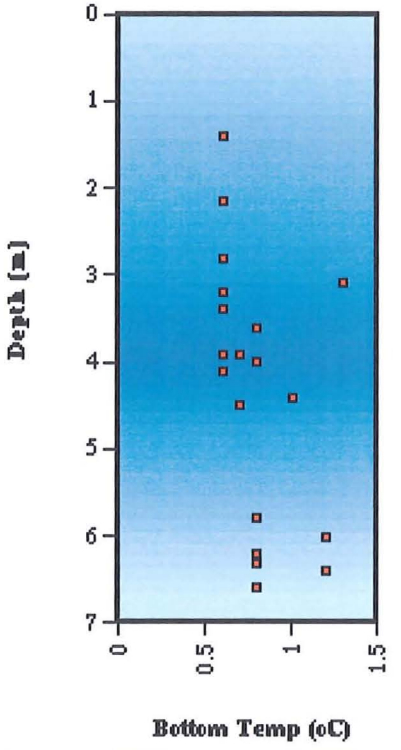

Figure 5.16. Table and graph showing temperature (°C) variation with depth (m) in the western Spillway Lake basin between the 8th and 10th of November 2001. See figure 5.14 for an isothermal map of the lake bottom temperatures in the western Spillway Lake basin.

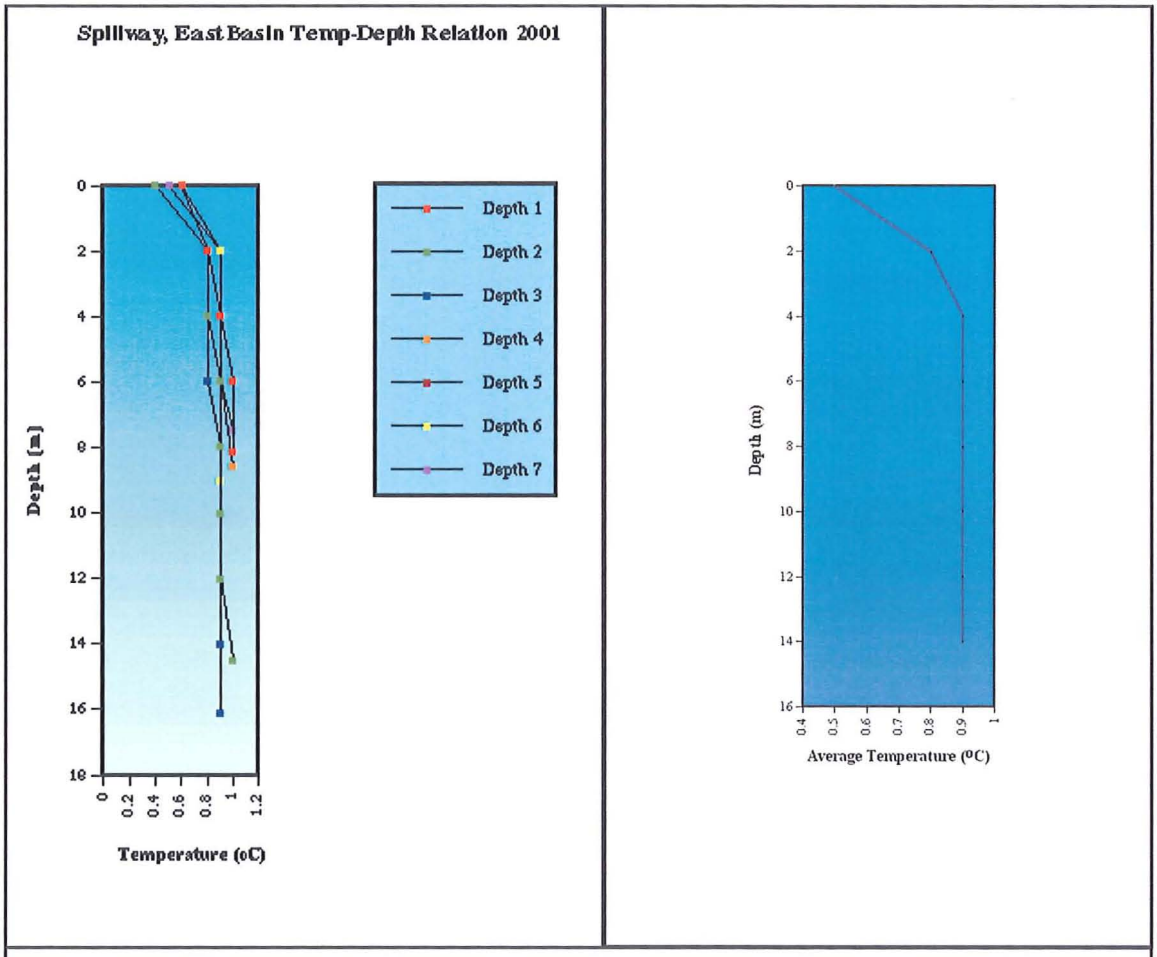

Point 1		Point 2		Point 3		Point 4		Point 5		Point 6		Point 7	
Depth (m)	Temp (oC)	Depth (m)	Temp (oC)	Depth (m)	Temp (oC)	Depth (m)	Temp (oC)	Depth (m)	Temp (oC)	Depth (m)	Temp (oC)	Depth (m)	Temp (oC)
0	0.6	0	0.4	0	0.6	0	0.6	0	0.4	0	0.6	0	0.5
2	0.8	2	0.8	2	0.8	2	0.8	2	0.8	2	0.9	2	0.9
4	0.9	4	0.8	4	0.8	4	0.9	4	0.8	4	0.9	4	0.9
6	1	6	0.9	6	0.8	6	0.9			6	0.9	6	0.9
8.15	1	8	0.9	8	0.9	8.6	1			8	0.9	7.5	1
		10	0.9	10	0.9					9.05	0.9		
		12	0.9	12	0.9								
		14.5	1	14	0.9								
				16.1	0.9								

Average Lake Depth (m)	Average Lake Temp (oC)	Average Lake Surface Tempemperature (oC)	Average Lake Bottom Temperature (oC)
9.7	0.826829268	0.942857143	0.740740741

Figure 5.17. Table and graphs showing temperature (°C) variation with depth (m) in the eastern Spillway Lake basin on the 22nd October 2001.

Figure 5.18.

Table and graph showing temperature (°C) variation with depth (m) in the perched pond to the south of the Spillway Basin. The measurements were taken on 24th October 2001.

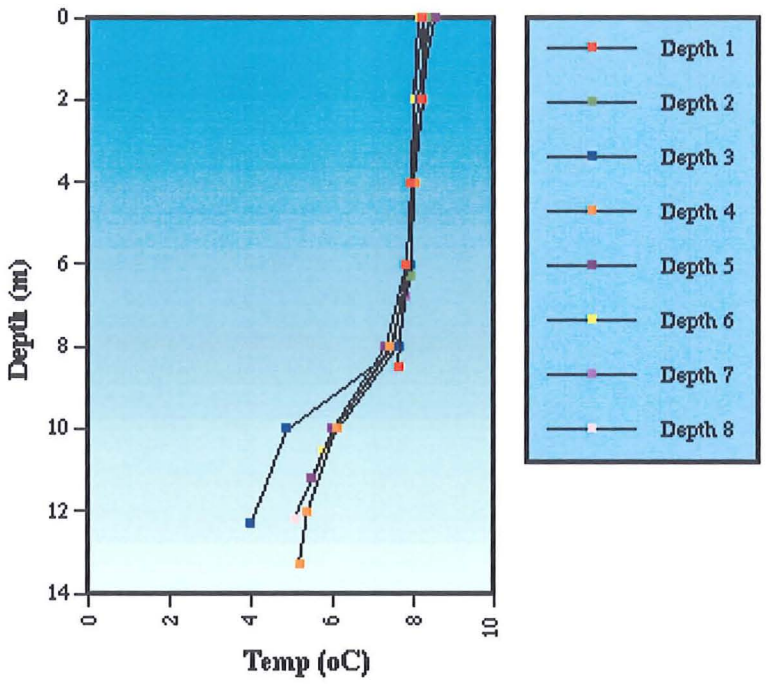

Point 1		Point 2		Point 3		Point 4	
Depth (m)	Temp (oC)	Depth (m)	Temp (oC)	Depth (m)	Temp (oC)	Depth (m)	Temp (oC)
0	8.2	0	8.3	0	8.3	0	8.3
2	8.2	2	8.2	2	8.1	2	8.2
4	7.9	4	7.9	4	7.9	4	8
6	7.8	6.3	7.9	6	7.9	6	7.9
8.5	7.6			8	7.6	8	7.4
				10	4.9	10	6.1
				12.3	4	12	5.4

Point 5		Point 6		Point 7		Point 8	
Depth (m)	Temp (oC)	Depth (m)	Temp (oC)	Depth (m)	Temp (oC)	Depth (m)	Temp (oC)
0	8.5	0	8.1	0	8.2	0	8.4
2	8.1	2	8	2	8	2	8.1
4	7.9	4	7.9	4	7.9	4	7.9
6	7.8	6	7.9	6	7.9	6	7.8
8	7.3	8	7.6	6.8	7.8	8	7.5
10	6	10.5	5.8			10	6.1
11.2	5.5					12.2	5.1

Average Lake Temp (oC)	Av. Lake Surface Temp (oC)	Av. Lake Bottom Temp (oC)
7.434693878	6.1125	8.2875

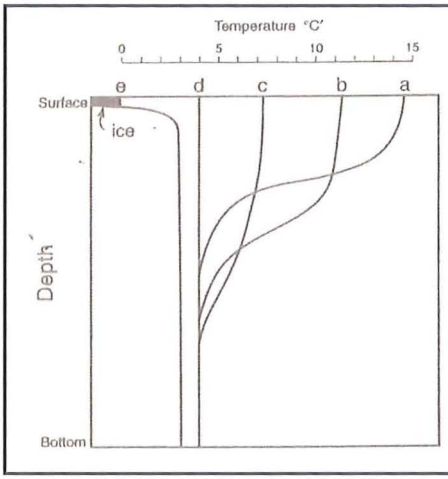

Figure 5.19.

Figure showing the hypothetical evolution of thermal structure in a lake between summer (a) and winter (e). From Smith and Ashley (1985).

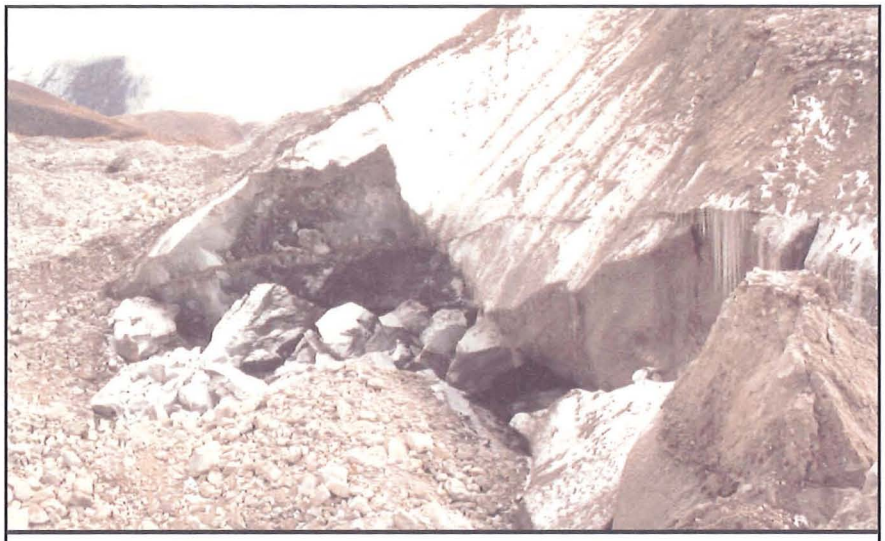

Figure 5.20. Collapse of an ice face above an englacial conduit in October 1999. View looking southeast.

Figure 5.21. Continued collapse of the conduit roof and retreat of the exposed ice face occurred between October 1999 and October 2000.

Figure 5.22. Further subsidence occurred to the north of the area of collapse in 2000.

Figure 2.23. The small pond to the north of the collapsed area in October 2001. The pond first appeared in October 2000 and had undergone calving retreat along structural weaknesses within the ice controlled by the rate of thermo-erosional notching at the waterline.

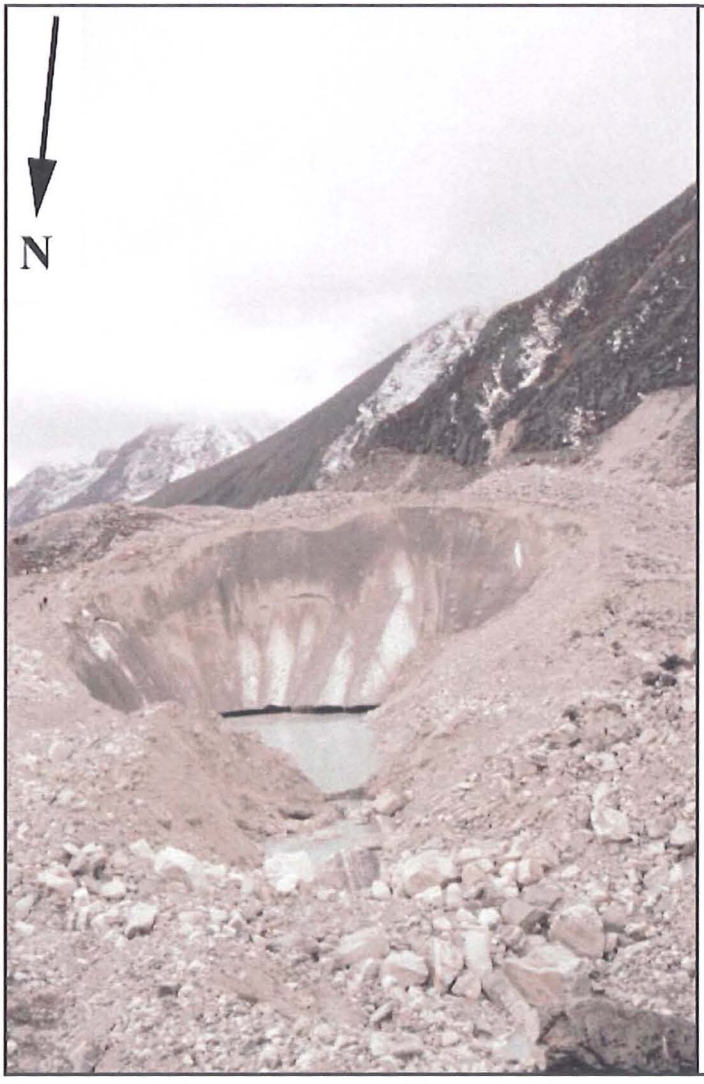

Figure 5.24.

The exposed ice face in 2001 with water running beneath the ice. Note the channel-like shape of the feature confirming that collapse occurred along the line of an englacial conduit.

Figure 5.25. View looking south. The perched pond (H), situated 54m south of the Spillway basin, will amalgamate with the Spillway Lake in the future.

Figure 5.26. The westernmost of the two small ponds situated 41m east of the Spillway Lake basin. Meltwater from the ice face and a subaerial stream entering the pond have a cooling effect on the water temperature. Both ponds will be amalgamated into the Spillway basin within the next few years.

Chapter 6

Paraglacial Reworking on the Ngozumpa Moraines

6.1. Introduction

Determining the rate of paraglacial reworking of moraines bordering debris-covered Himalayan glaciers is important because of the natural tendency for this type of glacier to form moraine-dammed lakes at or near to the terminus. Research into the rates of moraine degradation and stability provides invaluable information about how, where, why, and possibly when, moraine dams will fail. This chapter will examine the processes and rates of paraglacial reworking on the ice proximal slopes of the Ngozumpa moraines. The mechanisms of moraine reworking and the rates of retreat were examined in detail at three sites on the western lateral moraine. This allows the longevity of the moraines at the Ngozumpa to be estimated, with particular reference to the timing of possible flood events from the lateral moraine-dammed lakes in the western tributary valleys.

6.2. Description of the Ngozumpa Moraines

Large multi-crested Ghulkin-type lateral and terminal moraines encompass the Ngozumpa Glacier from the headwalls down to and around the terminus (Figures 6.1 6.2 and 6.3, see also Chapter 2, section 2.6.2). The moraine consists of particles that range in size from very fine silts and sands to large boulders measuring up to tens of metres in length. It is estimated that moraine deposition at the Ngozumpa Glacier began during the Chhukung Stage (c. 10ka) and continued episodically throughout the Holocene (See Chapter 3, section 3.3.1). The innermost moraine units are likely

to have been abandoned at the onset of glacier thinning following the Little Ice Age maximum.

Downwasting of the glacier has left the moraine crests standing between c. 20 and 120 m above the present glacier surface. The barrier formed by the moraine has resulted in the ponding of water on the glacier surface and the restriction of meltwater drainage from the glacier to a spillway through the western lateral moraine around 1 km from the glacier terminus (see Chapter 5). A second smaller spillway channels meltwater off the glacier surface through the southeastern terminal moraine. The existence of a complete moraine loop is one of the main controlling factors on the growth and subsequent failure of large and potentially dangerous supraglacial moraine-dammed lakes. In addition to restricting drainage from the glacier surface, the western lateral moraines of the Ngozumpa Glacier have dammed drainage from the tributary valleys causing the formation of five lateral moraine-dammed lakes (see Chapter 3, section 3.3.1 and Figure 6.1). A sixth lateral lake, the Gyajumba Tsho, that formed in the northern-most of the western tributary valleys, burst out through the western lateral moraine onto the glacier surface sometime during 1998 (Wiseman, 2004) (See Chapter 3, Figure 3.15), leaving behind a series of smaller ponds. The integrity and rate of degradation of the western lateral moraine is therefore important to the stability of the laterally-dammed lakes as well as to the formation and possible failure of a supraglacial moraine-dammed lake at the glacier terminus. An area of particular concern is the village of Gokyo (4750 m) that has been built on a large debris fan that extends from below the crest of the outermost moraine to the eastern shore of the Dudh Pokari, the third lateral moraine-dammed lake (Figure 6.4). The trekking village, which is permanently occupied and visited by thousands of tourists every year, is threatened as paraglacial reworking causes retreat of the inner moraine edge. Determining the rate of paraglacial mass wasting of the Ngozumpa moraines is crucial to predictions of when the Dudh Pokari and other marginal lakes are likely to flood out onto the glacier surface.

6.3. Glacier Downwasting and Moraine Stability

The outer and inner moraine slopes at the terminus of the Ngozumpa Glacier are generally well vegetated and relatively stable (Figures 6.5 and 6.6). In contrast, the inner moraine slopes from around 1-2 km upglacier of the terminus are unvegetated and are undergoing rapid paraglacial reworking and retreat. Along most of their length, the inner moraine slopes have developed a free face and talus slope profile, although landslipping of blocks of moraine frequently modifies the general slope profile.

The height of the moraine crests, relative to the level of the glacier surface, increases with distance from the glacier terminus. This is due to the increase in the downwasting rate upglacier resulting from the general increase in debris thickness downglacier. Consequently, the length of inner moraine slope increases with distance from the glacier terminus, which in turn causes an increase in slope activity on the inner moraine in an upglacier direction (Figures 6.5 and 6.6).

Activity on the upglacier inner moraine slopes seems to have increased slightly between 1984 and 2000 (Figures 6.5 and 6.6). Paraglacial reworking of these slopes was evident in the increased incidence of landslipped blocks on the lateral moraines. The most active slopes in both years were the inner western moraine slopes near to the Gyajumba Tsho (c. 11 km upglacier from the terminus). This is due to the relatively thin debris cover and the increased rates of surface downwasting in this area. Further evidence for high rates of surface downwasting adjacent to the Gyajumba Tsho is the pronounced increase in the number of supraglacial ponds that have developed in this part of the glacier since 1984.

6.3.1. Debris Thickness

Measurements of debris thickness were made in October 2001 around the Spillway Lake basin and the immediate environs, around the Pond 7092 basin and at several points across the glacier surface c. 12km from the glacier terminus where ice faces

were exposed. The debris thicknesses were determined by measuring the depth of the debris layer at the top of exposed ice faces using a Leica TR1000 theodolite and a Dior 3002S Distomat and reflector. The first measurement determined the distance (L) and angle (α_1) to the top of the debris layer and a second measurement was made of the angle (α_2) to the ice-debris interface, which is assumed to be vertically below the first point (Figure 6.7). The thickness of the debris layer (d) was then determined as follows:

$d = z_1 - z_2$

Where,

$z_1 = \text{Sin}(\alpha_1) \times L$

$z_2 = \text{Sin}(\alpha_2) \times L$

The assumption that the second measurement lies vertically below the first, although unlikely to be strictly true, was deemed to be acceptable. Any errors introduced are likely to be small due to the large distance of (L) relative to the depth of the debris layer (d) and the similar elevations of the survey stations and the tops of the measured ice faces.

In the vicinity of the Spillway Lake, debris thicknesses ranged from 0.1 m to 7.4 m and the average debris thickness was 1.8 m. Across the second transect in the vicinity of Site B, the depth of the debris cover ranged from 0.1 m to 6.4 m with an average depth of 2 m. Debris thicknesses across the third transect, taken around 12km from the terminus were much lower and ranged between 0.1 m and 3.2 m with an average thickness of 0.6 m. These thicknesses should be considered to represent the minimum depth of the debris cover because the debris depth could only be measured at the tops of ice faces where the debris thicknesses are expected to be lowest.

The decrease in debris thickness and the resulting higher downwasting rates upglacier has brought about an increase in the height of the moraine crests above the level of the glacier surface upglacier. At the terminus the minimum height of the moraine above the glacier surface is c. 20 m. The minimum height of the moraine

crest increases to 40 m around 4km from the terminus, and ~12km from the terminus the moraine crests are situated between 60 m and 120 m above the glacier surface. Further upglacier the minimum height of the moraine crest increases to >120 m above the glacier surface.

6.4. Moraine Case Study Areas

The outer moraine slopes of the Ngozumpa Glacier are well vegetated and generally stable, although relict slope failure scars, terracing and fans provide abundant evidence that these slopes were once highly active (Figures 6.4, 6.5 and 6.6). In contrast to the outer moraine slopes, the inner moraine slopes are extremely active. These slopes are long, steep and unvegetated as a result of the continued lowering of the glacier surface (Figure 6.8). Many slope processes are active on the inner moraine slopes including sliding, rock fall, debris flow, gullying, debris avalanching, and wind erosion. As a result of these processes, the inner moraine slopes are undergoing rapid retreat.

Three study sites were chosen to examine rates and processes of paraglacial reworking of the lateral moraines at the Ngozumpa (Figure 6.1). Site A is located about 1.5 km from the glacier terminus beside the Spillway Lake, Site B lies above the village of Gokyo approximately 4 km from the terminus, and Site C is situated around 4.5 km up glacier from the terminus. The sites were chosen to illustrate the range of processes operating on the moraine slopes at an increasing distance from the glacier terminus. Additional observations were made of the moraines at other locations, including the effects of snow melt, the amount of vegetation present, the effects of wind erosion, the failure mechanisms active on the moraine slopes, and signs of future slope failure events.

6.4.1. Site A

In October 1999, four moraine transects were measured on the moraines at Site A using a tape measure, Abney Level and compass. The average height of the moraine crests above the glacier surface at Site A was c. 39 m. The maximum inner moraine slope gradient was 41° and the average inner moraine slope gradient was 23.7°. The moraines near the terminus have good vegetation cover on both the inner and outer slopes, which suggests that these moraines are generally stable at present (Figure 6.9 and 6.10). Between September 1999 and 2001, no observable change occurred on the moraine slopes at Site A. The stability of these slopes reflects the low glacier downwasting rates near the terminus due to the thick debris cover.

6.4.2. Site B

The moraines at Site B are much less stable than those near the glacier terminus. Although the outer moraine slopes are vegetated and generally stable, the inner moraine slopes are free of vegetation and highly active (Figures 6.11 and 6.12). The main moraine crest is situated 34.5 m west of the actively eroding inner moraine edge and is situated 94 m above the glacier surface and 66.5 m above the Dudh Pokari Lake at the toe of the outer moraine slope (Figure 6.13). The altitude of the Dudh Pokari is therefore calculated to be 27.5 m higher than the glacier surface at present and this will increase as downwasting of the glacier surface continues. The top of the active inner moraine slopes are ~76 m above the glacier surface and consist of 1) upper cliffs of intact moraine material and 2) lower fans of reworked talus. A series of small ridges parallel to the moraine have been built up on the glacier surface at the base of the moraine in several places.

Over the period between October 1999 and October 2001, annual measurements of the position of the moraine edge, relative to a series of ten painted boulders labelled B (1-10), were made using a tape measure. From these measurements a mean retreat rate of 0.48 m a^{-1} was derived, although the rates vary between sites (Table 6.1). Retreat of the moraine edge was the result of a number of slope processes active on the inner moraine slopes including gullying, rockfall and debris avalanching.

Variations in the retreat rate reflect the dominant processes active at each site, which are discussed below.

Table 6.1. Moraine Edge Retreat at Site B from 1999-2001.

Painted Boulder No.	Distance between Boulder and Moraine Edge (m)			Total Amount of Edge Retreat (m)			
	1999	2000	2001	2000	2001	Total Retreat (m)	Mean Annual Retreat Rate ($m\ a^{-1}$)
B(1)	6.7	6.09	5.22	0.61	0.87	1.48	0.74
B(2)	1.65	1.58	1.58	0.07	0	0.07	0.04
B(3)	3.05	1.91	1.91	1.14	0	1.14	0.57
B(4)	4.07	2.04	1.96	2.03	0.08	2.11	1.06
B(5)	3.82	3.82	3.61	0	0.21	0.21	0.11
B(6)	4.84	4.84	4.8	0	0.04	0.04	0.02
B(7)	5.9	5.5	4.76	0.4	0.74	1.14	0.57
B(8)	1.98	0.66	0.07	1.32	0.59	1.91	0.95
B(9)	6.83	6.33	5.45	0.5	0.88	1.38	0.69
B(10)	2.75	2.72	2.72	0.03	0	0.03	0.02
Average Edge Retreat (m)				**0.61**	**0.34**	**Overall Mean Retreat Rate ($m\ a^{-1}$)**	**0.48**

6.4.2.1. Gullying

Along much of the length of the inner moraines deep gullies have been incised into the very steep scarp edges (Figures 6.14 and 6.15). Gullies can rapidly increase in size due to the channelling of snowmelt and rainfall. Extensive gullying of lateral moraines may also result from the melting out of buried ice cores within the moraine (Mattson & Gardner, 1991; Ballantyne & Benn, 1996), although no direct evidence of this process was found at the Ngozumpa. Rockfall from the gullies is a regular occurrence due to the exposure of large stones and boulders through the continuous removal of the supporting fine-grained matrix by weathering processes. Without the support of a matrix the larger clasts embedded in the moraine fall under the force of gravity. Very large boulders were observed to remove more morainic material as they fell, and even to trigger minor slope failures on the lower moraine slopes.

Gullying of the moraine slopes at Site B was observed directly in front of B(1), B(6) and B(8). A large gully was also opened up 2.9 m to the north of B(2) (Figure 6.16).

Average yearly edge retreat rates for B(1) and B(8) were among the highest rates observed (0.74 m a^{-1} and 0.95 m a^{-1} respectively), indicating that the formation of gullies along the moraine edge is an important process of moraine degradation. The gully below B(6) did not develop as rapidly as at B(1), B(2) and B(8); and indeed the moraine edge at this point retreated by a total of only 4 cm over the two years. It is believed that this was due to armouring of the gully head by several medium-sized boulders and the stabilisation of the soil by large and substantial plant roots.

6.4.2.2. Toppling and Rockfall

The moraine edge at B(4) underwent the greatest amount of retreat over the two year period, totalling 2.11 m. The retreat of the slope was the result of the toppling of a large boulder situated on the edge of the moraine crest during the period between the 1999 and 2000 field seasons. After the initial retreat of 2.03 m in the first year the slope retreat was slowed with only 0.08 m of retreat experienced in the period between the 2000 and 2001 field seasons. The toppling of large boulders from the crests of the moraines can therefore be seen as another process of moraine edge retreat (Figure 6.17). Rocks and boulders embedded within the moraine were observed to fall out of the supporting moraine matrix on several occasions, triggering further rockfalls and slope failures on the lower moraine slopes (cf. Blair, 1994). During the 2001 field season, a large boulder approximately 5 m in length fell from the eastern moraine causing the failure of the slope in several places where the boulder made contact with the slope (Figures 6.18 and 6.19). The slope failure appeared to take the form of a cohesionless grain flow with rocks and boulders colliding with each other as they tumbled down slope under gravity. At least two smaller slope failures were observed in quick succession subsequent to the large boulder falling. It is hypothesised that the large boulder was destabilised after a period of snow melt triggered debris flows in the immediate vicinity, removing some of the matrix material supporting the boulder. Blair (1994) suggested that after a wet period, shrinkage of the fine supporting matrix during drying can also cause large blocks to fall out of the moraine. The shrinkage of the fine matrix may also have been a factor in triggering the large rock fall event witnessed at the Ngozumpa.

The moraine edge in front of B(10) is believed to be a site of potential toppling failure. During the study period, a large boulder protected the moraine edge at this point and consequently it experienced the lowest rate of retreat at Site B over the two-year period (0.03 m a^{-1}). As mentioned previously, the moraine edge at B(6) was similarly armoured with several rocks and large roots that slowed the rate of moraine edge retreat. Interestingly, the moraine edge in front of B(10) experienced noticeable retreat at either side of the protective boulder. It is likely, therefore, that once the boulder has toppled, the retreat rate at the site will increase.

6.4.2.3. Debris Avalanching

The free face beneath B(2), B(3) and B(5) was considerably steeper than at the other sites measured on the moraine, and represents ungullied parts of the slope. No retreat was monitored for B(5) between the 1999 and 2000 seasons; however, 0.21 m of retreat was recorded for the period between 2000 and 2001. Similarly at B(3), 1.14 m of retreat was recorded during the period 1999 to 2000, and then activity ceased between 2000 and 2001. The moraine edge in front of B(2) underwent only 0.07 m of retreat during the period 1999 to 2000 after which time retreat was halted. The start-stop retreat rates of the areas of moraine between the gullies suggests that as the gullies on the scarp slope widen and become more incised the intervening areas are steepened and narrowed until they eventually become destabilised and fail in large but infrequent debris avalanching events.

At B(7) and B(9) the rate of yearly retreat was slightly greater than average (0.57 m a^{-1} and 0.69 m a^{-1} respectively), and it is likely that both of these sites will undergo debris avalanche activity in the near future. At B(9) tension cracks were starting to appear back from the moraine edge in September 2001 and 1.04 m of vertical displacement was recorded for the period between the 2000 and 2001 field seasons (Figure 6.20). This vertical displacement could be evidence of deeper shear planes within the moraine wall and could give rise to a debris slide causing a large segment of the moraine crest to fail as a solid unit. The sliding of large blocks downward

toward the glacier surface may be a contributing factor for the build up of ridges at the base of the moraine slope at the ice-moraine interface.

6.4.2.4 Summary

The dominant processes of moraine edge retreat on the Ngozumpa moraines at site B are believed to be 1) gullying followed by debris avalanching in the intervening areas and 2) the toppling of boulders from the moraine crest and the falling of stones and boulders from within the moraine matrix.

6.4.3. Site C

In common with Site B, the moraine at Site C (Figure 6.1) has vegetated outer slopes and steep active inner slopes. The moraine edge is situated c. 100 m above the glacier surface. The inner moraine slope profile is broken up by the downward displacement of two slipped masses of moraine material; termed Block 1 and Block 2 (Figure 6.21). The movement and erosion rate of the two blocks at Site C was monitored between October 1999 and October 2001 by annual laser distomat surveys of the top of the blocks. The surveys were used to draw up maps of the progress of the two blocks as they slumped down the inner moraine slope (Figures 6.22 and 6.23).

6.4.3.1. Block 1

In October 1999, Block 1 measured 213.3 m long and had a maximum width of 21.3 m. Between 1999 and 2000, Block 1 had slumped approximately 0.34 m down the moraine slope with a horizontal displacement of c. 2.5 m (Figures 6.22, 6.23, 6.24 and Table 6.2, p207). The middle of the block had experienced slightly more slumping than the edges and this caused a small decrease in the block length to c. 200 m. The edge of the block had undergone gullying and debris avalanching and had experienced an average of 4.3 m a^{-1} of retreat during this period. The block slumped by around a further 10.2 m down-slope between 2000 and 2001 and was displaced horizontally by c. 4.6 m (Figures 6.22 6.23, 6.24, 6.25 and Table 6.2, p207). The rate of edge retreat by gullying and debris avalanching had slowed to an

average of 2.7 m a^{-1} over this period. The southern end of Block 1 experienced a slight tilt between October 2000 and October 2001, causing the block surface to become more parallel with the glacier surface. Discrepancies with regard to the vertical displacement of the block (see Table 6.2, p207) are the result of debris avalanching from the rectilinear slopes above, causing the progradation of debris fans on the surface of the block. The survey data suggest that Block 1 underwent little change in the first year (1999-2000) before undergoing a large translational slide between the 2000 and 2001 field seasons which consequently triggered several debris avalanches on the rectilinear slope above the block.

In October 2001, it was noticed that a large tension crack was forming on the main moraine edge c. 25 m to the south of Block 1 (Figure 6.22). It is expected that the moraine slope at this point will undergo rapid retreat involving the slip of large blocks of moraine in the near future.

6.4.3.2. Block 2

In October 1999, Block 2 was 366.7 m long and had a maximum width of 25.4 m. Block 2 slumped around 7.5 m down-slope between October 1999 and October 2000 and was horizontally displaced by 2.7 m (Figures 6.22, 6.23, 6.26 and Table 6.3, p208). The edge of the block experienced an average of 0.4 m a^{-1} of retreat by gullying and debris avalanching over this period. Block 2 began to break up between October 1999 and October 2000 and a large tension crack had appeared c. 165 m from the southern edge (Figures 6.22 and 6.27). The break up of the block caused the length of the block to increase to 373.3 m. Between October 2000 and October 2001, Block 2 slipped a further 5.93 m down-slope and was displaced horizontally by c. 6.25 m (Figures 6.22, 6.23, 6.26 and Table 6.3, p208). The retreat rate of the block edge decreased to an average of 0.3 m a^{-1} between October 2000 and October 2001. In October 2001, more large tension cracks were noticed to have appeared below the surface vegetation (Figure 6.27). It was also noted that a small section of the block had become completely detached and was perched around 8.3 m above the

main block surface (Figures 6.28 and 6.29). The continued break up of the block had caused a further increase in the block length to c. 380 m.

Disintegration of Block 2 is related to the large stresses placed on the block by sliding and rotation as it travels down-slope. Tilting of the Block 2 surface was most obvious at the southern end of the block. The surface of the block was tilted down towards the glacier surface between October 1999 and October 2000 as the block slipped down the moraine slope. Between October 2000 and October 2001, the block was rotated further, causing the surface of the block to slope back towards the moraine crest. The data indicates that the block underwent translational sliding between October 1999 and October 2000 followed by one or more rotational slides between October 2000 and October 2001, possibly caused by the removal of support at the base of the moraine. The rotation of Block 2 is demonstrated well in the slope profiles (Figure 6.26).

6.4.3.3. Summary

Blocks 1 and 2 are gradually landslipping towards the base of the inner moraine slope by translational and rotational sliding. Landslipping of blocks at the Ngozumpa usually occurs along shear planes within the moraine and the first sign that this type of slope failure is occurring is the appearance of tension cracks along the top of the moraine. As the landslipped blocks proceed down-slope they undergo edge retreat by gullying, avalanching, debris flow and wind erosion. Blocks are often broken up as they travel down-slope, but if they reach the base of the slope intact they can form a ridge of moraine on the glacier surface. These ridges often retain their vegetation cover after deposition. Where a high rate of landslipping occurs, a series of parallel ridges can form at the base of the inner moraine slope.

6.5. Slope Processes: Wider Implications

In addition to the slope processes discussed in the detailed studies above, several other processes were identified as being important on the Ngozumpa moraines. These processes are examined in turn below.

6.5.1. Wind Erosion

During the course of the fieldwork it became apparent that sand and other fines were being actively eroded from the inner moraine slopes by wind action (Figure 6.30). The amounts and rates of aeolian erosion were not quantified but observations indicated that wind erosion of fines is occurring along most of the length of the unvegetated inner moraine slopes. Evidence for wind erosion of the moraines was most prominent above gully heads when the wind was being channelled upwards. In some areas, and particularly above large gullies, accumulations of sand were found deposited on the moraine crests. The removal of fines from gullies in the moraine may serve to destabilise some of the larger stones and boulders lodged within the gully walls, causing rockfalls and other slope failures.

Average monthly and hourly wind speeds on the Ngozumpa were calculated from data from a temporary weather station positioned on the glacier surface between November 2001 and October 2002 (Nicholson, unpublished data). Figure 6.31 charts the average hourly wind speed for each month between November 2001 and October 2002. The data show that wind speeds follow a daily cycle, with maximum wind speeds of up to 6 m s^{-1} occurring at mid-day, between 12pm and 1pm. This is a due to a diurnal valley wind that blows upglacier in the early afternoon. The maximum daily rate of wind erosion is therefore expected to occur between 12pm and 1pm. Table 6.4 below, shows that the average monthly wind speeds are highest in September and October and lowest during November and December. This suggests that maximum rates of wind erosion occur during the months of September and October. The amount of precipitation will also affect the rate of wind erosion on the inner moraine slopes, as will melting of snow cover on the moraines. When the

moraines have a high moisture content less wind erosion will take place because cohesion of fines will be higher. The Ngozumpa moraines will be driest in the pre-monsoon and post-monsoon periods between April and May and September and October. Snow cover during the winter followed by snowmelt in the spring will cause a rise in moraine moisture content. The wettest period occurs during the summer monsoon between June and August. Since the periods of highest wind speed and lowest moisture content of the moraines coincide in September and October, it follows that this is also the period of highest wind erosion on the Ngozumpa moraines.

Table 6.4. Average Monthly Wind Speed (November 2001 – October 2002)

Month	Average Wind Speed ($m\ s^{-1}$)
November 2001	1.27
December 2001	1.41
January 2002	1.69
February 2002	1.78
March 2002	1.54
April 2002	1.63
May 2002	1.64
June 2002	1.69
July 2002	1.61
August 2002	1.63
September 2002	2.37
October 2002	3.53

6.5.2. Debris Flows

Small debris flows and mudflows are a common occurrence on the inner moraine slopes of the Ngozumpa (Figure 6.14). This observation concurs with research carried out in Norway by Ballantyne and Benn (1996) who suggested that debris flow is the main process responsible for paraglacial reworking of glacial drift deposits. During the period of observation, debris flow activity was most frequent after a period of snowfall. The meltwater generated from a melting snow pack causes pore-water pressures in the moraine drift slopes and gullies to rise, lowering the strength of the slope material and causing flow-type failures to occur (cf. Theakstone, 1982; Johnson, 1984; Van Steijn et al., 1988; Cooke & Doornkamp, 1990; Blair, 1991; Owen, 1991; Mattson & Gardner, 1991; Ballantyne et al., 1992; Owen & Sharma, 1998; Palacios et al., 1998). There was no evidence to suggest that

the presence of lake water below a slope affected the frequency of debris flow occurrence. Previous studies of hillslope debris flows suggest that debris flow initiation favours slopes with gradients greater than 28-30° (Innes, 1983; Zimmermann & Haeberli, 1992; Ballantyne & Benn, 1996; Palacios et al., 1998). The largest flows observed at the Ngozumpa moraines occurred on the gentler talus slopes below gullies in the upper cliffs (Figure 6.14). Debris flows at the base of the gullies serve to rework accumulated debris, redistributing it over the lower slopes and producing gentler slopes (cf. Statham, 1976; Ballantyne & Benn, 1996; Van Steijn et al., 1998). It is believed that the sustained and intense rains during the monsoon season will similarly cause a rise in pore water pressures in the moraine sediments and initiate debris and mud flows on the inner moraine slopes (cf. Owen & Sharma, 1998). The channelling of rainfall and snow melt into the gullies of the upper moraine slopes serves to set up a positive feedback system whereby the gullies are incised and enlarged further, enabling them to capture more drainage during subsequent rain and snow melt events. Debris flow failure on the Ngozumpa moraines may therefore be strongly related to season: with very little activity during the cold winter season and increased activity over the wet summer monsoon season. Increased debris flow activity would also be experienced during the spring thaw and during periods of post-monsoon snowfall and subsequent melt.

6.5.3. Ice Cores

Debris flow, mud flow and other forms of mass movement on moraine slopes can also be initiated by the melt out of buried ice cores (Johnson, 1971, 1984; Whalley, 1973; Mattson & Gardner, 1991; Ballantyne & Benn, 1996; Richardson & Reynolds, 2000). Ice cores present within the moraines may also act as a failure plane over which rapid sliding failures can occur. At the Boundary Glacier, Canada, 83% of all sliding failures over ice cores which occurred in the summer field seasons of 1984 and 1985 were triggered after periods of heavy rainfall (Mattson & Gardner, 1991). The reason for this is two-fold. Firstly, the saturation of the overlying sediments can add to the mass of the overburden material and on a slope this increases the shear

stress; and secondly, the presence of water at the ice core/moraine interface can reduce the shear resistance (Mattson & Gardner, 1991).

The presence of ice cores is often marked by the appearance of tension cracks parallel to the moraine (Johnson, 1984). Although no ice cores were discovered in the moraines of the Ngozumpa, it would be imprudent to disregard the possibility of their existence. Once exposed at the surface a melting ice core will cause the direct input of water to the moraine slope increasing the adjacent pore water pressures and facilitating debris flows on the surrounding moraine (Johnson, 1971, 1984). Failure of slopes around an ice core may uncover further cores within a slope setting up a positive feedback cycle (Mattson & Gardner, 1991). Johnson (1984) reported that the melt out of ice cores within the moraines of the Donjek Glacier, Yukon Territory, Canada, causes erosion rates of up to 1.5 m per week during the summer months. An ice-cored kame terrace in Adams Inlet, Alaska, was measured as having a surface lowering rate of c. 0.25 m a^{-1} and backwasting rates between 1966 and 1983 were calculated to be 4.3 m a^{-1} (McKenzie & Goodwin, 1987).

In addition to exposure by low magnitude slope failure events, ice cores can also be uncovered by the debuttressing of moraine slopes during a rapid calving retreat (Kirkbride & Warren, 1999) and during large glacier flood events (Johnson & Power, 1985). Both of these scenarios are important considerations for the stability of the Ngozumpa Glacier moraines should the formation of a large glacial lake, followed by a Glacial Lake Outburst Flood, occur in the future. The stability of moraine slopes underlain by ice cores will only be achieved after all of the cores present within those slopes have been removed.

Although ice cores were not observed to contribute to wastage of the Ngozumpa moraines during the study period, they almost certainly exist beneath the talus aprons, and possibly deeper within the moraines. The presence of buried ice cores may accelerate the wastage rate of the Ngozumpa moraines in the future.

6.5.4. Seismic Activity

Nepal experiences major earthquakes approximately once every 50 years, due to subduction of the Indian plate under the Eurasian plate. The Khumbu Region is situated over the Main Central Thrust, which has been a focal point of tectonic activity in the past (Sharma, 1990). Tectonic disturbances can trigger landsliding, debris flow and other mass movements in moraine deposits (Johnson, 1984) and can also expose ice cores buried within the moraine, leading to increased erosion rates subsequent to an earthquake event. Thus, the long-term erosion rates of the Ngozumpa moraines may be larger than those observed during the study period. The estimates of moraine retreat should therefore be regarded as minima.

6.5.5. Vegetation

The presence of vegetation on a moraine slope has a stabilising effect because it increases the shear strength of the slope (Coppin & Richards, 1990). The plant roots bind together and strengthen the topsoil, whilst shoots and leaves protect the surface from rainsplash and aeolian erosion, which in turn helps to prevent rill erosion and gullying. A good vegetation cover will also act as an insulator protecting any buried snow layers or ice cores within the moraine (McKenzie & Goodwin, 1987). However, vegetation colonisation rates on Himalaya moraines and glacier forelands are low because of the extreme climate, the effects of altitude and the high rates of paraglacial slope reworking (Sharma, 1990). Vegetation has a stabilising effect on the outer moraine slopes and around the slowly ablating terminus of the Ngozumpa, but has only a limited effect on the more active slopes that border most of the glacier.

6.6. Longevity of the Ngozumpa Moraines

The average inner moraine edge retreat rate for Site B is currently c. 0.48 m a^{-1}. At this rate it would take approximately 675 years before the Dudh Pokari, and possibly the other marginally dammed lakes in the western tributary valleys, flood out over the glacier surface. However, the long-term retreat rate is likely to be much higher.

Observed retreat at Site B was mainly caused by gullying, debris avalanching, rockfall, small-scale debris flow, and wind erosion. Higher rates of moraine retreat at the Ngozumpa were experienced at Site C where landslipping of detached blocks occurred. The melt out of buried ice or the external influence of earthquake activity could also rapidly increase the rate of paraglacial reworking on the Ngozumpa moraines.

Additionally, the rate of moraine retreat is predominantly controlled by the rate of downwasting of the glacier surface. Increases in the length of the inner moraine slope will increase the rate of landslipping and cause the reactivation of the lower talus slopes. If the current warming of the Nepal Himalaya continues, the downwasting rate is likely to increase and this in turn will bring about an increase in the rate of paraglacial reworking of the Ngozumpa moraines. In order to fully understand the rate of paraglacial reworking on the moraines of debris-covered Himalayan glaciers, it is necessary to determine the average rate of downwasting on these types of glacier and examine how future rises in global temperature will affect surface downwasting rates.

6.7. Summary

The relationship between rates of downwasting and paraglacial reworking of the moraines is paramount to our understanding of moraine morphology and stability. The moraines at the Ngozumpa Glacier have restricted the drainage of meltwater from the glacier surface and therefore the stability of the moraines at the terminus of the glacier will affect the future development of the Spillway Lake into a large and potentially dangerous moraine-dammed lake. Following the formation a large lake at the glacier terminus, the stability of the moraines around the lake margins could determine when and where the moraine dam is likely to fail. The stability of the western lateral moraines adjacent to the large laterally dammed lakes in the five western tributary valleys are also important due to the height difference between the lakes and the glacier surface. The degradation of the moraine will eventually cause these lakes to flood out over the glacier surface. The rate of paraglacial retreat is

especially important for the village of Gokyo situated on the outer western moraine slopes beside the Dudh Pokari Lake.

It is evident from the research at the Ngozumpa Glacier that the moraines surrounding the glacier terminus are considerably more stable than those upglacier. The crests of the lateral moraines become progressively higher above the glacier surface and moraine slopes become steeper and more active up valley due to the decrease in average debris thickness with distance from the glacier terminus. Slope activity on the inner moraine slopes is therefore lowest near the glacier terminus and then increases with distance from the terminus due to the increasingly faster downwasting rates upglacier.

Processes of moraine edge retreat were observed to occur along almost the entire length of the glacier proximal side of the western and eastern lateral moraines of the Ngozumpa. The only area in which no edge retreat was observed was at the terminus of the glacier where the inner moraine slopes were more stable and had become vegetated. Up to a distance of around 4.5 km from the Ngozumpa terminus, paraglacial retreat of the inner moraine slopes is predominantly by small-scale slope failures such as gullying, debris avalanching and debris flow. Upglacier from this point, the dominant process of slope retreat is landslipping. At Site B, located c. 4 km from the glacier terminus, the mean rate of moraine retreat by small-scale slope failures was calculated to be 0.48 m a^{-1}. Landslipping is a much faster process of moraine retreat. In 1999, the average widths of the surveyed landslipped blocks at Site C were 15.9 m and 19.3 m respectively. As downwasting proceeds and the slope length increases, the zone of landslipping will migrate downglacier and the moraine retreat rate will increase. The rates of moraine retreat recorded here should be considered minima because they do not account for the effects of ice cores buried within the moraine or high magnitude events such as earthquakes on the rate of moraine retreat.

Table 6.2. Horizontal and Vertical Displacement and Average Edge Retreat Rate (m) at Block 1, Site C.

Block 1 Profile A	**1999**	**2000**	**2001**	**Total Edge Retreat (1999-2001)**
Block Width	9.51 m	8.89 m	8.63 m	**0.88 m**
Edge retreat		0.62 m	0.26 m	
	1999-2000			
	Horizontal Displacement		**Vertical Displacement**	
Edge	1.27 m		0.45 m	
Back of Block	1.89 m		0.45 m	
	2000-2001			
	Horizontal Displacement		**Vertical Displacement**	
Edge	5.53 m		10.16 m	
Back of Block	5.80 m		9.78 m	
Block 1 Profile B	**1999**	**2000**	**2001**	**Total Edge Retreat (1999-2001)**
Block Width	17.51 m	16.04 m	14.58 m	**2.94 m**
Edge retreat		1.48 m	1.46 m	
	1999-2000			
	Horizontal Displacement		**Vertical Displacement**	
Edge	3.84 m		0.22 m	
Back of Block	5.32 m		-0.75 m	
	2000-2001			
	Horizontal Displacement		**Vertical Displacement**	
Edge	3.79 m		10.19 m	
Back of Block	5.25 m		10.94 m	
Average Edge Retreat at Block 1				
	1999	**2000**	**2001**	**Mean Annual Edge Retreat Rate**
Av. Block Width	15.9 m	11.6 m	8.9 m	3.5 m a^{-1}
Av. Edge Retreat		4.3 m	2.7 m	

Table 6.3. Horizontal and Vertical Displacement and Average Edge Retreat Rate (m) at Block 2, Site C.

Block 2 Profile A	1999	2000	2001	Total Edge Retreat (1999-2001)
Block Width	13.07 m	12.98 m	10.56 m	**2.51 m**
Edge retreat		0.10 m	2.41 m	
1999-2000				
	Horizontal Displacement		**Vertical Displacement**	
Edge	4.06 m		8.48 m	
Back of Block	4.16 m		2.82 m	
Base of Scarp	0.83 m		4.16 m	
2000-2001				
	Horizontal Displacement		**Vertical Displacement**	
Edge	3.14 m		8.18 m	
Back of Block	5.55 m		10.96 m	

Block 2 Profile B	1999	2000	2001	Total Edge Retreat (1999-2001)
Block Width	25.10 m	22.90 m	15.99 m	**4.17 m**
edge retreat		2.20 m	1.97 m	
1999-2000				
	Horizontal Displacement		**Vertical Displacement**	
Edge	1.29 m		6.49 m	
Back of Block	-0.91 m		0.24 m	
Base of Scarp	1.91 m		0.53 m	
2000-2001				
	Horizontal Displacement		**Vertical Displacement**	
Edge	9.36 m		3.68 m	
Back of Block	16.27 m		10.08 m	

Average Edge Retreat Block 2				
	1999	2000	2001	Mean Annual Edge Retreat Rate
Av. Block Width	19.3 m	18.9 m	18.6 m	0.35 m a^{-1}
Av. Edge Retreat		0.4 m	0.3 m	

Chapter 6 Figures

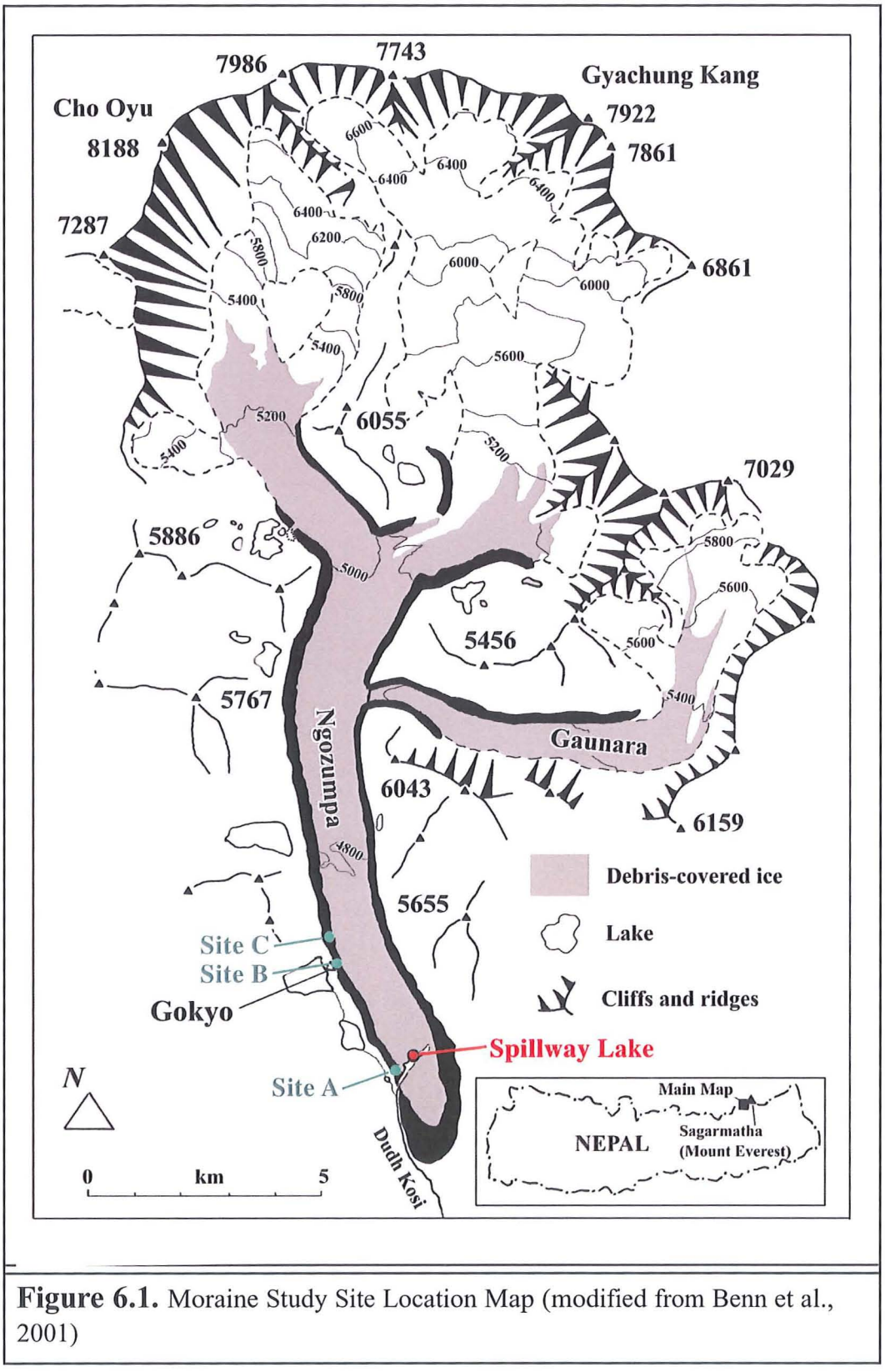

Figure 6.1. Moraine Study Site Location Map (modified from Benn et al., 2001)

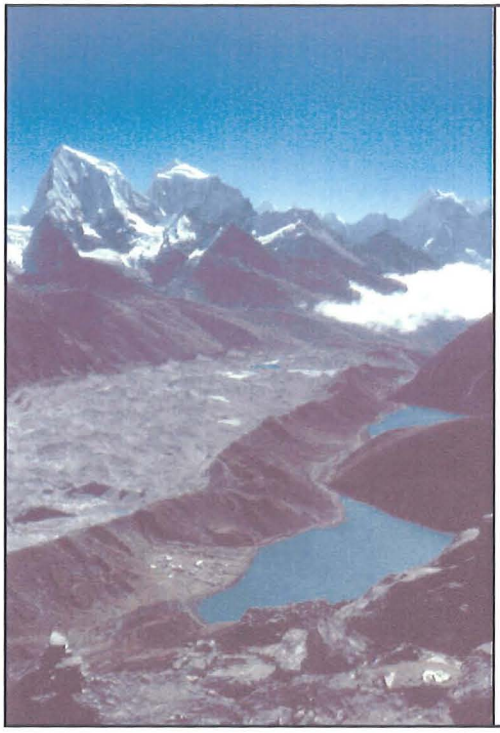

Figure 6.2. Extensive lateral moraines encompass the glacier. The moraines restrict the drainage of meltwater from the glacier surface and have dammed drainage from the tributary valleys to the west causing the formation of five laterally-dammed lakes. View looking south from Gokyo Ri.

Figure 6.3. The large terminal moraine of the Ngozumpa Glacier. View looking north.

Figure 6.4. The village of Gokyo situated on the outer slope of the western lateral moraine. The moraine has dammed drainage from the tributary valley forming the Dudh Pokari Lake, the surface of which is currently situated 27.56m above the glacier surface. View looking southeast.

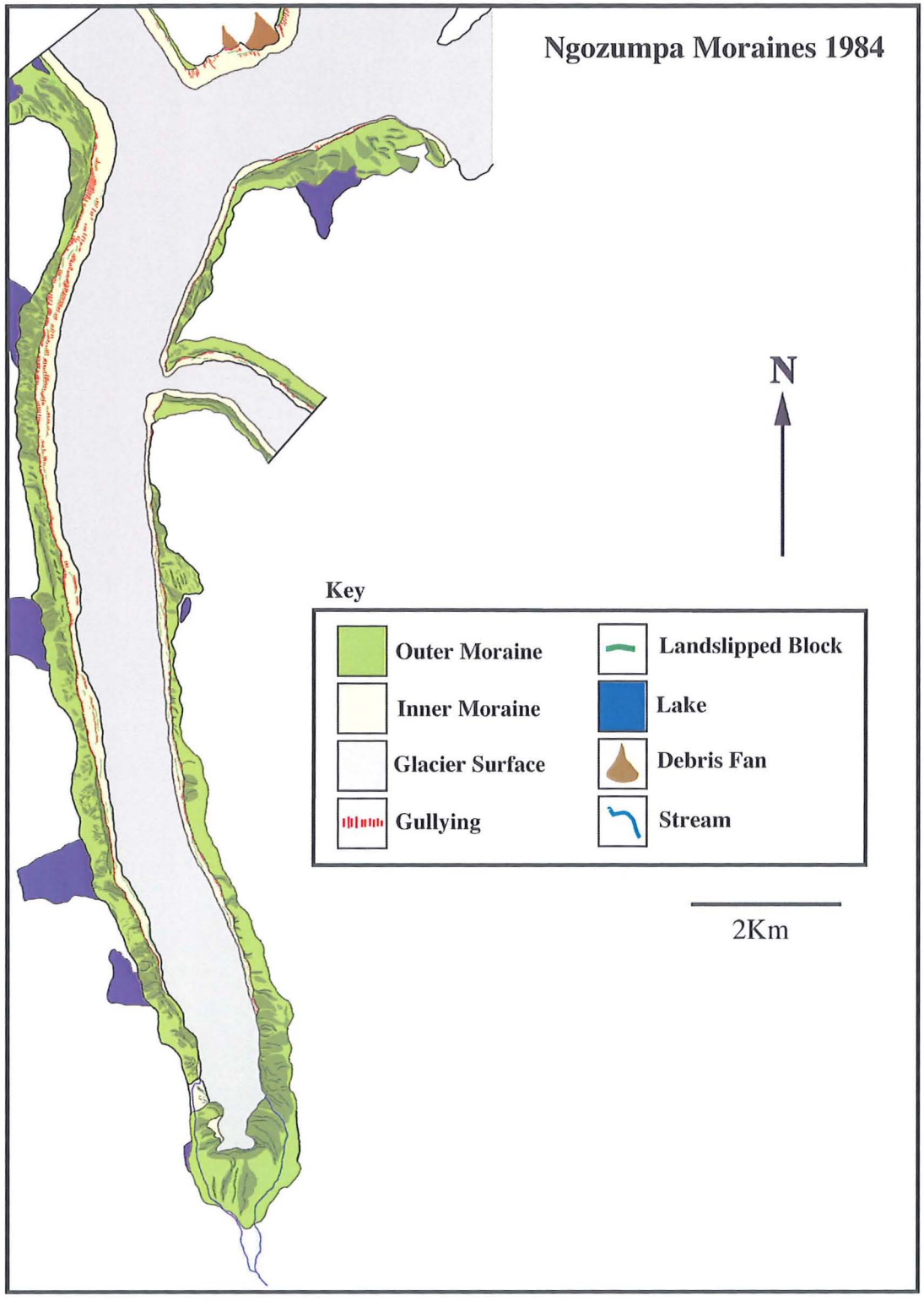

Figure 6.5. Map of the Ngozumpa moraines in 1984. Drawn from the 1984 1:35,000 aerial photograph (no. 123). See figure 3.28 for aerial photograph.

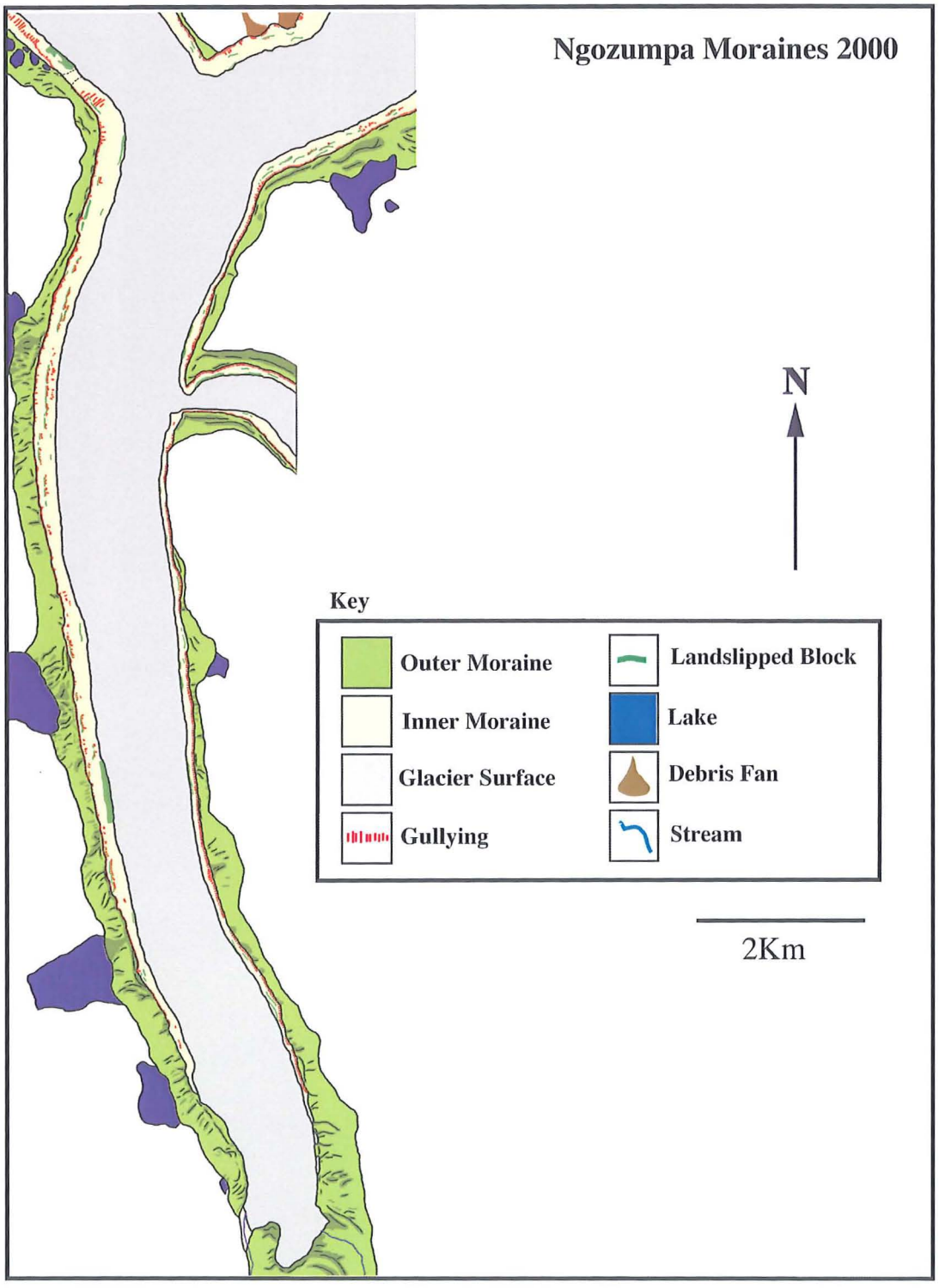

Figure 6.6. Map of the Ngozumpa moraines in 2000. Drawn from a panchromatic SPOT image (scene 227/294) taken on 6th October 2000. Figure 3.29 shows the SPOT image.

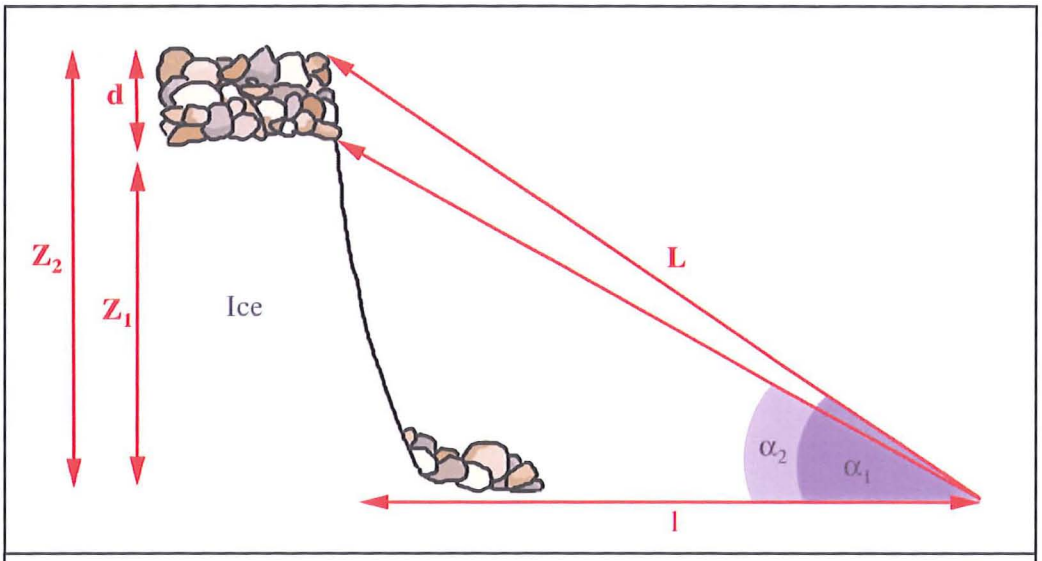

Figure 6.7. Diagram showing how debris thicknesses on the Ngozumpa Glacier were calculated.

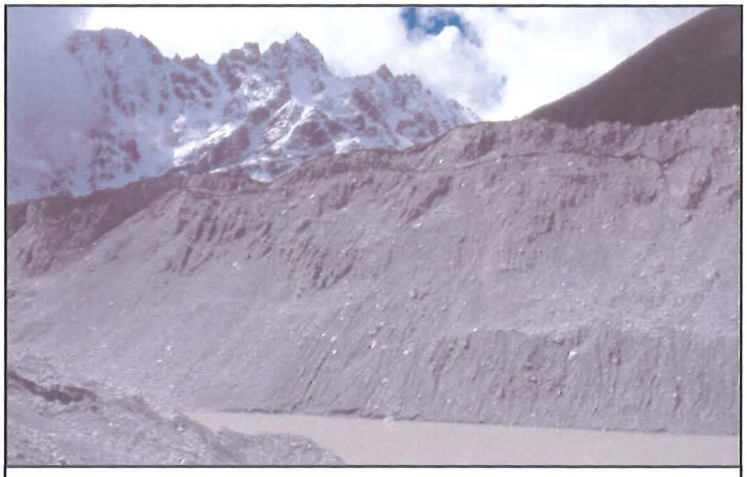

Figure 6.8. The inner lateral moraine slopes upglacier from the Spillway Lake are steep and unvegetated, and are undergoing rapid parallel and vertical retreat by paraglacial slope reworking. Viewed from the glacier surface looking southwest at the western lateral moraine.

Figure 6.9. Site A. The inner slopes of the western lateral moraine at the Spillway Lake in September 1999. The slopes have a thin vegetation cover which suggests that the moraine slopes are reasonably stable here. The relative stability of these inner moraine slopes indicates that the downwasting rate of the glacier surface is lower near to the glacier terminus. Viewed from the glacier surface looking southwest.

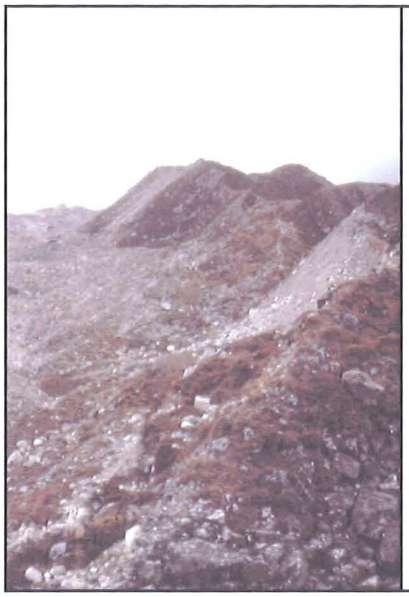

Figure 6.10. The western lateral moraine inner slope c. 100m upglacier from the Spillway Lake. The inner moraine slopes still have a thin vegetation cover but the slope angles are slightly steeper and the crests stand several metres higher above the glacier surface. View looking south from the moraine crest.

Figure 6.11. Site B. The inner western lateral moraine adjacent to Pond 7092. The slope is undergoing rapid paraglacial reworking. Note the recti-linear shape of the exposed slope and the landslipped block. Viewed from the glacier surface looking west.

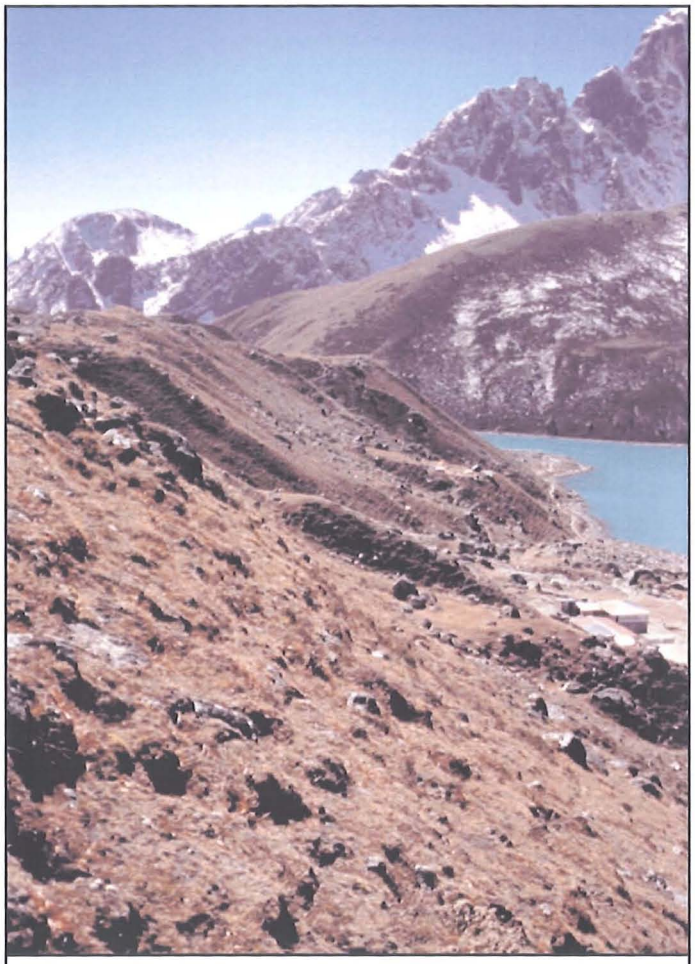

Figure 6.12. The outer slopes of the lateral and terminal moraines are generally well vegetated and relatively stable. View looking southwest.

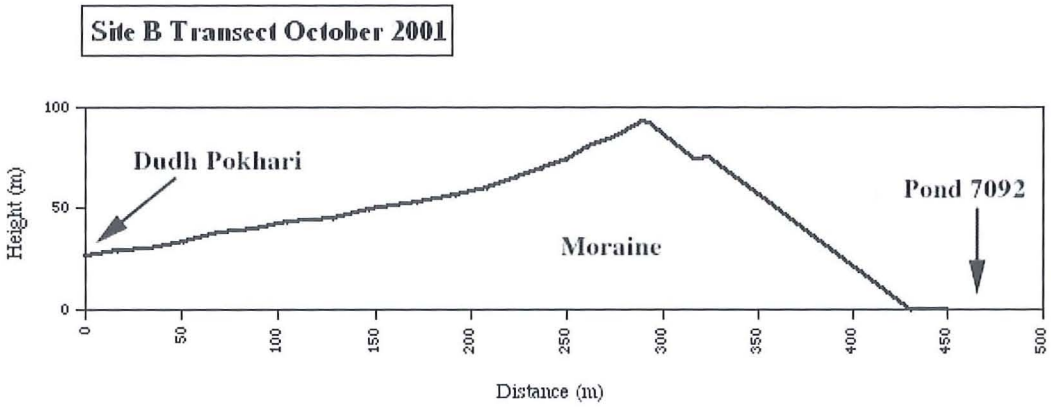

Figure 6.13. Transect of the western lateral moraine at Site B showing the height of the Dudh Pokari Lake and the glacier surface relative to the moraine crest.

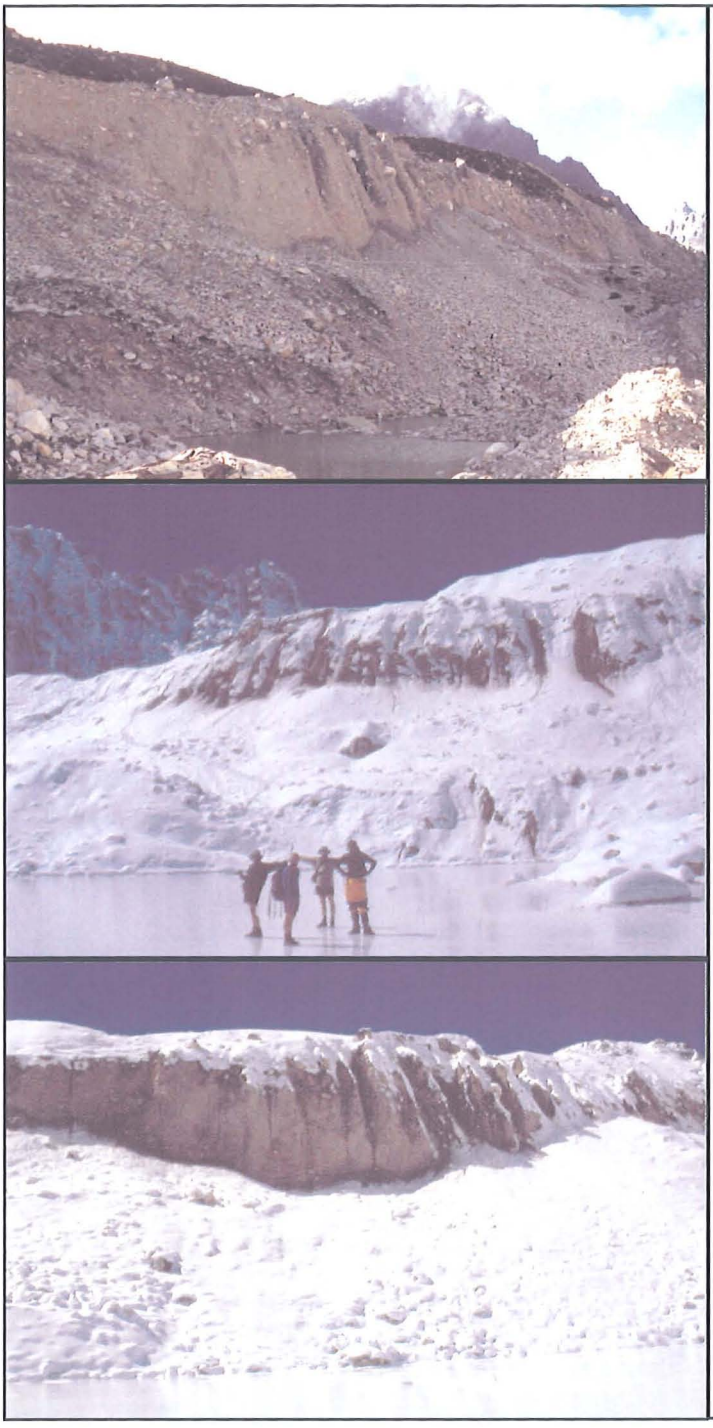

Figure 6.14. Site B viewed from the glacier surface looking northwest and west. Gullying of the free face is most intense during and after periods of heavy rain and snowfall. The three pictures show the development of gullies before and after c. 1m of snow fell on the Ngozumpa Valley during October 1999. Note the mud flows from the gullies in the centre picture. People for scale.

Figure 6.15. Site B in October 2001. Viewed from the glacier surface looking west. The gullies had widened and deepened since October 1999. As gullies are widened and incised the intervening areas become narrower and steeper before eventually failing by debris avalanching.

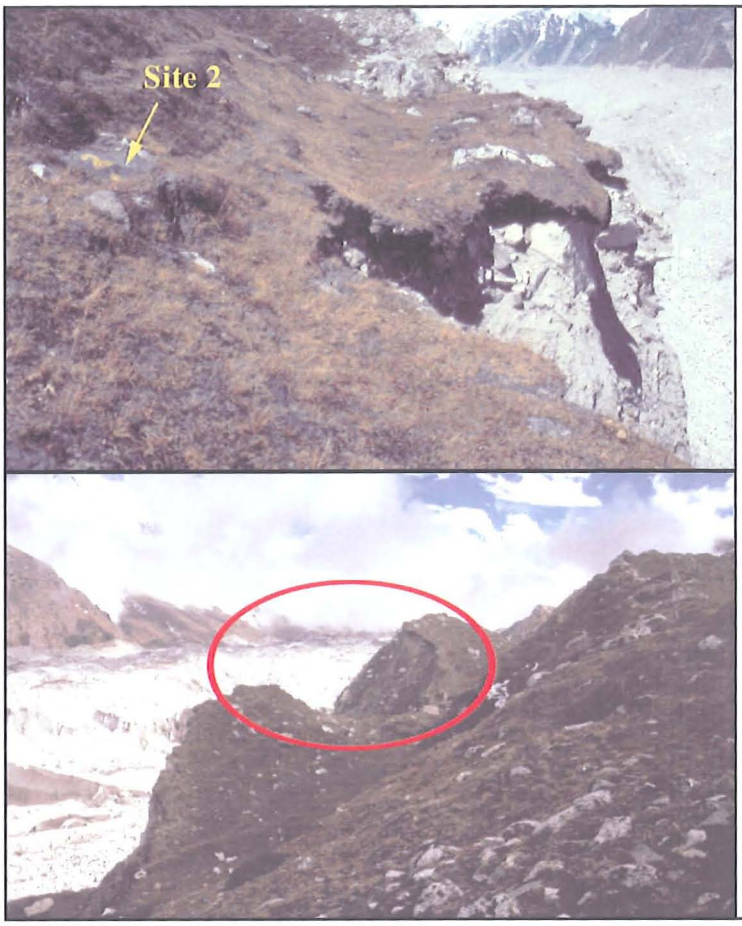

Figure 6.16. Retreat of the moraine slope edge by gullying at Site B. The top photograph shows the development of a gully at Site B (2) in 2000. The lower photograph shows the extent of the moraine edge erosion by gullying at Site B(8) in 2001. Viewed from the moraine looking north and south respectively.

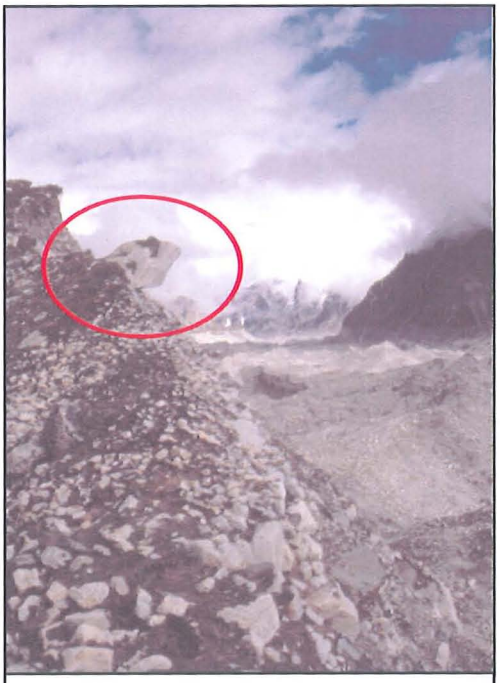

Figure 6.17. A boulder perched precariously on the moraine edge at Site B in October 1999. The boulder toppled sometime between October 1999 and October 2000. Viewed from the western lateral moraine looking north.

Figure 6.18. The eastern inner lateral moraine slope viewed from the western lateral moraine looking east in 1999. Note the extensive gullying of the upper part of the slope.

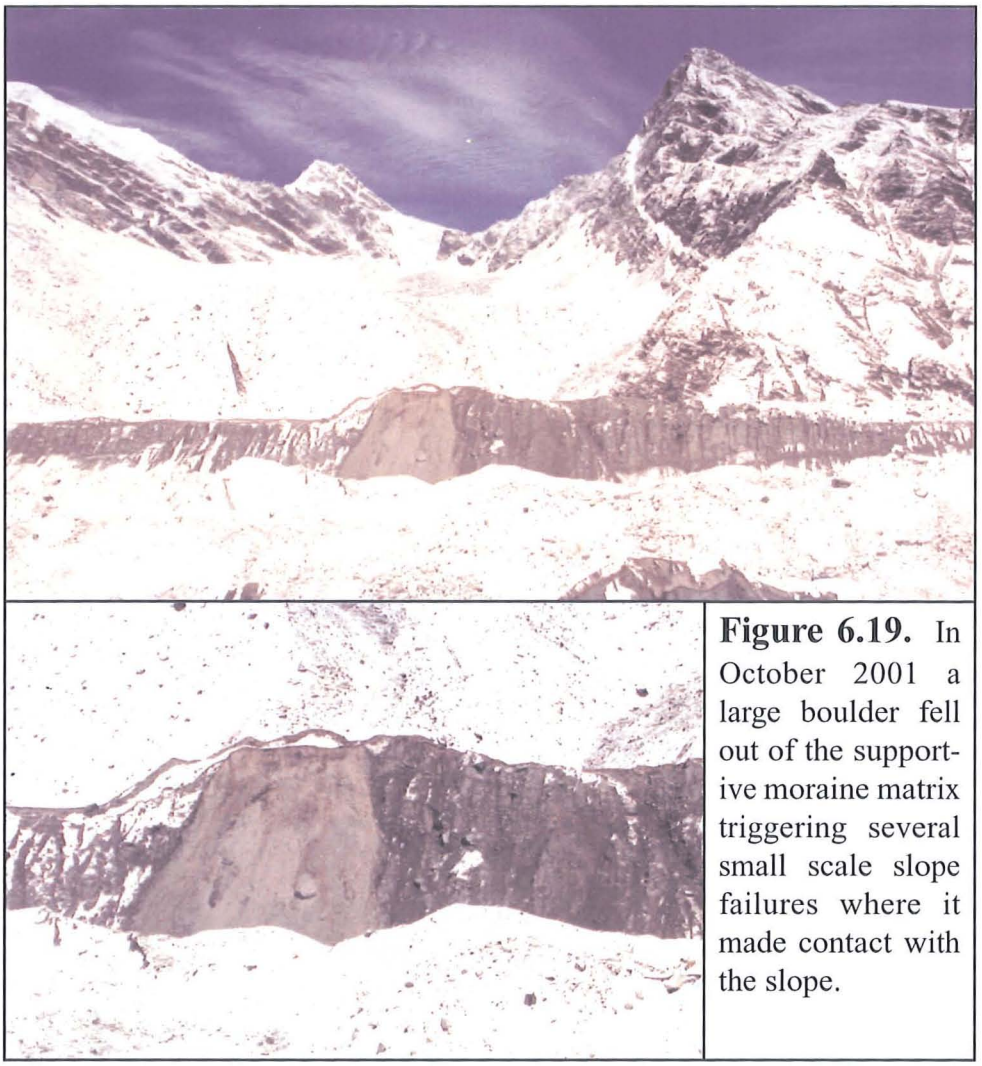

Figure 6.19. In October 2001 a large boulder fell out of the supportive moraine matrix triggering several small scale slope failures where it made contact with the slope.

Figure 6.20. The moraine slope at Site B(9) underwent 1.04m of vertical displacement between October 2000 and October 2001. Person for scale.

Figure 6.21. Site C. The inner lateral moraine slopes above Pond 7093 in October 1999. Note the two large land-slipped blocks near the top of the slope. Viewed from the glacier surface looking west.

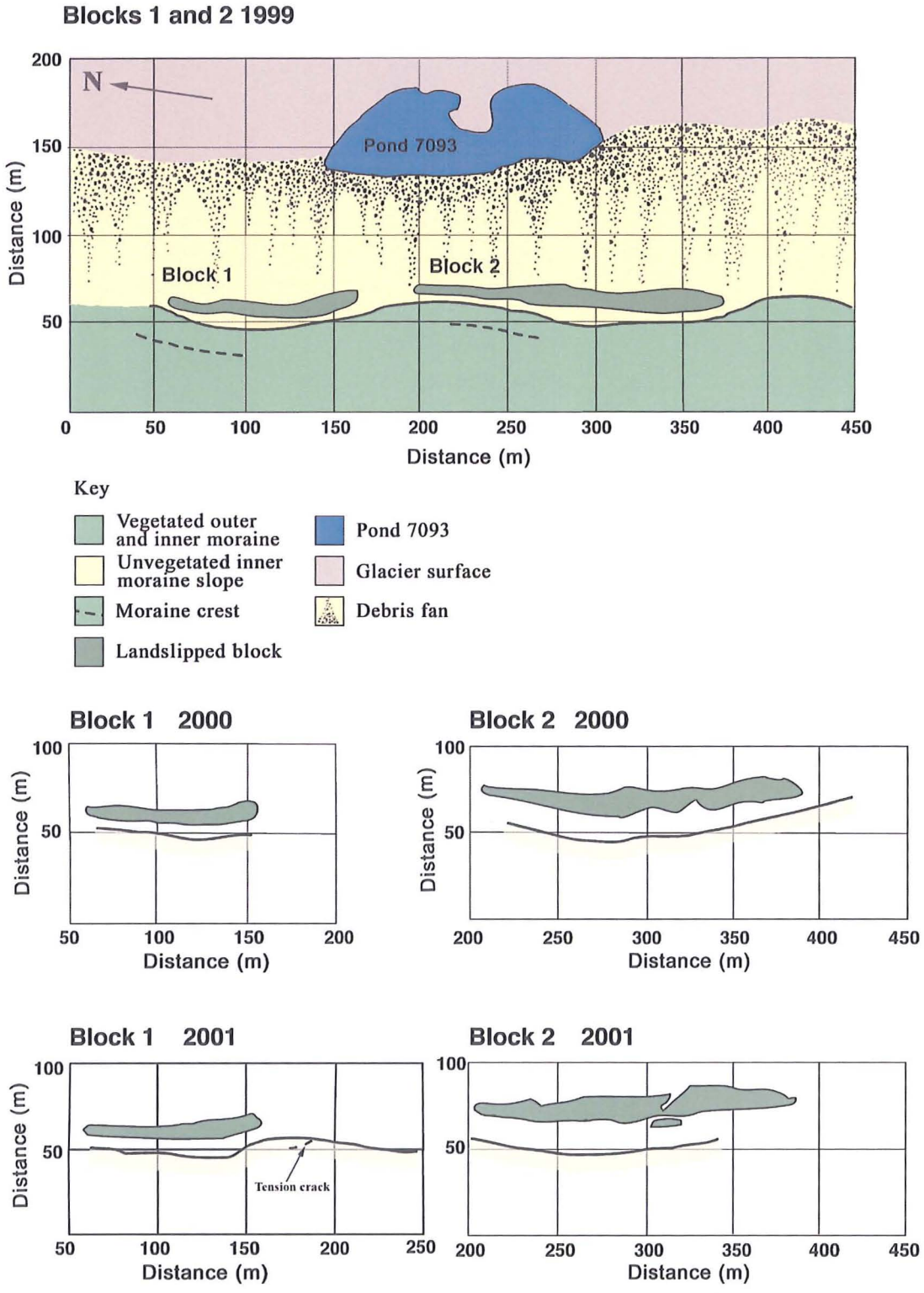

Figure 6.22. Map showing the position of the landslipped blocks at Site C between October 1999 and October 2001.

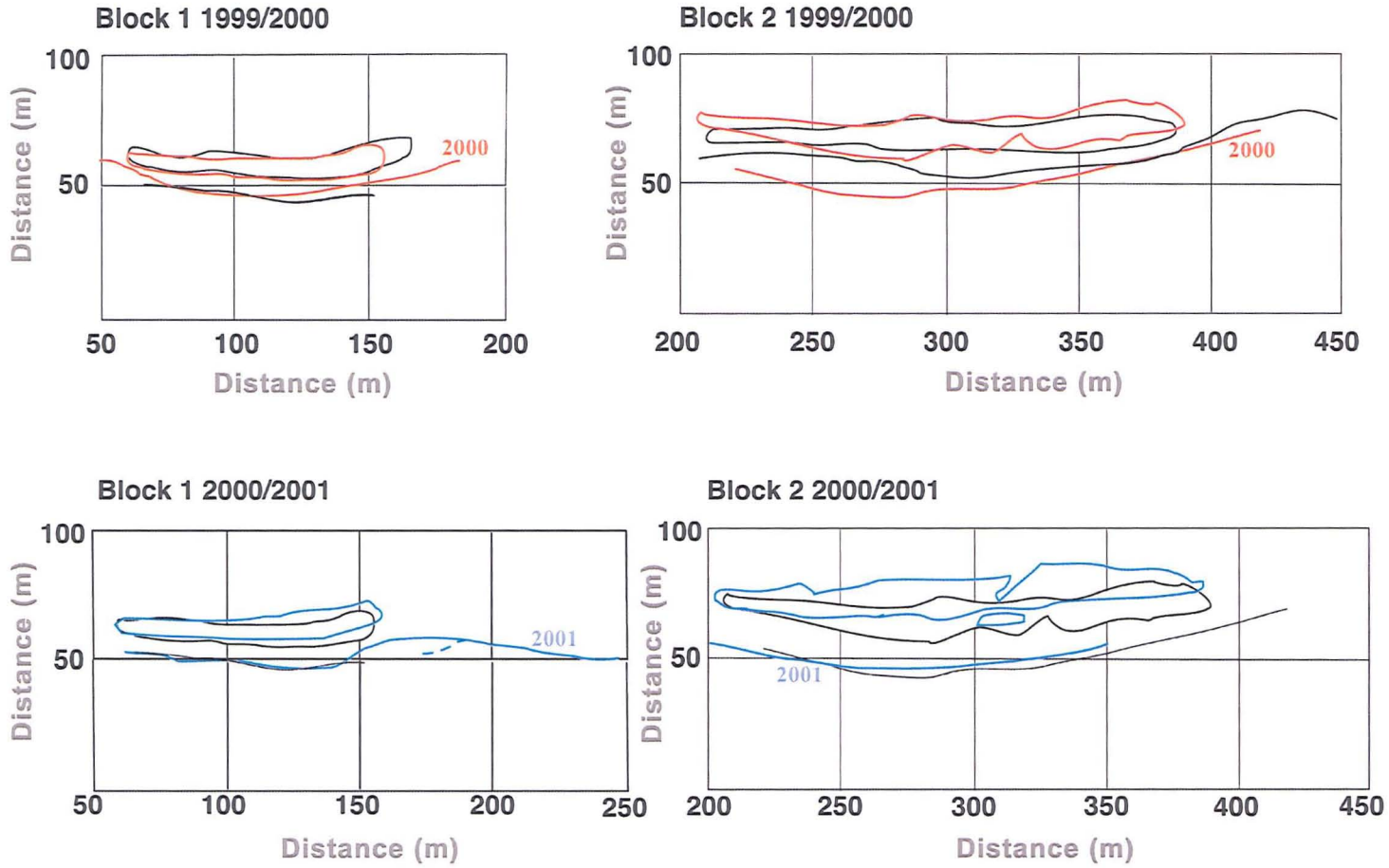

Figure 6.23. Map overlaying the position of the landslipped blocks at Site C between October 1999 - October 2000 and October 2000 - October 2001.

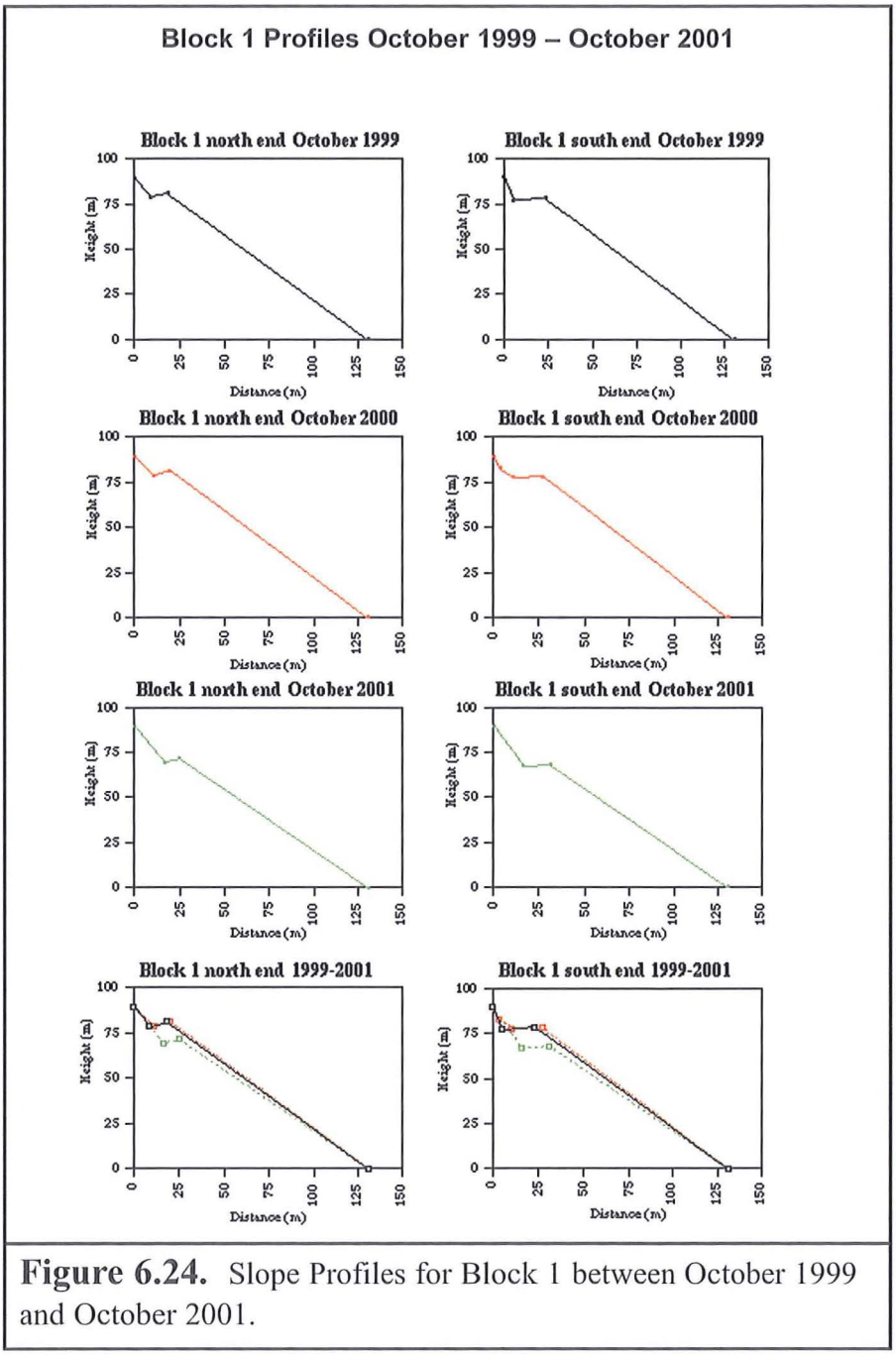

Figure 6.24. Slope Profiles for Block 1 between October 1999 and October 2001.

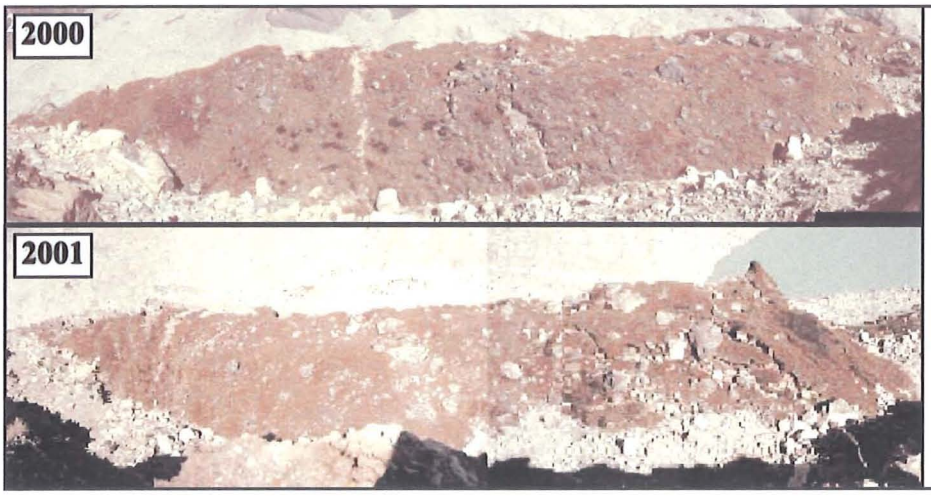

Figure 6.25. The surface of Block 1 in October 2000 and October 2001

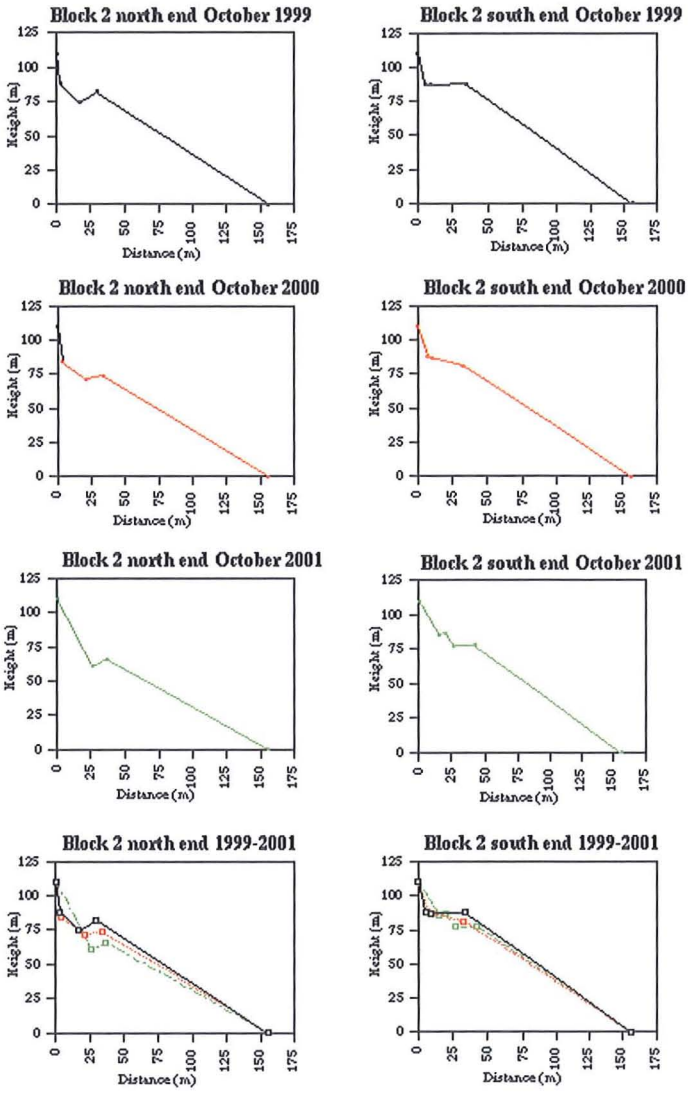

Figure 6.26. Slope Profiles for Block 2 between October 1999 and October 2001.

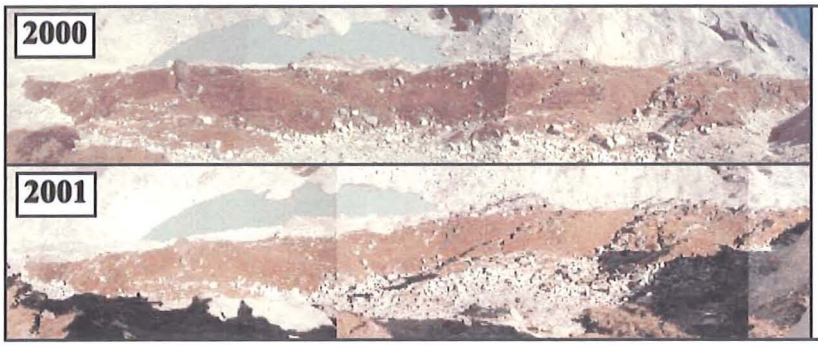

Figure 6.27. Site C. Block 2 in plan view in October 2000 and October 2001

Figure 6.28. Site C. Block 2 viewed from the crest of the western lateral moraine looking south in October 1999.

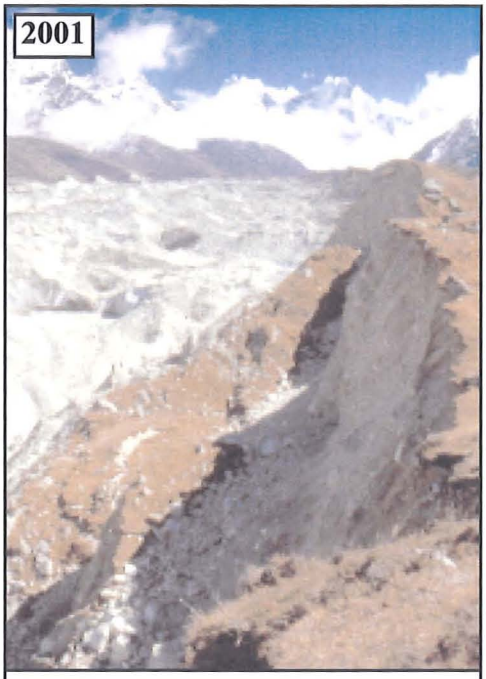

Figure 6.29. Site C. Block 2 viewed from the western lateral moraine looking south-southwest in October 2001.

Figure 6.30. Wind erosion removes the fine sediments from the inner moraine slope. Viewed from the western lateral moraine looking southeast.

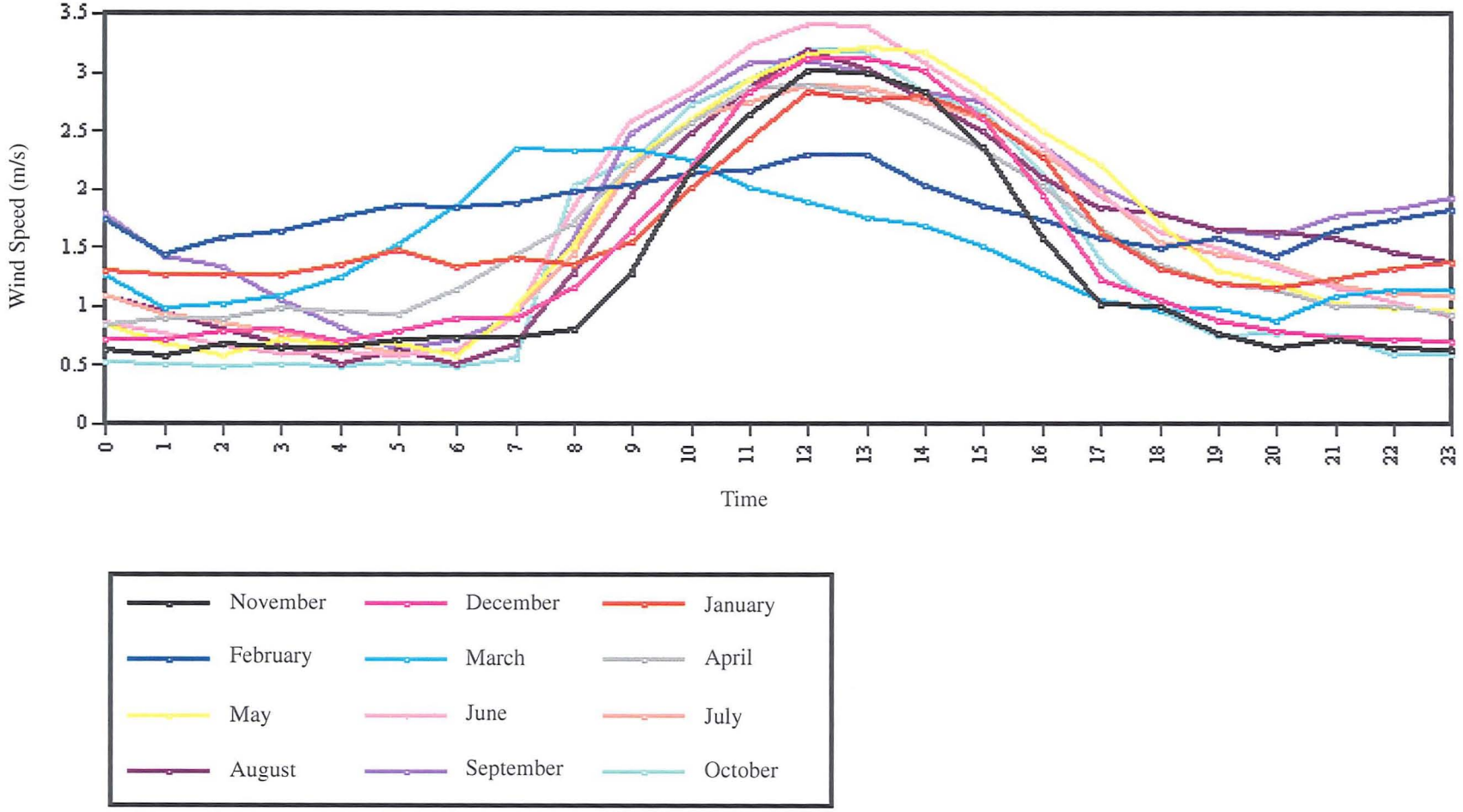

Figure 6.31. Average hourly wind speeds (m/s)

Chapter 7

Synthesis and Conclusions

7.1. Introduction

The research described in this thesis allows a comprehensive overview of the processes controlling the evolution of ponds and the developing hazard potential on the Ngozumpa Glacier. This chapter summarises 1) the processes that control the evolution of perched supraglacial pond basins on the debris-covered Ngozumpa Glacier; 2) the role of the Spillway Lake in controlling meltwater drainage from the glacier surface; 3) the processes of basin enlargement around the Spillway Lake basin; 4) the possible development of a large and potentially hazardous lake at the terminus of the Ngozumpa Glacier; and 5) the processes of paraglacial reworking operative on the Ngozumpa moraines and the implications of moraine stability for lakes dammed by the western lateral moraine. The chapter concludes by discussing the predictive and preventative measures that might be taken to avoid the occurrence, or mitigate the effects, of a glacier lake outburst flood from the Ngozumpa Glacier and makes some suggestions as to the possible direction of future research.

7.2. Downwasting and Evolution of the Debris Cover

The Ngozumpa Glacier has an almost continuous debris cover extending from around 5500 m to the glacier terminus. Several clean ice streams originating from the snowfields at the base of Cho Oyu (8188 m a.s.l.) and Gyachung Kang (7922 m a.s.l) taper out c. 5 km from the glacier headwalls (Figure 7.1). Downglacier from this point the debris cover is only broken where supraglacial ponds have formed, ice faces have been exposed on the sides of ice-cored debris mounds, or cracks have opened up on the glacier surface. The depth of the debris cover on the Ngozumpa

Glacier in the vicinity of the Spillway Lake ranges from 0.1 m to 7.4 m and the average debris thickness was 1.8m. Around 4km from the glacier terminus, the depth of the debris cover ranges from 0.1 m to 6.4 m with an average depth of 2m. Debris thicknesses around 12 km from the terminus were lower, ranging between 0.1 m and 3.2 m, with an average thickness of 0.6m. Given that the measurements of debris depth were made at the tops of exposed ice faces, where debris thicknesses are lowest, the thicknesses presented here represent the minimum depth of the debris mantle.

7.2.1. Source of Debris

The debris is mainly delivered to the glacier surface by snow and ice avalanching from the steep headwalls. Over time, as the avalanched snow turns into firn and eventually glacier ice, the avalanche debris becomes incorporated within the body of the glacier in stratified planes, forming englacial debris bands. As the debris bands are transported downglacier they are rotated and eventually become exposed at the glacier surface below the equilibrium line by downwasting of the glacier surface. In the ablation zone, debris is also delivered to the glacier margin by reworking of the inner lateral moraine slopes. As a general rule, debris generated above the equilibrium line becomes incorporated into the englacial transport system; below this point the debris is most likely to be transported supraglacially. However, it is also possible for supraglacial debris to enter the englacial transport system via crevasses, moulins, and subaerial conduits.

7.2.2. Evolution of the Debris Cover

As the Ngozumpa downwastes, the debris bands within the ice are exposed at the surface of the glacier. Supraglacial and englacial meltwater can also distribute and re-distribute debris on and within the glacier. Another possibility is that debris can be brought to the surface from the bed of the glacier by thrusting (Clayton, 1964; Boulton, 1967; Glazyrin, 1975; Gomez & Small, 1985; Bozhinsky et al., 1986; Kirkbride, 1995; Krüger & Aber, 1998; Ensminger et al., 2001). However, it has not been possible to ascertain whether this process is applicable to the Ngozumpa

Glacier due to limited exposure of englacial structures. Accumulation of debris on the glacier surface has resulted in the evolution of an almost continuous debris mantle on the Ngozumpa Glacier. Supraglacial debris is advected towards the glacier terminus by ice flow. The debris thickness at a point is therefore the result of cumulative melt-out of debris from the ice as it travels downglacier. This has resulted in an increase in the average debris thickness towards the glacier terminus.

7.2.3. Downwasting of the Glacier Surface

Ablation on the surface of the Ngozumpa Glacier is greatly increased on areas where ice faces have been exposed in the debris cover. Ice faces are exposed where debris has slumped on the sides of ice-cored debris mounds, around the margins of supraglacial ponds, and where subsidence above englacial karst features has occurred. Melt rates are highest on southeast to southwest facing ice faces. The melting of exposed ice faces can account for up to 80% of the total ice loss from debris-covered glaciers (Purdie & Fitzharris, 1999).

During periods of negative mass balance, the increase in the average debris thickness towards the Ngozumpa terminus causes an increase in the average downwasting rates with distance from the glacier terminus. This has resulted in a lowering of the glacier surface gradient. Wiseman (2004) ascertained that the surface gradient of the Ngozumpa between the altitudes of 4680 m and 5040 m (from the glacier terminus to the point where the Kyajumba Glacier feeds into the main glacier) was 2.04°. Where the glacier surface gradient lies between 2° and 10°, small isolated ponds can form (cf. Reynolds, 2000; Wiseman 2004). Melting and calving retreat of exposed ice faces around supraglacial ponds is considered to be the dominant processes of surface ablation and downwasting on the Ngozumpa Glacier. Furthermore, as downwasting proceeds and the overall glacier surface gradient is reduced, the number of ponds on the glacier surface increases. The increase in the number of ponds on the glacier surface accelerates the rate of downwasting and further reduces the overall surface gradient setting up a positive feedback cycle.

Reynolds (2000) found that on debris-covered glaciers in Bhutan large potentially dangerous lakes form where glacier surface gradients were between 0° and 2°. The surface gradient at the Ngozumpa terminus is 2.04° (Wiseman, 2004) and therefore the formation of a large and potentially hazardous lake in the vicinity of the Spillway Lake is a distinct possibility in the future.

7.2.4. Development of Surface Topography

The depth of the debris mantle covering the surface of the Ngozumpa is not uniform. Superimposed on the general increase in the maximum debris thickness towards the glacier terminus are large local variations in debris thickness. Such variations reflect a complex sequence of processes, which include the rate of debris emergence at the glacier surface, uneven melting, and debris redistribution by gravity and other processes. Wiseman (2004) suggested that ogives and crevasses, generated as glacier ice travelled through the icefalls of the Ngozumpa, also influence the patterns and rates of debris emergence at the glacier surface, and therefore have also affected the development of an undulating surface topography. Once an irregular glacier surface is established, further development of the glacier surface topography becomes self-perpetuating, as redistribution of the debris layer by slope processes and fluvial reworking bring about topographic inversions. Topographic high points (ice-cored debris mounds) are generated where there are thick accumulations of debris on the glacier surface and consequently low ablation rates. The debris mounds increase in height as the surrounding glacier ice downwastes more rapidly. An ice-cored debris mound will continue to grow until the slopes are too steep to support a debris cover. The debris is then transferred down the slopes of the ice-cored debris mound onto the surrounding, lower lying areas. The transfer of the protective debris covering causes an increase in the downwasting rate of the debris mound, and increases the insulation of the glacier surface where the debris thickness is increased in the surrounding low areas. Over time the topographic lows become ice-cored debris mounds as the former topographic high points downwaste to become topographic low points. Cycles of topographic inversion on a debris-covered glacier can occur many times as the glacier downwastes towards the bed (Watson, 1980). The process

of topographic reversal facilitates the lateral transfer of debris across the glacier surface, bringing about a fairly uniform average downwasting rate (Watson, 1979; Kirkbride & Warren, 1999; Nakawo et al., 1999). On the Ngozumpa Glacier irregular surface melt and topographic inversion have generated relief of up to c. 50 m on the glacier surface.

7.2.5. Stagnation and Glacial Karst Development

The negative mass balance and low ice flow velocities experienced at the Ngozumpa Glacier have gradually brought about the stagnation of the glacier terminus. Stagnation and the evolution of a thick debris mantle on the Ngozumpa Glacier have resulted in the widespread development of glacial thermokarst features such as englacial conduits and voids, sinkholes, and small supraglacial ponds. Such features are able to persist for long periods of time due to low ice flow velocities, low ice overburden pressures, and the insulation of the glacier ice by the thick debris mantle. The development of topography on the glacier surface is a prerequisite for supraglacial pond development (Clayton, 1964). The undulating topography of the Ngozumpa glacier creates natural basins that encourage the ponding of meltwater in the glacier ablation zone. In the lower areas of the Ngozumpa, the ice flow velocities are low enough to allow supraglacial ponds to survive and expand over several melt seasons.

7.2.6. Moraine Abandonment

Debris sliding from the surface of the glacier has caused the formation of large and extensive lateral and terminal moraines. These multi-crested Ghulkin-type terminal and lateral moraines encompass the glacier from the terminus up to the headwalls. The outer moraine slopes are generally well vegetated and relatively stable. In contrast, the inner moraine slopes are unvegetated and highly unstable. This is due to the continued lowering of the glacier surface by downwasting processes, which steadily increase the length of the inner moraine slopes, preventing the slopes from attaining a stable angle of repose. Downwasting of the glacier surface has left the moraine crests standing between c. 20 m and 120 m above the glacier surface.

The extensive moraines have exerted a profound influence on the hydrology of the Ngozumpa Glacier by inhibiting the drainage of meltwater from the glacier. The moraine barriers prevent meltwater from leaving the surface of the glacier and thereby encourage ponding of water on the surface. Most of the meltwater generated by the Ngozumpa Glacier is channelled into the Spillway Lake and out through the over-spill channel in the western lateral moraine, approximately 1km from the glacier terminus. The altitude of the over-spill channel determines the level of the englacial watertable at the Ngozumpa Glacier and exerts a control on the evolution and drainage of ponds upglacier.

The growth of the Spillway Lake is ultimately dependent on the level of the over-spill channel. Provided that this channel is not enlarged or deepened, the Spillway Lake will continue to expand and deepen over time. If growth of the Spillway Lake continues unchecked, then it is likely that the lake will form the nucleus for the formation of a large and potentially hazardous moraine-dammed lake.

7.3. Perched Supraglacial Pond Inception and Growth

The location of perched supraglacial ponds on the Ngozumpa is largely dependent on the glacier surface topography, the exposure of bare ice faces, the gradient of the glacier surface, and the development and extent of glacier karst and conduit networks. As exposure of clean ice faces, backwasting and topographic reversals take place on the glacier surface, the locations of supraglacial ponds will adjust accordingly. Additionally, the number of ponds present on the glacier surface has increased over time due an overall reduction in the glacier surface gradient.

7.3.1. Initial Pond Inception

The prerequisites of supraglacial pond formation on debris-covered Himalayan glaciers are as follows: a negative mass balance and low ice flow velocities; an

overall glacier surface gradient of between 2° and 10°; and the development of topographic hollows due to differential ablation.

Sliding and slumping of debris from the slopes of ice-cored debris mounds can expose bare ice faces. Once exposed, the ice faces experience much higher rates of ablation and backwasting. The meltwater generated from the ablation of exposed ice faces collects in topographic hollows due to the impermeable nature of the underlying glacier ice (Figure 7.2). Unless the exposed ice becomes covered over again by debris sliding or slumping from above, the ice face will gradually steepen over time. As the ice face steepens, debris will begin to slide away from the edges and the top of the face, lengthening and enlarging the exposure. This will lead to an increase in meltwater production and an enlargement and deepening of the pond (Figure 7.2). These mechanisms of pond inception were observed on the Ngozumpa Glacier at Pond 7093b between October 1999 and October 2001 (See Chapter 4, Section 4.2).

7.3.1.1. Water Inputs and Outputs

In addition to meltwater generated by surrounding exposed ice faces, perched supraglacial ponds on the Ngozumpa can also receive inputs of water from melting under the debris cover, englacial conduits, surface meltwater channels, melt-out of calved ice bergs, and precipitation (Figures 7.2 and 7.3). Over time, the input of water into the basin will cause the pond to increase in size and deepen. Water-level increases can also be achieved by displacement of the pond water by rock debris falling or sliding into the pond. Conversely, decreases in water level can occur by evaporation, seepage of pond water through subaqueous englacial debris bands, and drainage of pond water through englacial conduits. The water level of a perched supraglacial pond will also fluctuate over time due to seasonal and annual variations in melt rates, precipitation, evaporation, and debris inputs (Benn et al., 2001).

7.3.2 Basin Enlargement

Perched supraglacial ponds on the Ngozumpa Glacier develop and expand at different rates. The rate of basin expansion is controlled by:

- the type and length of the pond perimeter
- the subaerial rate of melt at exposed ice faces
- calving and the extent of structural weaknesses within ice faces surrounding the pond
- the water temperature and sediment concentration of the pond
- the rate of subaqueous melting
- the presence, or proximity of basins to englacial conduits and other supraglacial ponds.

7.3.3 Processes of Pond Enlargement

Studies of perched supraglacial ponds on the Ngozumpa have revealed that four processes are responsible for the enlargement of pond basins on the glacier. These processes are (1) subaerial melting of exposed ice faces around the basin; (2) thermo-erosional notching; (3) calving; and (4) melting at the pond floor (Figures 7.2 and 7.3)

7.3.3.1 Subaerial Ablation of Exposed Ice Faces

Exposed ice faces on the Ngozumpa glacier undergo daily melt cycles. Subaerial melting causes backwasting of exposed ice faces around the margins of perched pond basins and contributes to basin enlargement. The meltwater generated by subaerial melting contributes to the volume of water contained within a pond and can lead to an increase in the pond water level, which in turn can initiate, or increase the rate of, calving at exposed ice faces in contact with the pond (Figure 7.2). Furthermore, as melting proceeds, the overlying debris mantle is destabilised and sliding and slumping of debris from the top and sides of an ice face can cause an enlargement of the ice face and an increase in the rate of basin expansion. In basins where the pond water is not in contact with exposed ice faces around the pond margins, subaerial melting is the most important process of basin expansion.

The calculated ablation rates of exposed ice faces on the Ngozumpa in October 1998 were typically 0.03-0.045 m d^{-1}, with the highest rates recorded on southeast- to southwest-facing slopes (Benn et al., 2001; Wiseman, 2004). Between October 1999 and October 2000, the calculated ablation rate at exposed ice faces that were not undergoing calving retreat was 0.04 m d^{-1}. The average subaerial melt rate for exposed ice faces between October 2000 and October 2001 was calculated to be 0.045 m d^{-1}.

The longer-term and seasonal variations in melt rates of exposed faces are not known for the Ngozumpa Glacier. It is expected that very little ablation occurs over the winter (between December and February) due to colder air temperatures and extensive snow cover, that can raise the albedo of the glacier surface to around 0.67 (Benn et al., 2001). Early heavy snowfall and low air temperatures, such as those experienced during October 1999, can effectively shorten the melt season by ceasing surface ablation (Benn et al., 2001; Wiseman, 2004). Melt rates will begin to increase throughout the spring, and probably reach a maximum during the summer monsoon period (from the end of May through to the beginning of September).

7.3.3.2. Calving

The most rapid basin enlargement on the Ngozumpa occurs in basins undergoing calving retreat. Rapid calving retreat occurs in pond basins where ice faces are in contact with the pond water. There are four types of calving that occur around the edges of supraglacial pond margins on the Ngozumpa Glacier: thermo-erosional notch controlled calving, full-height slab calving, flake calving, and subaqueous calving.

Thermo-erosional Notching

As the water level of a pond increases, the protective talus slopes at the foot exposed ice faces become submerged and the ice-faces are brought into direct contact with the pond water. Perched supraglacial ponds on debris-covered Himalayan glaciers typically have low surface albedos (<0.05) and high turbidity, and therefore readily

absorb solar radiation at the pond surface (Chikita et al., 1998; 1999; Benn et al., 2001). Supraglacial ponds undergo diurnal cycles of heating and surface temperatures of around 5° can be experienced during the day (Chikita et al., 1997; 1998; 1999). The contact between an ice face and the relatively warm surface water of a pond instigates thermo-erosional notching at the water-line (Figure 7.2). It is difficult to determine the rate of thermo-erosional notching around pond margins on debris covered glaciers due to problems of safely accessing exposed ice faces.

As water-line melting proceeds the thermo-erosional notch is deepened and undercuts the ice face. Eventually the roof of the notch is destabilised and collapses. Notch-controlled calving was the most frequent form of calving observed in the supraglacial ponds on the Ngozumpa during the study period.

Full-Height Slab Calving

Full-height slab calving is the process by which large pillars or blocks of ice become detached from an ice face by toppling failure. Several full-height slab calving events were witnessed in supraglacial ponds on the Ngozumpa between October 1999 and October 2001 (See Chapter 4) and most of these occurred on ice faces over 15 m in height (Benn et al., 2000; 2001; Wiseman, 2004). Full-height slab calving on the Ngozumpa tends to occur along pre-existing weaknesses in the ice, such as steeply dipping debris bands and crevasse traces. In the days leading up to the calving of a large pillar or block from an ice face, the planes of weakness that defined the block were gradually opened up and widened due to the force imbalance at the ice face.

Flake Calving

Flake calving or spalling on the Ngozumpa occurs more frequently than full-height slab calving but involves smaller masses of ice. Flake calving tended to occur up from the water-line along stress-release fractures orientated parallel to the ice surface (Benn et al., 2001).

Subaqueous Calving

As an ice face experiences calving retreat in a supraglacial pond, an 'ice ramp' or 'ice foot' can develop at the base of the ice face. The ramp is subjected to buoyancy forces that can cause subaqueous calving to occur along structural weaknesses within the ice. At the Ngozumpa Glacier subaqueous calving events are rare because the debris mantle covering the floor of supraglacial ponds offsets the buoyancy of the ice. Only one subaqueous calving event was witnessed at the Ngozumpa between October 1999 and October 2001.

Cycle of Calving

The different types of calving observed at the Ngozumpa Glacier generally operated independently of each other and did not follow a cycle of calving, such as the model proposed for the Maud Glacier, New Zealand, by Kirkbride & Warren (1997) (see Chapter 4, Section 4.3.5.4). The rate of calving at exposed ice faces on the Ngozumpa was predominantly controlled by the location and spacing of suitably orientated crevasses behind the face. Where no structural weaknesses were present behind an exposed face, notch-controlled calving and flake calving up from the water-line were the main calving processes, and the rate of calving was controlled by the rate of water-line melting.

7.3.3.3. Subaqueous Melting and Pond Thermodynamics

The thick debris mantles that cover the floors of perched supraglacial ponds on debris-covered Himalayan glaciers reduce the subaqueous melt rate (Sakai et al., 2000). Bathymetric data from the Spillway Lake indicated that the minimum rate of melt at the bottom of the pond was in the region of 0.67-1.2 m a^{-1}. This is significant because it indicates that bottom melting is an important process of ablation and basin enlargement.

Although it was not possible to measure pond temperatures throughout the year, it is suggested that the perched ponds on the Ngozumpa Glacier are dimictic and undergo two overturning periods: one in November and the other in April or May during the

spring melt. The dimictic nature of the perched ponds on the Ngozumpa allows expansion and deepening of the pond basins to occur throughout the year. In the summer, higher water temperatures at the pond surface induce thermo-erosional notching and notch-controlled calving retreat at exposed ice margins. As air temperatures are reduced during the autumn, the pond surfaces cool and develop an ice cover that inhibits thermo-erosional notching and calving retreat. The freezing over of perched ponds during the winter phase changes the thermodynamics of the ponds, producing lower temperatures at the top of the water column than at depth. The surface ice increases the albedo of the pond surface and reduces the amount of shortwave radiation received at the pond surface. Furthermore, the cap of ice greatly reduces the amount of mixing and turbulence in the pond by inhibiting wind induced currents. However, the cold temperature of the ice layer also reduces the loss of longwave radiation from the pond surface allowing the water temperature at the bottom of supraglacial ponds to remain high enough to cause continuous subaqueous melting of pond floors, possibly throughout the winter season. It is therefore suggested that subaqueous melting is the dominant process of ablation and basin expansion in perched supraglacial ponds during the winter.

7.3.4. Pond Margin Conditions and Basin Enlargement Rates

The classification of pond perimeter type is important to our understanding of how supraglacial ponds will enlarge and over what time period. Different types of pond margin behave in different ways and exert distinct influences over the rate and direction of pond growth. There are three main types of supraglacial pond boundaries that occur on the Ngozumpa Glacier: ice perimeters, debris-covered ice perimeters, and moraine perimeters (Figure 7.4). Over time, the perimeter conditions of a pond may change and exert new influence over the future development of the pond. Furthermore, as a pond increases in area, the length of the perimeter also increases, thereby potentially increasing the amount of melting and expansion that can take place around the pond margin in a positive feedback cycle (Figure 7.2).

7.3.4.1. Ice Perimeters

The development and expansion rate of a supraglacial pond basin on the Ngozumpa is mainly controlled by the area of exposed ice that is present around the edge of the pond. Exposed ice faces ablate at a much more rapid rate than debris-covered ice margins that are insulated from solar radiation. Therefore, the larger the percentage of ice exposed around the pond margins, the higher the rate of ablation both above and below the water level, and the higher the rate of basin enlargement. The orientation of the exposed ice faces will also affect the rate of basin enlargement and will exert an influence on the direction of basin expansion.

As exposed ice faces around a pond margin ablate, the meltwater produced increases the volume and depth of water stored in the pond. This in turn increases the amount of melting around the pond margin and the rate of backwasting at exposed ice faces. A rise in water level can also bring subaerial faces into contact with the pond water and initiate thermo-erosional notching and calving retreat. As the length of the ice margin increases the amount of meltwater generated also increases, setting up a positive feedback cycle of exponential basin enlargement (Figure 7.2).

Ice margins around supraglacial ponds can be subdivided into melting ice margins and calving ice margins. The average retreat rate at melting ice margins between October 1999 and October 2001 was calculated to be 15.4 m a^{-1}. The highest rates of retreat were experienced at southwest and northwest facing faces. At calving margins the average retreat rate between October 1999 and October 2001 was calculated to be 20.4 m a^{-1}. The melt rate of a thermo-erosional notch in the Pond 7092 basin was measured on the 29th September 2001 and was calculated to be between 0.9 and 3.1 cm h^{-1}. This was on average around 3.2 times the melt rate experienced at an adjacent ice face. The rate of retreat at ice margins that experienced full-height slab calving events was faster than at ice margins where the retreat rate was controlled by waterline melting. At ice margins that experienced full-height slab calving events the average retreat rate was 29 m a^{-1}.

Calving and Exponential Growth of Pond Basins

Once calving retreat has been initiated in a supraglacial pond, rapid basin enlargement ensues (Figure 7.2). Calving is a much more rapid backwasting process than subaerial melting, removing larger volumes of ice from exposed faces around the pond margin. As the calving ice faces steepen up, the calving rate is increased and debris mantling the tops and sides of the face begins to slide off, increasing the length of the exposure. Melting of calved ice blocks increases the water level in a pond. A rise in water level can bring more faces into contact with the pond water and can promote further exposure of ice faces around the pond margin by encouraging sliding on debris mantled slopes. Very large calving events, however, can cause the average pond temperature to drop as icebergs melt out, temporarily reducing the rate of basin expansion by subaqueous and water-line melting. Rapid calving retreat and rising water levels also impede the progradation of talus fans that can protect the base of an ice face. In these ways, calving at exposed ice margins can become self-perpetuating setting up a positive feedback cycle of increasingly expeditious calving retreat and basin enlargement.

Seasonal Variations in Calving Rate

Supraglacial ponds on the Ngozumpa start to ice over towards the end of November; or earlier if heavy snowfall and low air temperatures are experienced, as in late October 1999. The lower pond surface temperatures significantly decrease the rate of thermo-erosional notching at the water-line and calving controlled by the rate of water-line melting. Thermo-erosional notch-controlled calving retreat in ponds will begin again during the spring melt season and will attain a maximum rate during the summer monsoon when pond water levels are at their highest.

Slumping of Debris

The enlargement of a pond basin often increases the ice face surface area around the perimeter. As a pond enlarges the existing ice margins and adjacent debris-covered ice slopes may steepen up, encouraging debris to slough off into the pond, thereby increasing the amount of exposed ice around the pond perimeter and the rate of basin

expansion. This is particularly noticeable at exposed ice margins undergoing calving retreat.

Although slumping and sliding of surficial debris can expose new ice faces, high rates of debris delivery into a pond below an ice margin can also cause the build up of protective debris cones along the ice margin which inhibit melting below the water-line and the development of thermo-erosional notches (Figure 7.5). This process is most likely to occur in shallow supraglacial ponds where the calving rate is low. Protection of an ice margin by debris cones can gradually bring about the cessation of calving and a reduction in slope angle. Slumping and sliding of debris from the top of lower angled ice faces can cause the exposed ice to become covered over once, more producing a debris-covered ice boundary that will slow the backwasting rate and affect the direction of pond enlargement.

7.3.4.2. Debris-covered Ice Perimeters

A debris-covered ice margin, although still ablating, will retreat at a much slower rate than an exposed ice margin. The depth of the debris cover controls the rate of retreat at a debris-covered ice margin. Debris-covered ice margins tend to have lower surface slope angles and do not experience any calving retreat (Figure 7.4). The debris cover also protects the underlying ice from thermo-erosional notching and notch-controlled calving. Debris-covered ice margins around supraglacial ponds restrict pond growth rates and exert a control over basin shape. Ponds that have very large percentages of debris-covered ice margins will experience little or no growth, and the volume of water contained therein can diminish due to evaporation of the pond water or infilling of the pond by the progradation of talus cones. However, debris-covered ice margins tend to steepen over time in a similar way to ice-cored debris mounds (See Chapter 2, Section 3.3 and Section 3.3 above). Additionally, melting at the pond floor increases the length of the perimeter slopes and will augment the steepening of debris-covered ice margins. Eventually, steepening of debris-covered slopes will trigger slope failure processes such as debris sliding, slumping and rockfall. These slope processes will cause an increase in the suspended

sediment concentration of the pond water. High suspended sediment concentrations can increase the amount of solar heating at the pond surface and therefore increase the rate of water-line thermo-erosional notching and notch-controlled calving at exposed ice margins. More importantly, slumping and sliding of debris at the pond margin can expose the underlying ice surface and can initiate a shift in margin type from a debris-covered ice margin to an exposed ice margin (Figure 7.2).

7.3.4.3. Moraine Perimeters

Ponds that form at the glacier margins tend to have straight perimeters where they are bordered by lateral moraines (Figure 7.4). Although the moraines generally act as a barrier to pond growth, it is possible for a moraine margin to cause pond expansion or shrinkage through advance, or retreat of the margin by slope processes (Benn et al., 2001).

Moraine margins also affect pond thermodynamics. Active inner moraine slopes are a large debris source and slope processes (such as debris flow, slope wash, and translational or rotational sliding, often initiated by periods of heavy precipitation or snowmelt) can increase the sediment concentrations of the ponds situated below. The ice/moraine margin can also act as a natural channel along which surface meltwater streams can enter or exit a pond.

7.3.4.4. Changes in Perimeter Conditions

Over time the perimeter conditions of a supraglacial pond will undergo several changes. Ice faces can gradually relax and become covered with debris as material slides down from the top of the ice face. Similarly, slope processes active on a debris-covered perimeter may expose the underlying ice and can eventually produce a new ice margin that will undergo rapid melting and possibly calving retreat. Moraine perimeters are the most stable type of pond boundary and will undergo relatively little change during the life span of a perched supraglacial pond.

7.4. Pond Quiescence

Although the onset of calving in perched supraglacial ponds initiates rapid basin enlargement at exposed ice margins, the positive feedback cycle of increasingly rapid growth can be interrupted. As an ice margin backwastes, debris from the top of the face is destabilised and slides or falls into the pond. If there is a thick debris cover at the top of the exposed face then the rate of debris delivery into the pond will be high and this can cause the progradation of protective debris cones along the ice margin. Debris cones inhibit melting below the water-line and the development of thermo-erosional notches (Figure 7.5). The depth of the pond and the rate of calving also influence the rate of progradation of debris cones. Shallow ponds, where the ice face retreat rate is low, are more likely to experience progradation of debris cones at the base of exposed ice margins. Over time the progradation of debris cones can cause the cessation calving retreat at an ice margin and bring about a reduction in the surface gradient of the ice face. Lower angled ice faces can eventually be converted into debris-covered ice margins as debris slides from the top of the face producing a debris-covered ice boundary that will slow the rate and affect the direction of pond enlargement. After calving retreat has ceased around the margins of the pond, the exposed ice faces can become further distanced from the pond margin through continued backwasting by subaerial melting. Ponds with predominantly debris-covered ice perimeters may experience a reduction in volume and pond area because of infilling of the pond basin by debris and evaporation.

Ultimately, the progradation of debris cones can bring about a period of pond quiescence in which the margins of the pond are predominantly debris-covered and little expansion of the basin occurs. This process occurred on the Ngozumpa Glacier at Pond 7093 between October 1999 and October 2001 (See Chapter 4, Sections 4.3.2 to 4.3.4).

Pond quiescence is not a permanent state and future expansion of a quiescent basin will occur if water levels in the pond rise and bring exposed ice faces into contact

with the pond perimeter or if debris-covered ice margins are converted into ice margins by reworking of the debris mantle.

7.5. Pond Drainage

This study provides direct evidence for the drainage of supraglacial ponds. The presence of large empty basins and raised deltas on the surface of the Ngozumpa Glacier show that such drainage events are common and limit the growth of perched supraglacial ponds (Figure 7.6). Satellite imagery, aerial photograph surveys and old picture postcard photographs also attest to the appearance and disappearance of perched ponds over time. There are two main causes of perched supraglacial pond drainage at the Ngozumpa Glacier: (1) pond water can overflow and drain out along an ice/moraine boundary; (2) backwasting of an exposed ice face, or melting of the lake floor, can cause a connection to be made with an englacial conduit below the water-line (Figure 7.2). The latter process is the most common cause of pond drainage on the Ngozumpa, evidence for the former being restricted to the eastern ice-moraine boundary downglacier from the Gaunara meltwater stream.

As exposed ice faces around perched pond margins backwaste they may expose englacial conduits. At the upglacier end of the pond exposed conduits can provide inputs of meltwater to the pond, increasing the volume of water stored within the basin. If, however, an englacial conduit is exposed below the level of the pond in a downglacier direction, or at the pond floor, then partial or complete drainage of the pond will ensue (Figure 7.2). The amount of drainage that occurs initially depends on the position of the connection. As drainage proceeds, thermal and mechanical erosion of the conduit walls caused by the rapid flow of relatively warm pond water enlarges the size of the conduit allowing increasingly more rapid drainage to occur.

In some cases the drainage of a pond can be interrupted, for instance if large calved icebergs block the conduit. This process was witnessed at Pond 7192 in October 2001 (see Chapter 3, Section 3.4.6).

7.5.1. Evolution of Drained Perched Pond Basins

Enlargement of basins on the surface of the Ngozumpa continues after the drainage of pond water from the basin but at a much slower rate. The exposed ice faces around the basin continue to backwaste through direct ablation. The most rapid melting takes place around the edges of exposed conduits and debris bands and where thin films of debris cover ice faces. Spalling and dry calving around structural weaknesses in the exposed ice faces also occurs. Over time these ice faces develop more relaxed surface slopes and may become covered over by debris slumping, sliding or falling from the top of the face (Figure 7.2). Large thicknesses of deltaic sediments covering a basin floor restrict melting to those areas of the basin where ponding of meltwater still occurs or where small supraglacial streams flow. Where pond floor sediments are very thick, topographic reversal can result in elevation of old basin floors above the surrounding topography.

Re-flooding of a drained basin by melting of exposed ice faces, inputs of water from precipitation or from conduits channelling meltwater from upglacier can initiate further calving retreat and enlargement of the basin in the future.

7.5.2. Temporary Storage of Water

Meltwater from the Ngozumpa is channelled downglacier through the englacial and supraglacial drainage systems. Most of this water eventually enters the Spillway Lake near the glacier terminus and exits the glacier surface through a channel cut down through the western lateral moraine. A small proportion of the total meltwater produced flows out through an exit stream cut down through the eastern terminal moraine. Evaporation of meltwater from supraglacial ponds and streams also contributes to the loss of meltwater from the glacier surface. No evidence of meltwater seepage through the lateral or terminal moraines was discovered at the Ngozumpa.

The transfer of meltwater from upglacier into the Spillway Lake is not always a straightforward process. The existence of extensive glacial karst and englacial

conduit networks suggest that meltwater on the Ngozumpa can take a very circuitous route before reaching the Spillway Lake. Many perched supraglacial ponds receive meltwater inputs from exposed englacial conduits along upglacier ice margins. The meltwater is temporarily stored in the pond until a drainage event releases the pond water downglacier. Temporary storage of meltwater may also be possible within large englacial voids and ice caves. This pattern of meltwater drainage provides a valid explanation of why old empty pond basins on the surface of the Ngozumpa are suddenly re-flooded. It is possible that meltwater draining from upglacier will be stored in several different perched supraglacial ponds before finally reaching the Spillway Lake and draining out through the western lateral moraine. Indeed it could take several melt seasons for meltwater to eventually reach the Spillway Lake basin. Alternatively, meltwater from the drainage of perched ponds may be channelled directly into the Spillway Lake (See Chapter 5, section 5.5). This situation is most likely to arise when drainage occurs out of ponds further downglacier into more established englacial conduits or during the drainage of very large pond basins where the volume of meltwater causes rapid thermal and mechanical enlargement of a conduit.

Given that most meltwater on the Ngozumpa is produced during the summer monsoon season, it follows that the englacial drainage network is most fully developed at this time of year. During the winter months drainage from the glacier is much reduced and the conduit network shuts down. Some of the smaller conduit networks will change and shift position on a yearly basis with new conduits developing along englacial fractures, crevasse traces and debris bands. Other englacial conduits will be re-activated during the spring melt and summer monsoon periods. As a result of shifting and migration of conduit networks, compounded by the development of new pond basins on the glacier surface, meltwater from upglacier can be directed in different directions and into different pond basins annually. Drained pond basins that were once connected with englacial conduit networks can become re-flooded once more if the conduits that drained them close up, migrate, melt out or become blocked by debris or collapsed material.

7.5.3. Future Implications for Drainage of Perched Pond Basins

At present, the complete or partial drainage of lakes through englacial conduits provides a check on rapid calving retreat and exponential basin enlargement on the Ngozumpa. However, the ultimate control on perched supraglacial lake drainage is not the proliferation of glacier karst and englacial conduits but the altitude of the Spillway Lake. As surface downwasting continues and the overall glacier surface gradient is reduced, perched ponds upglacier will eventually form at the same altitude as the Spillway Lake and rapid drainage of pond basins through englacial conduits will no longer take place. Instead ponds that make contact with the englacial conduit network will become dynamically connected to the Spillway Lake and enlargement of the pond basins will continue unabated. Eventually this could lead to the development of a large and potentially hazardous lake at the terminus of the Ngozumpa.

7.6. Spillway Lake

The Spillway Lake is the largest supraglacial pond on the Ngozumpa and it is not perched above the englacial base level like the other ponds on the glacier surface. The Spillway Lake has a continuous through-flow of water and does not undergo cycles of rapid growth followed by complete or partial drainage. Because the Spillway Lake represents the base level for englacial drainage on the Ngozumpa Glacier, it exerts an important control on the development of the perched ponds upglacier.

Meltwater enters the lake via a supraglacial stream at the easternmost end of the lake and also via an englacial conduit on the north lake shore around 150 m from the western lake margin. Additional sources of meltwater to the lake are from melting and calving of exposed ice faces, melting of debris-covered ice margins, and precipitation. Lake water exits the Spillway lake through an over-spill channel cut down through the western lateral moraine. This over-spill channel appears to be armoured by large boulders and no changes in the channel morphology or depth were observed between October 1999 and October 2001. The rate of down-cutting

of the over-spill channel controls the level and growth rate of the Spillway Lake and provided that the channel remains at the same altitude, the lake will continue to expand and deepen over time. In the future it is believed that the Spillway Lake will be the nucleus for the development of a large and potentially hazardous moraine-dammed lake on the Ngozumpa Glacier.

7.6.1. Mechanisms of Spillway Basin Expansion

The perimeter of the Spillway Lake is predominantly debris-covered ice and expansion of the basin between October 1998 and October 2001 has been concentrated in three areas: (1) at the large ice face in the western basin, (2) at the exposed ice margins in the eastern basin, (3) around an englacial meltwater conduit that enters the north shore of the lake (See Chapter 5).

Basin expansion at the Spillway Lake occurs in the same way as in the perched pond basins. However, the continuous through-flow of meltwater causes the water temperatures in the Spillway Lake to be lower than for perched ponds on the glacier surface. The development of thermo-erosional notching at the exposed ice margins is therefore much slower than in perched ponds, as is the rate of calving retreat. It is thought that the main process of basin expansion at the Spillway Lake is subaerial melting and small scale flaking and spalling of ice at the exposed ice margins.

7.6.1.1. Subaqueous Melting

The Spillway Lake, like the perched ponds on the Ngozumpa, is dimictic. However, the colder water temperatures in the Spillway Lake cause the onset of freezing at the lake surface to occur a few weeks ahead of the perched ponds. As a result, the ablation period for subaerial ice faces is slightly shorter for the Spillway Lake than for the perched ponds. Minimum bottom melting rates in the Spillway Lake were estimated to be around 2.4 m a^{-1} for the western basin and between c. 0.89-1.6 m a^{-1} for the eastern basin. However, the rate of bottom melting is expected to increase in the future because the cooling effect of cold englacial meltwater entering the lake will decrease as the lake increases in area and depth.

7.6.1.2. Collapse on the Glacier Surface

As downwasting of the glacier surface proceeds, glacier karst features such as englacial conduits and voids are brought closer to the glacier surface. This can often cause the collapse of englacial conduit or cave roofs. Subsidence of these features exposes clean ice surfaces and the area of collapse will undergo rapid ablation and enlargement. Ablation is often increased by the presence of running or ponded meltwater. Subsidence at the foot of ice-cored debris mounds can cause the exposure of ice faces as slope processes remove debris from the slopes of the mound. Subsidence below ice faces can trigger fracturing and dry calving above the area of collapse. Areas of collapse can also form nuclei for the development of supraglacial ponds.

Between October 1999 and October 2001, collapse of an englacial conduit roof on the Ngozumpa occurred to the north of the Spillway Lake basin. In October 1999, the subsidence of the glacier surface was indicated by the appearance of several cracks and holes in the glacier surface below a small ice face. However, by October 2000, the area of collapse had expanded northwards and the ice face had been greatly enlarged by backwasting, and possibly dry calving, along fractures in the ice above the hole. The area of collapse was directly upglacier from the englacial conduit in the north shore of the Spillway Lake and it is therefore suggested that the collapse was occurring along the up-glacier continuation of this conduit. It is possible therefore, that the collapse of the conduit roof may have been encouraged by the rapid drainage of the perched Pond 7092 into the Spillway Lake during the summer monsoon in 2000 (Chapter 4, Section 4.4.3). As drainage of Pond 7092 proceeded, it caused enhanced thermal erosion of the walls along the length of the englacial conduit and brought about exposure of the englacial conduit at the surface of the Spillway Lake. This initiated the rapid retreat of the newly exposed ice margin on the north shore (Chapter 5, Section 5.3.2). Following the drainage of Pond 7092, the roof of the enlarged englacial conduit began to collapse due to the proximity of the conduit to the surface of the glacier north of the Spillway Lake.

A long u-shaped channel, containing three small ponds had formed in the area of collapse by October 2001. Continued backwasting of the conduit entering the Spillway Lake and the ice face surrounding the southernmost part of the collapsed rift zone will almost certainly cause coalescence and inundation of the collapsed conduit over the next few years. Further collapse along the length of the englacial part of the conduit may also occur.

Subsidence of glacial karst features in the environs of the Spillway Lake may increase in the future as the glacier surface continues to downwaste and perched ponds upglacier of the Spillway Lake undergo rapid drainage. Areas of subsidence along englacial conduits adjacent to the Spillway basin may also be flooded as the lake continues to expand.

7.6.2. Future Enlargement of the Spillway Basin

Expansion of the Spillway Lake basin will continue at the exposed ice margins of the lake. The location and length of the exposed ice faces will change over time as slumping of debris exposes new ice faces and causes existing faces to become debris-covered and insulated once more. Where the lake perimeter consists of low-angled debris-covered slopes or large thicknesses of deltaic sediments, little expansion of the basin is expected. Enlargement of the Spillway Lake basin will also occur by amalgamation with surrounding supraglacial ponds and by flooding of areas of collapse in the immediate vicinity of the Spillway Lake basin.

Ultimately, the growth of the Spillway Lake is dependent on the altitude of the over-spill channel in the western lateral moraine. At present the channel is armoured by large boulders and appears to be stable. If the channel remains at its present altitude, then the following scenario may develop. As surface downwasting and the reduction of the overall glacier surface gradient continues, supraglacial ponds will eventually form at the same altitude as the Spillway Lake. When this occurs, the periodic drainage of ponds, through connection with englacial conduits below the water-line, will no longer take place. Ponds that connect with the englacial conduit network at

the same altitude as the over-spill channel in the western lateral moraine will become dynamically connected to the Spillway Lake and rapid basin enlargement will continue. As the number of ponds that connect with the englacial drainage network at the englacial base level increases, the connected pond basins on the glacier surface with amalgamate with each other, with other perched supraglacial ponds, and with the Spillway Lake basin. Eventually the amalgamation of ponds on the glacier surface will result in the formation of a large and potentially hazardous lake at the terminus of the Ngozumpa. By analogy with the evolution of the surfaces of glaciers elsewhere in the Himalaya, it is hypothesised that the formation a large and potentially hazardous moraine-dammed lake on the Ngozumpa Glacier could take place within the next two decades.

7.7. Paraglacial Reworking of Moraines

As the glacier surface has downwasted the lateral moraines bounding the glacier have been abandoned. The crests of the moraines now stand between 20 and >120 m above the glacier surface. The distance between the moraine crests and the glacier surface increases up glacier, due to the increase in downwasting rates with distance from the glacier terminus. The outer moraine slopes are well vegetated and are relatively stable. The inner moraine slopes upglacier of the Spillway Lake are unvegetated and are undergoing rapid paraglacial reworking and retreat. Downwasting of the glacier surface continually lowers the base of the inner moraine slopes, preventing the slopes from attaining a stable angle of repose and encouraging active paraglacial retreat. Slope activity on the inner moraines therefore increases upglacier, where higher rates of downwasting are experienced.

The lateral and terminal moraines that encompass the Ngozumpa Glacier play an important role in the formation of supraglacial lakes on the glacier surface. The moraines form an essentially impermeable barrier that inhibit drainage from the glacier surface and thereby encourage ponding on the glacier surface. The moraines will also support the formation of a large and potentially hazardous lake at the Ngozumpa terminus, acting as a moraine dam. The stability of the moraine and the

rate of degradation are therefore important to our understanding of where, how and when the moraine dam will fail, should the growth of a large lake on the Ngozumpa occur. Furthermore, the western lateral moraine has caused the formation of five laterally dammed lakes by damming back drainage from the western tributary valleys. These lateral lakes are now perched above the level of the glacier surface and will eventually flood out as paraglacial reworking causes degradation and retreat of the moraine.

7.7.1. Processes of Moraine Retreat

A number of processes were observed to cause the retreat of the inner lateral moraines at the Ngozumpa. These include gullying, debris avalanching, rockfall, landslipping, and wind erosion. The rates of gullying and debris flow failure on the Ngozumpa moraines were increased after periods of rainfall or snowmelt. Intensive gullying of the moraine edge was often followed by debris avalanching activity in the areas between the gullies. The removal of the supportive matrix around embedded boulders by gullying and wind erosion often triggered rockfalls. Large rockfall events were observed to trigger further slope failures, such as debris avalanching, on the lower talus slopes. Gullying, debris avalanching and rockfall were the dominant processes of moraine edge retreat on the western lateral moraine of the Ngozumpa, between October 1999 and October 2001 (See Chapter 6, Section 6.2.2). The average rate of retreat 4 km from the glacier terminus was calculated to be around 0.48 m a^{-1}.

Further upglacier, around 4.5 km from the glacier terminus, the rate of moraine edge retreat had been accelerated by the detachment and consequent landslipping of large blocks of moraine. Detachment of blocks occurs along failure planes within the moraine and is usually preceded by the appearance and propagation of tension cracks. The detached blocks are tilted as they travel downslope and start to break up, due to stresses caused by sliding and rotation. The front edges of the landslipped blocks also experience retreat by gullying, debris avalanching and rockfall activity.

The extent of landslipping on the moraines increases upglacier due to the increased distance between the moraine crest and the glacier surface (cf. Blair, 1994). Landslipping will therefore become an increasingly important process as downwasting proceeds. Detachment and consequent landslipping of blocks of moraine are believed to be responsible for the formation of ridges at the base of the moraine slope. Some of the ridges observed still supported a vegetation cover. High rates of detachment and landslipping were evidenced by the formation of a series of ridges at the foot of the moraine slope.

7.8. Final Conclusions

Ablation on the debris-covered Ngozumpa Glacier is largely restricted to where ice faces have been exposed on the glacier surface. The highest retreat rates are experienced at exposed ice faces surrounding supraglacial pond basins, and in particular at ice margins where rapid calving retreat is occurring. The evolution of pond basins on the Ngozumpa is therefore of fundamental importance to the downwasting rate of the glacier. As downwasting and lowering of the glacier surface gradient proceeds, the number and the size of perched supraglacial ponds increases. This in turn leads to an increase in the downwasting rate of the glacier surface in a positive feedback cycle.

At present, the growth of perched supraglacial ponds is limited by connection with the extensive englacial drainage network. As perched supraglacial pond basins expand they connect with englacial conduits below the water-line and undergo complete or partial drainage. The altitude of the over-spill channel determines the base level for englacial drainage on the Ngozumpa and controls the rate of growth of the Spillway Lake. Currently, the over-spill channel is armoured by large boulders and appears to be reasonably stable. If the altitude of the over-spill channel does not alter by downcutting of the meltwater stream then, as downwasting and surface gradient lowering on the Ngozumpa Glacier proceeds, perched supraglacial ponds will form at the englacial base level. The growth of perched ponds at the altitude of the englacial base level will not be limited by periodic drainage events. Connection

with the englacial drainage network will dynamically link the ponds with the Spillway Lake. Over time, ponds connected at the base level for englacial drainage will continue to grow in size and will amalgamate with neighbouring ponds, both perched and connected, and with the Spillway Lake. This could result in the formation of a large and potentially hazardous moraine-dammed lake at the terminus of the Ngozumpa Glacier within the next two decades.

If the safety of the infrastructure and people along the flood path of the Dudh Kosi is to be assured, then drainage of the Spillway Lake should be initiated before the lake becomes hazardous. Continued monitoring of the growth of the Spillway Lake and frequent excavation of the over-spill channel through the western lateral moraine could help to ensure that the development of a potentially hazardous lake does not occur on the Ngozumpa Glacier. Failing this, it is imperative that an early warning system is put in place in the Ngozumpa Valley in order to secure the safety of the people and infrastructure situated in the flood path of a potential Glacier Lake Outburst Flood (GLOF) from the Ngozumpa Glacier.

The research documented within this thesis is not limited to the situation at Ngozumpa Glacier and other debris-covered glaciers in the Khumbu Himal. It also has wide-reaching applications for understanding the expansion mechanisms of perched supraglacial ponds on debris-covered glaciers across the globe. Furthermore, the thesis provides the first direct evidence for drainage of perched supraglacial ponds on a debris-covered glacier and outlines how connection to the englacial conduit network can provide a check on rapid pond growth. It is proposed that once perched ponds connect at the base level for englacial drainage, they will no longer drain out and instead will continue to expand exponentially. This is important to understanding how large and potentially dangerous moraine-dammed lakes develop on debris-covered glaciers. The research at the Ngozumpa could therefore be applied to other debris-covered glaciers to enable prediction and improved monitoring of potentially dangerous moraine-dammed lake growth on other glaciers around the world.

If the safety of infrastructure and people living in the Khumbu Region, and other areas of the world threatened by the occurrence of GLOFs, is to be ensured then an integrated long term strategy for hazard mitigation and prevention must be enforced at a national level (Reynolds, 1995). Sometimes the time period between discovery of a potentially hazardous lake and remedial action can be up to 10 years (Reynolds, 2000). These issues must be overcome if any real headway is to be made in countering the threat of GLOFs. Of all the hazard mitigation strategies the safest and most cost effective are those which pre-empt the growth of very large lakes. Dealing with the problems generated by individual lakes should be considered an emergency procedure and more steps should be taken to identify where dangerous subaerial ice- and moraine-dammed lakes are likely to form in the future.

7.9. Suggestions for Future Research

At the Spillway Basin the following research could be undertaken:

- Continued observation of the Spillway Lake basin is required in order to monitor changes in the size of the basin and to determine any increase in the rate of basin expansion.
- More detailed investigation is required at the over-spill channel in order to accurately determine the rate of down-cutting. It would also be useful to monitor the annual variations in the rate and volume of meltwater flow through the channel.
- Year round monitoring of the Spillway Lake thermodynamics would enable a more precise estimate of the rate of subaqueous melting.
- Investigation of the thickness of the Ngozumpa Glacier, particularly at the glacier terminus. Determining the thickness of the ice at the terminus would allow a better estimate of the potential size and volume of a large moraine-dammed lake on the Ngozumpa.

Knowledge of the evolution of perched supraglacial pond basins could be expanded by:

- Calculation of seasonal variations in the rate of ablation and calving retreat at exposed ice faces around supraglacial pond basins.
- Further examination of the thermodynamics of perched ponds and how this relates to seasonal variations in subaqueous melting and the rate of thermo-erosional notching and notch-controlled calving events. Research into how the suspended sediment concentration and the albedo of pond surfaces affect pond thermodynamics would also be useful.
- Determining the extent of the englacial drainage network would allow more accurate prediction of when perched ponds on the glacier will drain. It would also allow a detailed analysis of what percentage of the meltwater generated on the Ngozumpa is channelled directly into the Spillway Lake and how much is stored in perched pond basins. However, there are many problems associated with this type of research due to the thickness of the debris cover and the large number of conduit connections. It is unlikely that a comprehensive study of englacial drainage on the Ngozumpa is feasible.
- Quantification of the contribution of ponds to the mean downwasting rates on the glacier compared with sub-debris melt rates (Nicholson, unpublished data).

The stability of the Ngozumpa moraines could be further analysed in the following ways:

- Further investigation on how debris thickness and downwasting rates on the Ngozumpa affect the rates of paraglacial reworking of the inner lateral moraines would be useful in determining the longevity of the moraines.
- GPR and electrical resistivity studies on the Ngozumpa moraines could identify the existence of buried ice cores. The melt out of buried ice cores would increase the rate of paraglacial reworking of the moraines and could compromise the stability of the moraine dam if a large lake were to form on the Ngozumpa terminus.

Chapter 7 Figures

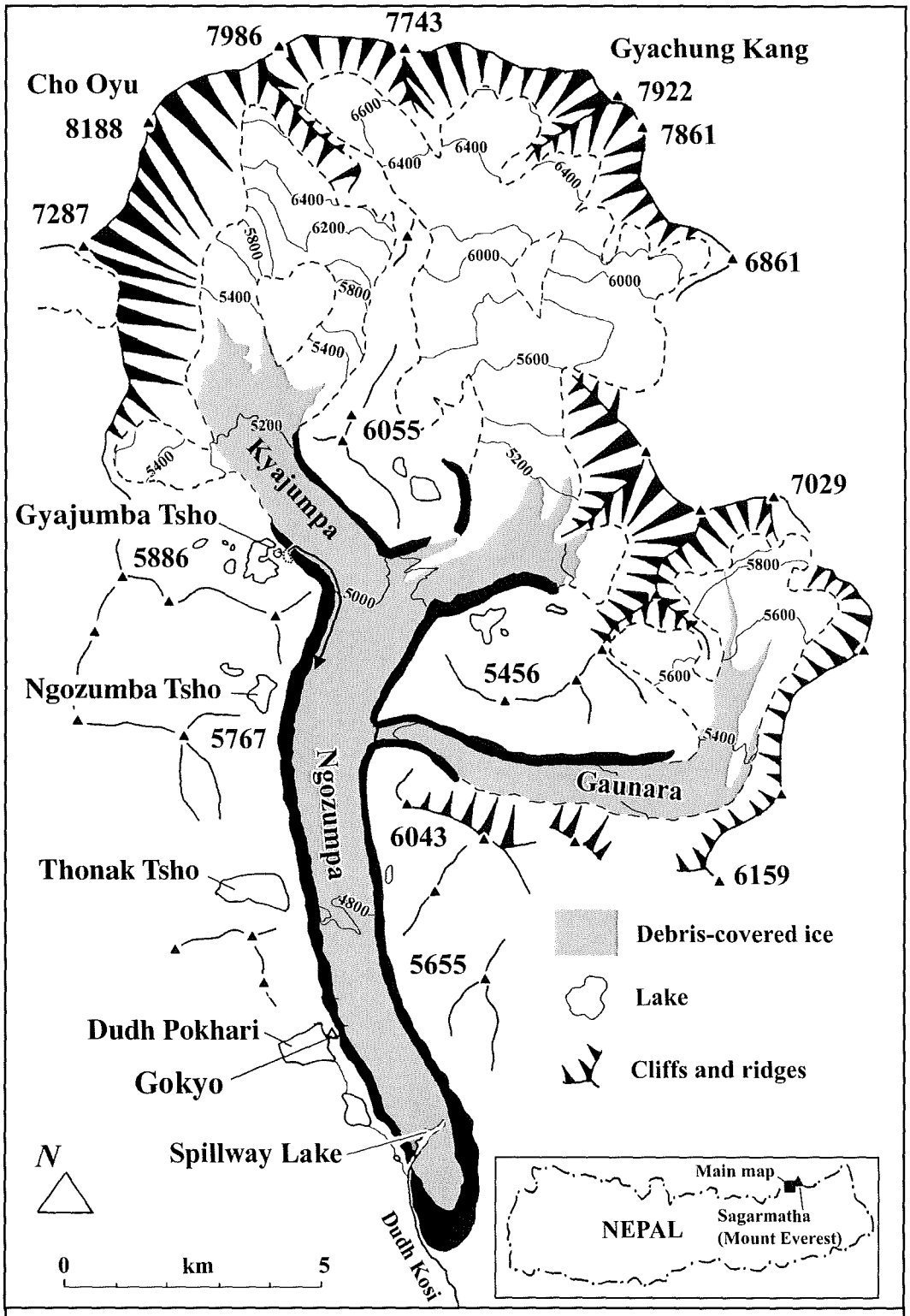

Figure 7.1. Ngozumpa Glacier Location Map (from Benn et al., 2001).

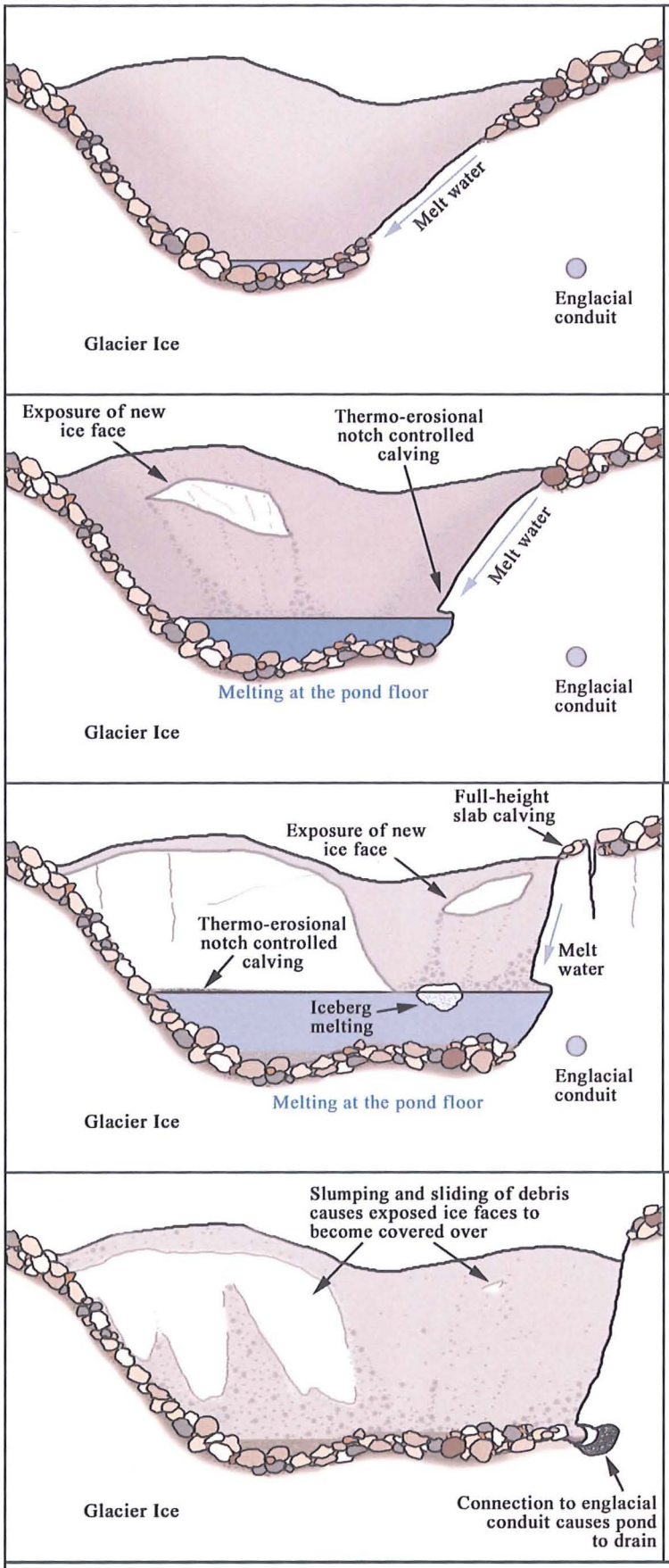

Stage 1. Slumping and sliding of debris on an ice-cored debris mound exposes an ice face. Melt water from the ice face ponds in the topographic hollow.

Stage 2. As the pond water level rises, the water is brought into contact with the exposed ice and initiates thermo-erosional notch controlled calving. The retreat rate of the ice face is increased and the pond enlarges more rapidly. As the pond margins steepen, new ice faces become exposed.

Stage 3. The pond basin continues to enlarge by melting and calving retreat at the exposed ice margins. Calved icebergs and melting at the pond floor provide additional water inputs. New ice faces are exposed and existing ones enlarged, initiating rapid exponential growth of the pond basin.

Stage 4. Retreat of the ice margin causes a connection to be made with the englacial conduit network and the pond drains. Over time the exposed ice margins become less steep and sliding and slumping of debris can cause them to become debris-covered.

Figure 7.2. Conceptual model illustrating the life cycle of a perched supraglacial pond from inception to drainage.

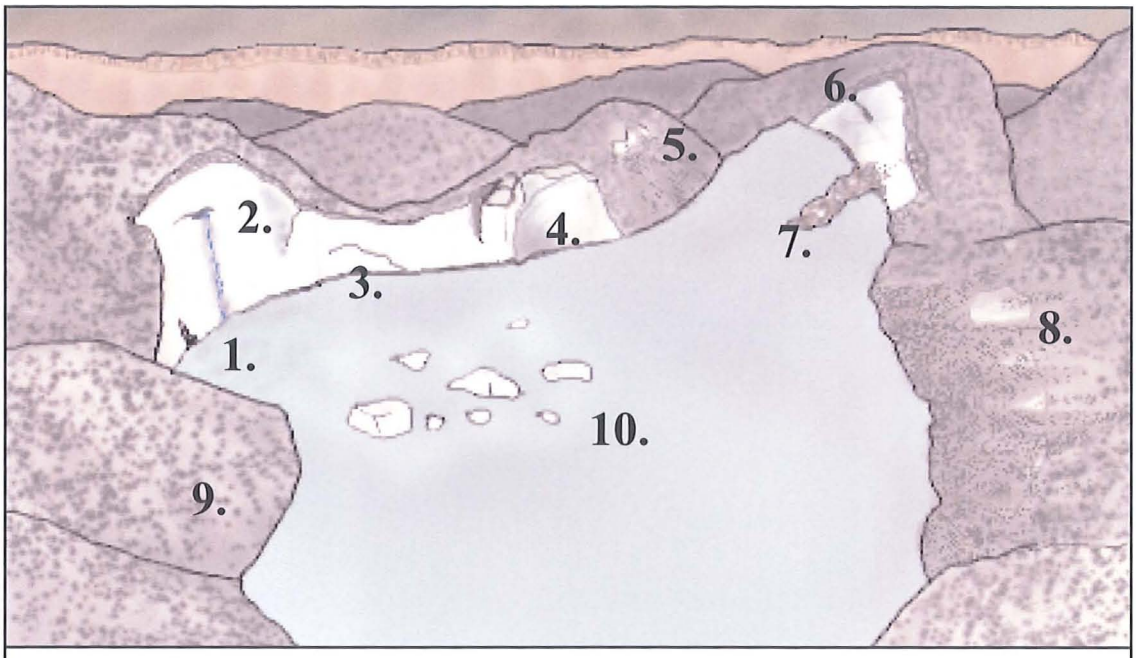

Figure 7.3. Subaerial processes of perched supraglacial pond evolution.

1. Englacial stream entering at the water level
2. Englacial conduit providing inputs of meltwater
3. Thermo-erosional notching and waterline calving
4. Full-height slab calving
5. Exposure of ice faces as debris slides down a steepening debris-covered ice margin
6. Englacial conduit exposed by ice face retreat
7. High rates of debris delivery into the pond causes a spit of debris to form
8. Progradation of talus cones causes an ice face to become debris-covered
9. Debris-covered ice margin
10. Calved icebergs provide inputs of water into a pond and can temporarily reduce the pond temperature

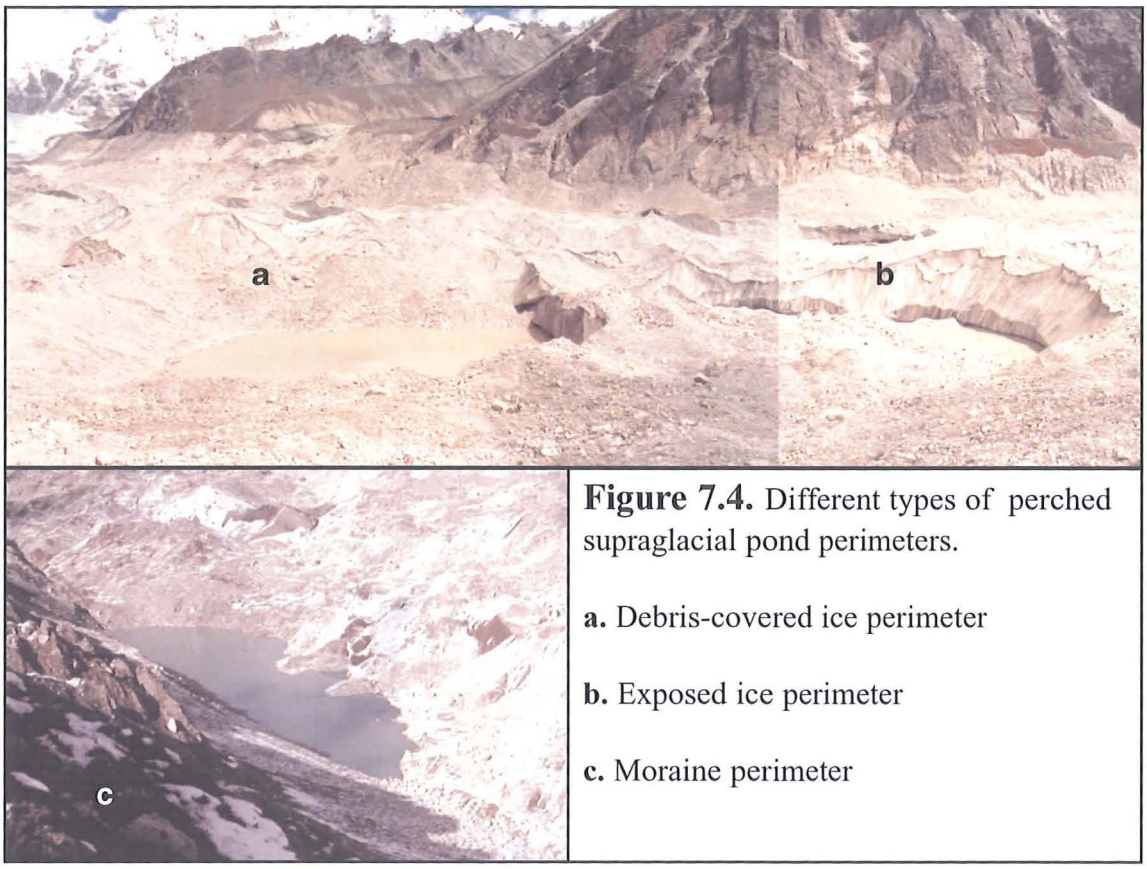

Figure 7.4. Different types of perched supraglacial pond perimeters.

a. Debris-covered ice perimeter

b. Exposed ice perimeter

c. Moraine perimeter

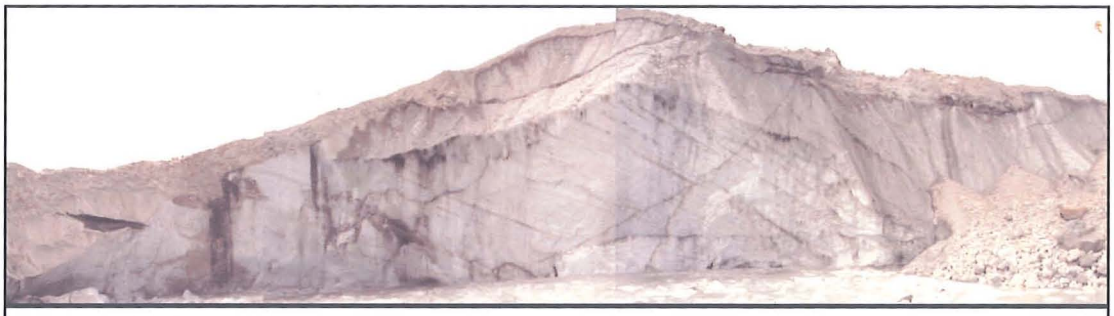

Figure 7.5. The deposition of debris cones can protect the base of an ice face from melting below the waterline and thermo-erosional notching.

Figure 7.6. Former pond floor sediments left behind after the drainage of a perched supraglacial pond. People for scale.

References

Ageta, Y. & Higuchi, K. 1984. Estimation of mass balance components of a summer-accumulation type glacier in the Nepal Himalaya. *Geografiska Annaler* **66A**, 249-255.

Ageta, Y., Ohata, T., Tanaka, Y., Ikegami, K. & Higuchi, K. 1980. Mass balance of glacier AX010 in Shorong Himal, east Nepal during the summer monsoon season. *Seppyo* **41**, 34-41.

Ageta, Y., Iwata, S., Yabuki, H. Naito, N., Sakai, A., Narama, C. & Karma. 2000. Expansion of glacier lakes in recent decades in the Bhutan Himalayas. *International Association of Hydrological Sciences, Special Publication* **264**, 165-175.

Anderson, R.S. 2000. A model of ablation-dominated medial moraines and the generation of debris-mantled glacier snouts. *Journal of Glaciology* **46**, 459-469.

Aoki, T. & Asahi, K. 1998. Topographical map of the ablation area of the Lirung Glacier in the Langtang Valley, Nepal Himalaya. *Bulletin of Glacier Research* **16**, 19-31.

Arnold, N.S., Willis, I.C., Sharp, M.J., Richards, K.S. & Lawson W.J. 1996. A distributed surface energy-balance model for a small valley glacier. I. Development and testing for Haut Glacier d'Arolla, Valais, Switzerland. *Journal of Glaciology* **42**, 77-89.

Ballantyne, C.K. 1995. Paraglacial debris-cone formation on recently deglaciated terrain, western Norway. *The Holocene* **5**, 25-33.

Ballantyne, C.K. & Benn, D. I. 1994. Paraglacial slope adjustment and resedimentation following recent glacier retreat, Fåbergstølsdalen, Norway. *Arctic and Alpine Research* **26**, 255-269.

Ballantyne, C.K. & Benn, D.I. 1996. Paraglacial slope adjustment during recent deglaciation and its implications for slope evolution in formerly glaciated environments. In Anderson, M.G. & Brooks, S.M. (eds.). *Advances in Hillslope Processes (Volume 2).* John Wiley & Sons Ltd, Chichester, 1173-1194.

Benn, D.I. & Evans, J.A; 1998; *Glaciers and Glaciation*; Arnold, London.

Benn, D.I. & Lehmkuhl, F. 2000. Mass Balance and equilibrium-line altitudes of glaciers in high-mountain environments. *Quaternary International* **65/66**, 15-29.

Benn, D.I. and Owen, L.A. 2002. Himalayan glacial sedimentary environments: a framework for reconstructing and dating former glacial extents in high mountainous regions. *Quaternary International* **97/98**, 3-26.

Benn, D.I., Wiseman, S. & Warren, C.R. 2000. Rapid growth of a supraglacial lake, Ngozumpa Glacier, Khumbu Himal, Nepal. *International Association of Hydrological Sciences, Special Publication* **264**, 177-186.

Benn, D.I., Wiseman, S. & Hands, K.A. 2001. Growth and drainage of supraglacial lakes on the debris-mantled Ngozumpa Glacier, Khumbu Himal, Nepal. *Journal of Glaciology* **47**, 626-638.

Benn, D.I., Kirkbride, M.P. and Owen, L.A. 2003. Glaciated Valley Landsystems. In D.J.A. Evans (ed.) *Glacial Landsystems*. Arnold, London, pp. 372- 406.

Benedict, J.B. 1976. Khumbu glacier series, Nepal. *Radiocarbon* **18**, 177-178.

Bennett, M.R. & Glasser, N.F. 1996. *Glacial Geology: Ice Sheets and Landforms*. Wiley, Chichester.

Blair, R.W. 1994. Moraine and valley wall collapse due to rapid deglaciation in Mount Cook National Park, New Zealand. *Mountain Research and Development* **14**, 347-358.

Boulton, G.S. 1967. The development of a complex supraglacial moraine at the margin of Sørbreen, Ny Friesland, Vestpitsbrgen. *Journal of Glaciology* **6**, 717-735.

Bozhinsky, A.N, Krass, M.S. & Popovnin, V.V. 1986. The role of debris cover in the thermal physics of glaciers. *Journal of Glaciology* **32**, 255-266.

Brower, B. 1983. Mountain hazards and the people of the Khumbu-Pharag. Unpublished paper, University of California, Berkley.

Cenderelli, D.A. & Wohl, E.E. 2001. Peak discharge estimates of glacial-lake outburst floods and "normal" climatic floods in the Mount Everest Region, Nepal. *Geomorphology* **40**, 57-90.

Chikita, K., Yamada, T., Sakai, A. and Ghimire, R.P. 1997. Hydrodynamic effects of the basin expansion of Tsho Rolpa Glacier Lake in the Nepal Himalaya. *Bulletin of Glacier Research* **15**, 59-69.

Chikita, K., Jha, J. & Yamada, T. 1998. The basin expansion mechanism of a supraglacial lake in the Nepal Himalaya. *Journal of Faculty of Science, Hokkaido University, Series VII (Geophysics)*, **11**, 501-521.

Chikita, K., Jha, J. & Yamada, T. 1999. Hydrodynamics of a supraglacial lake and its effect on the basin expansion: Tsho Rolpa, Rolwaling Valley in the Nepal Himalaya. *Arctic, Antarctic and Alpine Research,* **31**(1), 58-70.

Chikita, K., Joshi, S.P., Jha, J. & Hasegawa, H. 2000a. Hydrological and thermal regimes in a supraglacial lake: Imja, Khumbu, Nepal Himalaya. *Hydrological Sciences Journal* **45**, 507-521.

Chikita, K., Joshi, S.P., Jha, J. & Hasegawa, H. 2000b. The expansion mechanism for supraglacial lakes in the Nepal Himalaya. *Proceedings of the International Association of Theoretical and Applied Limnology* **27**.

Chikita, K., Jha, J. & Yamada, T. 2001. Sedimentary effects on the expansion of a Himalayan supraglacial lake. *Global and Planetary Change* **28**, 23-34.

Church, M. & Ryder, J.M. 1972. Paraglacial sedimentation: a consideration of fluvial processes conditioned by glaciation. *Geological Society of America Bulletin* **83**, 3059-3072.

Clague, J.J. 1987. Catastrophic outburst floods. *GEOS* **16** (2), 18-21.

Clague, J.J. & Evans, S.G. 1992. A self-arresting moraine dam failure, St Elias Mountains, British Columbia. *Geological Survey of Canada Paper* **92**-1A, 185-188.

Clague, J.J. & Evans, S.G. 1994. Formation and failure of natural dams in the Canadian Cordillera. *Geological Survey of Canada Bulletin* **464**, 1-35.

Clague J.J. & Evans, S.G. 2000. A review of catastrophic drainage of moraine-dammed lakes in British Columbia. *Quaternary Science Reviews* **19**, 1763-1783.

Clague, J.J., Evans, S.G. & Blown, I.G. 1985. A debris flow triggered by the breaching of a moraine-dammed lake, Klattasine Creek, British Columbia, Columbia. *Canadian Journal of Earth Sciences* **22**, 1492-1502.

Clark, D.H., Clark, M.M. & Gillespie, A.R. 1994. Debris-covered glaciers in the Sierra Nevada, California and their implications for snow-line reconstructions. *Quaternary Research* **41**, 139-153.

Clayton, L. 1964. Karst topography on stagnant glaciers. *Journal of Glaciology* **5**, 107-112.

Conway, H. & Rasmessen, L.A. 2000. Summer temperature profiles within supraglacial debris on Khumbu Glacier, Nepal. *International Association of Hydrological Sciences, Special Publication* **264**, 89-97.

Cooke, R.U. & Doornkamp, J.C. 1990. *Geomorphology in Environmental Management*. Clarendon Press. Oxford.

Coppin, N.J. & Richards, I.G. (eds). 1990. *Use of Vegetation in Civil Engineering.* Butterworths, London, pp. 49-86.

Costa, J.E. & Schuster, R.L. 1988. The formation and failure of natural dams. *Geological Society of America Bulletin* **100**, 1054-1068.

Drewry, D.J. 1972. A quantitative assessment of dirt-cone dynamics. *Journal of Glaciology* **11**, 431-446.

Eckert, E.R.G. & Drake, R.M. 1959. *Heat and Mass Transfer.* M°Graw-Hill, New York.

Eisbacher, G.H. 1982. Mountain torrents and debris flows. *Episodes* 1982 (4), 12-17.

Eisbacher, G.H. & Clague, J.J. 1984. Destructive mass movements in high mountains. *Geological Survey of Canada Paper* 84-16, 230.

Ensminger, S.L., Ensminger, S.L., Alley, R.B., Evenson, E.B., Lawson, D.E & Larson, G.J. 2001. Basal-crevasse-fill origin of laminated debris bands at Matanuska Glacier, Alaska, U.S.A. *Journal of Glaciology* **47**, 412-422.

Eyles, N. & Rogerson, R.J. 1978. A framework for the investigation of medial moraine formation: Austerdalsbreen, Norway, and Berendon Glacier, British Columbia, Canada. *Journal of Glaciology* **20**, 99-113.

Finkel, R.C., Owen, L.A., Barnard, P.L. & Caffee, M.W. 2003. Beryllium-10 dating of Mount Everest moraines indicates a strong monsoon influence and synchroneity throughout the Himalaya. *Geology* **31**, 561-564.

Fountain, A.G. & Walder, J.S. 1998. Water flow through temperate glaciers. *Reviews of Geophysics* **36**, 299-328.

Fushimi, H. 1977. Glaciations in the Khumbu Himal (1). *Seppyo* **39**, 60-67.

Fushimi, H. 1978. Glaciations in the Khumbu Himal (2). *Seppyo* **40**, 71-84.

Fushimi, H., Yoshida, M., Watanabe, O. & Upadhyay, B.P. 1980. Distributions and grain sizes of supraglacial debris on the Khumbu Glacier, Khumbu Region, East Nepal. *Seppyo* **41**, 18-25.

Glazyrin, G.E. 1975. The formation of ablation moraines as a function of the climatological environment. *International Association of Hydrological Sciences, Special Publication* **104**, 106-110.

Gomez, B. & Small, R.J. 1985. Medial moraines of the Haut Glacier D'Arolla, Valais, Switzerland: debris supply and implications for moraine formation. *Journal of Glaciology* **31**, 303-307.

Grove, J.M. 1988. Little Ice Age. Methuen, London.

Haffner, W. 1979. Nepal Himalaya. Untersuchungen zum vertikalen Landschaftsaufbau Zentral- und Ostnepals. *Erdwissen-schaftliche Forschung* **12**. Weisbaden: Steiner.

Hanisch, J., Delisle, G., Pokhrel, A.P., Dixit, A.M., Reynolds, J.M. & Grabs, W.E. 1998. *The Thulagi glacier lake, Manaslu Himal, Nepal - Hazard assessment of a potential outburst.* (In Moore, D. & Hunger, O. Eds. 1998. Proceedings Eighth International Congress International Association for Engineering Geology and the Environment. 21-25th September 1998/ Vancouver, Canada. pp2209-2215.)

Hanson, B. & Hooke, R. LeB. 2000. Glacier calving: a numerical model of forces in the calving speed/water-depth relation. *Journal of Glaciology* **46**, 188-196.

Healy, T.R. 1975. Thermokarst - a mechanism of de-icing ice-cored moraines. *Boreas* **4**, 19-23.

Hewitt, K. 1989. Hazards to water development in high mountain regions. The Himalayan sources of the Indus. In : *Hydrology of Disasters, Proceedings of Technical Conference, Geneva, November 1988.* World Meteorological Organisation. James & James, London. pp294-312.

Hewitt, K. 1993. Altitudinal organisation of Karakoram geomorphic processes and depositional environments. In J.F. Shroder (ed.) *Himalaya to the sea.* Routledge, London, pp. 159-183.

Higuchi, K., Fushimi, H., Ohata, T., Iwata, S. Yokoyama, K., Highuchi, H. Nagoshi, A. and Iozawa, T. 1978. Preliminary report on glacier inventory in the Dudh Kosi region. *Seppyo* **40**, 78-83.

Hochstein, M.P, Claridge, D., Henrys, S.A., Pyne, A., Nobes, D.C. & Leary, S.F. 1995. Downwasting of the Tasman Glacier, South Island, New Zealand: changes in the terminus region between 1971 and 1993. *New Zealand Journal of Geology and Geophysics* **38**, 1-16.

Inoue, J. 1977. Mass Budget of Khumbu Glacier. *Seppyo* **39**, 15-19

Inoue, J. & Yoshida, M. 1980. Ablation and heat exchange over the Khumbu Glacier, Khumbu region, east Nepal. *Seppyo* **41**, 26-33.

Innes, J.L. 1983. Debris flows. *Progress in Physical Geography* 7(4), 469-501

Iwata, S. 1976. Late Pleistocene and Holocene moraines in the Sagarmatha (Everest) region, Khumbu Himal. *Journal of the Japanese Society of Snow and Ice* 38, 109-114.

Iwata, S., Aoki, T., Kadota, T., Seto, K. & Yamaguchi, S. 2000. Morphological evolution of the debris cover on Khumbu Glacier, Nepal, between 1978 and 1995. *IAHS Publication* **264**, 3-11.

Jansson, P., Näslund, J., Pettersson, R. Richardson-Näslund, C. & Holmlund, P. 2000. Debris entrainment and polythermal structure in the terminus of Storglaciären. *International Association of Hydrological Sciences* **264**, 143-151.

Johnson, P.G. 1971. Ice-cored moraine formation and degradation, Donjek Glacier, Yukon Territory, Canada. *Geografiska Annaler* **53**A, 198-202.

Johnson, P.G. 1984. Paraglacial conditions of instability and mass movement. A discussion. *Zeitschrift für Geomorphologie* **28**, 235-250.

Johnson, P.G. & Power, J.M. 1985. Flood and landslide events, Peyto Glacier, Alberta, Canada. *Journal of Glaciology* **31**, 86-91.

Kalesnik, S.V. 1937. Gornye lednikovye rajony SSSR.

Kayastha, R.B., Ohata, T. & Ageta, Y. 1999. Application of a mass balance model to a Himalayan Glacier. *Journal of Glaciology* **45**, 559-567.

Kayastha, R.B., Takeuchi, Y., Nakawo, M. & Ageta, Y. 2000. Practical prediction of ice melting beneath various thickness of debris cover on Khumbu Glacier, Nepal, using positive degree-day factor. *IAHS Publication* **264**, 71-81.

Kick, W. 1962. Variations in some central Asiatic glaciers. In: *Variations of the regime of existing glaciers*. Commission of Snow and Ice. IAHS Publication **58**, 223-229.

Kirkbride, M.P. 1989. The influence of sediment budget on geomorphic activity of the Tasman Glacier, Mount Cook National Park, New Zealand. Unpublished PhD thesis, University of Canterbury, New Zealand, p 395.

Kirkbride, M.P. 1993. The temporal significance of transitions from melting to calving termini at glaciers in the central Southern Alps of New Zealand. *The Holocene* **3**, 232-240.

Kirkbride, M.P. 1995. Relationships between temperature and ablation on the Tasman Glacier, Mount Cook National Park, New Zealand. *New Zealand Journal of Geology and Geophysics* **38**, 17-27.

Kirkbride, M.P. 1995. Ice flow vectors on the debris-mantled Tasman Glacier 1957-1986. *Geografiska Annaler* 77A, 147-157.

Kirkbride, M.P. & Spedding, N. 1996. The influence of englacial drainage on sediment-transport pathways and till texture of temperate valley glaciers. *Annals of Glaciology* **22**, 160-166.

Kirkbride, M.P. and Warren, C.R. 1996. Controls on glacier calving in freshwater lakes. Unpublished report, NERC, Swindon.

Kirkbride, M.P. & Warren, C.R. 1997. Calving processes at a grounded ice cliff. *Annals of Glaciology* **24**, 116-121.

Kirkbride, M.P. & Warren, C.R. 1999. Tasman Glacier, New Zealand: Twentieth Century thinning and predicted calving retreat. *Global and Planetary Change* **22**, 11-28.

Knighton, A.D. 1973. Grain size characteristics of supraglacial dirt. *Journal of Glaciology* **12**, 522-524.

Kodama, H & Mae, S. 1976. The flow of glaciers in the Khumbu region. *Seppyo* **38**, 33-36.

Krüger, J. 1994. Glacial processes, sediments, landforms, and stratigraphy in the terminus region of Myrdalsjökull, Iceland. *Folia Greogr. Dan.* **21**.

Krüger, J. & Aber, J.S. 1999. Correspondence. Formation of supraglacial sediment accumulations on Kottujökull, Iceland. *Journal of Glaciology* **45**, 400-402.

Lewkowicz, A.G. 1987. Nature and importance of thermo-karst processes, Sand Hills moraine, Banks Island, Canada. *Geografiska Annaler* **69**A, 321-327.

Lliboutry, L. 1971. Les catastrophes glaciaires. *La Recherche* **2**, 417-425.

Lliboutry, L., Morales, B., Pautre, A. & Schneider, B. 1977a. Glaciological problems set by the control of dangerous lakes in Cordillera Blanca, Peru. I. Historical failure of moraine dams, their causes and prevention. *Journal of Glaciology* **18**, 239-254.

Lliboutry, L., Morales, B. & Schneider, B. 1977b. Glaciological problems set by the control of dangerous lakes in Cordillera Blanca, Peru. III. Study of moraines and mass balance at Safuna. *Journal of Glaciology* **18**, 275-290.

Loomis, S.R. 1970. Morphology and Ablation Processes on Glacier Ice. *Proceedings of the Association of American Geographers* **2**, 88-92.

Luckman, B.H. 1977. The geomorphic activity of snow avalanches. *Geografiska Annaler* **59**A, 31-48.

Lundstrom, S.C., McCafferty, A.E. & Coe, J.A. 1993. Photogrammetric analysis of 1984 - 1989 surface altitude change of the partially covered Eliot Glacier, Mt. Hood, Oregon, U.S.A. *Annals of Glaciology* **17**, 167-170.

McKenzie, G.D. & Goodwin, R.G. 1987. Development of collapsed glacial topography in the Adams Inlet area, Alaska, U.S.A. Journal of Glaciology **33**, 55-59.

McSaveney, M.J. 1975. The Sherman Glacier rock avalanche of 1964: its emplacement and subsequent effect on the glacier beneath it. Unpublished PhD thesis, Ohio State University.

Mattson, L.E. & Gardner, J.S. 1989. Energy exchanges and ablation rates on the debris-covered Rakhiot [Raikot] Glacier. *Zeitschrift fur Gletscherkunde und Glaziologie* **25**(1), 17-32.

Mattson, L.E. & Gardner, J.S. 1991. Mass wasting on valley-side ice-cored moraines, Boundary Glacier, Alberta, Canada. *Geografiska Annaler* **73**A, 123-128.

Mayewski, P.A. & Jeschke, P.A. 1979. Himalayan and Trans-Himalayan glacier fluctuations since AD 1812. *Arctic and Alpine Research* **11**, 267-287.

Mayewski, P.A., Pregent, G.P., Jeschke, P.A. & Ahmad, N. 1980. Himalayan and Trans-Himalayan glacier fluctuations and the monsoon record. *Arctic and Alpine Research* **12**, 171-182.

Müller, F. 1980. Present and late Pleistocene equilibrium line altitudes in the Mt Everest region – an application of the glacier inventory. World Glacier Inventory **126**, 75-94.

Müller, F. & Keeler, C.M. 1969. Errors in short term ablation measurements on melting ice surfaces. *Journal of Glaciology* **8**, 91-105.

Naito, N., Nakawo, M., Aoki, T., Asahi, K., Fujita, K., Sakai, A., Kadota, T., Shiraiwa, T. & Seko, K. 1998. Surface flow on the ablation area of the Lirung Glacier in Langtang Valley, Nepal Himalayas. *Bulletin of Glacier Research* **16**, 67-73.

Naito, N., Nakawo, M., Kadota, T. & Raymond, C.F. 2000. Numerical simulation of recent shrinkage of Khumbu Glacier, Nepal Himalayas. *International Association of Hydrological Sciences* **264**, 245-253.

Nakawo, M. 1979. Supraglacial debris of G2 Glacier in Hidden Valley, Mukut Himal, Nepal. *Journal of Glaciology* **22**, 273-283.

Nakawo, M & Rana, B. 1999. Estimate of ablation rate of glacier ice under a supraglacial debris layer. *Geografiska Annaler* **81**A, 695-701.

Nakawo, M. & Takahashi, S. 1982. A simplified model for estimating glacier ablation under a debris layer. *International Association of Hydrological Sciences* **138**, 137-145.

Nakawo, M & Young, G.J. 1981. Field experiments to determine the effect of a debris-layer on ablation of glacier ice. *Annals of Glaciology* **2**, 85-91.

Nakawo, M. & Young, G.J. 1982. Estimate of glacier ablation under debris layer from surface temperature and meteorological variables. *Journal of Glaciology* **28**, 29-34.

Nakawo, M., Iwata, S., Watanabe, O. and Yoshida, M. 1986. Processes which distribute supraglacial debris on the Khumbu Glacier, Nepal Himalaya. *Annals of Glaciology* **8**, 129-131.

Nakawo, M., Yabuki, H. & Sakai, A. 1999. Characteristics of Khumbu Glacier, Nepal Himalayas: recent changes in the debris covered area. *Annals of Glaciology* **28**, 118-122.

Näslund, J.O. & Hassinen, S. 1996. Correspondence. Supraglacial sediment accumulations and large englacial water conduits at high elevations in Myrdalsjökull, Iceland. *Journal of Glaciology* **42**, 190-192.

Østrem, G. 1959 Ice melting under a thin layer of moraine and the existence of ice cores in moraine ridges. *Geografiska Annaler* **41**, 228-230.

Østrem, G. 1964. Ice-cored moraines in Scandinavia. *Geografiska Annaler* **46**, 282-237.

Owen, L.A. 1991. Mass movement deposits in the Karakoram Mountains: their sedimentary characteristics, recognition and role in Karakoram landform evolution. *Zeitschrift für Geomorphologie* **35**, 401-424.

Owen, L.A. 1994. *Glacial and non-glacial diamictons in the Karakoram Mountains and western Himalayas.* (In Warren, W.P. & Croot, D.G. Eds. 1991. Proceedings of the meeting of the Commission on the formation and deformation of glacial deposits. Balkema, Rotterdam. 9-28.)

Owen, L.A. & Derbyshire, E. 1989. The Karakoram glacial depositional system. *Zeitschrift für Geomorphologie* **76**, 33-73.

Owen, L.A. & Sharma, M.C. 1998. Rates and magnitudes of paraglacial fan formation in the Garhwal Himalaya: implications for landscape evolution. *Geomorphology* **26**, 171-183.

Owen, L.A., Derbyshire, E. & Fort, M. 1998. The Quaternary glacial history of the Himalaya. *Quaternary Proceedings* **6**, 91-120.

Palacios, D., Parilla, G. & Zamorano, J.J. 1999. Paraglacial and postglacial debris flows on a Little Ice Age terminal moraine: Jamapa Glacier, Pico de Orizaba (Mexico). *Geomorphology* **28**, 95-118.

Paterson, W.S.B. 1994. *The Physics of Glaciers, 3rd ed.* Pergamon, New York.

Pearce, F. 1999. Flooded Out. *New Scientist* 19th June, 4.

Pearce, F. 2002. Meltdown. *New Scientist* 2nd November, 44-48.

Powell, R.D. 1983. Glacial marine sedimentation processes and lithofacies of temperate tidewater glaciers, Glacier Bay, Alaska. In Molnia, B.F. (ed.), *Glacial-Marine Sedimentation.* Plenum Press, New York, 195-232.

Purdie, J. & Fitzharris, B. 1999. Processes and rates of ice loss at the terminus of Tasman Glacier, New Zealand. *Global and Planetary Change* **22**, 79-91.

Reynolds, J.M. 1998. High-altitude glacial lake hazard assessment and mitigation: a Himalayan perspective. In: Maund, J.G. & Eddleston, M. (eds.) Geohazards in Engineering Geology. Geological Society, London. Engineering Geology Special Publications **15**, 25-34.

Reynolds, J.M. 1999. Glacial hazard assessment at Tsho Rolpa, Rolwaling, central Nepal. *Quarterly Journal of Engineering Geology* **32**, 209-214.

Reynolds, J.M. 2000. On the formation of supraglacial lakes on debris-covered glaciers. *International Association of Hydrological Sciences* **264**, 153-161.

Richards, B.W.M., Benn, D.I., Owen, L.A., Rhodes, E.J. & Spencer, J.Q. 2000. Timing of late Quaternary glaciations south of Mount Everest in the Khumbu Himal, Nepal. *Geological Society of America Bulletin* **112**, 1621-1632.

Richardson, S.D. & Reynolds, J.M. 2000a. Degradation of ice-cored moraine dams: implications for hazard development. *International Association of Hydrological Sciences* **264**, 187-197.

Richardson, S.D. & Reynolds, J.M. 2000b. An overview of glacial hazards in the Himalayas. *Quaternary International* **65/66**, 31-47.

Röthlisberger, F. & Geyh, M.A. 1986. Glacier variations in Himalayas and Karakoram. *Zeitshcrift für Gletscherkunde und Glazialgeologie* **21**, 237-249.

Ryder, J.M. 1971. The stratigraphy and morphology of paraglacial alluvial fans in South-central British Columbia. *Canadian Journal of Earth Science* **8**, 279-298.

Sakai, A., Fujita, K., Aoki, T., Asahi, K. & Nakawo, M. 1997. Water discharge from the Lirung Glacier in Langtang Valley, Nepal Himalayas, 1996. *Bulletin of Glacier Research* **15**, 79-83.

Sakai, A., Nakawo, M. & Fujita, K. 1998. Melt rate of ice cliffs on the Lirung Glacier, Nepal Himalayas, 1996. *Bulletin of Glacier Research* **16**, 57-66.

Sakai, A., Takeuchi, N., Fujita, K. & Nakawo, M. 2000a. Role of supraglacial ponds in the ablation process of a debris-covered glacier in the Nepal Himalayas. *International Association of Hydrological Sciences* **264**, 119-130.

Sakai, A., Chikita, K. & Yamada, T. 2000b. Expansion of a moraine-dammed lake, Tsho Rolpa, in Rolwaling Himal, Nepal Himalaya. *Limnology and Oceanography* **45**, 1401-1408.

Sakai, A., Yamada, T. & Chikita, K. 2001. Thermal regime of a moraine-dammed lake, Thso Rolpa, in Rolwaling Himal, Nepal Himalaya. *Bulletin of Glaciological Research* **18**, 37-44.

Searle, M.P. and Treloar, P.J. 1993. Introduction: Himalayan Tectonics. *Geological Society of London*, Special Publication **74**, 1-8.

Searle, M.P. 1999a. Extensional and compressional faults in the Everest-Lhotse massif, Khumbu Himalaya, Nepal. *Journal of the Geological Society, London* **156**, 227-240.

Searle, M.P. 1999b. Emplacement of Himalayan leucogranites by magma injection along giant sill complexes: examples from Cho Oyu, Gyachung Kang and Everest leucogranites (Nepal Himalayas). *Journal of Asian Earth Sciences* **17**, 773-783.

Searle, M.P., Simpson, R.L., Parrish, R.R. & Waters, D.J. 2003. The structural geometry, metamorphic and magnetic evolution of the Everest massif, High Himalaya of Nepal-South Tibet. *Journal of the Geological Society, London* **160**, 345-366.

Seko, K., Yabuki, H., Nakawo, M., Sakai, A., Kadota, T. & Yamada, Y. 1998. Changing surface features of Khumbu Glacier, Nepal Himalayas revealed by SPOT images. *Bulletin of Glacier Research* **16**, 33-41.

Sharma, C.K. 1990. *Geology of Nepal Himalaya and Adjacent Countries.* Sangeeta Sharma & Bishal Nagar, Kathmandu, Nepal.

Shaw, J. & Archer, J. 1979. Deglaciation and glaciolacustrine sedimentation conditions, Okanagan Valley, British Columbia, Canada. In Schluchter, C (ed.), *Moraines and Varves.* Balkema; Rotterdam, 347-355.

Shroder, J.F., Bishop, M.P., Copland, L. & Sloan, V.F. 2000. Debris-covered glaciers and rock glaciers in the Nanga Parbat Himalaya, Pakistan. *Geografiska Annaler* **82**A, 17-32.

Small, R.J. 1983. Lateral moraines of Glacier De Tsidjiore Nouve: form, development, and implications. *Journal of Glaciology* **29**, 250-259.

Small, R.J. & Clark, M.J. 1974. The medial moraines of the lower glacier de Tsidjiore Nouve, Valais, Switzerland. *Journal of Glaciology* **13**, 255-263.

Small, R.J., Clark, M.J. & Cawse, T.J.P. 1979. The formation of medial moraines on Alpine glaciers. *Journal of Glaciology* **22**, 43-52.

Smith, N.D. & Ashley, G.M. 1985. Proglacial lacustrine environments. In Ashley, G.M., Shaw, J. and Smith, N.D. (eds), *Glacial Sedimentary Environments.* SEPM Short Course 16, 135-215.

Souchez, R.A. 1971. Ice-cored moraines in south-western Ellesmere Island, N.W.T., Canada. *Journal of Glaciology* **10**, 245-254.

Spedding, N. 2000. Hydrological controls on sediment transport pathways: implications for debris-covered glaciers. *International Association of Hydrological Sciences* **264**, 133-141.

Statham, I. 1976. Debris flows on vegetated screes in the Black Mountain, Carmarthenshire. *Earth Surface Processes* **1**, 173-180.

Szilder, K, Lozowski, E.P., & Sharp M.J. 1997. Glacial lake drainage: a stability analysis. *Annals of Glaciology* **24**, 175-180.

Takeuchi, Y., Kayastha, R.B. & Nakawo, M. 2000a. Characteristics of ablation and heat balance in debris-free and debris-covered areas on Khumbu Glacier, Nepal Himalayas, in the pre-monsoon season. *IAHS Publication* **264**, 53-61.

Takeuchi, N., & Koshima, S. 2000b. Effect of debris cover on species composition of living organisms in supraglacial lakes on a Himalayan glacier. *IAHS Publication* **264**, 267-275.

Theakstone, W.H. 1982. Sediment fans and sediment flows generated by snowmelt: observations at Austerdalsisen, Norway. *Journal of Geology* **90**, 583-588.

Theakstone, W.H. 1989. Further catastrophic break-up of a calving glacier: observations at Austerdalsisen, Svartisen, 1983-1987. *Geografiska Annaler* **71**A, 245-253.

Tufnell, L. 1984. *Glacier Hazards*. Longman, London.

Van Der Veen, C.J. 1998. Fracture mechanics approach to penetration of bottom crevasses on glaciers. *Cold Regions Science and Technology* **27**, 213-223.

Van Steijn, H, de Ruig, J. & Hoozemans, F. 1988. Morphological and mechanical aspects of debris flows in parts of the French Alps. *Zeitschrift für Geomorphologie* **32**, 143-161.

Vere, D.M. & Benn, D.I. 1989. Structure and debris characteristics of medial moraines in Jotunheimen, Norway: implications for moraine classification. *Journal of Glaciology* **35**, 276-280.

Vuichard, D. 1984. Geology of Khumbu area. Unpublished paper, University of Berne.

Vuichard, D. & Zimmermann, M. 1986. The Langmoche flash-flood, Khumbu Himal, Nepal. *Mountain Research and Development* **6**, 90-93.

Vuichard, D & Zimmermann, M. 1987. The 1985 catastrophic drainage of a moraine-dammed lake, Khumbu Himal, Nepal – cause and consequences. *Mountain Research and Development* **7**, 91-110.

Warren, C.R. 1992. Iceberg calving and the glacioclimatic record. *Progress in Physical Geography,* **16**, 253-282.

Warren, C.R. 1993. Rapid recent fluctuations of the calving San Rafael Glacier, Chilean Patagonia: climatic or non-climatic? *Geografiska Annaler* **75**, 111-125.

Warren, C.R. 1999. Calving speed in freshwater at Glacier Ameghino, Patagonia. *Zeitschrift für Gletscherkunde und Glazialgeologie* **35**, 21-34.

Warren, C.R., Greene, D.R. & Glasser, N.F. 1995. Glacier Upsala, Patagonia: rapid calving retreat in fresh water. *Annals of Glaciology* **21**, 311-316.

Warren, C.R., Glasser, N.F., Harrison, S., Winchester, V., Kerr, A.R. & Rivera, A. 1995b. Characteristics of tide-water calving at Glaciar San Rafael, Chile. *Journal of Glaciology* **41**, 273-289.

Warren, C.R. & Kirkbride, M.P. 1998. Temperature and bathymetry of ice-contact lakes in Mount Cook National Park, New Zealand. *New Zealand Journal of Geology and Geophysics* **41**, 133-143.

Warren, C.R., Benn, D.I., Winchester, V. & Harrison, S. 2000. Buoyancy-driven lacustrine calving, Glaciar Nef, Chilean Patagonia. *Journal of Glaciology* **47**, 135-146.

Watanabe, O., Iwata, S. & Fushimi, H. 1986. Topographic characteristics in the ablation area of the Khumbu Glacier, Nepal Himalaya. *Annals of Glaciology* **8**, 177-180.

Watanabe, T., Ives, J.D. & Hammond, J.E. 1994. Rapid growth of a glacial lake in Khumbu Himal, Himalaya: prospects for a catastrophic flood. *Mountain Research and Development* **14**, 329-340.
Watanabe, T., Kameyama, S. & Sato, T. 1995. Imja Glacier dead-ice melt rates and changes in a supraglacial lake, 1989-1994, Khumbu Himal, Nepal: danger of lake drainage. *Mountain Research and Development* **15**, 293-300.

Watson, R.A. 1980. Landform development on moraines of the Klutlan Glacier, Yukon Territory, Canada. *Quaternary Research* **14**, 50-59.

Weeks, W.F. & Campbell, W.J. 1973. Icebergs as a fresh-water source: an appraisal. *Journal of Glaciology* **12**, 207-233.

Wenshou, W. 1992. Properties and structure of the seasonal snow cover in the continental regions of China. *Annals of Glaciology* **32**, 93-96.

Whalley, W.B. 1973. An exposure of ice on the distal side of a lateral moraine. *Journal of Glaciology* **12**, 327-329. [Letter].

Whalley, W.B., Palmer, C.F., Hamilton, S.J. & Kitchen, D. 1996. Supraglacial debris transport variability over time, examples from Switzerland and Iceland. *Annals of Glaciology* **22**, 181-186.

Williams, Van S. 1983. Present and former equilibrium-line altitudes near Mount Everest, Nepal and Tibet. *Arctic and Alpine Research* **15**, 201-211.

Wiseman, S. 2004. The inception and evolution of supraglacial lakes on debris-covered glaciers in the Nepal Himalaya. Unpublished PhD thesis, University of Aberdeen.

Wright, H.E. 1980. Surge moraines of the Klutlan Glacier, Yukon Territory, Canada: origin, wastage, vegetation succession, lake development and application to the late glaciation of Minnesota. *Quaternary Research* **14**, 2-18.

Xu, D. & Feng, Q. 1994. Dangerous lakes and their outburst features in the Tibetan Himalayas. *Bulletin of Glacier Research* **12**, 1-8.

Yafeng, S. & Jinwen, R. 1990. Glacier recession and lake shrinkage indicating a climatic warming and drying trend in Central Asia. *Annals of Glaciology* **14**, 261-265.

Yamada, T. 1998. *Glacier lake and its outburst flood in the Nepal Himalaya.* Monograph No. 1, Data Center for Glacier Research, Japanese Society of Snow and Ice.

Yamada, T. & Sharma, C.K. 1993. Glacier lakes and outburst floods in the Nepal Himalaya. *International Association of Hydrological Sciences* **218**, 319-330.

Yongjian, D. & Jingshi, L. 1992. Glacier lake outburst flood disasters in China. *Annals of Glaciology* **16**, 180-184.

Zimmermann, M. & Haeberli, W. 1992. Climatic change and debris flow activity in high-mountain areas – a case study in the Swiss Alps. *Catena Supplement* **22**, 59-72.

Zimmermann, M., Bichsel, M. & Kienholz, H. 1986. Mountain hazards mapping in the Khumbu Himal, Nepal, with prototype map, scale 1:50,000. *Mountain Research and Development* **6**, 29-40.